Menzies Research Institute

UTAS

EXERCISE AND INSULIN: MUSCLE HAEMODYNAMICS AND METABOLISM

By

Renee M. Ross
BHM(Hons), GradDipSci(Hons)

A thesis submitted in requirement for the degree of
Doctor of Philosophy (Medical Research)

Menzies Research Institute (Biochemistry)
University of Tasmania

November 2007

TABLE OF CONTENTS

STATEMENT

The work in this thesis has been undertaken exclusively for the use of a PhD in the area of Biochemistry and has not been used for any other higher degree or graduate diploma in any university. All written and experimental work is my own except that which has been referenced accordingly.

Renee M. Ross

AUTHORITY OF ACCESS

This thesis may be available for loan and limited copying in accordance with the *Copyright Act 1968.*

Renee M. Ross

ABSTRACT

Insulin resistance is a disease characterised by an inability of the body to effectively respond to insulin in terms of increased glucose uptake. However, in most cases, the response to exercise to increase glucose uptake is largely unaffected in insulin resistance. This thesis focuses on the differences and similarities between these two stimuli with a view to further understanding the cause of insulin resistance and the possibility of developing new treatments for this disease.

There is evidence to suggest that the ability of insulin and muscle contraction to increase muscle glucose uptake is due in part, to their ability to increase blood flow, in particular microvascular perfusion. Accordingly, the hyperinsulinaemic euglycaemic clamp technique, in conjunction with electrical stimulation to simulate exercise, was used in anaesthetised rats to examine factors which control muscle microvascular perfusion. Additionally, an assessment was made of how microvascular perfusion related to glucose uptake and insulin resistance in skeletal muscle, the main site where insulin normally acts to increase glucose uptake.

This study used two techniques to measure changes in muscle microvascular perfusion. The first, an established method involving the capillary endothelial metabolism of infused 1-methylxanthine; the second, a relatively new technique, contrast enhanced ultrasound (CEU), which has been adapted from its use in measuring microvascular perfusion in heart.

A component of this thesis applied model systems to validate the use of CEU to measure microvascular perfusion and showed that this was independent of changes in bulk flow, and that CEU can be used to measure changes in skeletal muscle microvascular perfusion regardless of the microvascular architecture involved.

In another component, again using CEU, changes in microvascular perfusion in response to electrical stimulation were measured. The rapid increase in femoral blood flow in response to muscle contraction was found to reverse quickly, however microvascular perfusion remained enhanced up to 60 min after contraction. In addition, it was also shown that while insulin-mediated vasodilation was nitric oxide-dependent and thus was indicative of the main mechanism by which insulin causes vasodilation in muscle, a local infusion (via the epigastric artery) of a nitric oxide synthase inhibitor during contraction did not block microvascular perfusion, even though it inhibited the accompanying increase limb (femoral arterial) blood flow. The nitric oxide synthase inhibitor blocked ~35% of the contraction-mediated increase in muscle glucose uptake, but by not affecting the accompanying increase in microvascular perfusion, the results suggested that a non-nitric oxide compensatory mechanism (such as adenosine, potassium ions, or neural inputs) may be involved.

Interleukin-6 (IL-6) is released by muscle during exercise and thought to have a role in glucose homeostasis. Its involvement in insulin resistance is controversial and its effects on insulin-mediated changes were thus explored. The infusion of this cytokine during a hyperinsulinaemic euglycaemic clamp suppressed the insulin-mediated increase in microvascular perfusion. Interestingly, this inhibition did not result in insulin resistance as IL-6 was able to increase muscle glucose uptake through its own signalling pathway. However, it is possible that elevated plasma IL-6 when maintained over longer periods may lead to insulin resistance due to the inhibition of insulin's microvascular effects.

Because chronically elevated levels of endothelin-1 (ET-1) may also be implicated in insulin resistance of muscle through actions on the microvasculature, another component of this thesis explored the acute effects of ET-1 *in vivo*. Infusion of ET-1 into anaesthetised rats in conjunction with insulin led to a hyperinsulinaemic state, found to be due to a decrease in

insulin clearance. Muscle insulin resistance also resulted and was concluded to result from an attenuation of insulin-mediated increase in microvascular perfusion.

Collectively, the findings of this thesis confirm an important role for microvascular perfusion in mediating the stimulatory responses of both insulin and exercise on muscle glucose uptake. In most cases there was a close association between increases in microvascular perfusion and glucose uptake. However, contraction-mediated microvascular perfusion was maintained even when muscle glucose uptake was blocked by infusion of a nitric oxide synthase inhibitor, suggesting a non-vascular myocyte source of nitric oxide that is involved in contraction-mediated glucose uptake. ET-1 was found to play an important part in opposing the insulin-mediated increases in microvascular perfusion, thus consistent with growing evidence that ET-1 may be a major contributor to insulin resistance in muscle. Finally there are data to suggest that in the short term, the body may be able to compensate for a decrease in insulin- or contraction-mediated microvascular perfusion, but that the compensatory mechanisms may unsustainable in the longer term and insulin resistance may develop because of the reduced microvascular perfusion.

ACKNOWLEDGEMENTS

I would like to extend my sincere thanks to my supervisors Prof. Michael Clark for his guidance and tireless enthusiasm for research and to Assoc. Prof. Steve Rattigan for his technical assistance and advice. I feel very fortunate to have worked with such dedicated scientists and have learned a great deal from you both.

I would like to acknowledge the work of two groups in Melbourne which I have collaborated with on two of the studies in this thesis. I would like to acknowledge Glenn Wadley and Glenn McConell at The University of Melbourne, for their contribution to Chapter 5. Glenn Wadley assayed the muscle samples collected during the contraction and nitric oxide synthase inhibition protocol for nitric oxide content, nitric oxide synthase phosphorylation, and AMPK activation (Fig. 5.9-5.12). I would also like to acknowledge the work of Derek Yuen and Mark Febbraio at the Baker Heart Institute in Melbourne for their contribution to Chapter 7. Derek assayed the muscle samples collected during the IL-6 and insulin protocol for Akt activation (Fig. 7.13).

I would also like to thank many past and present members of the muscle research group, including Eloise Bradley, Cate Wheately, Hema Mahajan, Zhang Lei, Georgie Vollus, Maree Smith, Phil St-Pierre, Amanda Genders, Kathleen Downey, John Newman, Carol Bussey, Geoffrey Appleby and Stephen Richards for your help and friendship. Thanks also to Marcus, Murray and Barbra down at the animal house for all of your hard work, and an extra special thank you to Cathryn Kolka for all her help (especially in the early days!) and continued friendship.

Finally, I would like to thank my family, for their continued love, support and encouragement, and to the Dwyer family for their support and generosity throughout the last 5 years. To my Nicholas, thank you; this thesis is dedicated to you.

ABBREVIATIONS

1-MU	1-methylurate
1-MX	1-methylxanthine
2-DG	2-deoxy-D-[1-^{14}C] glucose
ACC	Acetyl Co-A carboxylase
AI	Acoustic intensity
AICAR	5'-aminoimidazole-4-carboxamide riboside
ALP	Allopurinol
AMP	Adenosine monophosphate
AMPK	AMP activated protein kinase
ANOVA	Analysis of variance
AS160	Akt substrate of 160 KDa
ATP	Adenosine triphosphate
BCS	Biodegradable counting scintillant
BSA	Bovine serum albumin
CaMK	Calmodulin-dependent protein kinase
CEU	Contrast enhanced ultrasound
cGMP	cyclic guanosine monophosphate
CO_2	Carbon dioxide
COMB	Combined calf muscle
EDL	Extensor digitorum longus
EDTA	Ethylenediaminetetra-acetic acid
ELISA	Enzyme-linked immuno-sorbent assay
eNOS	Endothelial nitric oxide synthase
EPOC	Excess post exercise oxygen consumption
ERK	Extracellular signal-regulated kinase
ES	Electrical stimulation
ET	Endothelin
ET_A	Endothelin receptor type A
ET_B	Endothelin receptor type B
FAT	Epididymal fat pad
FBF	Femoral blood flow
FFA	Free fatty acid

FITC	Flourescein isothiocyanate
GIR	Glucose infusion rate
GLUT	Glucose transporter
GSK	Glycogen synthase kinase
GU	Glucose uptake
HGU	Hindlimb glucose uptake
HPLC	High performance liquid chromatography
ICV	Intracerebroventricular
IL-6	Interleukin-6
IRS1	Insulin receptor substrate
JNK	Jun N-terminal kinase
LDF	Laser Doppler flowmetry
L-NMMA	N^G-monomethyl-L-arginine
L-NAME	N^G-nitro-L-arginine methyl ester
LR	Lactate release
MAPK	Mitogen activated protein kinase
MB	Microbubble
MIRKO	Muscle-specific insulin receptor knock out mouse
nNOS	Neuronal nitric oxide synthase
NO	Nitric oxide
NOS	Nitric oxide synthase
NOx	Nitrites and nitrates
PDK-1	Phosphoinositide-dependent protein kinase
PI	Pulsing interval
PI3-kinase	Phosphatidylinositol 3-kinase
PKC	Protein kinase C
PLA	Plantaris
PP	Perfusion pressure
Ra	Rate of glucose appearance
Rd	Rate of glucose disappearance
RG	Red gastrocnemius
R'g	Rate of radioactive 2-DG glucose uptake
RU	Resistance units
SEM	Standard error of the mean

SOCS	Suppressor of cytokine signalling
SOL	Soleus
TNF-α	Tumour necrosis factor-α
TIB	Tibialis anterior
VO_2	Oxygen uptake
VR	Vascular resistance
WG	White gastrocnemius

PREFACE

Some of the data presented in this thesis has been published or presented at scientific meetings and has been listed below.

Publications arising directly from this thesis

Ross RM, Kolka CM, Rattigan S, Clark MG. 2007. Acute blockade by endothelin-1 of haemodynamic insulin action in rats. *Diabetologia* 50(2): 443-451.

Rattigan S, Bussey CT, **Ross RM**, Richards SM. 2007. Obesity, insulin resistance, and capillary recruitment. *Microcirculation* 14(4): 299-309.

Ross RM, Wadley GD, Clark MG, Rattigan S, McConell GK. Local NOS inhibition reduces skeletal muscle glucose uptake but not capillary blood flow during in situ muscle contraction in rats. (*Diabetes*: Accepted for publication in August 2007).

Ross RM, Downey K. Newman JMB, Richards SR, Clark MG, Rattigan S. Contrast enhanced ultrasound measurement of microvascular perfusion relevant to nutrient and hormone delivery in skeletal muscle: a model study *in vitro*. (*Microvascular Research:* Accepted for publication November 2007)

Ross RM, Yuen DYC, Matthews V, Southgate RJ, Clark MG, Febbraio MA, Rattigan S. IL-6 blunts the effect of insulin on endothelial cell signalling and capillary recruitment, but augments its effect on skeletal muscle insulin action. (Manuscript prepared for submission to *Diabetes*)

Ross RM, Rattigan S. Clark MG. Brief muscle contraction results in sustained capillary recruitment and glucose uptake. (Manuscript prepared for submission to *Diabetologia*)

Other publications

Newman JMB, **Ross RM**, Rattigan S, Richards SM, Clark MG. Insulin and contraction increase nutritive blood flow in rat muscle in vivo: Determined by microdialysis of [^{14}C]-L-glucose (*The Journal of Physiology,* Accepted for publication in August 2007)

Abstracts/Posters at conferences

AMPK 2004 3rd International Symposium on AMP-activated protein kinase. Melbourne, Australia. March 2004. Steinberg GR, **Ross RM**, Carey AL, Rogers S, Richards S, Rattigan S, Kemp BE, Clark MG, Febbraio MA. Interleukin-6 increases glucose uptake but does not increase AMPK activity in L6 myotubes and perfused rat hindlimb muscle.

Diabetes and Exercise: Impact on Muscle Blood Flow. Tasmania (Freycinet), Australia. 2004. Wheatley C. **Ross RM**, Richards S, Rattigan S, Clark MG. Prior exercise-mediated recruitment may sensitize muscle to insulin.

42nd European Association for the Study of Diabetes Annual Meeting. Copenhagen, Denmark. September 2006. **Ross RM**, Rattigan, S, Clark MG. Endothelin-1 infusion *in vivo* decreases insulin clearance and causes acute muscle insulin resistance through impaired capillary perfusion.

Exercise, Insulin sensitivity and diabetes – Whats is new? International Symposium. Copenhagen, Denmark. September 2006. **Ross, RM**, Newman JMB, Richards SR, Rattigan S, Clark MG. Laser Doppler flowmetry, but not contrast enhanced ultrasound, influenced by flow when measuring changes in muscle capillary recruitment – a study *in vitro*

Exercise, Insulin sensitivity and diabetes – Whats is new? International Symposium. Copenhagen, Denmark. September 2006. Newman JMB, Clark MG, **Ross RM**, Richards SR, Rattigan S. Use of microdialysis to assess capillary recruitment in muscle – a study *in vitro*.

American College of Sports Medicine conference on the integrative physiology of exercise: Discovery and application of cardiovascular, pulmonary and metabolic science. September 2006. Clark MG, **Ross RM**, Newman JMB, Richards SR, Rattigan S. A Comparison of Ultrasound and Laser Doppler for Measuring Capillary Recruitment Using Models *in vitro*.

67th Scientific Sessions - American Diabetes Association Annual Meeting. Chicago, USA. June 2007. **Ross RM**, Wadley GD, Richards SM, Clark MG, Rattigan S, McConell GK. Local NOS Inhibition Attenuates Contraction-Mediated Muscle Glucose Uptake in Rate Hindlimb Muscle.

67th Scientific Sessions - American Diabetes Association Annual Meeting. Chicago, USA. June 2007. Bradely EA, **Ross RM,** Clark MG, McConell GK, Rattigan S. Local L-NAME administration blocks Insulin-mediated but not Contraction mediated Capillary Recruitment in Rat Hindleg Muscles.

67th Scientific Sessions - American Diabetes Association Annual Meeting. Chicago, USA. June 2007. Newman JM, **Ross RM,** Richards SM, Rattigan S, Clark MG. L-Glucose: A superior Tracer for Microdialysis Assessment of Microvascular Flow Response to Exercise or Insulin in Muscle.

Australian Diabetes Society/Australian Diabetes Educators Association Annual Scientific Meeting. Christchurch, NZ. September 2007. Yuen YC, **Ross RM,** Matthews V, Southgate RJ, Clark MG, Rattigan S, Febbraio MA. Interleukin-6 blunts the effect of Insulin on Endothelial Cell Signaling and Capillary Recruitment. (abstract submitted)

Oral presentations at conferences

Australian Conference of Science and Medicine in Sport and Third National Sporting Injury Prevention Conference. Canberra, Australia. October 2003. **Ross RM,** Dwyer D. Caffeine increases sprint performance after prolonged exercise in trained cyclists.

CHAPTER 1:

INTRODUCTION

1.1 INTRODUCTION

In Australia, there are currently 699 600 people (3.5% of the population) medically diagnosed with diabetes mellitus, 83% of these having type 2 diabetes, with an annual health cost of one billion dollars [1]. In the United States of America 7% of the population (20.6 million people) has medically diagnosed type 2 diabetes, with another 54 million people diagnosed with pre diabetes. This results in an annual expenditure in the United States of 92 billion dollars in diabetes treatment and care [2]. The World Health Organisation estimates that more than 180 million people worldwide have diabetes, 90% of which have type 2 diabetes, and this figure is expected to double by 2030 [3].

Type 2 diabetes is a chronic disease characterised by the body's inability to effectively utilise insulin [3]. Type 2 diabetes is related to other disease states such as cardiovascular disease and renal diseases, and over time may cause damage to the eyes (diabetic retinopathy), kidney (diabetic nephropathy), nerves (diabetic neuropathy), heart (resulting in poor blood circulation and possible limb amputation), as well as increasing the risk of heart disease and stroke [3]. Although traditionally known as a disease which occurs in the older population (over 45 years of age), as rates of obesity and inactivity (major risk factors for type 2 diabetes) increase, people are being diagnosed with the disease as early as adolescence [4].

Type 2 diabetes was identified as an Australian national health priority area in 1996 [1]. Research into the prevention and management of the disease is important in order to improve the quality of life and to increase life expectancy for people with type 2 diabetes.

1.2 THE DEVELOPMENT OF INSULIN RESISTANCE

Discovered in the 1920's, insulin is a 5808 Da protein which has various metabolic effects on numerous cells in the body. Undoubtedly its most important role is that of glucose metabolism and homeostasis.

Insulin resistance is defined as the failure of insulin, at relatively physiological concentrations, to exert its normal effects and results from a decrease in glucose homeostasis, hyperinsulinaemia and elevated circulating free fatty acid levels [5]. Insulin resistance develops from a progressive decrease in glucose control as insulin's ability to increase muscle glucose uptake and suppress hepatic glucose production are impaired leading to an increase in fasting plasma glucose concentrations. Impaired insulin secretion may occur concomitantly. Even so, persistent hyperglycaemia may then require the β cells of the pancreas to function at near maximal levels to maintain normoglycaemia. As β cell function declines, glucose tolerance is also diminished resulting in type 2 diabetes [6].

Insulin resistance and type 2 diabetes is associated with hypertension [7], endothelial dysfunction (associated with increased plasma concentrations of endothelin-1 and impaired nitric oxide function) [8] and increased inflammation (associated with increased levels of tumour necrosis factor -α and interleukin-6) [9]. However the condition is improved with exercise [10], suggesting that insulin and contraction regulate glucose metabolism through different pathways.

What makes insulin resistance and type 2 diabetes such a difficult disease to investigate is that there are multiple causes. Insulin resistance appears to result from a combination of factors which differ from patient to patient and depend on their level of fitness, weight, genetic predisposition and diet to name only a few. However, it is a common feature of the disease that skeletal muscle insulin resistance is a major contributor to the development of type 2 diabetes [11-13]. There are three main areas to be considered when discussing insulin mediated glucose uptake. The delivery of insulin and glucose to the site of disposal, movement across the interstitium from the vasculature to the cell and the insulin signalling cascade for glucose uptake which occurs once insulin has bound to its receptor on the cell surface [14]. This thesis focuses on factors which influence the delivery of insulin and glucose to the skeletal muscle, and how this affects glucose uptake in that tissue.

1.3 STRUCTURE OF THE MICROVASCULAR VASCULAR SYSTEM/CAPILLARY ARCHITECTURE

The connection between arteries and veins, the capillaries, were discovered in the 17th century, however their physiological behaviour had not been investigated until the 1900's. Danish scientist August Krogh demonstrated that capillaries are independently controlled units, regulated by their metabolic requirements [15]. Krough [15] showed that at rest, only a small percentage (~33%) of the capillaries are perfused, and that a small level of activity greatly increased this percentage. He demonstrated in the frog tongue that capillary dilation is not a passive process resulting from an increase in arterial pressure and that capillaries control their own level of perfusion by relaxation of the contractile elements of the capillary walls [15].

The arteries are classified according to their size and branching sequence and are important in the control of capillary perfusion [16, 17]. The first and second order arterioles are larger vessels, greater than 50 μm in diameter with corresponding venules. These larger vessels control resistance and consequently blood flow in the tissue and are termed feed arterioles [16, 18]. From these arterioles branch 3rd order transverse arterioles which run across the skeletal muscle fibres, and are not paired with a venule. They play a primary role in the control of microvascular blood flow distribution, as do the 4th order arteriole [16, 17]. The 4th order branch arterioles are approximately 25 μm in diameter, and give rise to between three and eight 5th order arterioles which may be as small as 10 μm in diameter. The 5th order inflow arterioles each control a capillary 'module' or 'unit' which are architecturally similar in nature, and consist of between 20-30 capillaries [16, 19, 20]. These capillaries run parallel to the muscle fibres for a distance of approximately 1 mm before entering the muscle fibres, each of which is perfused by at least four capillary modules [16, 20]. When capillaries are recruited, the entire module becomes perfused, not just a portion, and this is controlled by the transverse and branch arterioles from which the capillary module arises [16, 20].

The structure and number of modules can differ between muscle types and depending on the energy requirements of the tissue. Williams and Segal [18], showed differences in the soleus, a slow twitch red fibre type muscle, and the extensor digitorum longus

(EDL), a fast twitch white fibre muscle in terms of capillary perfusion. They found that the feed artery pressure was higher and that the segment length of the microvascular structure was 50% greater in the EDL than the soleus. The soleus also had a decreased extraction of oxygen at rest and didn't exhibit the same functional hyperaemia as the EDL muscle. The EDL also exhibits a greater blood flow response to exercise which correlated with greater vascular conductance demonstrating the relationship between tissue structure and function.

At rest, approximately one third of capillaries are perfused [15] and as much as 50% of total resistance to blood flow resides in the feed arterioles supplying the tissue [18]. Control of microvascular perfusion appears to be a local response, with local application of potassium, phenylephrine, acetylcholine, adenosine and halothane shown to induce vasoconstriction or vasodilation in upstream arterioles [16, 17]. Depending on the stimulus, increased perfusion is controlled by different signals. Due to its rapid nature, much research has focused on exercise induced increases in capillary flow and functional hyperaemia. It is thought that exercise increases capillary perfusion by transmitting membrane potential changes along gap junctions in the vessel walls to upstream arterioles [17]. Different mechanisms however, are responsible for insulin mediated increases in blood flow and capillary recruitment, as the increase in perfusion occurs over a longer period of time. The mechanisms leading to exercise and insulin mediated increases in capillary perfusion are discussed in section 1.5 and 1.6

1.4 MEASUREMENT OF MICROVASCULAR PERFUSION

A number of methods have been used to measure total blood flow such as venous occlusion plethysmography, radioactive microspheres, thermodilution, and positron emission topography, however measurements of capillary perfusion which are separate to total blood flow changes are more difficult to obtain. Outlined below are four methods which are used to measure microvascular blood flow.

1.4.1 1-methylxanthine metabolism

A biochemical method has been developed by Rattigan et al. [21] which measures the metabolism of exogenously added 1-methylxanthine (1-MX), a substrate for the capillary bound enzyme xanthine oxidase. Xanthine oxidase is concentrated in the capillary endothelial cells of various tissues including the heart, kidney, intestine, liver, lung and skeletal muscle, with only very small amounts found in the endothelium of larger vessels [22-24]. 1-MX is not vasoactive and is metabolised by xanthine oxidase to form a single product, 1-methylurate (1-MU). The extent of 1-MX metabolism is indicative of the capillary surface area. By determining the arterio-venous differences across the hindlimb of 1-MX metabolism to 1-MU (by high performance liquid chromatography) we are able to assess any changes in the perfused state of the microvasculature [21]. One of the limitations of this technique is that it is restricted to use in animals, as the arterial concentrations of 1-MX do not reach high enough levels without the competitive inhibition of xanthine oxidase by oxypurinol, which is not possible in humans [21, 25].

The advantage of the 1-MX method is that it measures changes in the perfusion of the microvasculature and is not affected by total flow changes. This was demonstrated by Rattigan et al. [21] when comparing a hyperinsulinemic euglycaemic clamp and epinephrine infusion *in vivo*. Insulin (10 $mU.kg^{-1}.min^{-1}$) significantly increased 1-MX metabolism, with no change in 1-MX extraction, compared to saline. This increase in microvascular perfusion was also accompanied by a concomitant increase in total blood flow. To show the dissociation between total flow and microvascular flow on 1-MX metabolism, the vasodilator epinephrine (0.125 $\mu g.min^{-1}.kg^{-1}$) was infused to simulate the total flow increase seen by insulin. Epinephrine had no effect on hindleg 1-MX metabolism compared to saline, and significantly decreased 1-MX extraction proportionate to the increase in total flow. This study demonstrated that changes in total flow will not necessarily lead to changes in microvascular perfusion and that these two parameters can be differentiated by the 1-MX method.

1.4.2 Contrast Enhanced Ultrasound

The use of contrast enhanced ultrasound (CEU) has been adapted from its application in cardiovascular imaging for use in imaging the skeletal muscle microvasculature [26, 27]. The technique involves the infusion of phospholipid or albumin microbubbles systemically into the circulation. The microbubbles are visualised by a linear array transducer (connected to an ultrasound system) positioned over the area of interest, such as the hindlimb skeletal muscle. The microbubbles are simultaneously imaged and destroyed with a pulse of high-frequency sound wave. The acoustic signal (pulse) transmitted during the destruction of these microbubbles is recorded and quantified as acoustic intensity. Once the microbubbles under the probe have been destroyed the area is replenished with microbubbles from the systemic circulation. By varying the amount of time between pulses a measure of microvascular volume may be calculated. Shorter pulsing intervals (0-1 s) are considered to be indicative of larger vessel (>100 μm in diameter) perfusion, with the longer pulsing intervals (10-20 s) allowing the greatest amount of refill, reflecting the microvascular blood volume [28]. The signal received from the larger vessels (shorter pulsing interval) is subtracted from the signal from the longer pulsing intervals to obtain a true measure of microvascular blood volume. The rate at which the capillary vessels fill may also be assessed and a measure of microvascular blood flow may be determined by multiplying the microvascular volume and microvascular fill rate.

Supporting the results obtained with the 1-MX method, CEU has also confirmed insulin's ability to increase microvascular perfusion. Zhang et al.[29] compared the 1-MX and CEU techniques during hyperinsulinemic euglycaemic clamps in rats at 1.5, 3 or 10 $mU.min^{-1}.kg^{-1}$ and showed an increase in capillary perfusion with both methods at each dose, regardless of changes in total blood flow. Dawson et al. [28] showed that insulin administration and contraction results in over a two fold increase in microvascular volume, with contraction accompanied by a five-fold increase in red blood cell velocity (insulin showed no change). Also, the calculation of microvascular blood flow showed that the increase in microvascular perfusion was greater than the changes in femoral artery blood flow [28]. These data lends support to the notion that microvascular perfusion and total blood flow are controlled separately and that this method is able to distinguish between the two [28]. This technique is

relatively non invasive in comparison to other methods, and allows multiple measurements of capillary perfusion over a time course, as opposed to the 1-MX method which is only used to obtain an end point measurement.

1.4.3 Laser Doppler flometry

Laser Doppler flometry (LDF) has been adapted for use in skeletal muscle from its origins in measuring skin microvascular flow [30]. The LDF probe is made up of optical fibre light guides that emit low power laser light into the surrounding tissue. The light is scattered by reflective components with in the tissue, and by moving components (the red blood cells) and some of this light is reflected back to the probe. This received light is processed against the light that was emitted and the Doppler shift or volume of flow in the tissue is calculated. This method is highly sensitive to movement, and also very specific to its surrounding tissue, however only changes in movement, and not exact volume measurements can be determined using LDF [30].

Serne et al. [31] used LDF to show that microcirculatory blood flow increased in the skin during hyperinsulinaemia, and de Jongh et al. [30] showed a similar result in both the skin and muscle. Clark et al. [32] showed that an increases in LDF signal correlated with increased metabolism (as shown by oxygen consumption) in the erythrocyte-perfused rat hindlimb. In this same study, the LDF signal showed increases in microvascular perfusion during a hyperinsulinemic euglycaemic clamp which preceded increases in total flow changes by 30 min [32]. However, in a separate study, Clark et al.[33] used a series of models made from polymer tubes, to show that the vessel architecture and the flow distribution within the vessels may in fact alter the LDF signal, showing that the LDF signal measures mainly non-vectorial cell speed, and not cell number.

1.4.4 Microdialysis

Microdialysis is a technique used to monitor the chemical components of the fluid in the extracellular space, and has the advantage of identifying changes in biochemical composition prior to changes in the systemic circulation. The microdialysis probe is a small, permeable thin walled tubing which is inserted in to the tissue of interest (eg.

skeletal muscle). A perfusion fluid is pumped through the microdialysis probe at a low flow rate allowing the infused solution to equilibrate with the local environment of interest. Changes of substances in the tissue surrounding the probe are reflected in the collected perfusate.

Newman et al.[34] used microdialysis to determine the interstitial concentrations of glucose and lactate during the infusion of various vasoconstrictors in the constant flow perfused rat hindlimb. They showed that increased capillary perfusion enhances the exchange of glucose and lactate by improving the supply of glucose and the removal of lactate from the interstitium. Gudbjornsdottir et al.[35] used microdialysis to demonstrate a decreased capillary perfusion in type 2 diabetic subjects which was accompanied by a decreased capillary permeability for glucose during insulin infusion, resulting in a low level of passage for glucose and insulin across the interstitial space.

1.5 THE HAEMODYNAMIC EFFECTS OF INSULIN

1.5.1 Insulin and macrovascular blood flow

Type 2 diabetes patients experience a number of problems related to blood flow that include hypertension, heart disease (stroke, angina, oedema, ischaemic heart disease), peripheral vascular disease and other circulatory disorders [1]. It is thought that insulin's ability to increase blood flow is an important mediator of its ability to increase glucose uptake, particularly in the skeletal muscle which makes up 40% of the weight of man, and is responsible for over 85% of glucose disposal during hyperinsulinaemic euglycaemia [11].

Insulin's haemodynamic effects were first realised in 1939 when Abramson and colleagues [36] found that very high doses of insulin (40-280 units) caused increases in blood flow (measured by plethysmographic method) in the human forearm, hand and leg in patients with schizophrenia. They found that insulin increased blood flow up to 8 times the basal flow rate, and that the administration of glucose (without insulin) also leads to a transient increase in blood flow. Since this time, there have been many studies assessing insulin's impact on total blood flow using various techniques,

undertaken in animals [29, 37-41] and humans [42-50] with mixed results. Liang and colleagues [37] found femoral blood flow (measured by radioactive microspheres) doubled after insulin (4 or 8 $mU.kg^{-1}.min^{-1}$) administration in the canine. Baron and Brechtel [43] showed a 60% increase in leg blood flow (measured by thermodilution method) where systemic insulin reached 212 $pmol.l^{-1}$, and Tack et al. [50] showed a ~124 ± 51% increase in forearm blood flow (measured by venous occlusion plethysmography) during local insulin infusion into the brachial artery where forearm insulin concentrations reached ~540 $pmol.l^{-1}$. In contrast, Yki-Jarvinen and colleagues [48] found that insulin at an average systemic level of 61 $\mu U.ml^{-1}$, with or without glucose infusion, had no effect on the rate of blood flow (measured by capacitance plethysmography) across the forearm. Using the same technique to measure blood flow, Ebeling et al. [46] also found no increase in forearm blood flow using low dose insulin infusion (1.5 $mU.kg^{-1}.min^{-1}$) in both trained athletes and sedentary subjects.

Under the more physiological conditions of a mixed meal, Høst et al. [51] found forearm blood flow increased after a high carbohydrate and protein meal while Fugmann and colleagues [52] found that both a normoglycaemic hyperinsulinaemic clamp and a mixed meal similarly increased calf blood flow (measured by venous occlusion plethysmography). The vasodilatation induced by the mixed meal however, was greater than during hyperinsulinaemia, even though insulin levels were lower. The author suggested that muscle nerve sympathetic activity and haemodynamic changes are stimulated by insulin, however the mechanisms involved in digestion, as apposed to a superficial insulin infusion, may play a role in increasing blood flow [52].

Insulin's effect on flow is still a controversial area, with the discrepancies in data being attributed to insulin dose, the method of administration and the length of time the subject is exposed to insulin [53], factors which have been shown to be the main determinants of insulin's effect on blood low. Regardless of the controversy surrounding insulin and total blood flow, it was suggested by Baron [54], and confirmed by subsequent studies [21, 28, 29, 55, 56], that the effect of insulin to increase total blood flow and the effect of insulin to increase microvascular perfusion (principally in the muscle) are two separate and unrelated events. The structure of the arteriole and capillary network (described in section 1.3) help to demonstrate that the

capillary perfusion is not necessarily controlled by changes in total flow and mean arterial pressure.

1.5.2 Insulin and microvascular blood flow

Rattigan et al. [21] demonstrated that there are alternate blood flow routes in muscle, and that an increase in total flow alone will not lead to an increase in glucose uptake. *In vivo* experiments were performed, using a 10 $mU.min^{-1}.kg^{-1}$ hyperinsulinemic euglycaemic clamp in the rat, which increased femoral blood flow (measured by a Transonic™ flow probe) by 80%. Insulin increased 1-MX metabolism (described in section 1.4.1) by 50% over basal showing an increase in capillary perfusion, which was also accompanied by an increase in glucose uptake. The infusion of epinephrine was used as a control, and the dose was matched to cause a similar increase in femoral blood flow to that caused by insulin. Epinephrine did not increase 1-MX metabolism above basal, and did not lead to an increased glucose uptake, demonstrating that increased microvascular perfusion and not total flow, is important for insulin mediated glucose uptake. This was further supported by work from Zhang et al. [29] and Vincent et al. [56] who showed insulin ability to increase microvascular perfusion occurred prior to its effects on glucose uptake and total flow. Using the 1-MX method and contrast enhanced ultrasound to measure microvascular perfusion Zhang and colleagues [29] showed that increases in capillary perfusion occurred at very low doses of insulin (1 $mU.min^{-1}.kg^{-1}$) in the absence of a total blood flow increase and without an increase in glucose uptake. Glucose uptake increased in a dose dependent fashion (from 1 to 10 $mU.min^{-1}.kg^{-1}$), however microvascular recruitment appeared to be maximal at 1 $mU.min^{-1}.kg^{-1}$. In this study, the microvascular recruitment was reversed by 30 min post-insulin infusion. Using contrast enhanced ultrasound, Vincent and colleagues [56] demonstrated that insulin recruited capillaries within 5-10 min of its infusion, preceding both activation of the insulin signalling pathways and increased glucose uptake.

These data may explain the discrepancies regarding total flow changes between studies, as insulin may act to increase microvascular perfusion (particularly at low doses such as during the studies of Ebeling et al.[46] and Yki-Jarvinen [48]) and glucose uptake, but may not increase total flow.

1.6 THE HAEMODYNAMIC EFFECTS OF EXERCISE

1.6.1 Exercise mechanisms to increase microvascular flow

Exercise, even small amounts, rapidly increases blood flow and microvascular perfusion in the working muscles [57-59]. This appears to be a local response, as contraction of a just a single muscle fibre or multiple fibres, will result only in vasodilation of the vessel region which is overlying the active portion of muscle [60]. The exact mechanism of how this phenomenon occurs so rapidly (less than 2 s) is still largely unknown, however the speed at which the initial response occurs suggests that the mechanism occurs too slowly to be due to conduction in the nerve fibres and too rapidly to be due to a vasodilator substance [61]. This is not to say that vasodilation is not maintained by these factors, however the initial response is thought to be produced by the capillaries themselves and then propagated via gap junctions centrally located in the vessel wall, in to the larger arterioles resulting in vasodilation [16, 17, 59, 61].

Vasodilation in response to exercise contains three components [60, 62]. Firstly, the initial lag time between the start of contraction and the initial increase in vessel diameter, which may be representative of the initial signal from the capillaries via the vessel wall. Secondly, the early (and sometimes transient) peak and increase in arteriolar diameter, and thirdly the slow increase in arteriolar diameter which attains steady state in 80-100 s [60, 62]. These later phases may be mediated by vasodilator substances such as nitric oxide, prostaglandins, acetylcholine or adenosine [63]. Wunsch et al. [57] assessed this issue in primary arterioles isolated from the soleus and gastrocnemius muscles of Sprague-Dawley rats, which were perfused with various concentrations of adenosine, potassium, acetylcholine or the nitric oxide donor sodium nitroprusside. All of these substances caused the arteriole to vasodilate, but this effect took over 4 s to occur. This time frame is too slow to be responsible for the initial hyperaemia caused by exercise, but these substances may be involved in maintaining microvascular perfusion throughout exercise. That particular study was undertaken in primary arterioles, however the vasodilitary response is propagated upstream from the terminal arterioles, therefore the time taken for vasodilation to occur in this study may be different to the time taken for the signal to arise in the terminal arterioles and be propagated upstream.

The increase in blood flow is also mediated by metabolism and it has been shown that the metabolic needs of the muscle, such as oxygen consumption, are tightly correlated with blood flow [64, 65]. At rest, blood flow to the muscles is directly related to the percentage of slow-twitch oxidative fibres in the muscle. During exercise, while blood flow increases to most working muscles, the increase is proportional to the percentage of fast twitch high oxidative fibres in the muscle [66] and is dependent on the exercise intensity [67].

1.6.1.1 The muscle pump

There is the possibility that this initial increase in blood flow during exercise is due to mechanical stimulation of the contracting muscle. Tschakovsky et al.[68] showed that the muscle pump is responsible for 45% of the initial rise in blood flow during muscular contraction of the hand. Similarly, Radegran and Saltin [62] found a single passive leg movement increased blood flow by ~50%, however blood flow was further increased during voluntary contraction. These authors showed the initial increase in blood flow is most rapid during the first phase of exercise (0-4 s) and is facilitated by the muscle pump, with a more potent vasodilitary phase occurring at ~4 s which may be substance mediated. The later phases of blood flow increased with greater exercise intensities [62]. These two studies show that the muscle pump is involved in the initial rise in blood flow initiated by exercise, however it only accounts for half the flow response. There are a number of mechanisms both metabolic and neural which may, alone or in combination, account for exercise-induced hyperaemia.

1.6.1.2 Potassium ions

Potassium ions (K^+) are released into the interstitium via voltage dependent K^+ channels as the muscle cell repolarises during muscle contraction. The mechanism by which K^+ causes vasodilation still requires further investigation, but may result from the increased activity of the Na^+-K^+ pump [69] and activation of K^+ (K_{IR}) channels [70]. K^+ rapidly accumulates in the interstitium following contraction and decreases rapidly during recovery [71] with the increased concentrations proportional to the intensity of the exercise bout [72]. In support of K^+ involvement in the exercise hyperaemia

response is that the time course of K^+ release in to the venous blood follows changes in blood flow in response to exercise [73]. However, although the infusion of K^+ into the femoral artery at rest increases leg blood flow in a dose dependent manner, the magnitude of the increase (0.39 ± 0.06 to 0.71 ± 0.17 $l.min^{-1}$) suggests that K^+ only accounts for a small portion, if any, of reactive hyperaemia [72].

1.6.1.3 Adenosine

Adenosine is formed via AMP derived from the hydrolysis of ATP and its levels are increased during hypoxia or times of increased oxygen consumption and metabolism, such as during exercise. Adenosine may be released from both the muscle and the endothelial cells and readily diffuses from the intracellular compartment into the interstitium and leads to vasodilation by a number of mechanisms including binding to adenosine receptors producing vasodilation via adenylate cyclase, nitric oxide and cyclic GMP [57].

A bolus injection of adenosine increases femoral blood flow at rest mimicking the hyperaemic response seen during exercise [74, 75], while adenosine receptor blockade causes a 20% decrease in femoral blood flow and vascular conductance during knee extensor exercise [75]. Similarly, Ballard et al. [76], calculated that adenosine contributed approximately 15% to total vasodilation after 1 min of exercise in the canine, which rose to 40% between 5 and 20 min of contraction. This suggests that adenosine may play a role in maintaining perfusion but may only contribute to the initial blood flow response, and given the pathways involved this response may involve nitric oxide (the effects of nitric oxide are discussed in section 1.9).

1.6.1.4 Acetylcholine

Acetylcholine may play a role in the ascending vasodilation seen during exercise, and along with the sheer stress of muscle contraction, it may also act to stimulate the release of nitric oxide from the endothelial cells [77]. Acetylcholine is released from the motor nerve terminals and binds to nicotinic receptors triggering fibre contraction. It is rapidly cleared from the synaptic cleft by cholinesterase and neurotransmitter diffusion promoting muscle fibre relaxation. Acetylcholine is also in close enough proximity to activate muscarinic receptors and trigger vasodilation in capillaries [64].

Application of acetylcholine to isolated feed arteries results in hyperpolarisation at the site of application, and conduction of the signal along the endothelium contributing to ascending vasodilation. The same response was seen during muscle contraction [64, 78], and the ascending response was blocked by causing endothelial damage. This response was confined to a central segment of the arteries, resulting in acetylcholine or contraction causing vasodilation distal to the damaged segment, however the propagation of the signal could pass through the damaged region. This shows that exercise hyperaemia is not caused by flow induced vasodilation, but conduction of the signal along the endothelium [78]. A cholinesterase inhibition doubles the vasodilitary response to exercise, while muscarinic receptor antagonism with atropine inhibits vasodilation by 65% in feed arteries and reduces functional hyperaemia by 50% [64]. Such studies suggest a role for acetylcholine in hyperaemia due to exercise via co-activation of muscarinic receptors and increased conduction into the feed arteries.

1.6.1.5 Prostacyclin

The vasodilators prostaglandin and prostacyclin are produced from the conversion of arachidonic acid by cyclooxygenase enzymes and released from the endothelial cells. The concentration of arachidonic acid is increased by enhanced intracellular calcium levels, such as those seen during exercise and induced in shear stress. Prostaglandin and prostacyclin act on receptors on the nearby smooth muscle cells which lead to the activation of adenylate cyclase resulting in a decrease in the smooth muscle cell calcium levels and vasodilation [58].

There are mixed results concerning the role of prostaglandins in the hyperaemic response to exercise. Wilson and Kapoor [79] showed that inhibition of prostaglandin release at rest and during wrist flexion exercise decreased forearm blood flow. In contrast, Shoemaker et al. [80] showed that inhibition of prostagladins had no effect on the time course of, or the magnitude of, forearm blood flow during handgrip exercise. Interestingly, Schrage et al. [81] found that while nitric oxide inhibition decreased femoral blood flow, prostaglandin inhibition only caused a transient decrease in blood flow. These data suggest that while prostaglandins may be involved in the

vasodilitary response, their contribution is minimal and may be compensated for by other vasodilitary factors.

While a number of factors have been shown to affect the initial increase in blood flow seen at the onset of exercise, none has been found to be solely responsible for this effect. Therefore it is likely that this initial effect is due to a number of different mechanisms involving both mechanical and neural input and this response may then be sustained by a separate set of vasodilitary factors.

1.7 INSULIN RESISTANCE AND MICROVASCULAR FLOW IN RESPONSE TO EXERCISE OR INSULIN INFUSION

The ability of insulin to increase perfusion is blunted in diabetics and models of insulin resistance [41, 44, 82]. The obese Zucker (*fa/fa*) rat is a commonly used model of insulin resistance, and is characterised by insulin resistant muscle [83], hyperinsulinaemia [41], dislipidaemia [84], elevated plasma endothelin-1 levels [85] and hypertension [86]. Wallis and colleagues [41] showed the differences in response to exercise and insulin by performing a 2 h, 20 $mU.min^{-1}.kg^{-1}$ clamp on obese Zucker rats and their lean litter mates. The lean rats showed an increase in femoral blood flow, muscle glucose uptake, glucose infusion rate and capillary perfusion. In comparison, the obese Zucker rat showed only a small increase in glucose infusion rate (7.7 ± 1.4 versus 22.2 ± 1.1 $mg.min^{-1}.kg^{-1}$ in the lean rat), and no increase in femoral blood flow or muscle glucose uptake. Above all, capillary perfusion was 2.6-fold greater in the lean rat compared to the obese rat, demonstrating the obese Zucker rat has an impairment in its insulin mediated haemodynamic response to insulin. In contrast, the contraction mediated haemodynamic response was still apparent, as the Zucker rat shows near normal increases in femoral blood flow, glucose uptake and capillary perfusion in response to electrical stimulation for one hour [87] Others showed an improved vascular function after a five week treadmill exercise protocol [84].

The inflammatory cytokine tumour necrosis factor (TNF)-α is often increased in states of insulin resistance and type 2 diabetes [88-90]. In incubated soleus and epitrochlearis muscle preparations 45 min of exposure to TNF-α had no effect on insulin stimulated

tyrosine phosphorylation of the insulin receptor, insulin receptor substrate (IRS)-1 or phosphoinositide-3 kinase (PI3-Kinase) associated IRS-1[91], unlike preparations involving heptoma cells [92], adipocytes [93] and fibroblasts [94] which show a decreased signalling response to insulin with TNF-α incubation. TNF-α in muscle incubation also had no effect on insulin stimulated 2-deoxyglucose uptake [91]. The infusion of TNF-α *in vivo* however abolishes insulin mediated increases in bulk flow and microvascular perfusion [95] as well as decreasing glucose uptake by 50-70% [95, 96], suggesting TNF-α causes insulin resistance by decreasing insulin mediated haemodynamics *in vivo*. In contrast, TNF-α infusion during contraction *in vivo* had no effect on haemodynamic parameters or glucose metabolism [97].

The haemodynamic and glucose uptake response to insulin infusion in type 2 diabetic patients, as would be expected, is blunted as type 2 diabetic and obese patient have impaired skeletal muscle blood flow response [44, 98, 99]. In addition, translocation of glucose transporter type 4 (GLUT4) protein to the plasma membrane is decreased and this is accompanied by an attenuation of glucose transport. [100]. During exercise however, type 2 diabetic patients have a normal response to exercise, with no difference in GLUT4 translocation when compared to control subjects [101].

1.8 INSULIN SENSITISATION AND SIGNALLING POST EXERCISE

Exercise training causes changes in gene and protein expression and fuel utilisation, in addition to its well known beneficial effects on insulin sensitivity [102]. However studies in both animals [103-105] and humans [106-108] show an increased in insulin sensitivity after only a single bout of exercise. The time period of increased insulin sensitivity varies depending on the type and intensity of exercise, however Mikines et al. [109] have shown that insulin sensitivity may be improved up to 48 h after a single cycling exercise bout. Immediately after exercise however, insulin sensitivity may be impaired before a sensitisation effect is seen, possibly due to an increase in the circulating levels of free fatty acids, catecholamines, intracellular glucose metabolites, and inflammatory cytokines [110]. Furthermore, eccentric exercise, known to cause muscle damage, increases this time period due to an increase in the release of inflammatory factors known to cause insulin resistance. For example, Del Agulia et

al. [111] showed that an insulin resistant state persistent 24 h after downhill running (eccentric exercise). This decrease in insulin mediated glucose uptake was associated with a decrease in IRS-1 phosphorylation, decreased activation of PI3-kinase and Akt, as well as increased levels of TNF-α.

The first study to recognise this post exercise sensitisation effect were Richter et al. [112] who found that after 45 min of treadmill running in rats, glucose utilisation was increased and the concentration of insulin required to maximally stimulate glucose uptake was decreased. This effect lasted 4 h (but was not present at 24 h) with exercise also enhancing insulin's ability to incorporate glucose into glycogen. Increased insulin sensitisation post exercise is thought to increase in two phases. Firstly, by increasing non-insulin stimulated and insulin stimulated glucose uptake in order to replenish glycogen stores. Secondly, once glycogen levels are restored, there is an increased insulin sensitivity, which may account for the super-compensation of glycogen stores seen post exercise [113]. Muscle glycogen content has an effect on both insulin sensitivity and GLUT4 translocation post exercise and both exercise and insulin mediated increase in glucose transport is proportional to increases in GLUT4 protein expression [114-116]. GLUT4 mRNA and protein levels are increased over 2-fold 16 h post-exercise. A high carbohydrate diet results in GLUT4 mRNA and protein levels returning to baseline levels within 42 h, however a carbohydrate free diet results in elevated GLUT4 protein levels up to 66 h post exercise [117, 118]. Also, treatment with insulin immediately after exercise results in greater glycogen accumulation (over a 3 h period) and GLUT4 content than exercise controls without insulin [115]. Interestingly, Chou et al. [119] found an increase in GLUT 4 protein levels and a concurrent increase in muscle glycogen stores in rats 16 h post exercise. If insulin was injected immediately following exercise, there was a further increase in muscle glycogen content compared to the control rats, however the increase in GLUT4 protein and whole body glucose tolerance was attenuated. In a similar fashion to the activation of AMP activated protein kinase (AMPK) in response to a decrease in energy stores, there may be a negative feedback mechanism in place to help regulate muscle glucose uptake and glycogen storage to ensure energy stores are fully replenished after exercise. The attenuation of GLUT4 may also act as a protective mechanism in order to inhibit the possibility of insulin resistance caused by hyperglycaemia or glucose toxicity due to a rapid influx of glucose in to the cell and

increased activation of the hexosamine pathway [120]. An inverse relationship between glycogen content and glucose transport has been shown and although GLUT4 protein may initially regulate insulin mediated glucose uptake post exercise, the glycogen content of the muscle will determine the degree of insulin sensitivity and glucose uptake [121, 122].

Increased insulin sensitivity in response to exercise occurs mainly in the working muscle and independent of changes in insulin signalling. In humans, prior exercise had no effect on insulin induced receptor tyrosine kinase, serine phosphorylation of Akt, serine phosphorylation of glycogen synthase kinase (GSK) or GSK-3 activity [123]. Similarly in rodents, prior exercise decreases the effect of insulin on the insulin receptor and IRS-1 phosphorylation by ~25%, as well as decreasing IRS-1 associated PI3-kinase activity [124]. Furthermore, muscle specific insulin receptor knockout mouse has normal glucose uptake at rest and during exercise, with no response to insulin stimulation. Yet, when insulin is administered post exercise there is a synergistic effect on glucose uptake which occurs without increasing insulin receptor tyrosine phosphorylation or PI3-kinase activity [125]. Prior exercise does however increase insulin stimulated IRS-2 associated PI3-kinase activity in humans [126], and a study in IRS-2 deficient mice showed that while post-exercise, insulin stimulated phosphotyrosine associated PI3-kinase activity was attenuated, there was still a small increase in phosphotyrosine associated PI3-kinase activity [104]. This presents the possibility that there is another tyrosine phosphoprotein which is able to activate PI3-kinase in response to insulin post-exercise.

In recent times, Akt substrate of 160 kDA (AS160) has emerged as a signalling molecule phosphorylated by both insulin and exercise. AS160 is a Rab GTPase activating protein and is the most distal signalling event linked to GLUT4 translocation found to date [127, 128]. Insulin signalling leads to the activation of Akt via PI3-kinase dependent mechanisms. AS160 is an Akt substrate , which contains a GTPase activating protein domain and its phosphorylation inhibits GAP activity, leading to formation of GTP or Rab proteins causing GLUT4 translocation [129]. Insulin stimulation has been shown to phosphorylate AS160 in both adipocytes [130] and skeletal muscle [128, 131] with this affect inhibited by wortmanin treatment *in vitro* [131], and in the Akt2 knockout mouse *in vivo* [128], suggesting insulin mediated

phosphorylation of AS160 is dependent on Akt activation. Interestingly, type 2 diabetic patients have a 39% decrease in AS160 phosphorylation in response to insulin stimulation compared to control subject. This is accompanied by a 51% decrease in Akt Thr^{308} phosphorylation, however Akt Ser^{473} phosphorylation is not affected [132]. These data suggest that GLUT4 translocation is impaired in type 2 diabetic patients due to a defect in the phosphorylation of Akt Thr^{308} and AS160. However, contraction stimulated phosphorylation of AS160 is still functional in the diabetic state as sciatic nerve stimulation in the obese Zucker rat increased glucose uptake without a change in the activation of IR, IRS-1 or Akt, but with an increase the phosphorylation of AS160 [133].

Contraction mediated phosphorylation of AS160 is mediated through separate mechanisms to insulin as PI3-kinase inhibition only partially blocked AS160 phosphorylation in skeletal muscle and was unaffected in the Akt2 knockout mouse [128]. AMPK has been shown to have a positive correlation with AS160 during exercise with both compounds phosphorylated to a greater extent in longer duration higher intensity exercise [134, 135]. AICAR and contraction phosphorylate AS160 in skeletal muscle, and this response is blunted in AMPK α2 knockout mice [136]. The combination of PI3-kinase inhibition in an AMPK α2 inactive mouse however only partially inhibited contraction mediated phosphorylation of AS160 [128] suggesting there are additional regulatory mechanisms involved in contraction mediated control of this process. It is possible that AS160 may be involved in post-exercise insulin sensitisation as Arias et al. [105] showed that AS160 phosphorylation was positively correlated with insulin independent glucose transport immediately post-exercise, and the increase in AS160 phosphorylation was still evident 4 h post-exercise. Further research is required to confirm the involvement of this substrate and to further elucidate the mechanisms through which the muscle is sensitised to insulin after exercise.

As discussed previously, insulin and exercise both have positive effects on microvascular perfusion. It may be that microvascular perfusion remains slightly elevated for a period of time post exercise, increasing the surface area and delivery of nutrients to the muscle. Alternatively, previous exercise may help to sensitise the vasculature to the insulin action, decreasing the time, or increasing the efficiency by

which insulin increases perfusion, leading to an increase in glucose metabolism. At the present time, the reversal of microvascular perfusion after exercise has not been assessed. Despite the vast amount of literature addressing post exercise sensitisation, the mechanisms and pathways by which insulin and exercise increase and regulate GLUT4 translocation and glucose uptake still require further investigation. Furthermore, the interactions between the two stimuli also warrant additional research to increase our understanding of glucose regulation and to elucidate possible therapeutic targets for the treatment of diabetes.

1.9 MEDIATORS OF MICROVASCULAR PERFUSION: NITRIC OXIDE

Nitric oxide (NO) is a small, uncharged molecule which may easily diffuse into tissues resulting in both autocrine and paracrine effects. Nitric oxide production from the conversion of L-arginine to citrulline, is stimulated by a variety of factors including insulin, acetylcholine, bradykinin and shear stress [and] results in endothelium dependent vasodilation. The reaction is catalysed by nitric oxide synthase (NOS), using molecular oxygen and NADPH as co-substrates, and eventually results in un-reactive nitrite and nitrate accumulating in the biological system which can be used as a quantitative measure of nitric oxide synthesis [(137)]. There are three separate forms of NOS which may be involved in nitric oxide production, inducible NOS (iNOS) which is located in the macrophages and induces nitric oxide formation in inflammatory cells, endothelial NOS (eNOS) found predominantly in the blood vessels and neuronal NOS (nNOS) found in the neural tissue [(138)].

Skeletal muscles expresses both eNOS, and nNOS (mainly in fast-twitch fibre type) which play a role in regulating vascular tone through continuous production of nitric oxide [(137)]. The production and release of nitric oxide by nNOS and eNOS activation may be activated by a number of different mechanisms including stimulation by calcium release from the sarcoplasmic reticulum during exercise. Nitric oxide release not only leads to vasodilation but also increases skeletal muscle glucose uptake via calcium calmodulin-dependent protein kinase (CaMK) and/or Protein Kinase C (PKC), however the precise mechanisms are still to be elucidated [(139)]. It has been recently discovered that eNOS may be phosphorylated and activated by Akt [(140)]

suggesting possible stimulation by insulin via this route. Nitric oxide may also bind to haemoglobin as S-nitroheamoglobin which is released in response to hypoxia suggesting a link between nitric oxide and skeletal muscle metabolism [141, 142], or may also act via a second messenger by activating soluble guanylate cyclase in the vascular tissue leading to an increase in cyclic GMP levels resulting in vasodilation [58, 137].

As explained in Section 1.6.1, it is unlikely that nitric oxide is involved in the initial recruitment of capillaries in response to exercise, as its release and subsequent actions occur too slowly to account for this effect. However, nitric oxide may be involved in maintaining the pattern of increased microvascular perfusion during exercise and at rest. The recruitment of capillaries by insulin occurs over a longer time period than during exercise and is thought to be nitric oxide dependent. Therefore the mechanisms which initiate the increase in microvascular perfusion are different, however the maintenance of this perfusion may be similar between the two stimuli.

1.9.1 Nitric oxide and exercise mediated microvascular recruitment

Exercise training results in the up-regulation of eNOS and nNOS [143] and increased nitric oxide production [144]. It also results in the vascular smooth muscle endothelium becoming more responsive to nitric oxide stimulation due to contraction enhancing endothelial nitric oxide formation and its release into the extracellular space [58, 144]. Both acute exercise [145] and endurance training lead to increased eNOS and nNOS protein and expression [146, 147].

Pharmacological inhibition of NOS has no effect on the initial rise in femoral blood flow during exercise, but does affect blood flow at rest and during recovery from exercise [77, 148]. Bradley et al. [149] showed that NOS inhibition had no effect on leg blood flow during cycling exercise, but did result in a 40-50% decrease in leg glucose uptake compared with the saline infused control subjects. Furthermore, co-infusion of L-arginine (resulting in increased nitric oxide) restored glucose uptake during NOS inhibition. A similar result was also seen by McConell et al. [150] where L-arginine infusion during cycling resulted in increased glucose clearance rate. In a follow up study, Kingwell et al. [151] found the infusion of NOS inhibitor N^G-monomethyl-L-

arginine (L-NMMA) had no effect on leg blood flow, but reduced leg glucose uptake by 34 ± 14% in normal controls and this effect was even greater in type 2 diabetic patients whose glucose uptake decreased by 75 ± 13%. This study suggests that type 2 diabetic patients rely on nitric oxide during exercise to increase glucose uptake to a greater extent than control subjects and shows that nitric oxide is involved in exercise mediated glucose uptake. However, non of the above studies involved an assessment of microvascular perfusion, which may have impacted on glucose uptake

In animal models, data relating NOS inhibition to exercise mediated perfusion and glucose uptake is both for and against. In rats Roberts et al.[152] found NOS inhibition resulted in complete blockade in glucose transport stimulation during treadmill running, which is consistent with a muscle effect of nitric oxide reported by Balon et al.[143]. These authors found NOS inhibition reduced both basal and exercise stimulated (but not insulin stimulated) glucose uptake in incubated rat extensor digitorum longus muscles. They also reported a stimulatory effect of sodium nitroprusside (a nitric oxide donor) which increased glucose uptake in a dose dependent manner. Higaki et al.[153] also found that sodium nitroprusside had an additive effect on glucose uptake in combination with both insulin and exercise stimulation in incubated muscle, but NOS inhibition however, had no effect on exercise stimulated glucose uptake in incubated epitrochlearis muscle [153, 154]. It may be speculated that the decreased glucose uptake seen *in vivo* may be due to the haemodynamic aspects of nitric oxide which are absent in incubated muscle, however a study in the conscious mouse model, where the vascular effects of NOS may be seen has shown that N^G-nitro-L-arginine methyl ester (L-NAME) infusion had no effect on exercise mediated fatty acid and glucose uptake. In that study, however blood flow was not measured and the L-NAME, a specific inhibitor of nitric oxide synthase, was delivered in the drinking water which may not increase circulating levels to a high enough concentration to block NOS as is seen in other studies using intravenous infusion [155]. In support of this theory are studies from Hirai et al. [156] and Musch et al. [157] who found NOS inhibition reduced vascular conductance [157] and decreased blood flow to the hindlimb muscles, as well as decreasing blood flow to the kidneys and organs of the gut during treadmill exercise in rats [156]. Hirai, et al. [156] also found that the inhibition of NOS and consequent reduction in blood flow which was greatest in the red muscle fibres. Unfortunately glucose uptake was not measured in these

studies and the systemic L-NAME treatment caused an increase in mean arterial pressure which may have affected the pattern of blood flow. Furthermore, as previously discussed changes in bulk flow can be independent of changes in microvascular perfusion, which may play a critical role in control of glucose uptake [53] and therefore the effects of NOS inhibition on glucose uptake and muscle perfusion requires further investigation.

Some of the discrepancies in the data may be due to two factors. Firstly, the delivery of NOS inhibitor (systemic or local), and the inhibitor used. For example, when infused locally L-NAME does not affect mean arterial pressure however, systemically, L-NAME may affect mean arterial pressure and heart rate, which may disrupt blood flow resulting in effects on both macrovascular flow and microvascular perfusion. Secondly, the method of measuring flow may cause confusion, and result in inaccurate or delayed measurements. For example, venous occlusion plethysmography requires exercise to cease during measurement, therefore flow is measured during recovery from exercise and not *during* exercise, therefore the decreased flow reported may be due to the effect NOS inhibition on recovery from exercise. In addition, these studies assess total flow which may not be representative of the changes in microvascular perfusion. Discrepancies between human and animal data may result from the different distribution of NOS protein expression in the different species [139].

1.9.2 Nitric oxide and insulin mediated microvascular recruitment

There are many studies showing that stimulations of nitric oxide release accounts for the vascular actions of insulin. Insulin simulated nitric oxide production in the heart, liver, kidney, muscle and endothelial cells *in vitro* increases in a rapid and dose dependent manner. This response is blocked by L-NAME [158-160] and is also prevented by PI3-Kinase inhibitor, wortmanin [159, 160]. Furthermore, activation of PDGF (a growth factor that signals through the tyrosine kinase receptor) dose not increase nitric oxide production suggesting an insulin specific signalling cascade is required [159] and in particularly, IRS-1 and PDK-1 are essential in the insulin signalling activation of eNOS [161].

In conscious humans, Steinberg et al.[162] showed that endothelium derived nitric oxide was responsible for 20% of basal leg blood flow and 40% of insulin mediated increases in leg blood flow during L-NMMA infusion into the femoral artery. Also in humans, Scherrer et al.[163] infused L-NMMA into the brachial artery 60 min prior to, and at the end of a 2h hyperinsulinemic clamp. L-NMMA infusion prior to the clamp caused a prolonged effect and decreased forearm blood flow during insulin infusion, preventing insulin induced vasodilation in both arms throughout the clamp. This resulted in an increased arterial pressure, however the glucose uptake remained unaltered, which may be due to L-NMMA being infused prior to the clamp and not as a co-infusion. In animal studies, Vincent et al. [56, 164] showed that the increase in both femoral blood flow and microvascular perfusion caused by insulin was blocked, and glucose uptake partially inhibited, by administering L-NAME. Roy et al. [165] also found glucose uptake to be inhibited *in vivo* and found that L-NAME failed to affect basal or insulin-stimulated glucose transport in isolated muscles. Such studies confirm a role for nitric oxide in insulin mediated glucose uptake which is possibly mediated by changes in microvascular perfusion.

1.9.3 Nitric Oxide and insulin resistance

Type 2 diabetes is associated with impaired NOS activity in skeletal muscle [166, 167]. Kashyap et al.[166] showed that although type 2 diabetes patients have the same NOS protein content (at basal and during insulin stimulation) as non-diabetic control subjects, their basal and insulin stimulated NOS activity is significantly decreased. Furthermore, the defect in insulin stimulated NOS activity closely correlated with the severity of the patient's insulin resistance. Similarly, eNOS content and total eNOS activity in skeletal muscle of obese women was significantly lower than lean women, and inversely related to percentage body fat and body mass index [168].

The Zucker obese fatty rat (a model of insulin resistance) has decreased eNOS expression and total NOS activity in microvessels [160], and skeletal muscle tissue [169] in comparison to its lean litter mates. Incubation of the soleus muscle from these rats with zaprinest (a selective cGMP phosphodiesterase inhibitor) increased cGMP levels and glucose uptake in the lean but not the obese rat. Incubation with sodium nitroprusside meanwhile, increased glucose uptake in both the lean and obese rats,

however this response was significantly less in the obese rats [169]. Similar results were also found in regard to insulin stimulation of vascular endothelial growth factor which was further stimulated by a cGMP analogue, with a blunted response in the obese rats [167]. Incubation of endothelial cells from the obese rat had a decreased insulin stimulated eNOS gene expression compared to its lean counterparts. Furthermore, incubation with PKC inhibitors enhanced eNOS expression, while PKC activators inhibited both insulin stimulated PI3-kinase and eNOS mRNA [160]. Such studies suggest a problem with the NO/cGMP signalling pathway in the insulin resistant state leading to abnormal glucose utilisation. This may occur due to hyperglycaemia, insulin resistance, and/or the activation of PKC [170] inducing inhibition of the PI3-Kinase activities in the vasculature, blunting insulin stimulated eNOS expression and decreasing insulin's effects on vasodilation [160].

In other animal models, eNOS knockout mice become insulin resistant in both the liver (showing an inability to suppress insulin stimulated endogenous glucose output) and peripheral tissues, whereas nNOS knockout mice only developed insulin resistance in the peripheral tissues [138]. Also, eNOS deficient mice have been shown to develop hypertension, hyperinsulinaemia, hyperlipidaemia and they have a 40% decrease in insulin stimulated glucose uptake as well as a 40% decrease in hindlimb muscle blood flow (measured by a laser Doppler probe) [171]. Also, both eNOS and nNOS knockout mice characteristically have hypertension and altered basal vascular tone [172, 173]. To further illustrate this problem, shear stress induced and flow dependent vasodilation mediated by nitric oxide is significantly blunted in hypertensive rats [174, 175] while intracerebroventricular (ICV) infusion of a NOS inhibitor results in hypertension and a state of insulin resistance by increasing basal glucose concentrations and decreasing insulin mediated glucose disposal [176]. These studies show the relationship of NOS in glucose and lipid metabolism as well as blood pressure and vascular dysfunction, which are both related to insulin resistance [177].

Nitric oxide therefore plays a role in insulin resistance possibly by either direct affects on muscle glucose uptake and/or through its modification of microvascular blood flow via a role in endothelial dysfunction, where it acts to regulate vascular tone in conjunction with endothelin through a balance of vasodilation and vasoconstriction.

1.10 MEDIATORS OF MICROVASCULAR PERFUSION: ENDOTHELIN-1

Endothelin-1 (ET-1) is synthesised by the endothelium and is the most potent of a family of three vasoactive peptides (ET-1, ET-2, ET-3) [178]. These 21 amino acid long endothelins are involved in vasomotor tone, cell proliferation and hormone production, however ET-1 is the only isoform released from the vascular endothelial cells [179]. Its release is stimulated by a number of factors including insulin, shear stress, hypoxia, growth factors, angiotensin II and catecholamines, and it is secreted abluminally to act on receptors located on the vascular endothelial or smooth muscle cells [179]. Even though ET-1 is cleared rapidly from circulation by the pulmonary, splanchnic and renal systems, and has a half life of approximately 3-4 min [180], its potent vasoconstrictor effects are long lasting [181].

Endothelial ET-1 is a paracrine signal, therefore plasma measures of ET-1 are not a true indication of its local concentrations. However, increased plasma concentrations are representative of over spill-over from increased secretion, which is the likely cause of elevated plasma ET-1 levels in disease states such as hypertension [7, 182], type 2 diabetes [183], and cardiovascular disease [184]. Plasma concentrations are approximately 540 fmol.l^{-1} in healthy humans, and 1 880 fmol.l^{-1} in patients with type 2 diabetes [183]. However, as plasma levels are only representative of the spill over from the local environment the reported plasma concentrations vary between studies [7, 182, 184].

Endothelin-1 has a high affinity for its two different guanine-nucleotide-binding (G) protein receptors, termed ET_A and ET_B receptors. ET-1 binding to the ET_A receptors, located on the vascular smooth muscle cells, results in a prolonged vasoconstriction caused by the stimulation of phospholipase C, which ultimately leads to vasoconstriction by increasing the intracellular Ca^{2+} stores [179, 181]. The ET_B receptors are located primarily on the endothelial cells, and to a lesser extent on the vascular smooth muscle cells. ET-1 binding to the ET_B receptor located on the vascular endothelial cells causes vasodilation by stimulating the production of prostacyclin and nitric oxide [185, 186] which in turn inhibit ET-1 release [179]. ET-1 binding to the ET_B receptor located on the vascular smooth muscle cells causes vasoconstriction by similar means to the ET_A receptor [179]. Therefore, due to these opposing effect and

the distribution of the ET-1 receptors, ET-1 infusion may cause a transient vasodilation followed by a prolonged and dose dependent vasoconstrictor effect [187].

Acute administration of ET-1 leads to an increase in mean arterial pressure in both humans [178, 180, 188] and animals [187, 189, 190]. This effect may be attributed to the strong vasoconstriction caused by ET-1 in the pancreas [191, 192], kidney [187-189, 193], mesenteric [187, 189], and splanchnic [188, 193] regions. Some studies have also reported a decrease in flow to the skeletal muscle however findings are inconsistent [178, 189, 194, 195].

1.10.1 ET-1, nitric oxide and endothelial dysfunction

Other than its potent vasoconstrictor effects, ET-1 also plays a role in regulating vascular tone, demonstrating the regulatory role of ET-1's two receptor mediated effects. It may be possible that if this response becomes unbalanced over time it may result in endothelial dysfunction, which has a close association with cardiovascular disease and its associated risk factors. Endothelial dysfunction involves alterations to the endothelial cell's capacity to maintain normal homeostatic and vascular function [8]. Therefore an imbalance between the secretion of ET-1 and nitric oxide may lead to pathophysiological conditions such as atherosclerosis, hypertension and/or insulin resistance which are disease states characterised by modified blood flow and increased plasma ET-1 concentrations.

Insulin release causes secretion of both ET-1 and nitric oxide which help to maintain vascular tone. Potenza et al. [196] showed that insulin resistance in the spontaneously hypertensive rat was due to an impairment in PI3-kinase dependent nitric oxide production and enhanced mitogen activated protein kinase (MAPK) dependent ET-1 secretion. The mechanisms or time line of how these deregulations leads to insulin resistance, or vice versa, are yet to be elucidated. It is possible that an over-secretion of ET-1 may lead to an imbalance in the regulation of the blood vessel tone, causing vasoconstriction leading to an insulin resistant state. Alternatively, insulin resistance may lead to an impairment in the insulin signalling pathway which decreases the ratio of nitric oxide to ET-1 decreasing blood flow and causing a further increase in insulin resistance [8].

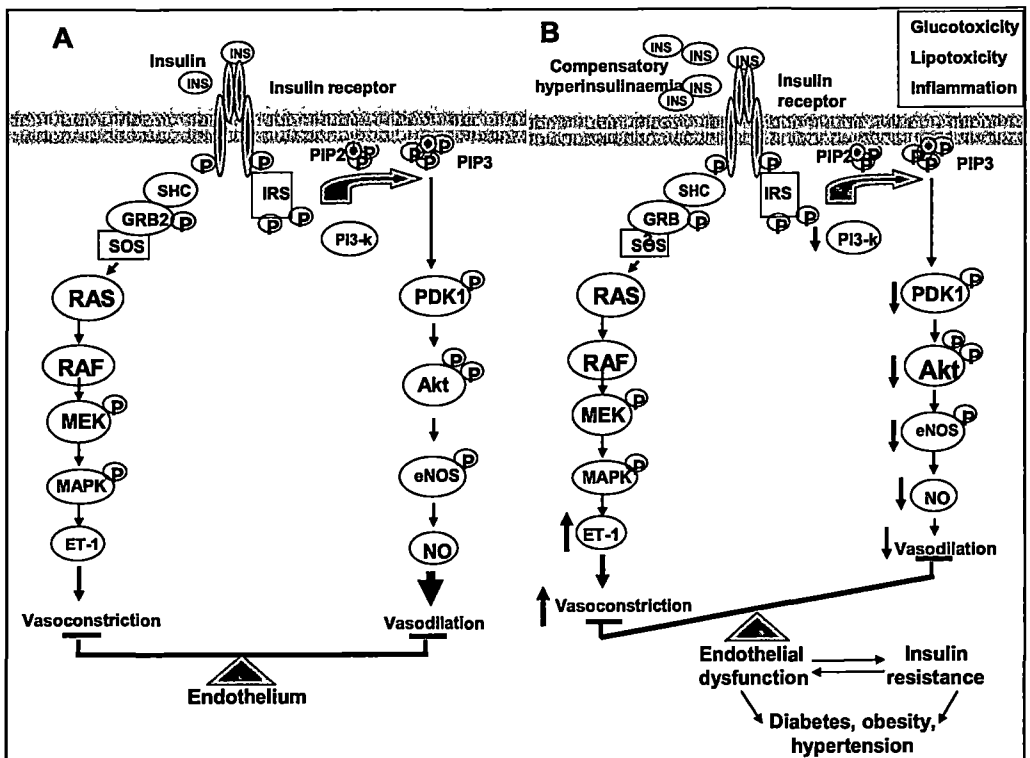

FIGURE 1.1 A SCHEMATIC REPRESENTATION OF THE INSULIN SIGNALLING PATHWAY. Panel A depicts the insulin signalling pathway related to nitric oxide and endothelin-1 production resulting in vasodilation or vasoconstriction. Panel B depicts the insulin signalling pathway under pathological conditions which may create an imbalance between insulin's vasodilator and vasoconstriction actions resulting in insulin resistance and hyperinsulinaemia (Diagram adapted from Muniyappa et al. [197]).

Mather et al. [198] showed that the ET_A antagonist BQ123 produced vasodilation in obese and diabetic humans. Vascular resistance decreased in the obese by 34% compared to only a 13% in lean subjects in response to BQ123 treatment. There was no change in nitric oxide flux, causing the authors to conclude that there is increased basal ET-1 constrictor tone in obese and type 2 diabetic subjects. Also, inhibition of nitric oxide release by L-NMMA results in similar symptoms as ET-1 infusion, such as increased plasma ET-1 concentrations and mean arterial pressure, decreased splanchnic and renal blood flow and decreased splanchnic glucose production [199]. These two studies help to demonstrate how imbalances in vascular control may have a negative impact on the vasculature leading to endothelial dysfunction and related disease states such as insulin resistance.

1.10.2 Endothelin-1 and insulin resistance

The obese Zucker rat is an animal model of insulin resistance and is characterised by increased plasma insulin, total cholesterol, triglycerides and glucose concentrations relative to their lean counterparts [200]. They also have elevated ET_A and ET_B receptor mRNA which is thought to be induced by their hyperinsulinemic state [200, 201]. Berthiaume et al. [202] treated obese Zucker rats for 6 weeks with an ET_A antagonist which lead to an increase in whole body glucose metabolism, and a normalisation of PI3-kinase, IRS-1 tyrosine and Akt signalling in the liver.

Chronic infusion of ET-1 in normal rats over 5 days caused symptoms resembling those associated with insulin resistance and type 2 diabetes. Treated rats had a decreased glucose transport and 30% decrease in insulin stimulated glucose disposal. These effects were accompanied by a decreased IRS-1 protein content and Akt phosphorylation and elevated plasma insulin concentrations [203]. Insulin resistance has also been observed during acute infusion of ET-1. Ottosen-Seeberger et al. [193] found co-infusion of ET-1 with insulin in humans, leads to a 31% decrease in whole body insulin mediated glucose uptake and a 26% decrease in leg glucose uptake. This was associated with decreased blood flow to the splanchnic and renal organs. Skeletal muscle blood flow in the leg and forearm remained unchanged, however microvascular perfusion was not assessed. Ahlborg et al. [178] also found a decrease in insulin sensitivity and blood flow with ET-1 infusion accompanied by an increase in circulating plasma insulin concentrations. While antagonism of the ET_B receptor did not prevent any of these effects, co-infusion of ET_A antagonist resulted in normal blood flow and insulin sensitivity.

In cell culture models, which negate ET-1's effects on haemodynamic parameters, Idris et al. [204] found 24 h of ET-1 exposure had no effect on basal glucose transport, but did inhibit insulin stimulated glucose uptake in a time dependent manner in 3T3-adipocytes. The L6 myoblasts, however were unaffected by the ET-1 treatment. Ishibashi et al. [205] found chronic treatment of 3T3 L1 adipocytes with ET-1 inhibited insulin stimulated glucose uptake and GLUT4 translocation. It also inhibited insulin stimulated tyrosine phosphorylation of IRS-1, PI3-kinase activity and Akt phosphorylation. Co-treatment with an ET_A receptor antagonist prevented these

inhibitions [205]. From these data, it is unlikely that chronically elevated ET-1 has a direct effect on insulin signalling mechanisms as it is the muscle, and not the adipose tissue which is responsible for over 85% of insulin mediated glucose uptake [11]. Also, many of the negative responses caused by ET-1 (hyperinsulinaemia, decreased glucose uptake and vasoconstriction) are prevented by blocking the ET_A receptor [85, 187, 206] suggesting the main mechanism by which ET-1 causes peripheral insulin resistance is by interacting with vascular receptors to cause haemodynamic actions, and thus inhibiting the access of insulin and glucose in the muscle.

1.10.3 Endothelin-1 and exercise

ET-1 is released during exercise and its proposed main function is to cause vasoconstriction in the non working muscles and organs. Maeda et al. [195] demonstrated ET-1's role in the redistribution of flow during a one leg 30 min cycle ergometer test. Femoral vein sampling showed an increase in ET-1 concentration and a larger arterio-venous difference in ET-1 in the non working leg, while concentrations in the working leg were unchanged. This concept is supported by others [207-210] and confirmed in a follow up study by Maeda et al. [211] in rats, where ET_A receptor blockade decreased the vasoconstrictor action of ET-1 during treadmill exercise, causing the amount of constriction normally seen to the stomach, intestine, spleen and kidneys to decrease compared to the control animals (therefore allowing greater blood flow) which in turn decreased blood flow to the active muscles. Therefore ET-1 does play an important role in exercise mediated distribution of flow and this effect is mediated by the ET_A receptor.

However, when ET-1 levels are elevated such as in hypertensive and cardiac patients, this leads to a decrease in exercise performance and tension development. McEniery et al. [209] measured the forearm blood flow response to handgrip exercise in hypertensive subjects and found that vasodilation in response to exercise was inhibited compared to normotensive controls. This response was enhanced by ET_A receptor antagonism in hypertensive controls, but had no effect on the normotensive subjects. Similarly , Kolka et al.[212] found ET-1 infusion reduced the aerobic capacity of the muscle during electrical stimulation. Therefore over-secretion of ET-1 may not

only affect insulin mediated effects but may also be detrimental to the positive vasodilitary effects of exercise.

Exercise training has also been shown to decrease circulating ET-1 levels which may produce beneficial effects on the cardiovascular system. However it is difficult to attribute the beneficial effects of exercise training to decreased ET-1 levels, given the vast number of physiological and metabolic changes which occur with training.

1.11 MEDIATORS OF MICROVASCULAR PERFUSION: INTERLEUKIN-6

Interleukin-6 (IL-6) is a pleiotropic protein well known for its effects on immune function and its role in the acute phase response [213]. In addition, it has a large scope of physiological effects playing a role in bone metabolism, reproduction, neural development, aging and haematopoiesis [214]. In recent times, the effect of this cytokine in the muscle and adipose tissue, and its role in glucose regulation and insulin signalling has also received much attention.

IL-6 is rapidly synthesised and secreted from a variety of tissues in the body including the blood, cartilage, bone marrow, skin, lung and central nervous system [215]. Most importunately, in regards to the action of insulin and exercise, it is also released by the adipose tissue and skeletal muscle. There are relatively low levels (~1-2 $pg.ml^{-1}$) of IL-6 circulating at rest in healthy individuals, with these levels increasing in disease states such as type 2 diabetes [216, 217], obesity [218-220] and heart disease [221, 222], with these increases attributed to an increased fat mass, leading to increased IL-6 secretion [218, 219, 223]. During exercise, the majority of IL-6 is secreted from the working skeletal muscle [224, 225].

IL-6 exerts its effects through a cell surface receptor consisting of a ligand-binding IL-6 receptor α chain and the signal transducer glycoprotein 130, which are located throughout the body on immune cells, osteoblasts, bladder, brain, in serum, adipose tissue and liver [214, 226]. These receptors appear at the cell surface after synthesis in the endoplasmic reticulum and have half lives of two to three h regardless of the presence of IL-6 [227]. Upon binding to its receptor, IL-6 may activate many signalling

pathways such as Janus Kinase tyrosine kinase, STAT or MAPK signalling cascades [226, 228], and due to its effects on fat oxidation and its release during exercise is also thought to activate AMPK.

1.11.1 Interleukin-6 and exercise

Exercise elevates circulating cytokines in similar proportions to those seen during sepsis, trauma and bacterial infection [229], with the concentrations of IL-6 increasing two fold above that of other released cytokines to ~100 $pg.ml^{-1}$ after strenuous exercise [224, 225, 230]. While the skeletal muscle produces very little IL-6 at rest [216], exercise results in an increase in IL-6 mRNA and IL-6 production localised in the working skeletal muscles [231]. This was demonstrated by Steensberg et al. [232] among others [224, 233], who showed a 19-fold increase in IL-6 production during leg extensor exercise in one leg, with no change in IL-6 concentrations of the control leg.

It was originally proposed that IL-6 was released in response to muscle damage, which is generally associated with eccentric exercise and an acute phase response. However, both eccentric and concentric exercise increase plasma concentrations, regardless of the mode of exercise [233], and the levels of creatine kinase (a marker of muscle damage) peak in the blood 24 to 72 h post exercise, by which time plasma IL-6 concentrations have returned to basal [224, 234]. In addition low intensity, long duration concentric exercise which elicits only a small elevation in creatine kinase levels still causes an increase in plasma IL-6 [233]. Other factor which may be responsible for increased IL-6 concentrations during exercise are changes in calcium homeostasis [235], impaired glucose availability [236, 237] or increased formation of reactive oxygen species [238, 239] which are all capable of activating the transcription factors which regulate IL-6 synthesis, however the exact mechanisms are still to be elucidated [240].

The level of IL-6 production increases in longer duration, higher intensity exercise where there is a high level of metabolism and energy stores become depleted [224, 241, 242]. It is therefore expected that IL-6 release is also greater when glycogen stores are depleted , as shown by Keller et al. [231] who found that low glycogen content in the

muscle (40% lower than control) during prolonged knee extensor exercise lead to a greater than two-fold increase in IL-6 concentration and a higher rate of IL-6 transcription than in the control leg. Steensberg et al. [243] found similar results with glycogen depletion increasing circulating IL-6 to 4.38 ± 2.8 $ng.l^{-1}$ during knee extensor exercise versus 0.36 ± 0.14 $ng.l^{-1}$ in the control leg. McDonald et al. [244] showed while there was no increase in IL-6 production or AMPK activation during cycling exercise in the fully glycogen loaded state, there was a correlation between IL-6 production and AMPK activation during exercise in the glycogen depleted state. As IL-6 production is also dependent of carbohydrate and glucose availability [236, 245], this data suggests a role for IL-6 in energy regulation during exercise, which may be mediated through activation of AMPK.

AMPK, like IL-6, activation is sensitive to the glycogen content in the muscle [246]. It is possible that both IL-6 and AMPK act independently as sensors of a low energy state in the muscle, however there is evidence to suggest that IL-6 is capable of acting directly on skeletal muscle or adipose tissue to activate AMPK [247, 248]. Also, *in vitro* experiments show that L6 myotubes infected with a dominant negative AMPKα subunit, blocked the effect of IL-6 treatment on fatty acid oxidation and glucose uptake [248], while siRNA mediated depletion of AMPK affected IL-6 mediated fatty acid oxidation and palmitate uptake in skeletal muscle cells [249]. Furthermore, AMPK activity is diminished at rest and its activation during exercise is also decreased in the skeletal muscle and adipose tissue of IL-6 knockout mice ($IL6^{-/-}$) compared to control mice. This shows that IL-6 is able to activate AMPK, and also demonstrates however, that IL-6 is not solely responsible for increased AMPK phosphorylation in response to exercise [247].

The release of IL-6 during prolonged or strenuous exercise may help to regulate energy expenditure and maintain homeostasis, by acting to increase the production of blood glucose and glycogen from glycerol and lactate, and helping to retain glucose stores by using excess fat stores for energy production. This may occur through IL-6s ability to increase fatty acid oxidation [250, 251] (possibly through AMPK and phosphorylation of acetyl-CoA carboxylase), which may lead to a state of insulin resistance, as is often seen for a short period of time after strenuous exercise [110, 111, 252].

1.11.2 Interleukin-6 and insulin

It is generally accepted that IL-6 administration *in vivo*, results in increase lipolysis and fat oxidation, in the absence of hypertriglycidaemia and without changes in catecholamines, glucagon or insulin [250, 251]. This data is supported by cell culture experiments where IL-6 alone increases fat oxidation in L6 myotubes [253], incubated muscle strips [254] and adipose tissue [255]. More contentious issues however, are those surrounding the role of IL-6 in glucose uptake and insulin action, where there have been conflicting reports, particularly when comparing human and animal studies.

In vitro studies show that, in addition to its well known effects on increased fatty acid oxidation [256], incubation of muscle cells and L6 myotubes with IL-6 results in an increase in glucose uptake and insulin sensitivity at basal and during incubation with insulin [248, 257-259] through increased GLUT4 translocation to the plasma membrane [248]. IL-6 may mediate its effects on glucose and fat metabolism through different pathways as Ali-Khalili et al.[256] showed that inhibition of PI3-kinase in skeletal muscle cells suppressed IL-6 mediated glucose metabolism but did not affect lipid metabolism, while diminished AMPK (by siRNA) decreased IL-6 mediated fatty acid oxidation without affecting glycogen synthesis [256]. In regards to the insulin signalling pathway, Glund et al. [259] found IL-6 had no effect on insulin stimulated glucose transport or phosphorylation of Akt, AS160 or IRS-1 associated PI3-Kinase. In contrast Weigert et al. [260] found IL-6 induced a rapid recruitment of IRS-1 to the IL-6 receptor complex while inducing a rapid and transient phosphorylation of Ser ^{318} of IRS-1 in the skeletal muscle (but not the liver). In addition, IL-6 induced phosphorylation of Ser^{473} of Akt and increased insulin mediated phosphorylation of glycogen synthase kinase-3 [257] resulting in an insulin sensitising effect.

Treatment of adipocytes with IL-6 causes an increase in IL-6 and TNF-α expression and release. A number of studies have found IL-6 disrupts insulin signalling in adipocytes by decreasing transcription of IRS-1 and GLUT4 [261]. A decrease in insulin stimulated tyrosine phosphorylation and insulin activation of IR-b, Akt and extracellular signal-regulated kinase (ERK) 1/2 has also been observed as well as an increase in suppressor of cytokine signalling (SOCS) 3 protein [262, 263], suggesting IL-6 may cause a state of insulin resistance in the adipocytes. In contrast, IL-6 has been

shown to increase AMPK activation [247, 258], glucose transport and glucose uptake in 3T3-L1 adipocytes, which was additive to the effect of insulin [258, 264], suggesting a insulin sensitising effect.

IL-6 administration at rest has no effect on whole body glucose disposal, glucose uptake or endogenous glucose production [253, 265]. Acute administration of IL-6 during a hyperinsulinemic euglycaemic clamp in healthy humans leads to an increase in the glucose infusion rate, and glucose oxidation without changes in exogenous glucose production [248]. Alternatively in rats, IL-6 infusion during a euglycaemic hyperinsulinaemic clamp had no effect on insulin stimulated whole body glucose homeostasis or insulin signalling [266], while an intravenous injection of IL-6 in the rat caused plasma glucagon and plasma glucose levels to increase, with a decreased hepatic glycogen [267]. Experiments in the conscious mouse also showed that IL-6 infusion blunts insulin's ability to suppress hepatic glucose production, however in contrast to the human and rat studies there was a decreased insulin simulated glucose uptake in the skeletal muscle, which was associated with defects in IRS-1 associated PI3-Kinase activity and increased fatty acyl-CoA levels [268].

1.11.3 Interleukin-6 and insulin resistance

A link has been established between obesity and insulin resistance and a state of chronic low level inflammation [9] which may involve increased levels of circulating cytokines such as TNF-α and IL-6 [88, 216, 269]. TNF-α has been shown to causes insulin resistance by inhibiting insulin stimulated tyrosine kinase activity of the insulin receptor and down regulation of GLUT4 expression [92, 93]. In addition, TNF-α inhibits the insulin stimulated increases in femoral blood flow and microvascular perfusion [95, 97], and TNF-α blockade before a hyperinsulinaemic euglycaemic clamp improves insulin sensitivity [270]. As TNF-α increases the secretion of IL-6 from the adipose tissue it may be thought that IL-6, like TNF-a may be involved in insulin resistance. Injecting TNF-α into the adipose tissue of mice elevated serum IL-6 levels and reduced serum lipo-protein lipase activity by 70% [271]. As insulin stimulates lipo-protein lipase in order to increase fatty acid uptake into the cell, these cytokines may regulate the adipose tissue by stimulating lipolysis (as TNF- α also stimulates hormone sensitive lipase release [272]) and inhibiting lipoprotein lipase and insulin

action causing insulin resistance. There are differences between these cytokines as unlike IL-6, TNF-α release is not increased during exercise [216], and while TNF-α has a strong correlation with decreased insulin sensitivity, IL-6 has a stronger correlation with increased fat mass and body mass index [90, 218], suggesting they may have separate actions concerning insulin action and energy metabolism.

Whether elevated plasma IL-6 concentrations occur as a result of, or are the cause of, insulin resistance is still unknown, however inhibition of IL-6 with an anti-IL-6 receptor antibody in patients with rheumatoid arthritis, caused an increase in cholesterol and plasma glucose levels [273, 274]. Also, the IL-6 knockout mice develop obesity, and become glucose intolerant and dyslipidaemic [247, 275], suggesting that the absence of IL-6, rather than an increased presence, may contribute to insulin resistance. This was demonstrated by Wallenius et al. [275] who reversed the insulin resistant effect in the knockout mice through IL-6 replacement.

There is controversy surrounding the role which IL-6 plays in insulin resistance, however there are some consistencies, in that IL-6 appears to have different effects on the muscle, adipose tissue and liver. It appears that IL-6 induces hepatic insulin resistance which is demonstrated in both *in vitro* and *in vivo* experiments. Incubation of hepatocytes with IL-6 causes an increased glycogen degradation, and a greater than 50% inhibition of insulin mediated glycogen synthesis [276] as well as decreased tyrosine phosphorylation of IRS-1 and decreased association of the p85 subunit of PI3-kinase with IRS-1[277]. *In vivo* data supports these finding with five day subcutaneous infusion of IL-6 (resulting in a six-fold elevation of IL-6) in mice, causing an impairment of early insulin receptor signalling in the liver, including a 60% decrease in hepatic insulin receptor autophosphorylation, and a decrease in the tyrosine phosphorylation of IRS-1 and IRS-2. During this study, only hepatic insulin signalling, and not skeletal muscle insulin signalling, was impaired [278]. Similar results were seen in the conscious mouse during a euglycaemic hyperinsulinaemic clamp with IL-6 infusion. IL-6 blunted insulin's ability to suppress hepatic glucose production and insulin stimulated IRS-2 associated PI3-Kinase in the liver. This study however, also showed a decreased insulin stimulated glucose uptake in skeletal muscle [268]. IL-6 also activated suppressor of cytokine signalling proteins in the liver (with little effect in skeletal muscle [260]) leading to hepatic insulin resistance via

inhibition of hepatic insulin-dependent receptor autophosphorylation and IRS-1 tyrosine phosphorylation [277, 279].

As described above, IL-6 has been shown to increase [248, 264] or decrease [261, 263] insulin signalling and glucose uptake in skeletal muscle and adipose tissue. The controversy surrounding IL-6 and its role in insulin resistance may be due to the number of different cell lines, species, and concentrations of IL-6 and insulin used in each study. In addition, the discrepancies in the data may be due to the time of incubation or administration of IL-6. It appears that chronic treatment (>5 h) [247, 261, 263], results in insulin resistance, while shorter periods of incubation or acute administration [248, 257-259, 264], tend to cause an increase in glucose uptake and insulin sensitising effect. Chronic treatment may be more representative of disease states such as type 2 diabetes and obesity which are characterised by chronic elevation of circulating IL-6. While acute treatment may be compared to the short term release of IL-6 during exercise causing elevated IL-6 concentrations for only a few hours. Therefore from the data presented, it appears that IL-6 has specific effects in the muscle, liver and adipose tissue, and these effects may be modified depending on the time period of exposure to IL-6. In the short term, IL-6 may have a positive effect on glucose uptake and act to maintain glucose homeostasis and energy regulation during exercise. However in the long term, the inflammatory effects of IL-6 may play a role, and the involvement of IL-6 with TNF-α and its actions to increase plasma fatty acid concentrations [251] may lead to an insulin resistant state [95, 280].

1.12 SUMMARY OF STUDY AIMS

There is evidence to suggest the ability of insulin and contraction to increase glucose uptake is due in part, to their ability to increase total blood flow, and more importantly microvascular perfusion. The work in this study aims to assess the mechanisms through which this increase in perfusion occurs, and the similarities/differences in these pathways in response to insulin or contraction.

While it has been shown that changes in bulk flow correlate with the filling rate of the capillaries, research has been published using this method under the assumption that

the technique is able to discriminate changes between microvascular volume and total blood flow. Therefore the first aim of this study was to validate the technique of contrast enhanced ultrasound for use in detecting changes in skeletal muscle microvascular perfusion independent of changes in bulk flow.

The beneficial effects of exercise in terms of insulin sensitivity are well documented, however the mechanism behind this phenomenon are still to be elucidated. While there is a large body of work assessing the signalling pathways which may be responsible for this sensitisation post-contraction, the role of the microvasculature and capillary perfusion during this post-contraction period has not been assessed. The second aim of this study was to assess, using the contrast enhanced ultrasound technique, if an acute bout of contraction results in an increase in microvascular perfusion post-contraction and if this is associated with an increase in skeletal muscle glucose uptake.

Nitric oxide has been implicated in insulin mediated increases in microvascular perfusion, however its role in the hyperaemic response to exercise is still controversial. The effect of nitric oxide on total blood flow has been assessed with mixed results, however its effect on microvascular perfusion has not been assessed. This third aim of this study is to examine the role of nitric oxide in exercise induced vasodilation and its effects on microvascular perfusion and glucose uptake during contraction.

In conjunction with nitric oxide, endothelin-1 is responsible for maintaining the vascular tone of the vessels at basal, and possibly during insulin stimulation. An imbalance in the secretion of these compounds may result in disruption of the homeostatic regulation of the vessels leading to endothelial dysfunction and insulin resistance. This fourth aim of this study is assess if endothelin-1 is able modulate insulin mediated effects on total blood flow and microvascular perfusion and to examine if this leads to a state of insulin resistance in the skeletal muscle.

Another controversial area is the role of interleukin-6 during exercise and insulin stimulation. Due to its release in vast quantities during intense exercise, interleukin-6 is thought to play a positive role in maintaining glucose homeostasis and fuel stores,

however its effects on insulin action are still unknown. This laboratory has shown that a similar cytokine, TNF-α, when administered acutely causes insulin resistance by inhibiting insulin mediated haemodynamic effects. Therefore, the fifth aim of this thesis is to assess the role of acute IL-6 administration on insulin mediated microvascular perfusion and glucose uptake in the skeletal muscle.

In summary, the principal aim of this thesis is to assess *in vivo*, the mechanism involved in mediating microvascular perfusion and glucose uptake during stimulation by insulin or contraction in the rat. As these two stimuli act to increase glucose uptake through separate mechanisms, further insight into the metabolic and haemodynamic changes that occur in the microvasculature in response to these stimuli is important in understanding the development of disease states such as type 2 diabetes, and opens the possibility of finding new therapeutic targets for treatment of these diseases.

CHAPTER 2:

MATERIALS AND METHODS

2.1 MATERIALS

2.1.1 Infusion substances

Allopurinol

Sigma-Aldrich®; white powder

8.50 mg of allopurinol was dissolved in 4.9 ml of heparinised saline and 100 µl of 1 M NaOH and stored at -20°C as a 12.5 mM solution

Endothelin-1 (ET-1)

Calbiochem®; white powder, human and porcine ET-1

1 mg ET-1 powder was dissolved in 125 µl of 80% acetic acid and then diluted with 1.875 ml saline to give a stock solution of 200 µM. The solution was stored in 200 µl aliquots at -20°C and diluted to the appropriate concentration with heparinised saline prior to each experiment.

Fluorescein isothiocyanate (FITC)-labelled insulin

Sigma Aldrich ®; USA

A 200 µl solution of FITC-labelled insulin at a concentration of 1 $mg.ml^{-1}$ was made before each experiment using heparinised saline.

Insulin

Eli Lilly ®; 100$U.ml^{-1}$ solution

Humulin® R

0.1 U of insulin was diluted in a 0.9 ml 2% bovine serum albumin (BSA) solution. This solution was then further diluted with heparinised saline dependent on rat weight and the concentration required, and infused intravenously.

Interleukin-6 (IL-6)

R and D Systems Inc.; 50 μg rrIL-6 solution
97% purity (SDS-PAGE), recombinant rat (*E-coli*-derived) IL-6

The stock IL-6 was prepared with 14 μl of filtered 2% BSA and 669 μl of filtered PBS to give a final concentration of 50 $\mu g.ml^{-1}$. 200μl of the 50 $\mu g.ml^{-1}$ solution was then combined with 800 μl filtered PBS (10$ug.ml^{-1}$ stock solution) and stored at -4°C. The stock solution was then diluted to the appropriate concentration with heparinised saline prior to each experiment.

The IL-6 vehicle infusion solution consisted of 143 μl CH3CN, 3 μl TFA, 840 μl filtered PBS and 14 μl of 2% BSA, and was diluted in the same manner as the IL-6 solution.

N_{ω}-Nitro-L-arginine methyl ester hydrochloride (L-NAME)

Sigma-Aldrich®; white powder
≥98% purity (TLC)

The stock solution consisted of 16.18 mg powder dissolved in 20 ml heparinised saline and was stored at -20°C.

1-methylxanthine (1-MX)

Sigma-Aldrich®; white powder
≥97.0% purity (HPLC)

100 mg of 1-Methylxanthine was dissolved in 19.4 ml of heparinised saline and 600 μl of 1 M NaOH. This 5 $mg.ml^{-1}$ stock solution was stored at -20°C.

Microbubble contrast agents (MB)

The phospholipid microbubble solution was prepared in the laboratory.
Per 100 ml:

10.35 g 1,2-Propanediol
12.62 g Glycerol
0.66 g NaCl

0.075 g Lipid Blend (consists of 0.0043 g 1,2-Dipalmitoyl-SN-Glycero-3-Phospatidic acid, mono salt; 0.039 g 1,2-Dipalmitoyl-SN-glycero-3-phosphatidylcholine (DPPC); 0.0307 g 1,2-dipalmitoyl-SN-glycero-3-phospatidylethanolamine, monosodium salt, N-(methodxypolyethylene glycol 500 carbomyl) (MPEG5000-DPPE))

In separate 200 ml beakers, the 1,2-propanediol and lipid blend were heated in a 55°C water bath, and combined when the 1,2-propanediol reached 55°C. The NaCl was dissolved in 60 ml of water and added to glycerol before being heated to 55°C in a water bath. When dissolved, the lipid blend/propanediol mix was added to the NaCl/glycerol solution and dissolved in a 75°C water bath. The pH of the solution was adjusted to 6.5 using NaOH or HCl and filled to volume (100 ml) with distilled water. The solution was filtered through a sterilising filter (0.45 μm) into sterile falcon tubes before being transferred into 5ml glass vials. The head space was exchanged for octafluoropropane gas, the vials were sealed, and stored at -4°C.

2.1.2 Radioactive Material

2-Deoxy-D-[1-^{14}C] glucose (2-DG)

Amersham Pharmacia Biotech;
Aqueous solution, sterilised, 200 μCi.ml^{-1}

100 μl of 2-Deoxy-D-[1-^{14}C] glucose (2-DG) was freeze dried overnight. When required the 2-Deoxy-D-[1-^{14}C] glucose was resuspended in 100 μl of heparinised saline and given as a bolus injection in the jugular vein of the anaesthetised rat, as above.

D-[3-^{3}H] glucose

Amersham Pharmacia Biotech
Aqueous solution, sterilised, 1 mCi.ml^{-1}

An infusion solution of 0.1 μCi.min^{-1} of D-[3-^{3}H] glucose was made with heparinised saline before use.

2.2 IN VIVO EXPERIMENTS

2.2.1 Animals

Male Hooded Wistar rats (230-250g) reared in the University of Tasmania animal house were used. Animals were kept on a 12 h light/dark cycle maintained at 22°C. All animals were allowed free access to standard laboratory rat chow (21.4% protein, 4.6% lipid, 68% carbohydrate and 6% crude fibre with added vitamins and minerals) and water ad libitum.

Rats used during experiments that required the determination of glucose turnover were fasted overnight prior to the experiment.

2.2.2 Surgery

Rats were anaesthetised using sodium pentobarbital (50mg/100g body weight). A tracheotomy tube was inserted to allow the animal to spontaneously breathe room air throughout the experiment. The right carotid artery and both jugular veins were cannulated using Polyethylene cannulas (PE-60, Intramedic®) and secured using silk ligatures (size 3/0 waxed braided silk). After the cannulas were surgically implanted, the carotid artery was attached to a pressure transducer (Transpac IV, Abbott Critical Systems, Morgan hill, CA USA) allowing constant mean arterial pressure measurements. The carotid artery was also used for arterial sampling through out the experiment. The right jugular vein was used for the administration of various intravenous infusions (eg. saline, insulin, 1-Methylxanthine etc). This surgical procedure generally lasted approximately 20 min, after which the animals were maintained under anaesthesia for the remaining surgery and the duration of the experiment via a constant infusion of anaesthetic (0.6 $mg.min^{-1}.kg^{-1}$ pentobarbitone sodium) through the left jugular vein (Fig. 2.1). The body temperature of the animal was maintained at 37°C using a water-jacketed platform and a heating lamp positioned above the rat.

Once the animal was stabilised (ie. mean arterial pressure of approximately 110 mmHg and a heart rate between 300 and 400 $beats.min^{-1}$), a small incision was made in the skin overlaying the femoral vessels of both legs. The femoral artery was

separated from the femoral vein and saphenous nerve in each leg, and an ultrasonic flow probe (Transonic Systems™, VB series 0.5 mm Ithaca, NY USA) was positioned around each femoral artery distal to the rectus abdominis muscle (Note: some experiments only required blood flow measurements in one leg, as specified in the individual study protocols, and therefore only one flow probe was used). The cavity in the leg surrounding the flow probe was filled with lubricating jelly (H-R, Mohawk Medical Supply, Utica, NY USA) to provide acoustic coupling to the probe. The flow probes were then connected to a flow meter (Model T106 ultrasonic volume flow meter, Transonic™ systems Ithaca, NY USA). This in turn was interfaced with an IBM compatible PC computer, that acquired data at a sampling frequency of 100 Hz for femoral blood flow, heart rate and blood pressure using WINDAQ data acquisition software (DATAQ instruments, Akron, OH USA) (Fig. 2.1).

After surgery, a 45 min equilibration period was permitted to allow leg blood flow, mean arterial pressure and heart rate to become stable and constant before commencing the experiment.

2.2.2.1 Epigastric artery cannulation

When a local infusion in the rat hindlimb was required (ie. to prevent systemic effects), the epigastric artery was cannulated prior to the ultrasonic flow probe being positioned around the femoral artery. The cannula was made form a blunted insulin syringe needle attached to a small diameter polyethylene tubing (PE-20, Intramedic®). This in turn was connected to a larger sized polyethylene tubing (PE-50, Intramedic®) to allow the attachment of the infusion syringe. The skin above the epigastric artery and femoral artery was removed and the connective tissue overlying the vessels was separated. The connective tissue surrounding the epigastric artery was removed and a silk tie was loosely placed around the artery/vein bundle. A small incision was made in the artery using a sharp insulin syringe needle and then cannulated, with the tip of the needle positioned in the junction between the epigastric and femoral arteries and without disrupting blood flow. The cannula was secured using the silk tie around the artery/vein bundle. A successful cannulation resulted in arterial blood pulsing into the tubing upon which it was flushed with saline. Saline was infused at a rate of 1 $\mu l.^{-}$

^{1}min to ensure the cannula remained clear until the infusion substance was required (Fig. 2.1).

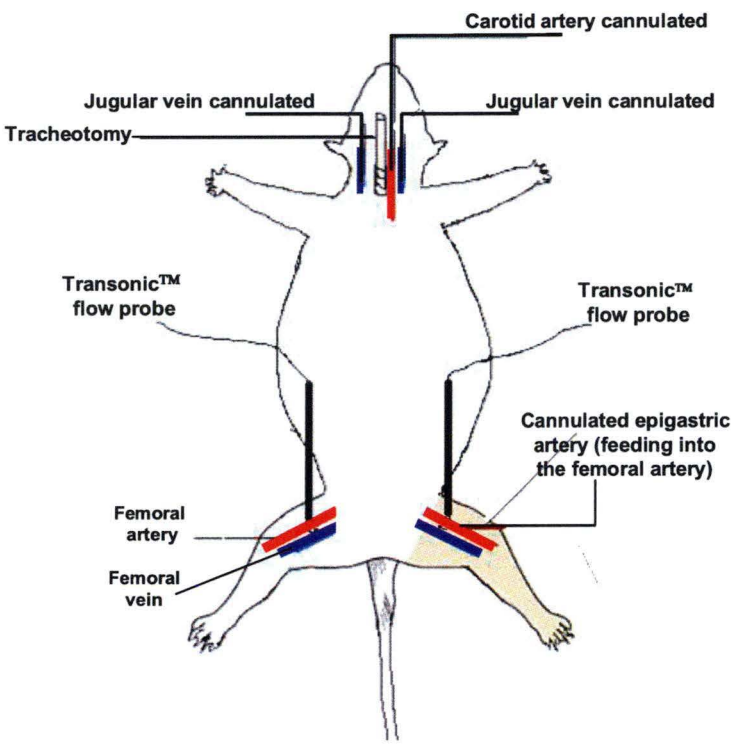

FIGURE 2.1: SCHEMATIC DRAWING OF THE *IN VIVO* SURGERY. Surgery details are given in section 2.2.2. This picture depicts the ventral view of the rat, showing cannulation of the jugular veins (used for intravenous infusions) and the carotid artery (used for arterial blood sampling and continuous measurement of mean arterial pressure and heart rate). A tracheotomy tube was inserted to allow spontaneous breathing of room air and a Transonic ™ flow probe was placed around either one, or both of the femoral arteries (depending on the study protocol), to measure femoral blood flow. The epigastric artery was only cannulated during experiments where a local infusion into the hindlimb was required. (Diagram adapted from Mahajan et al. [281])

2.3 EXPERIMENTAL PROCEDURES AND ANALYTICAL METHODS

2.3.1 In vivo procedure

After a 45 min equilibration period, two arterial samples were taken to determine blood glucose levels. During insulin infusion blood glucose was maintained at euglycaemia by infusion of a 30% w/v solution of glucose. Infusion volumes of glucose and insulin were matched during control experiments with the equivalent

volume of saline. Excess arterial and venous plasma samples taken throughout the experiment were stored at -20°C for use when required. Details of experimental protocols are given in individual chapters.

2.3.2 Microvascular flow measurements

2.3.2.1 1-methylxanthine metabolism

The surface area of the microvasculature was measured by a previously established method involving the infusion of 1-methylxanthine (1-MX; Sigma Aldrich Inc) and its metabolism by xanthine oxidase [21]. Xanthine oxidase is an enzyme located in the endothelium of capillaries and small arterioles in skeletal muscle [282]. As the number of perfused capillaries increases, as does the endothelial surface area exposed to the circulating 1-MX, therefore increasing its metabolism. The disappearance of 1-MX from the circulation and the appearance of 1-Methylurate (its metabolite) can be used to indicate an increase (or decrease) in capillary perfusion.

Xanthine oxidase rapidly metabolises 1-MX, thus it is necessary to partially inhibit the activity of the xanthine oxidase (particularly in non-muscle tissue) via a specific xanthine oxidase inhibitor, allopurinol [283, 284]. Allopurinol (10 $\mu mol.kg^{-1}$) was administered as a bolus (via the carotid artery), five min prior to commencing 1-MX infusion (0.4 $mg.min^{-1}kg^{-1}$) allowing a constant arterial concentration of approximately 15-25 μM of 1-MX to be maintained throughout the experiment.

In order to measure 1-MX metabolism arterial and venous samples were collected in cold eppendorf tubes. The blood samples were centrifuged at 13000 rpm for 10 min and the plasma removed and placed on ice. The 20 μl of plasma was deproteinised using 80 μl of 2 M perchloric acid and analysed using reverse-phase high performance liquid chromatography as previously described [21].

The metabolism of 1-MX ($nmol.min^{-1}$) was calculated by multiplying the arterial-venous 1-MX difference by femoral blood flow, and corrected for the volume accessible to 1-MX (0.871) which was determined from plasma concentrations after the addition of 1-MX standard to whole rat blood.

2.3.2.2 Contrast Enhanced Ultrasound

Contrast Enhanced Ultrasound (CEU) imaging of the muscle microvasculature is a recently developed technique adapted from its use in cardiovascular imaging [26]. Gas filled phospholipid microbubbles (section 2.1.1) were infused intravenously into systemic circulation at a constant rate and visualised using a linear-array transducer/probe (L7-4) interfaced with an ultrasound system (HDI-5000; Philips Medical Systems, Andover, MA).

The transducer was placed over the calf muscle region allowing imaging of the soleus, plantaris and the red and white gastrocnemius muscles. The tendons behind the knee were used as a reference point when positioning the probe (see Fig. 2.2) and a region of interest was selected around the muscles (Fig. 2.2) using Qlab advanced quantification software (Phillips Medical Systems, The Netherlands, B.V).

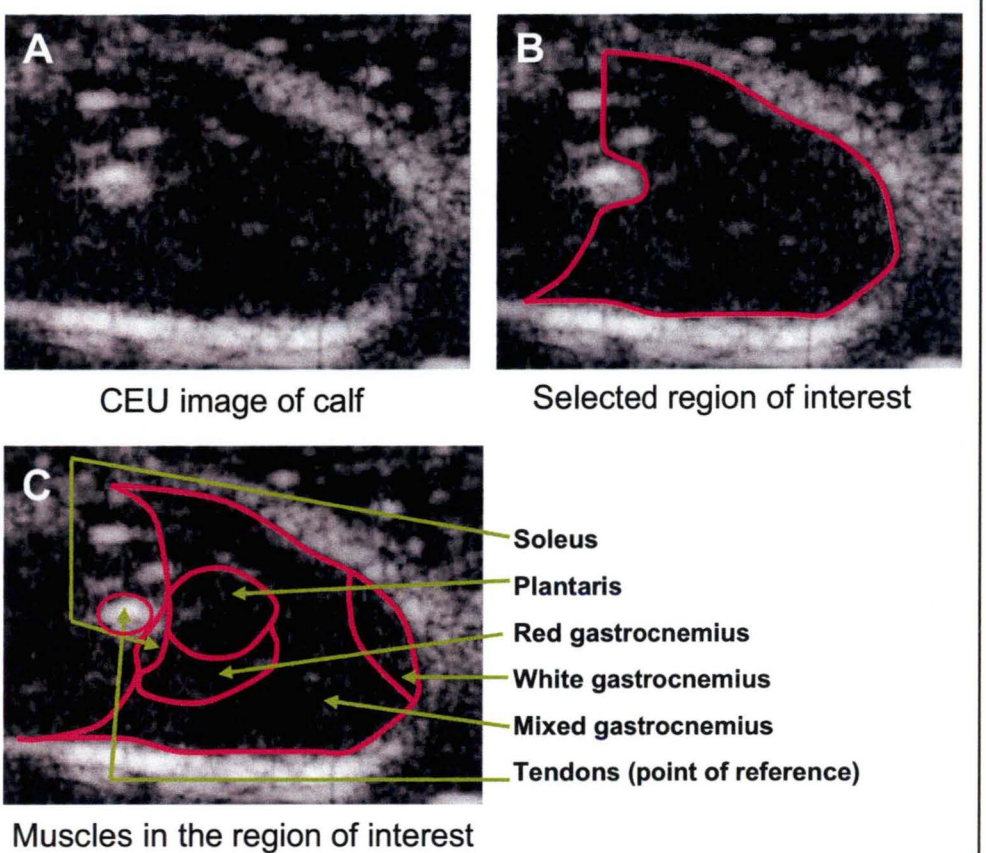

FIGURE 2.2: CONTRAST ENHANCED ULTRASOUND IMAGE OF THE CALF MUSCLE. A) The image as seen by contrast enhanced ultrasound. B) During the analysis a region of interest is selected to include only the muscles of the calf. C) The positioning of the muscles of the calf. The tendons are used as a point of reference when positioning the probe.

The microbubbles (that average 4 μm in diameter) have a similar rheology to erythrocytes, enabling them to stay in the microvasculature and act as a marker of microvascular space [56] . The microbubbles are echogenic as they expand under conditions of high pressure and compress under low pressure leading to changes in acoustic signal. As the microbubbles pass under the ultrasound beam they can be simultaneously imaged and destroyed, therefore as the time between high energy pulses from the ultrasound increases, the number of microbubbles able to fill the microvasculature increases, and the greater the amount of perfusion the greater the signal/intensity (Fig. 2.3).

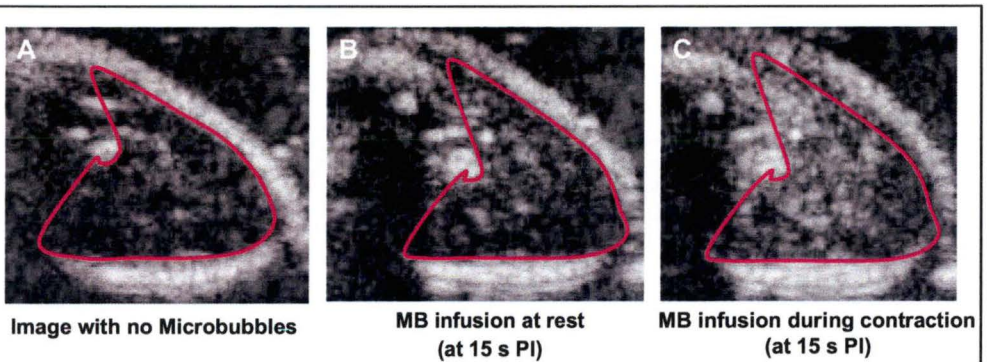

FIGURE 2.3: CONTRAST ENHANCED ULTRASOUND IMAGES OF THE CALF. Panel A shows the image without the infusion of microbubbles. Panel B shows the calf, with a systemic infusion of microbubbles at rest. Panel C shows the calf with a systemic infusion of microbubbles during contraction. All these images are taken at 15 s pulsing intervals (PI).

By controlling the amount of time between pulses we are able to measure the velocity at which the microvasculature fills and the amount of volume perfused (Fig. 2.4). Continuous pulsing, or pulses set at a small time interval (0.07-0.5 s) represent the microbubble fill time of the larger vessels (Fig. 2.4 A and B). Longer pulsing intervals (15-20 s) represent the microvasculature volume (Fig. 2.4 C and D). At the conclusion of the experiment the data is analysed using Qlab advanced quantification software (Phillips Medical Systems, The Netherlands, B.V). This software gives a measure of the received ultrasound signal (in decibels) in the selected region of interest. This value is then converted to acoustic intensity (AI) by the equation:

$$\text{Acoustic intensity} = 10 \text{ ^ } (\text{decibels} / 10)$$

Thus, using these values, we are able to subtract the signal intensity from the larger vessels and the background image, from the signal of the smaller vessels to gain a true measure of microvascular perfusion.

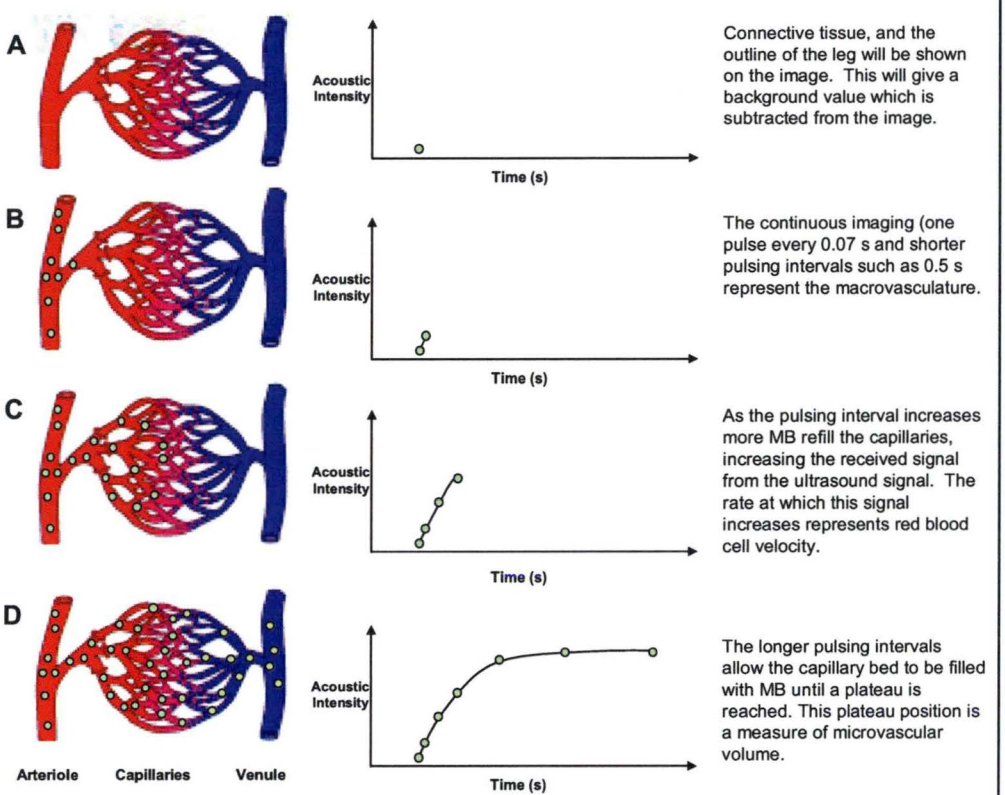

FIGURE 2.4: MEASUREMENT OF MICROVASCULAR VOLUME BY CONTRAST ENHANCED ULTRASOUND. As the time between pulsing intervals increases, a greater number of microbubbles may fill the microvascular space leading to an increase in signal. By manipulating the pulsing interval time a pulsing interval curve may be constructed and used to indicate the microvascular filling rate and microvascular volume.

The mechanical index [(peak acoustic pressure) × (frequency) $^{-1/2}$], a measure of acoustic power, was set to 0.8, and the gain settings were optimised and maintained through each separate experiment. The pulsing intervals were set to 0.2, 0.3, 0.5, 1, 2, 3, 5, 8, 12 and 15 s. At each pulsing interval five frames/images were captured. The signal/intensity (assessed using the using Qlab advanced quantification software (Phillips Medical Systems, The Netherlands, B.V)) from each of these five frames was averaged, the signal from the larger vessels and background were subtracted and the pulsing interval curve was constructed by plotting pulsing interval time versus acoustic intensity. The microvascular volume (*A*) and microvascular filling rate constant (β) values were determined using graphing software (Systat Software Inc.

California, USA) and the microvascular volume and velocity are calculated using the equation:

$$Y = A(1\text{-}e^{-\beta t})$$

Where:

Y = Acoustic intensity at a given pulsing interval

A = Acoustic intensity at the plateau position (an indicator of microvascular volume) (Figure 2.5)

β = The rate constant that provides a measure of the filling rate of the microvasculature (Fig. 2.5)

A measure of microvascular blood flow is achieved by multiplying the A and β values.

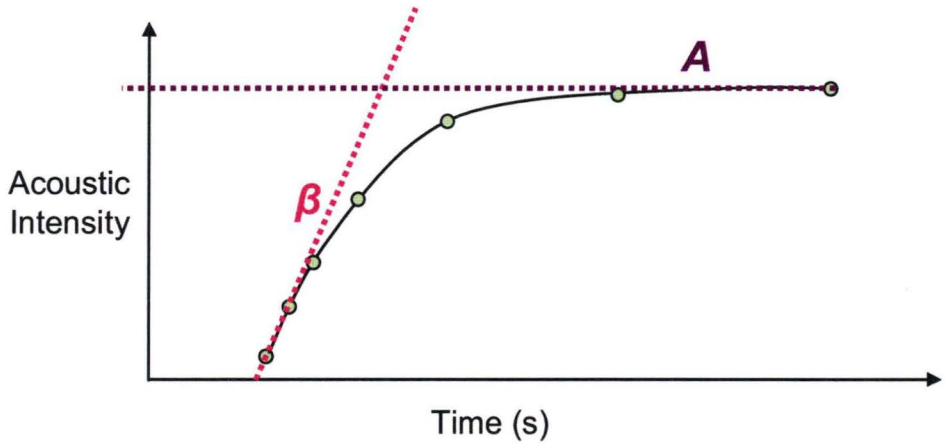

FIGURE 2.5: MICROVASCULAR VOLUME AND FILLING RATE CALCULATION. Once a pulsing interval cure has been constructed, we may measure the plateau position (A) which is a measure of microvascular volume, and the rate of increase (β) which is a measure of average filling rate of the microvasculature. By multiplying A and β values we have a measure of microvascular blood flow.

2.3.3 Muscle Glucose Uptake (R'g)

To asses the uptake of glucose into the individual muscles a 100 µl bolus of 2-deoxy-D-[1-^{14}C] glucose (specific activity = 56.0 mCi.mmol^{-1}, Amersham Pharmacia Biotech, IL, USA) was administered via the jugular vein, 45 min prior to the

completion of the experiment. To determine the clearance rate of 2-DG from the blood, arterial samples were taken 5, 10, 15, 30 and 45 min after the bolus injection, centrifuged and the plasma removed. The plasma (25 µl) was then added to four ml of Biodegradable Counting Scintillant BCS (Amersham Pharmacia Biotech, IL) and glucose radioactivity was determined using a scintillation counter (Perkin Elmer Inc., Tri-Carb 2800TR, IL, USA).

At the conclusion of the experiment, the soleus (SOL), plantaris (PLA), gastrocnemius red (RG), gastrocnemius white (WG), extensor digitorum longus (EDL) and tibialis anterior (TIB) muscles were dissected, freeze-clamped using liquid nitrogen-cooled tongs and stored at -80°C.

The frozen muscles were powdered under liquid nitrogen and 100 mg of muscle tissue was homogenised with 1.5 ml water using a Heidolph™ silent crusher M (27000 $rpm.min^{-1}$). Free and phosphorylated [^{14}C] 2-DG were separated by ion exchange chromatography using an anion exchange resin (AG® 1-X8, Bio-Rad laboratories, CA). Biodegradable Counting Scintillant (16 ml; Amersham Pharmacia Biotech, IL, USA) was added to each sample and the radioactivity determined using a liquid-scintillation counter (Perkin Elmer Inc., Tri-Carb 2800TR, IL, USA). R'g, which reflects the glucose uptake into the muscle, was calculated using these counts from the individual muscles and the decay rate (calculated from the arterial plasma radioactivity figures), as previously described by others [285, 286]. R'g is expressed as $\mu g.g^{-1}.min^{-1}$ of muscle (wet weight).

2.3.4 Glucose and Lactate Determination

Whole blood and plasma glucose and lactate concentrations were measured using a glucose analyser (Model 2300 Stat plus, Yellow Springs Instruments, OH) during the experiment. A sample of 25 µl was required for each assay and concentrations were determined by the glucose oxidase method.

Glucose uptake ($\mu mol.min^{-1}$) and lactate release ($\mu mol.min^{-1}$) were calculated by multiplying the arterial-venous glucose difference by femoral blood flow.

2.3.5 Hindlimb contraction by electrical stimulation

When the protocol required contraction (ie. exercise simulation), a Nerv-Muskel-Reizgerat stimulator (Hugo Sachs Electronics) was used to stimulate contraction of the lower leg muscles. The skin was removed from the knee area and an electrode attached, with a second electrode placed through the Achilles tendon. The foot was secured to minimise movement. Twitch stimulation was performed, with 0.1 ms pulses applied at 2 Hz. Voltage was set to 35 V.

When force measurements were required, the leg was stabilized in a jig, with a pin securing the bone around the knee. A hook was inserted through the Achilles tendon and attached by a metal rod to isometric transducer to allow a constant measure of tension development via the WINDAQ software program.

2.4 Data Analysis

All data are expressed as means ± SEM. Mean femoral blood flow, mean heart rate and mean arterial pressure were calculated using five second sub-samples of WINDAQ data, which represented 501 flow and pressure measurements. These measurements were taken every 15 min during the experiment. Vascular resistance in the hindlimb was calculated by dividing mean arterial pressure (mmHg) by femoral blood flow ($ml.min^{-1}$) and was expressed as resistance units (RU).

2.5 Statistical Analysis

To ascertain differences between treatment groups at the conclusion of the experiment, a one-way ANOVA was used. Differences between initial (samples taken before treatment) and final (samples taken at the conclusion of the experiment) values were assessed using a paired *t*-test. Comparisons were made between treatment groups over the course of the experiment using a two-way repeated-measures ANOVA and Student-Newman-Keuls post hoc test. Significance was accepted at a level of $p<0.05$. All tests were performed using SigmaStat software (Systat Software Inc. California, USA).

CHAPTER 3:

CEU OF CAPILLARY MODELS *IN VITRO*

3.1 INTRODUCTION

Contrast enhanced ultrasound (CEU) is a method used in cardiovascular research to measure myocardial blood flow [27, 287]. It is a relatively non invasive technique which requires a contrast agent, phospholipid microbubbles (MB), to be infused into the circulation and achieve a steady state concentration. A transducer (interfaced with an ultrasound system) which emits pulses of sound waves is placed over the region of interest, with each pulse resulting in acoustic signals produced by the microbubbles within the vasculature. This signal can then be visualised using the ultrasound system. By using a high mechanical index to destroy the microbubbles and manipulating the time between each pulse of ultrasound, the microvascular volume and the rate of fill of the microvasculature can be assessed.

CEU has been adapted for use in skeletal muscle and its application has shown increased microvascular perfusion during exercise and insulin infusion in both humans [25, 288], and rats [28, 38] *in vivo*. As discussed in Chapter 1, it is the ability of insulin and exercise to increase microvascular perfusion, and not bulk flow, which is important for glucose uptake. This is shown by experiments using low dose insulin, which increase microvascular perfusion and glucose uptake without affecting total blood flow. [29]. It has been proposed that capillary recruitment in response to stimuli such as contraction and insulin may occur by one of two methods. Firstly, by flow sharing into capillaries of similar properties, where capillary blood flow rate may be expected to decrease, or secondly, by redistributing flow from short to long tortuous capillaries where capillary blood flow would not be expected to change. It is not known whether CEU is able to distinguish between these two patterns of flow redistribution.

Unlike the method of 1-MX metabolism, which may only be used to measure microvascular perfusion at the end of an experiment (due to the large sample volume required), CEU has the advantage that multiple measurements may be made throughout the course of an experiment. In addition, CEU is able to make measurements of a large region of interest (such as the calf muscle), without disrupting the tissue (which may occur with microdialysis) or blood flow in that region. To date, only one modelling study using CEU has been reported and this

found bulk flow to correlate with measured filling rate, but capillary volume was not assessed [26].

The aim of this project was to validate the CEU technique in a capillary tube model and to assess the effect of bulk flow on microvascular volume. Furthermore, this study determines if CEU is able to discriminate between different flow patterns which may account for increased microvascular perfusion *in vivo*.

3.2 METHOD

3.2.1 Capillary Models

Preliminary experiments showed that the thickness of the tubing wall could affect the reflected signal received from the ultrasound, thus masking the signal from the microbubbles. Therefore, thin-walled microdialysis tubing (BAS Bioanalytical Systems Inc. IN, USA) with an external diameter of 320 μm and an internal diameter of 280 μm was used to construct the capillary models. The capillary tubing models were held in position by a Perspex frame positioned under the ultrasound transducer (Fig. 3.1). To allow conduction of ultrasound, the capillary tubing and head of the transducer were immersed in a beaker of water.

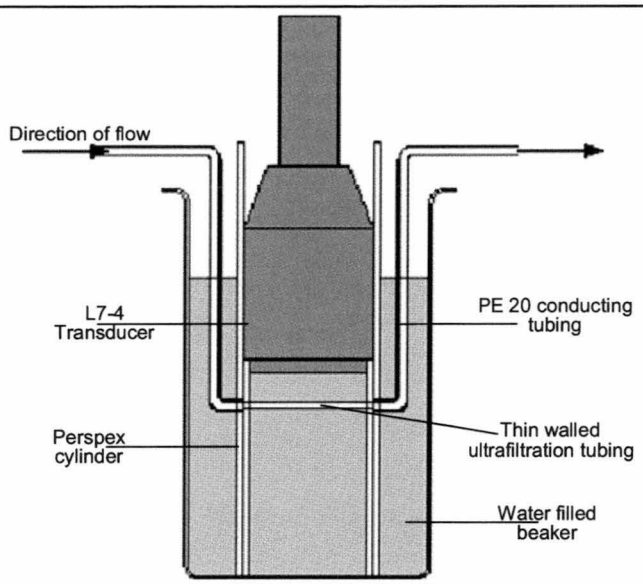

FIGURE 3.1: CAPILLARY MODEL APPARATUS. The capillary model was made from thin walled microdialysis tubing, adhered to thicker PE 20 plastic tubing to allow the delivery of microbubbles. The ultrasound transducer and the capillary model were held in place by a Perspex cylinder, and both were submersed in distilled water to allow conduction of the ultrasound signal.

Three separate capillary tubing models were made. The first model consisted of a single piece of tubing to test the effects of a microbubble delivery rate on the signal received (Fig. 3.3A). A 60 mm length of capillary tubing was used and a 23 gauge stainless steel needle (10 mm in length, which had been removed from a hypodermic needle and blunted) was inserted into one end of the tubing. This in turn was joined to a length of non-permeable conducting tubing (PE 20, Becton Dickinson; NJ, USA) by a short sleeve (1.5 cm) of PE 50 (Becton Dickinson; NJ, USA) tubing. All junctions were sealed with water-proof glue (Araldite®). The opposite end of the capillary tubing was similarly attached to another length of PE 20 to allow the continuous perfusion of microbubbles through the model (Fig. 3.2).

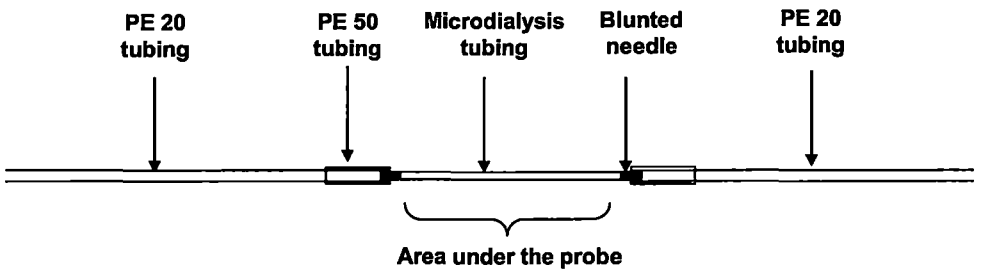

FIGURE 3.2: CAPILLARY MODEL CONSTRUCTION. Microdialysis tubing was used as the capillary model, and was the only portion of tubing within the field of measurement under the ultrasound probe. The microdialysis tubing was attached to a length of PE 20 plastic tubing at each end (in order to allow the flow of microbubbles through the model) via a blunted needle tip and a sleeve of PE 50 plastic tubing. All junctions were sealed with water-proof glue (Araldite®).

The second model aimed to compare the characteristics of a long tortuous capillary with a short capillary and consisted of a long piece of tubing connected in series versus one straight piece of tubing (as described above). The 'in series' model consisted of three lengths of microdialysis tubing joined with needles and PE 20 tubing as described above, so that each capillary doubled back under the face of the transducer, creating a zigzag pattern (Fig. 3.3B).

The third model was a manifold which allowed comparisons to be made between the perfusion of one, two, three or four capillaries. The microdialysis tubing was packaged so that 6 capillary tubes arose from one larger piece of tubing (similar in size to PE 20). Therefore, to construct the manifold these 6 lengths of microdialysis tubing were attached to PE 20 as described above. Two lengths were permanently sealed with snug-fitting stainless steel wire and the four remaining lengths were closed (when required) with removable clamps (Fig. 3.3C).

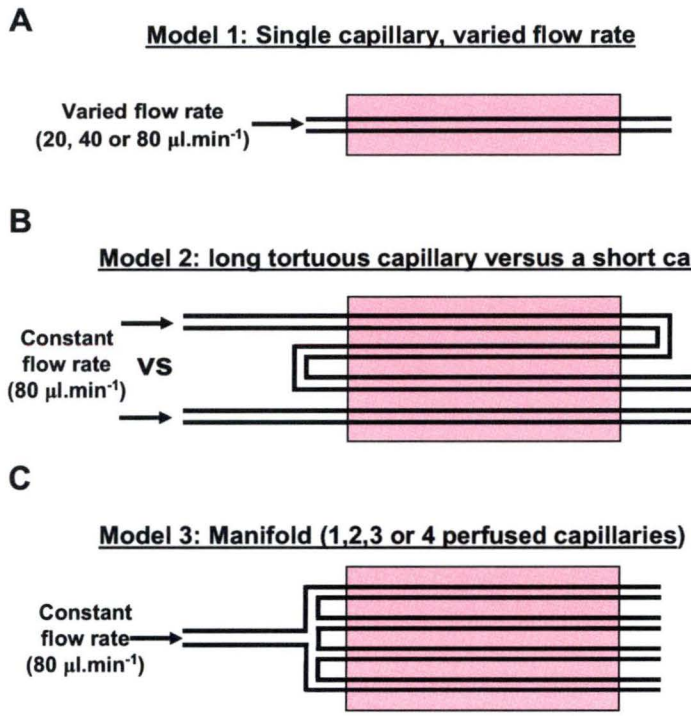

FIGURE 3.3: CAPILLARY MODEL ARRANGEMENTS. (A) The single capillary model where delivery rate was varied. (B) A tubing model connected in series, where the flow through a long tortuous capillary, which crosses the region of interest three times is compared to a short capillary. (C) A manifold model, where one, two, three or four capillaries were compared at a constant flow rate. The region of interest is shown by the coloured box around each model.

3.2.2 CEU measurements

Images were collected by CEU as described in section 2.3.2.2 with the following adaptations for use in a model system.

Commercially available perfluorocarbon gas-filled albumin microbubbles (MB; Optison™, Amersham), diluted with isotonic saline (previously gassed with perfluorocarbon) were used as the contrast medium (~750 MB.µl^{-1}). The microbubbles were delivered at 20, 40 or 80 µl.min^{-1} as specified, by a syringe pump, which was continuously mixed by rotation to maintain an even suspension. The delivery lines were also vibrated to prevent an uneven infusion of microbubbles. CEU measurements were made at a mechanical index of 1.0 that was capable of destroying all bubbles in the ultrasound beam. The capillary tubing was at a depth of

4.1 cm and the gain settings were held constant between all experiments. A region of interest was selected around all the tubing in the field of vision as shown in Figure 3.3. Pulsing intervals of 0.2, 0.3, 0.5, 1, 2, 3, 5, 8, 12 and 15 s were used, and 5 frames were captured at each interval. The intensity value at each of these frames was averaged and then plotted against time resulting in a pulsing interval curve. Capillary tubing volume (A) and capillary filling rate constant (β) were then calculated using the equation $y = A\ (1 - e^{-\beta t})$, where y is equal to the acoustic intensity at a given pulsing interval (see section 2.3.2.2). Capillary tubing volume (A) was multiplied by the capillary tubing filling rate constant (β) to give a measure of flow rate.

3.2.3 Experimental design

Initial experiments focused on establishing a suitable concentration of microbubbles for use in the model system, using the single capillary tubing model. The acoustic intensity at a pulsing interval of 8 s was graphed as a function of microbubble concentration (Fig. 3.4). The concentration infused was varied by diluting the commercial Optison™ suspension at 1:10; 1:20; 1:40; 1:60; 1:80; 1:100; and 1:120 with isotonic saline previously gassed with perflourocarbon. A 1:10 dilution corresponded to ~2400 microbubbles per µl. From this concentration curve an optimal dilution of 1:50 was determined and used for all capillary model experiments.

A single capillary, variable delivery rate model was used to determine if flow rate affected the volume (A) or filling rate constant (β). A single length of capillary tubing was positioned under the longer axis of the transducer. Microbubbles were infused at 20 $\mu l.min^{-1}$ and an image set consisting of 5 images captured at each intermittent pulsing interval was collected. This process was then repeated at flow rates of 40 and 80 $\mu l.min^{-1}$. The order of flow rate change was randomised in subsequent experiments. A pulsing interval curve was constructed for each flow rate and capillary tubing volume (A) and filling rate constant (β) was determined.

A tubing model connected in series was used to determine the flow pattern changes between a single short capillary and a long capillary which crossed the field of measurement three times. The long tortuous capillary and short capillary were under the same region of interest. The three lengths of tubing for the model connected in

series passed under the long axis of the transducer and were arranged vertically, with the space between each length approximately 5 mm. A single length of capillary tubing, with its own inflow and out flow tube, was positioned 5 mm below the tubing connected in series in the same region of interest allowing accurate comparisons to be made between the long and short capillary tubing models. The flow rate for both was set to 80 $\mu l.min^{-1}$ and an image set was captured as described above in a randomised manner between the two capillary tubing arrangements. Pulsing interval curves were constructed from each image set to determine capillary tubing volume (A) and filling rate constant (β).

A manifold arrangement was used to determine flow pattern change involving the sharing of flow from a single capillary to multiple capillaries. A manifold model of four identical lengths of capillary tubing was positioned with each length in parallel, and one above the other, under the long axis of the transducer. The space between each length of capillary tubing was approximately 5 mm. Flow was set to 80 $\mu l.min^{-1}$ and initially confined to only one capillary by using removable clamps to prevent flow into the other three capillaries. An image set was captured as described above. Flow was then shared between two capillaries and a second set of images was captured. Flow was then allowed to pass through three and then four capillaries, with an image set captured at each. Subsequent image sets were captured in a randomised manner for each of the tubing arrangements, with flow maintained at 80 $\mu l.min^{-1}$ throughout the experiment. Pulsing interval curves were constructed from each image set to determine capillary tubing volume (A) and the filling rate constant (β).

3.2.4 Statistical analysis

A one-way repeated measures ANOVA was used to determine differences between groups in the single tubing and manifold models. A paired t-test was used to determine differences between the long versus short capillary tubing model. Data are presented as mean ± standard error of the mean and significance was accepted at a level of $p<0.05$. All tests were performed using SigmaStat software (Systat Software Inc. California, USA).

3.3 RESULTS

3.3.1 Microbubble concentration

Figure 3.4 shows a graph of microbubble concentration versus acoustic intensity during 8 s pulsing intervals measured when microbubbles were infused into a single capillary tubing model. The graph shows that the microbubble concentrations begin to plateau at a dilution of 1 in 40 (approximately 600 MB per µl). Accordingly, a dilution of 1 in 50 (750 MB per µl) was chosen for all model experiments as this concentration fell in the linear portion of the graph. A higher concentration of microbubbles may have attenuated the received signal, while a lower concentration may not provide a strong enough signal to enable differences to be measured.

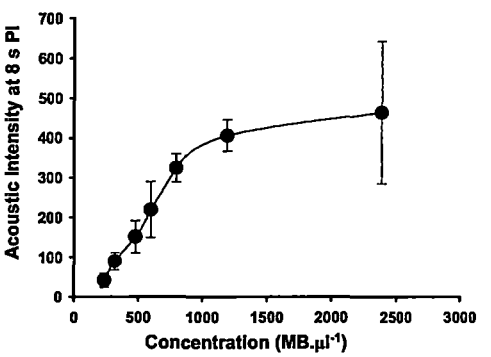

FIGURE 3.4: MICROBUBBLE CONCENTRATION CURVE. Optison™ microbubbles were infused into a single capillary tubing model at various concentrations to establish a concentration curve. The acoustic intensity at a pulsing interval (PI) of 8 s is graphed as a function of microbubble concentration. A concentration of approximately 750 microbubbles per µl (MB.µl^{-1}) was used for all model experiments. Values are means ± SEM (n=5)

3.3.2 Effect of flow rate on CEU signal

Figure 3.5 shows the A, β and A x β data for the single tubing model, where various flow rates were used. A representative ultrasound image is also shown. This model was used to demonstrate how the ultrasound can distinguish between changes in volume and fill rate. The calculated capillary volume, as represented by the A value, was unaffected by changes in flow rate. The refill rate constant (β) and consequently

the A x β measure of capillary flow rate, increased as the flow rate increased from 20 to 40 and 80 µl.min^{-1}.

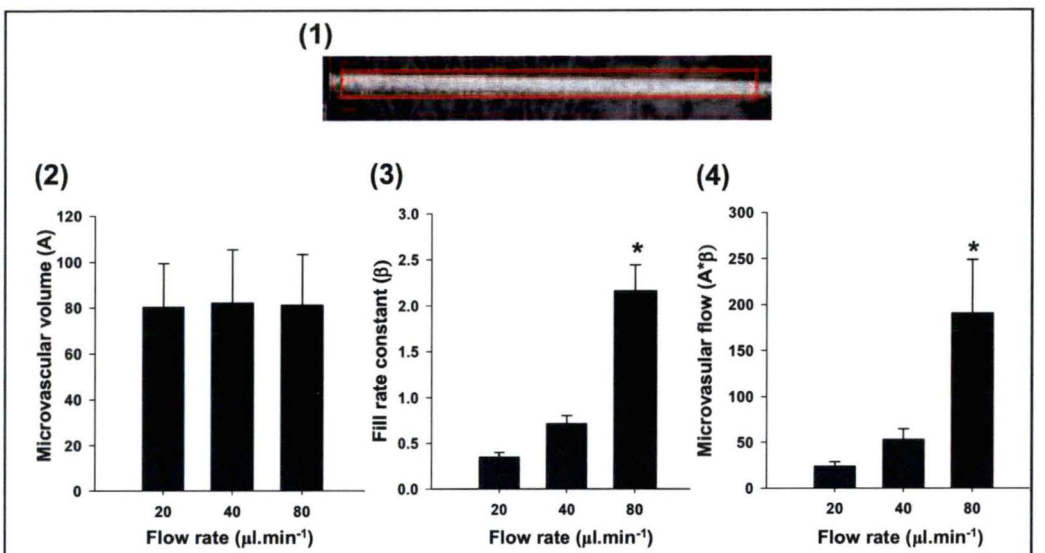

FIGURE 3.5: SINGLE CAPILLARY TUBING MODEL. Microbubbles were infused at 20, 40, or 80 µl.min^{-1}. Pulsing interval curves were conducted as described in the text. A, β and the product $\beta \times A$ were interpolated from the equation $y = A(1\text{-}e^{-\beta t})$. Panel 1 shows representative image of the single tubing model captured at a 15 s pulsing interval and the region of interest is outlined in red. The effect of flow rate on capillary tubing volume (A), filling rate constant (β), and microvascular flow ($\beta \times A$) as determined by CEU are shown in panels 2, 3 and 4 respectively. Values are means ± SEM (n=7). *, significantly different to 20 µl.min^{-1} and 40 µl.min^{-1} flow rates (p<0.05).

3.3.3 Effect of long tortuous capillary versus short capillary on CEU signal

Figure 3.6 shows the A, β and A x β data for the model simulating a shift in flow pattern for a long tortuous capillary passing through the ultrasound beam three times versus a short capillary passing through the ultrasound beam only once. Flow rate was set to 80 µl.min^{-1} and comparisons were made between pulsing interval curves constructed from the tubing connected in series versus a single capillary tube model. Both tubing arrangements were in the same region of interest as shown in Figure 3.6 (panel 1). The graph for the A value shows that the capillary volume of the long tortuous capillary was three times that of the short capillary. In contrast, the β value decreased, so that there was no change in the product A x β.

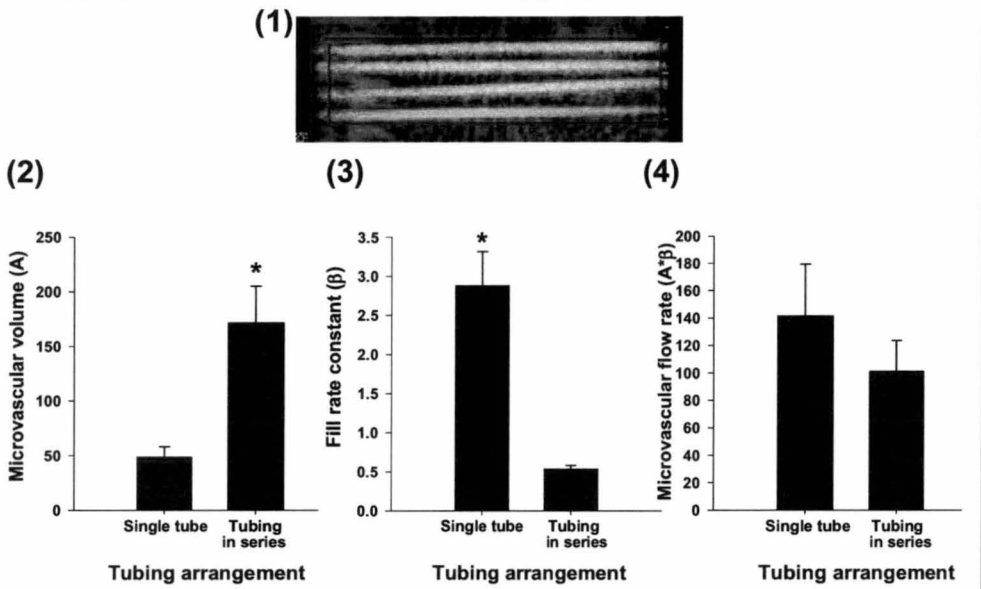

FIGURE 3.6: TUBING CONNECTED 'IN SERIES' MODEL. Panel 1 shows a representative image of the in series model captured at a 15 s pulsing interval, during perfusion of the longer tubing. The region of interest is outlined in red. The effect of flow pattern change from a single short capillary tube (labelled single tube) to a long capillary tubing crossing the field of measurement three times (labelled 'tubing in series') on capillary tubing volume (A), filling rate constant (β) and microvascular flow rate ($\beta \times A$,) as determined by CEU, are shown in panels 2, 3 and 4 respectively. Microbubbles were infused at a constant rate of 80 $\mu l.min^{-1}$. Pulsing interval curves were conducted as described in the text. β, A and the product $\beta \times A$ were interpolated from the equation $y = A(1\text{-}e^{-\beta t})$. Values are means ± SEM (n=9). *, significantly different to 'tubing in series' arrangement (p<0.05).

3.3.4 Effect of flow sharing on CEU signal

Figure 3.7 shows the A, β and A x β data and a representative ultrasound image for the manifold model, which was intended to simulate capillary recruitment. The flow rate was set at 80 $\mu l.min^{-1}$ and was shared between one, two, three or four capillary tubes. As the number of perfused capillaries increased, the capillary volume increased. This was accompanied by a proportional decrease in the filling rate constant resulting in an unaltered flow rate as measured by A x β value.

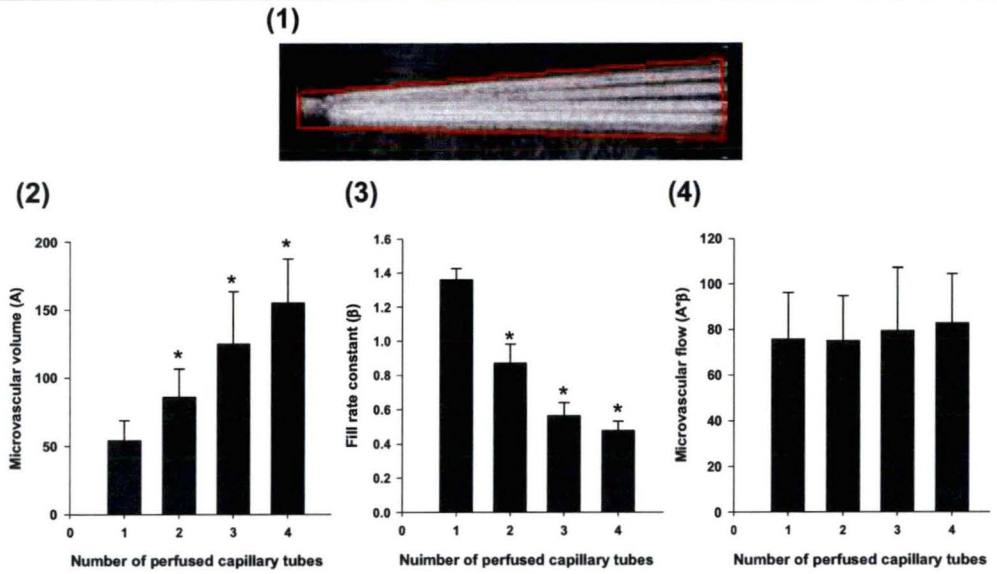

FIGURE 3.7: FLOW SHARING MANIFOLD MODEL. Panel 1 shows a representative image of the manifold model captured at a 15 s pulsing interval during perfusion of all four capillaries. The region of interest in outlined in red. The effect of flow pattern change involving the sharing of flow from a single capillary to capillaries on filling rate constant (β), capillary tubing volume (A) and flow rate ($\beta \times A$), as determined by CEU, are shown in panels 2, 3 and 4 respectively. Microbubbles were infused at a constant rate of 80 $\mu l.min^{-1}$. Pulsing interval curves were conducted as described in the text. β, A and the product $\beta \times A$ were interpolated from the equation $y = A(1\text{-}e^{-\beta t})$. Values are means ± SEM (n=7). *, significantly different to one tube (p<0.05).

3.4 DISCUSSION

The use of capillary tubing models has revealed a number of important findings. Firstly, providing thin-walled tubing is used, there is a dose dependent effect of microbubble concentration on acoustic intensity. Secondly, it was shown that the CEU technique measures changes in microvascular volume and is not influenced by increases (or decreases) in bulk flow. This was demonstrated by the single tubing, variable flow rate model, where a four-fold increase in flow gave identical measures of microvascular volume. This was accompanied by an increase in the rate of fill constant (β), demonstrating that the CEU recognised the increase in flow rate. This affect was also evident in the A x β value which showed an increase in microvascular flow as the flow rate increased. Accordingly, use of this technique *in vivo* is likely to detect a change in microvascular volume during muscle contraction or high doses

insulin, without being influenced by increased bulk flow. Independence between bulk and microvascular flow has been assumed in previous *in vivo* studies based on the knowledge that increases in bulk flow can be accommodated by increased flow in the non-nutritive route, however independence between bulk flow and microvascular perfusion has not been directly shown previously. Another assumption is that the acoustic signal emitted from the bursting microbubbles is only proportional to the microbubble number and not by the motion of the microbubbles that increases as flow increases. This study has confirmed these preconceived ideas. The CEU technique contrasts with laser Doppler flowmetry where the signal predominantly reflects non-vectorial motion rather than particle number, and may only be used as a measure of microvascular perfusion when bulk flow remains unchanged [33].

The β value and resulting A x β product in this model increased in direct proportion between the 20 and 40 µl.min^{-1} flow rates, but not at 80 µl.min^{-1}. This may be caused by the rapid filling of the tubing volume at this flow rate (demonstrated by the sharp rise in acoustic intensity during shorter pulsing intervals, Fig 3.8), which occurred to quickly for an accurate measure of the β value in this model. This higher flow rate was necessary however, to measure changes in the flow sharing models, where flow was ultimately distributed between four capillaries resulting in a flow rate of 20 µl.min^{-1} in each capillary.

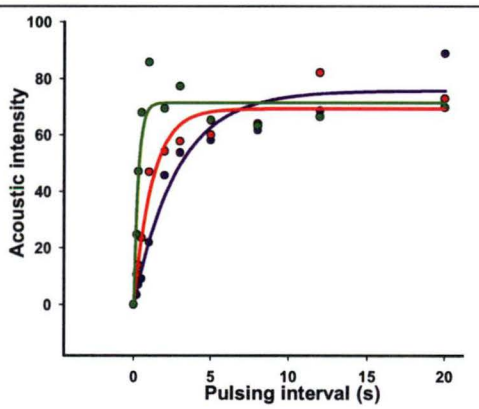

FIGURE 3.8: REPRESENTATIVE PULSING INTERVAL CURVES AT 20, 40 AND 80 µL.MIN^{-1} IN THE SINGLE CAPILLARY MODEL. This figure shows the acoustic intensity of each pulsing interval plotted against time for each flow rate (a representative plot from each) and shows the sharp increase in acoustic intensity during the 80 µl.min^{-1} flow rate (●) in comparison to the lower flow rates of 20 (●) and 40 ul.min^{-1} (●).

The third finding from this study was that the CEU method was not able to discriminate between the two flow pattern changes thought most likely to occur as a consequence of increased microvascular perfusion *in vivo*. These two flow pattern changes were chosen to reflect the possible changes which may occur *in vivo* in response to insulin or contraction. In one model, it has been proposed that insulin acts on the muscle microvasculature through a combination of vasodilation and vasoconstriction, possibly involving nitric oxide and endothelin respectively [289]. This combination may result in blood redistribution from relatively short, low resistance, high capacitance vessels to longer tortuous vessels. The active vasoconstriction may occur by restricting flow to the shorter vessels, and redistributing flow to the longer more tortuous vessels where a higher degree of nutrient exchange occurs [53]. In the other model, flow may be shared from one main route (as only one third of capillaries are perfused at rest [15]) to a number of different capillaries increasing the surface area for nutrient exchange.

The effects of these changes were shown by the tubing model connected in series. In this model, microvascular volume increased, and the rate of fill constant decreased, when perfusion was switched from a longer capillary to a shorter capillary. There was however no change in the calculated microvascular flow ($A \times \beta$) between the long or short capillary tube. A similar result was seen in the second flow sharing model, where flow initially in one capillary, was shared between one, two, three or four capillary tubes, at the same flow rate of 80 $\mu l.min^{-1}$. In this model, the microvascular volume increased with increased flow sharing, while the rate of fill constant decreased, resulting in unchanged microvascular flow ($A \times \beta$). The CEU technique is therefore unable to deduce the type of flow pattern changes that occur *in vivo*, since it can only detect volume filling rate and not red blood cell velocity as first thought [290]. If we had been able to measure red blood cell velocity, a decrease would have been expected in the flow sharing manifold model as increased perfusion occurs as a result of flow being distributed from one to a number of capillaries. In contrast, red cell velocity would not be expected to change if increased perfusion resulted from flow being redirected from a short to a longer capillary.

The use of these capillary tubing models shows the consequences of a redistribution of flow in the capillaries on CEU signal and how these results may be interpreted to show changes in capillary volume and capillary fill rate. However, there are short comings with these models as the results show a lack of proportionality between the different flow rates in each model. This may result from a number of factors. For example, as explained above (Fig. 3.8), the higher flow rate of 80 $\mu l.min^{-1}$ results in a very sharp increase in intensity resulting in possible error in the calculation of the microvascular fill rate. Furthermore, there is a slight variation in the microbubble concentration between experiments as the microbubble infusion solution is prepared before each experiment, which may result in variations in the acoustic intensity. This is not problematic during *in vivo* experiments as the microbubble solution is further diluted in the systemic circulation of the animal or human, minimising any inaccuracies. In the model system, any slight changes are magnified as the microbubbles are infused without further dilution into the model system. The error is also increased as the capillary tubing contributes to the background image making it harder to distinguish changes in the microbubble signal intensity. *In vivo*, the capillaries are considerably smaller and are not seen as a background image thus decreasing the intensity and reducing the interference of the background image, resulting in a more accurate measure of capillary flow. Despite these limitations, this model system shows that the CEU method is able to measure changes in capillary perfusion regardless of changes in total flow, and demonstrates how the data should be interpreted in terms of fill rate and capillary volume.

There are a number of studies which have assessed microvascular perfusion *in vivo* using the CEU technique. Dawson et al. [28] used the CEU method to assess the microvascular perfusion increase in the rat hindlimb in response to both hyperinsulinaemia and muscle contraction. Contraction resulted in a large increase in femoral blood flow (300% over basal) and an increase in both microvascular volume and the microvascular flow rate constant (β). Hyperinsulinaemia also increased femoral blood flow (by 50%) and microvascular volume, however there was no change in the flow rate constant which is most likely the result of flow sharing or flow redistribution in the hindlimb vasculature. Coggins et al.[25] confirmed insulin's ability to increase microvascular perfusion without influencing bulk flow in the forearm of normal healthy individuals. A low dose of insulin increased the capillary

blood volume by 54% and decreased the fill rate constant by 42%. As the data from the capillary model shows, the decrease in the fill rate constant is expected due to a redistribution of flow and an increase in the perfused surface area with insulin infusion. Similarly, Clerk et al.[99] found an increase in capillary blood volume and brachial artery flow, and a trend towards a decreased flow rate constant in healthy humans during a 1 $mU.min^{-1}.kg^{-1}$ euglycaemic hyperinsulinaemic clamp. Interestingly this increase in capillary blood volume was not seen in obese subjects. A similar pattern of results was also observed during low intensity handgrip exercise where brachial artery blood flow and microvascular blood volume increased and the flow rate constant decreased, supporting the notion of flow distribution and microvascular recruitment [288].

In summary, the CEU method measures changes in microvascular recruitment and is not affected by changes in bulk flow. Although changes in both microvascular volume (A) and the microvascular filling rate (β) can be distinguished by the CEU, these two parameters are inversely related and therefore are unable to discriminate between increased microvascular perfusion resulting from either flow redistribution from short to long tortuous capillaries and/or by flow sharing from one into many capillaries. The CEU method is however, a valuable tool in measuring changes in microvascular perfusion.

CHAPTER 4:

CONTRACTION-MEDIATED SENSITISATION OF SKELETAL MUSCLE

4.1 INTRODUCTION

Experiments using the perfused hindlimb model have shown that skeletal muscle contraction is capable of increasing glucose uptake without the presence of insulin [291, 292]. Furthermore, skeletal muscle contraction is able to increase glucose uptake in insulin resistance models and type 2 diabetic patients [87, 101, 292] and the addition of insulin infusion during contraction in normal subjects results in an additive effect on glucose uptake [293]. This implies that insulin and contraction have separate signalling mechanisms which result in the ability to increase glucose uptake into the cells. It has been suggested that there may be two pools of GLUT4, with each pool stimulated in response to either insulin or exercise, which may account for the additive effect when the two stimuli are combined [10].

An acute bout of exercise results in an increase in the sensitivity of the working muscles to insulin stimulation post exercise [112] and occurs independently of changes in the initial steps of the insulin signalling cascade (eg. the extent of insulin receptor tyrosine phosphorylation) [123, 124]. The magnitude of the sensitisation effect is related to the pre-existing level of glycogen present in the muscle, as glycogen depletion results in a greater response to insulin stimulation during recovery [117, 119]. This sensitisation may also involve the activation of AS160, an Akt substrate which is phosphorylated by both stimuli and is involved in GLUT4 translocation to the plasma membrane [105, 127]. While the insulin signalling pathway acts through PI3-kinase dependent mechanisms, the contraction mediated signalling pathway appears to be regulated by a number of different mechanisms (including Ca^{2+}-dependent kinases, calcium calmodulin protein kinase and/or protein kinase C, and AMPK) which are still to be established [129].

From a haemodynamic perspective, there are similarities between the actions of insulin and contraction, but there are also issues that have not been explored. Like insulin, contraction also results in an increase in microvascular perfusion. For insulin, the reversal in capillary perfusion after insulin stimulation (measured by 1-MX metabolism) occurs within 30 min after plasma insulin levels had returned to baseline levels from a hyperinsulinaemic euglycaemic clamp, showing that perfusion remains enhanced for some time after insulin stimulation [29]. This may also be true for

exercise, as the microvasculature may remain perfused in order to assist with the replenishment of nutrients and waste removal during the post exercise period. Also, as the microvasculature is initially recruited in response to the metabolic needs of the muscle during exercise [144], it is plausible that these requirements may also regulate the reversal of this response post exercise. Many of the current studies assessing insulin sensitisation post-exercise focus on the myocyte signalling cascades involved in mediating this effect, however there has been very little research assessing the involvement of blood flow in this response.

Honig et al. [294] found that capillaries in the gracilis muscle were recruited in response to twitch stimulation frequency at less than 0.5 Hz and these changes occurred independently of changes in total blood flow. That study highlighted the independence between bulk and microvascular flow, and shows that even though bulk flow returns to basal levels relatively quickly post exercise, it is possible that the microvasculature may remain perfused for some time after. However, using *in vivo* microscopic techniques, Klitzman et al. [295] found that microvascular perfusion in the cremaster muscle of the hamster had returned to basal levels within 120 s of the end of contraction. It is important to note though, that only a single muscle was examined, therefore these results may be only specific to that fibre type and the function of that muscle, reflecting the notion that as both flow and metabolism are influenced by fibre type [66]. In addition, since the procedures used required exposure of the muscle surgically, followed by denervation, the muscle may have altered the capillary response resulting from disruption of the surrounding vessels and the sympathetic control required to maintain vascular tone at rest. Furthermore, studies in this laboratory at the University of Tasmania have shown that cutting the sciatic nerve results in a substantial increase in femoral blood flow and hyperaemia.

Therefore, the present study aims to examine the effect of a single bout of contraction on metabolic and haemodynamic parameters *in vivo*, with a view to assessing the relationship between the parameters, in a relatively non-invasive manner, as well as the time course for the return to basal levels post-contraction. This study also used the erythrocyte perfused hindlimb as a means to separate the microvascular response to contraction (which is not seen in this fully dilated system) and the effect of contraction directly on the myocyte.

4.2 METHODS

4.2.1 In vivo experiments

4.2.1.1 Animals

Male hooded Wistar rats weighing 250 ± 7g were used for these experiments. They were raised as described in section 2.2.1.

4.2.1.2. In vivo surgery

Experiments were conducted using the anaesthetised rat model, with surgery as described in section 2.2.2. A Transonic™ flow probe was placed around each femoral artery in order to monitor blood flow in both the contracted and resting hindlimb.

4.2.1.3 In vivo experimental procedure

After a 45 min equilibration period, the lower leg muscles of one hind limb was stimulated to contract by electrical pulses (0.1 ms pulses applied 2 Hz, 35 V; as described in section 2.3.5) for 10 minutes. Saline was then infused at 10 $\mu l.min^{-1}$ for 60 min (Fig. 4.1) to measure post contraction events. At the conclusion of the experiments the muscles of the calf (soleus, plantaris, red gastrocnemius, white gastrocnemius, extensor digitorum longus and tibialis anterior) of both the control and treatment legs were removed and freeze clamped under liquid nitrogen. The muscle samples were then stored at -80°C until required for determination of muscle glucose uptake.

Arterial (via the carotid artery) and venous (via the epigastric vein) blood samples were taken at the times indicated in Figure 4.1 and analysed for blood glucose and lactate concentrations and used to calculate hindlimb glucose uptake (refer to section 2.3.4). Muscle glucose uptake was determined by using 2-deoxy-D-[1-^{14}C] glucose (2-DG; specific activity = 56.0 $mCi.mmol^{-1}$, Amersham Pharmacia Biotech) method as described in section 2.3.3.

The CEU method (refer to section 2.3.2.2) was used to determine microvascular perfusion. Two CEU 7-4 MHz transducers were used to measure flow in the contracting and contra-lateral control legs. A transducer was placed over the calf

muscle region of each limb allowing imaging of the soleus, plantaris, red and white gastrocnemius muscles during electrical stimulation or at rest. The mechanical index was set to 0.8, and gain settings were standardised for all experiments. A 40-fold dilution of gas-filled phospholipid microbubbles (see Section 2.1.1; 'microbubble contrast agent' for composition) was infused at a rate of 40 $\mu l.min^{-1}$ into the rat, via the jugular vein. The infusion pump and syringe containing the microbubble solution was continuously mixed to ensure the microbubbles maintained an even suspension and the delivery line to the rat was also vibrated. Microbubbles were infused 5 min prior to commencing 15 s pulsing intervals to allow the microbubble concentration to reach steady state. As the microbubbles interfere with the Doppler flow measurements, femoral blood flow was assessed in a separate group of experiments.

4.2.1.4 In vivo protocol

The time course of changes in microvascular volume, flow and glucose uptake were determined during 10 min of contraction and for 60 min post-contraction. Microvascular volume and flow were assessed using the CEU technique in continuous pulsing mode at intervals of 15 s throughout the basal and 10 min contraction period and for 60 min post-contraction. Pulsing intervals of 15 s were chosen as the PI curves obtained in previous experiments showed the PI curve had reached a plateau at this point (ie. 15 s) and thus was indicative of full microvascular perfusion (Fig. 4.1).

During the protocol (Fig. 4.1), muscle glucose uptake was assessed by using 2-DG method as described in section 2.3.3. At the conclusion of the experiments (60 min post exercise) the muscles of the calf (soleus, plantaris, red gastrocnemius, white gastrocnemius, extensor digitorum longus and tibialis anterior) of both the control and treatment legs were removed and freeze clamped under liquid nitrogen. The muscle samples were then stored at -80°C until required for determination of muscle glucose uptake.

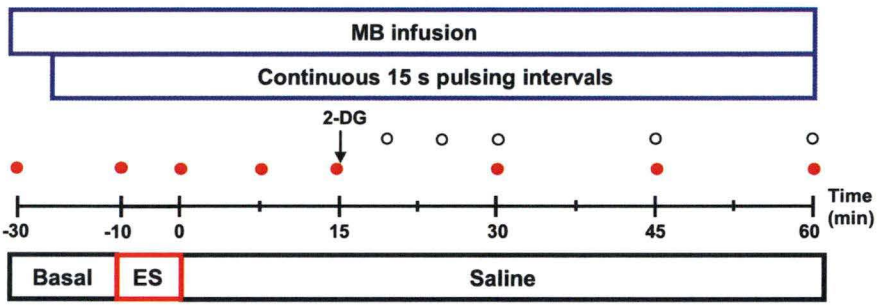

FIGURE4.1: ***IN VIVO* PROTOCOL:** Contrast enhanced ultrasound (CEU) was used to examine the time course of microvascular volume changes during basal, 10 min contraction with electrical stimulation (ES; 2Hz, 0.1msec pulse, 35 V) and 60 min post-contraction. Phospholipid microbubbles were infused throughout the experiment and continuous 15 s pulsing intervals were used to gain a measure of microvascular volume. To determine muscle glucose uptake 2-deoxy-D-[1-^{14}C] glucose (2-DG) was administered as a bolus at 15 min and the muscles of both the contracted and rested hindlimbs were freeze-clamped under liquid nitrogen at the conclusion of all experiments for further analysis.

Horizontal bars represent electrical stimulation, microbubble (MB) infusion, continuous 15 s pulsing interval CEU measurements and venous infusions, *red circles* represent arterial blood samples for determination of blood glucose and lactate, *white circles* represent arterial blood samples taken to determine the clearance rate of 2-DG, *arrows* indicate bolus injection of radioactive 2-DG.

4.2.1.5 Determination of plasma insulin concentrations

Arterial blood samples were taken prior to the start of the *in vivo* experiment, and at 60 min post contraction, centrifuged and the plasma was removed and stored at -20°C until required. The plasma was used to determine arterial insulin concentrations using an insulin ELISA kit (Mercodia AB; Sweden).

4.2.2 In vitro experiments

4.2.2.1 Animals

Male hooded Wistar rats weighing 180-190 g were used for these experiments. They were raised as described in section 2.2.1.

4.2.2.2 Hindlimb perfusion surgery

Surgery was essentially as described by Ruderman et al. [296] and is illustrated in figure 4.2. In brief, the surgery involved isolating the hindlimb by ligating the major

abdominal branches, removal of the entire gastrointestinal tract and cannulating the aorta and vena cava, and ligating the contra-lateral leg so that only one leg was perfused. In detail, male rats (180-200 g) were anaesthetised with an intraperitonal injection of pentobarbitone sodium (50 mg/100 g body weight). String ligatures were tied around the tail and the left tarsus (of the leg being perfused). Skin covering the stomach was cut away and a midline abdominal incision was made from the pubic region to the diaphragm. The superficial epigastric vessels were ligated on the right and left sides to allow the abdominal wall and skin to be removed with minimal bleeding. In order to prevent perfusate flow to the skin during perfusion, the vessel supplying the skin from the knee was ligated in the leg to be perfused (left). The small and large intestines were excised by ligating the descending colon twice. Cuts were made between them to limit bleeding. The superior portion of the intestine and the mesenteric artery were then ligated and the gut was removed. The blood vessels supplying the testes were tied and the testes removed, and a common ligature was placed around the seminal vesicles and the neck of the bladder, and the seminal vesicles were removed. The bladder was emptied using a syringe. The connective tissue covering the body wall was teased apart using cotton buds to allow access to the major vessels. The iliolumbar vessels, ureters, renal vessels and internal spermatic vessels were tied using one ligature on both the right and left sides. To prevent the perfusion of the contralateral limb, the right branch of the common iliac vessels was tied below the bifurcation using two silk ties (size 3/0 waxed braided silk). The vena cava and aorta were gently separated using blunt forceps and two silk ligatures were placed loosely around each vessel. Heparin (0.2 ml) was then injected into the vena cava (through fat if possible, to prevent bleeding), and allowed to circulate for one minute. The upper ligature on the vena cave was tightened and the vena cava was cannulated (Surflo® I.V. catheter, 18 G x 11/4", Terumo, Australia). The bottom ligature was tightened around the vessel and cannula, and the upper ligature was tightened around the cannula to keep it in place. The upper ligature on the aorta was then tightened and a small incision was made below the ligature, half way through the aorta. This opening was held open using a fine metal probe and the cannula (Surflo® I.V. catheter, 20 G x 11/4", Terumo, Australia), attached to a saline filled syringe, was inserted into the vessel. The bottom ligature was then tightened around the skin and vessel, and the top ligature secured around the cannula to keep it in place. Saline was then expelled into the vessel to determine if the catheter was

properly placed and to facilitate the removal of residual blood in the hindlimb (which may cause clots) and to minimise air bubbles entering the vasculature. The preparation was then transferred to the perfusion cabinet and attached to the perfusion apparatus connecting the aortic cannula to the tubing containing the oxygenated buffer medium. Once circulation was re-established through the perfusion apparatus, the animal was killed with a lethal dose of pentobarbitone sodium via an intracardiac injection. String was then used to tie off the abdomen (L3, L4 region) to prevent flow of perfusate into lower back muscles. Throughout surgery cotton thread was used as ligatures (unless otherwise specified) and surgery did not exceed 20 min.

All anaesthetic and surgical procedures were approved by the University of Tasmania Animal Ethics Committee.

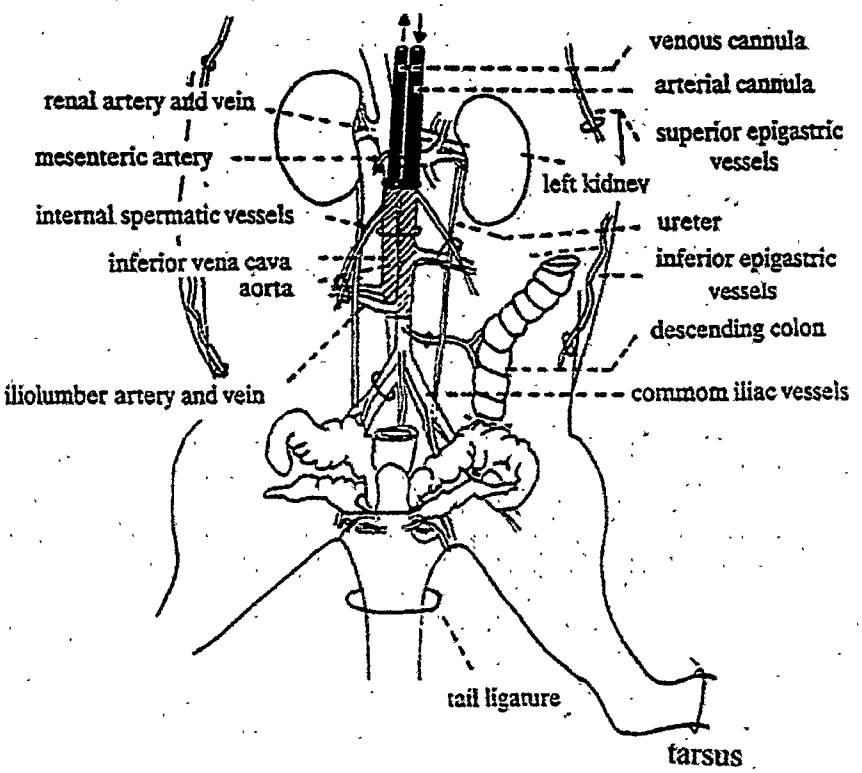

FIG. 4.2: SURGERY FOR THE PERFUSED RAT HINDLIMB: Surgery details are given in section 4.2.2.2 This picture depicts the ventral view of the rat, showing vessel ligation and cannulation performed to isolate blood flow to a single hindlimb (adapted from Ross [297] and Greene [298]).

4.2.2.3 Perfusion medium

4.2.2.3.1 Krebs-Henseleit buffer

Krebs-Henseleit buffer was prepared in distilled water and consisted of:

118 mM NaCl
4.74 mM KCl
1.19 mM KH_2PO_4
1.18 mM $MgSO_4$
25.0 mM $NaHCO_3$
8.30 mM D-glucose
40 $g.L^{-1}$ bovine serum albumin (BSA)*

The buffer was filtered through a 0.45μm filter.
(*, the modified Krebs-Henseleit preparation did not include BSA).

4.2.2.3.2 Erythrocyte preparation

Bovine blood was collected from the abattoir, mixed with a cold anticoagulant solution (consisting of saline containing 5 mM glucose and 0.2% EDTA) and kept on ice during transportation back to the laboratory.

The blood was then centrifuged at 1700 g for 30 min and the supernatant and white blood cell/platelet layer was removed. The erythrocytes were then resuspended in ice-cold saline (0.9% NaCl) and centrifuged again for 30 min at 1700 g. The supernatant and white blood cell/platelet layers were removed. The saline wash procedure was repeated three times. The blood was then resuspended in modified Krebs- Henseleit buffer which had been gassed with carbon dioxide in air (5% CO_2 and 95% air) one hour prior to use, centrifuged at 1700 g for 30 min and the supernatant removed. This procedure was also repeated three times. The erythrocytes were then resuspended in modified Krebs- Henseleit buffer and stored at 4°C in an airtight container.

4.2.2.3.3 Perfusion medium preparation

To prepare the perfusion medium for use, the suspended erythrocytes were centrifuged at 1700 g for 15 min and the supernatant was removed. The erythrocytes were then filtered through 6 layers of cheesecloth which had been soaked in modified Krebs- Henseleit buffer, and combined with a 4% BSA Krebs-Henseleit buffer

medium, in a ratio of 9:11 giving a haematocrit of ~35%. Pyruvate (final concentration of 1.2 mM) and 228 IU/L of heparin was added. The perfusion medium was then gassed with CO_2 (5%) in air for 30 min to give a pH of 7.4. Calcium chloride ($CaCl_2$) was then added to a final concentration of 2.54 mM. The buffer was introduced into the perfusion apparatus and allowed to circulate for 30 min. The buffer was gassed with CO_2 in air throughout the experiment.

4.2.2.4 Perfusion apparatus for in vitro experiments

The perfusion apparatus is illustrated in Figure 4.3. Experiments were conducted in a non-recirculating manner and polyethylene was used as the tubing between various components of the apparatus. The perfusion equipment was encased in a Perspex cabinet that was heated to and maintained at 37°C. The gassed perfusate was pumped from the buffer reservoir by a Cole-Parmer Masterflex® pump at a constant flow rate of 4 ± 0.1 ml.min^{-1}. The perfusate initially passed through a bubble trap and then through a bubble trap within a water-jacketed heat exchange coil, maintained at 37°C by a constant temperature water heater and pump. The perfusion medium entered a 'lung' of silastic tubing in a closed gassed (5% CO_2 in air) chamber, before passing through an infusion port (and the third bubble trap), where perfusion pumps (WPI®, SP101i syringe pump) were used to infuse treatments at a constant rate. Pressure was measured by a pressure transducer attached to the third bubble trap to monitor the arterial blood pressure of the hindlimb throughout the experiment. Before reaching the rat, the perfusate passed through an A-V difference analyser (A-Vox, San Antonio, TX, USA) that measured arterial oxygenated haemoglobin before entering the hindlimb via the arterial cannula. The venous effluent flowed out the vena cava cannula and passed back through the A-V difference analyser (A-Vox, San Antonio, TX, USA) to measure venous oxygenated haemoglobin and thus the difference in oxygenated haemoglobin in arterial versus venous blood at 660 nm (Fig. 4.3). Venous samples were also collected from this point during the experiment, before passing into a waste container. Data for arterial pressure (PP) and arterial-venous oxygen difference were collected throughout the experiment via a WinDaq data acquisition system software (DATAQ instruments, Akron, OH USA).

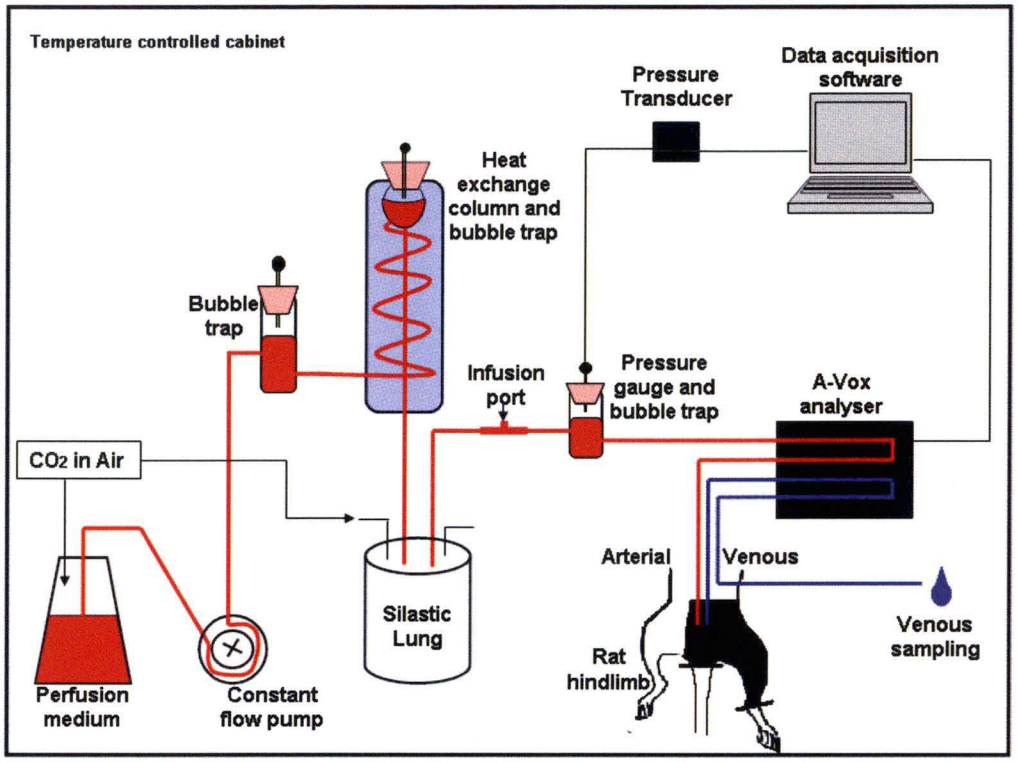

FIG 4.3: PERFUSION APPARATUS. The cabinet was maintained at 37°C and the perfusion medium was heated as it passed through a heat exchange column. The perfusion medium was gassed with 5% CO_2 in air, in the buffer reservoir and as it passed through the silastic tubing lung. The oxygen content of the perfusion medium was measured before and after it has passed through the rat hindlimb and analysed by an A-Vox analyser (A-Vox, San Antonio, TX, USA). Pressure was also measured via a pressure transducer attached to a bubble trap. Data were recorded throughout by WinDaq data acquisition system software (DATAQ instruments, Akron, OH USA).

4.2.2.5 Determination of glucose uptake and lactate release in vitro

All samples were analysed for glucose and lactate using a glucose analyser (Yellow Springs Instruments, Model 2300 Stat plus). Rates of glucose uptake and lactate release were calculated from arterial-venous differences in perfusate glucose/lactate concentrations, multiplied by the perfusate flow rate and divided by the weight of the perfused muscle. Glucose uptake and lactate release are expressed as $\mu mol.g^{-1}h^{-1}$.

4.2.2.6 Hindlimb perfusion protocol

The erythrocyte perfused hindlimb model was used to assess changes in perfusion pressure, oxygen uptake, glucose uptake and lactate release in response to a 10 min bout of contraction and throughout a 60 min recovery period. This model was used as it is a fully dilated system, and therefore the effects of increased microvasculature perfusion in response to contraction are not present. This allows the relative importance of microvascular perfusion to be compared with the *in vivo* system, and thus to separate the influences of microvascular perfusion and metabolic events in the myocyte that may lead to the sustained increase in glucose uptake during recovery from contraction. A similar protocol to the *in vivo* system was employed.

Figure 4.4 shows a diagram of the hindlimb perfusion protocol. After a 20 min equilibration period, at a flow rate of 4 ml.min^{-1} basal samples were taken for 15 min before 10 min contraction of the perfused hindlimb (via electrical stimulation at 2 Hz, 0.1 ms, 30 V) was initiated. During the contraction period, the flow rate was increased to 15 ml.min^{-1} to ensure adequate oxygen delivery to the muscle. This flow rate returned to 4 ml.min^{-1} during the 60 min recovery. Samples were taken every 5 min at basal and during recovery, and every 2 min during contraction for glucose and lactate determination.

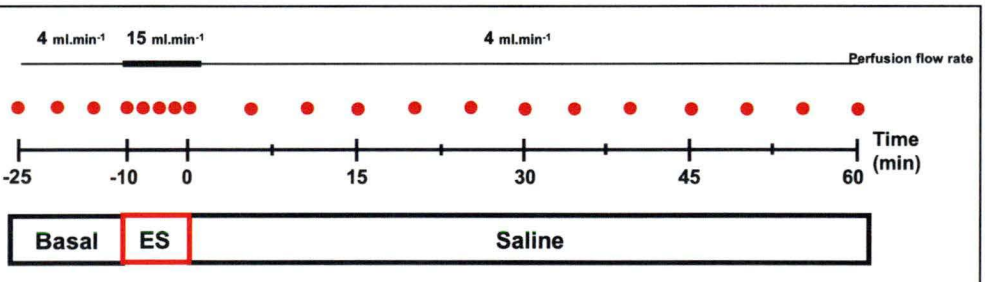

FIGURE 4.4: ISOLATED-PUMP PERFUSED HINDLIMB PROTOCOL. The hindlimb was equilibrated with an erythrocyte containing medium at 4 ml. min^{-1} during the basal period. After the basal period the flow rate was increased to 15 ml.min^{-1} and the perfused hindlimb was contracted via electrical stimulation (2Hz, 0.1 ms, 30 V) for 10 min at which time the flow rate was returned to 4 ml.min^{-1} and maintained at this rate during the 60 min post-contraction period.

Horizontal bars represent electrical stimulation and saline infusion, *red circles* represent arterial and venous perfusate samples for determination of glucose and lactate, *ES* represents electrical stimulation of the perfused hindlimb.

4.2.3 Data analysis

Heart rate, mean arterial pressure, femoral blood flow and vascular resistance data for *in vivo* experiments were calculated as described in section 2.4. CEU data were analysed using Qlab advanced quantification software (Phillips Medical Systems, The Netherlands, B.V). The continuous 15 s pulsing interval data was converted to acoustic intensity and graphed against time.

In the perfused hindlimb experiments, changes in arterial pressure were recorded via a pressure transducer. Calculations were made on the principle that for any fluid moving though a pipe of radius r, and length l, then according to Poiseuille's Law:

$$Q = \frac{\pi(P_i - P_o)\, r^4}{8\eta l}$$

Where:

Q = flow rate

P_i-P_o = pressure difference

η = viscosity of the perfusate

Therefore, assuming flow rate (Q), viscosity of the perfusate (η), length of tubing (l) and π remain constant, the pressure difference is proportional to $r^{1/4}$, and a small change in radius will lead to a large change in pressure.

Oxygen consumption in the perfused hindlimb was measured through an A-V oxygen difference analyser (A-Vox, San Antonio, TX, USA) that measures the spectral difference in arterial versus venous blood at 660 nm. VO_2 was then calculated from the arterio-venous difference in oxygen divided by the Bunsen coefficient (25.54), multiplied by the perfusate flow rate and divided by the weight of the perfused muscle. Oxygen consumption is expressed as $\mu mol.g^{-1}.hr^{-1}$.

All data are expressed as means ± SE.

4.2.4 Statistical Analysis

To ascertain differences between treatment groups at 60, a one-way repeated measures ANOVA was used. Comparisons were made between treatment groups over the course of the experiment using a two-way repeated measures ANOVA and Student-Newman-Keuls post hoc test. Significance was accepted at a level of $p<0.05$. All tests were performed using SigmaStat software (Systat Software Inc., USA).

4.3 RESULTS

4.3.1 Experimental groups

4.3.1.1 Hindlimb perfusion

There were two experimental groups assessed in the isolated pump-perfused hindlimb experiments, contraction with saline infusion (n=5) and a saline control (n=5).

4.3.1.2 In vivo

There were two *in vivo* experimental groups, contraction with saline infusion (n=5) and a saline control (n=5). The contra-lateral leg in each *in vivo* experiment was used as an internal control.

4.3.2 Systemic measurements during contraction and recovery in vivo

4.3.2.1 Heart rate and mean arterial pressure

Heart rate increased ($p<0.05$) in response to contraction of the hindlimb from 332 beats.min^{-1} at basal to ~372 beats.min^{-1} and was significantly different from saline control at 2 and 5 min. Although this remained elevated during recovery (Fig. 4.5A) it was not different from the saline control at 10 min or beyond. One leg contraction also had a small significant ($p<0.05$) effect on mean arterial pressure causing an increase from 110 mmHg at basal to ~116 mmHg that was significant at 2, 5, 8, and 10 min after the start of contraction, and 5 min into recovery. The pressure had returned to basal by 30 min post-contraction (Fig 4.5B).

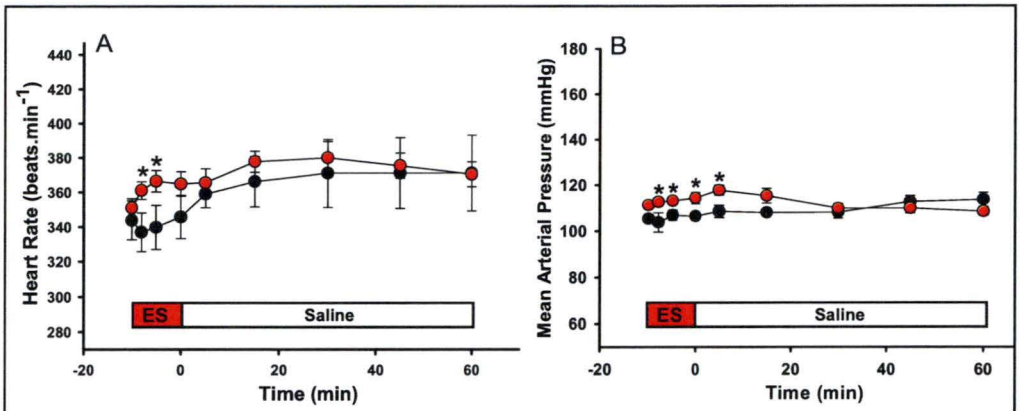

FIGURE 4.5: The effect of saline (●) or contraction (●) on heart rate or mean arterial pressure during contraction of one hind leg and up to 60 min post-contraction. Heart rate (A) and mean arterial pressure (B) were measured by a catheter placed in the carotid artery. Values are means ± SEM (n=5). *, significantly different to saline controls (p<0.05).

4.3.2.2 Blood glucose and lactate concentrations

Contraction had no affect on arterial blood glucose concentrations which remained stable at ~ 3.5 mM throughout contraction and during the post-contraction period (Fig 4.6A). Arterial blood lactate concentrations, increased significantly during the contraction period, but had returned to baseline levels by 10 min post contraction, where they remained at ~ 0.5 mM for the duration of the experiment (Fig. 4.6B).

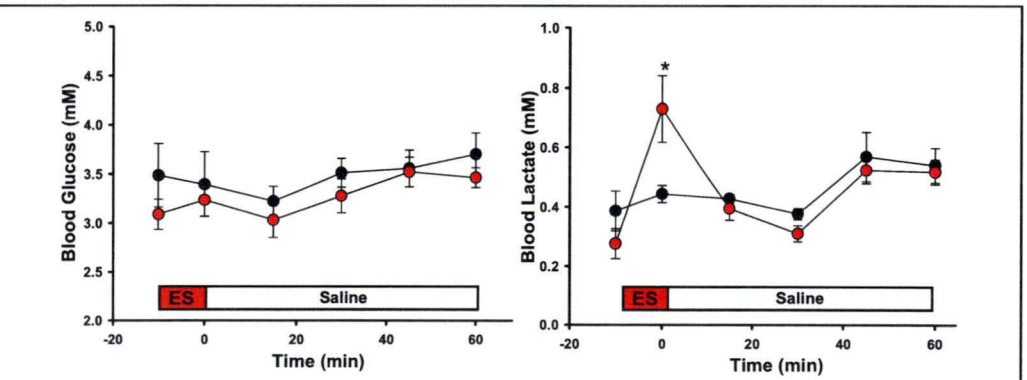

FIGURE 4.6: Effect of saline (●) or contraction (●) on arterial blood glucose and lactate concentrations during contraction of one hind leg and up to 60 min post exercise. Values are means ± SEM (n=5). *, significantly different to saline (p<0.05).

4.3.2.3 Plasma insulin concentrations

Table 4.1. shows the plasma insulin concentrations at basal and 60 min post-contraction. There was no difference in the plasma insulin concentrations between the saline control and contraction groups at basal or post-contraction.

TABLE 4.1: PLASMA CONCENTRATIONS OF INSULIN BEFORE CONTRACTION AND 60, 120 AND 180 MIN AFTER CONTRACTION OF ONE HINDLIMB.

	Saline	Contraction
	Plasma insulin concentrations ($pmol.l^{-1}$)	
Basal	205 ± 21	197 ± 17
60 min post exercise	151 ± 45	134 ± 23

Values are means ± SEM (n=5).

4.3.3 Measurements in the hindlimb during contraction and recovery in vivo

4.3.3.1 Femoral blood flow and vascular resistance

Femoral blood flow and vascular resistance were measured in the contracting and non-contracting legs within the same animal. Femoral blood flow was measured in both the test and contra-lateral resting leg by a Transonic™ flow probe placed around each femoral artery (n=5). Femoral blood flow increased rapidly (within 1 min) to ~ 5 $ml.min^{-1}$ ($p<0.05$) in response to contraction and returned to basal values (~ 1.5 $ml.min^{-1}$) within 5 min post-contraction (Fig. 4.7A). There was a tendency (but not significant) for a corresponding decrease in the femoral blood flow of the contra-lateral resting leg during contraction. Femoral blood flow remained stable during the saline control experiments, and there was no difference between the two groups or the test and resting legs during the post exercise period (5-60 min; Fig. 4.7A).

Contraction caused a significant decrease ($p<0.05$) in vascular resistance in the contracting hindlimb during exercise with a corresponding increase ($p<0.05$) in vascular resistance in the contra-lateral resting leg. Vascular resistance appeared to remain decreased in the contracted leg and increased in the contra-lateral leg for approximately 10 min post-contraction, but this was not significant. There was no change in vascular resistance in the saline control experiments (Fig. 4.7B).

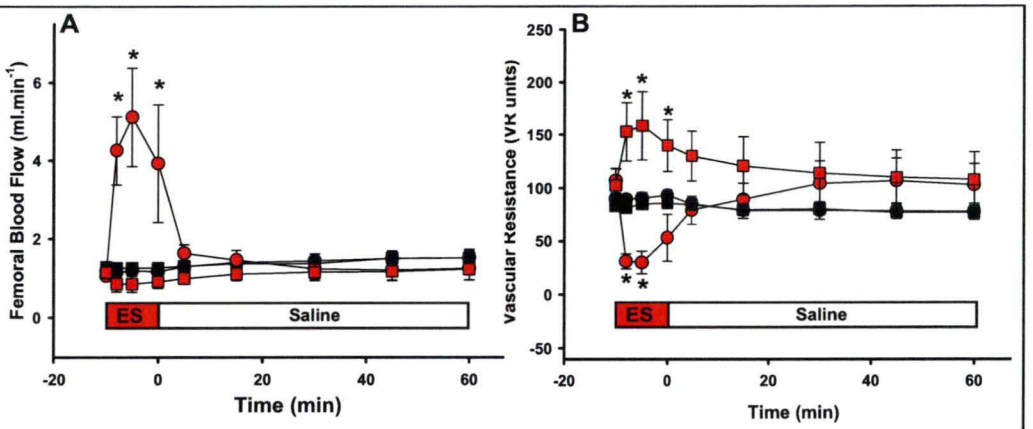

FIGURE 4.7: Effect of saline (•) or contraction (•) on femoral blood flow and vascular resistance during contraction of one hind leg and up to 60 min post exercise in the test leg (circles) and contra-lateral control leg (squares). Femoral blood flow (A) was measured via a flow probe around each femoral artery. Vascular resistance (B) was calculated by dividing blood pressure by femoral blood flow. Values are means ± SEM (n=5). *, significantly different to saline control (p<0.05).

4.3.3.2 Microvascular blood flow

Microvascular perfusion was measured in the contracting and non-contracting legs in separate animas. Contrast enhanced ultrasound measurements were made in the contracting hindlimb or during saline infusion without contraction. Continuous 15 s pulsing intervals were used to assess the time course of changes in microvascular perfusion during contraction, and for 60 min post exercise. The acoustic intensity from the 15 s pulsing intervals increased from an acoustic intensity of ~ 30 at basal to ~100 during contraction. This response decreased in the 10 to 20 min after contraction and reached a plateau position of ~50 for the remainder of the experiment. The acoustic intensity between 55-60 min post-contraction, was significantly elevated compared to basal levels (Fig 4.8).

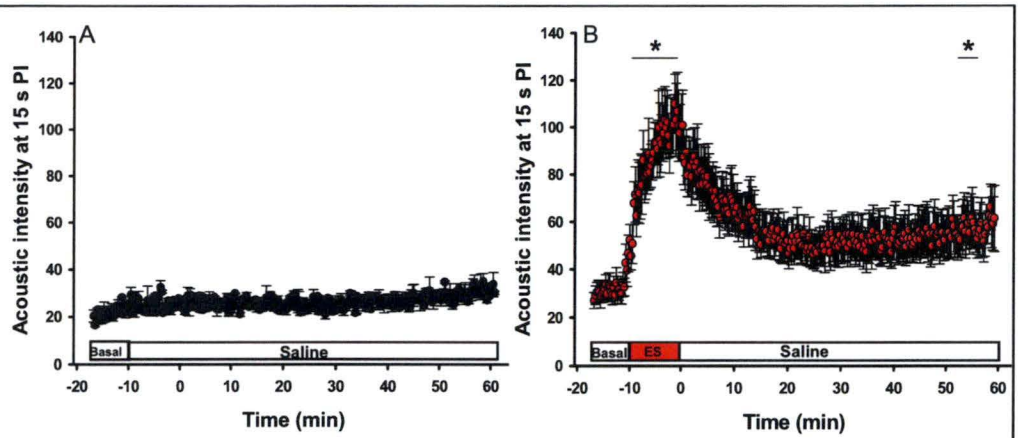

FIGURE 4.8: The time course of microvascular volume changes during saline infusion without contraction (panel A, •) and at basal, during 10 min contraction of one hind leg, and up to 60 min post contraction (panel B, •). Microvascular volume was measured by contrast enhanced ultrasound using phospholipid microbubbles during continuous 15 s pulsing intervals. Values are means ± SEM. (n=6). *, significantly different from basal (p<0.05).

4.3.3.3 Glucose metabolism and lactate release

Glucose uptake was measured in the contracting and non-contracting legs in the same animal. Hindlimb glucose uptake (measured by the arterio-venous difference multiplied by femoral blood flow) in the contracted hindlimb was significantly increased above the contra-lateral leg at 60 min (p=0.027; Fig. 4.9A). There was no difference however, between the lactate release (measured in the same way), when the two hindlimb were compared at this time (Fig. 4.9B).

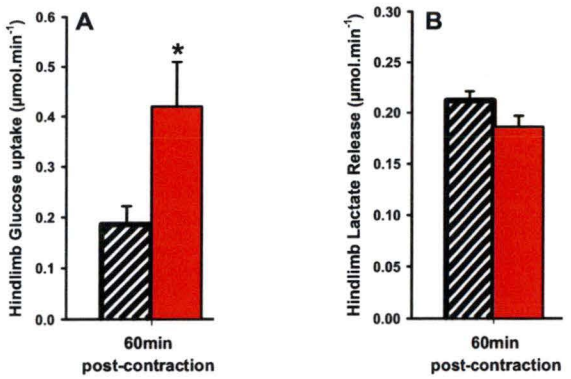

FIGURE 4.9: Effect of contraction on hindlimb glucose uptake and lactate release 60 min post contraction in the contracting test leg (■) and contra-lateral control leg (▨). Hindlimb glucose uptake and lactate release were measured by multiplying the arterio-venous difference in glucose concentration by femoral blood flow. Values are means ± SEM (n=5). * Significantly different to contra-lateral control leg (p<0.05).

Muscle glucose uptake was measured in two ways, using arterio-venous glucose difference as sampled from the femoral artery and vein, and by 2-DG uptake by muscles of the lower leg. Figure 4.10 shows data for 2-DG uptake measured in both the contracted test leg and contra-lateral control leg of each rat. At 60 minutes post-contraction, glucose uptake in all muscles (except the soleus) of the contracted test leg were significantly ($p<0.05$) increased compared to the muscles of the rested contra-lateral control leg (Fig 4.10). The combined muscle glucose uptake of the entire lower leg (aggregated by proportion of weight) of the contracted limb had a 250% increase in glucose uptake compared to the rested contra-lateral control lower leg muscles.

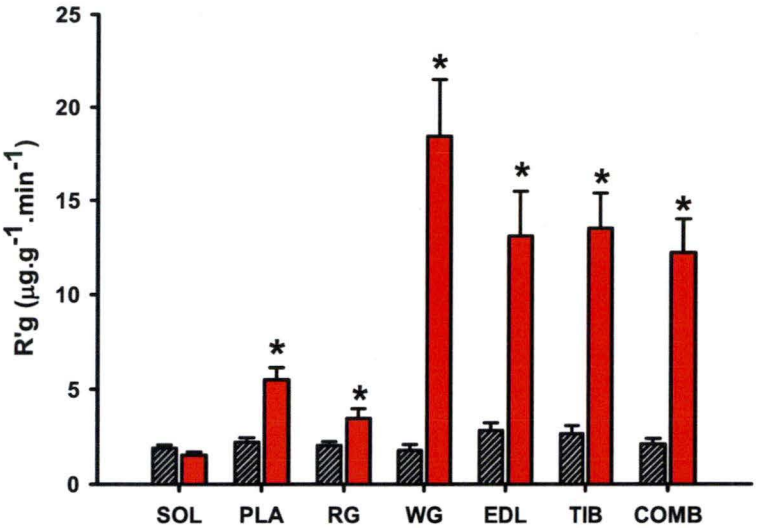

FIGURE 4.10: Muscle radioactive 2-DG uptake (R'g) for individual muscles of the lower leg of the contracting test leg (■) or contra-lateral control leg (▨) 60 min post-contraction. 2-DG was administered as a bolus at 45 min (Figure 4.1) prior to the end of the experiment and individual muscles (SOL, soleus; PLA, plantaris; RG, red gastrocnemius; WG, white gastrocnemius; EDL, extensor digitorum longus; TIB, tibialis anterior; COMB, combined muscles of the lower leg aggregated on proportion of weight) were excised at the completion of the experiment. Values are means ± SE (n=6). *, significantly different to contra-lateral control leg (p<0.05).

4.3.4 Measurements in the isolate, pump-perfused hindlimb during contraction and recovery

4.3.4.1 Perfusion pressure and oxygen consumption

Perfusion pressure significantly increased as expected, in both the saline control and contraction experiments when flow rate was adjusted from 4 ml.min^{-1} at basal to 15 ml.min^{-1} to accommodate the extra energy demand of contraction. A further consequence of this increase in flow was an elevated oxygen consumption in the saline control experiment. However oxygen consumption was further increased (p<0.05) in response to contraction (Fig 4.11B). Both perfusion pressure and oxygen consumption returned to basal levels immediately post-contraction and remained stable at basal values for the remainder of the experiment (Fig. 4.11).

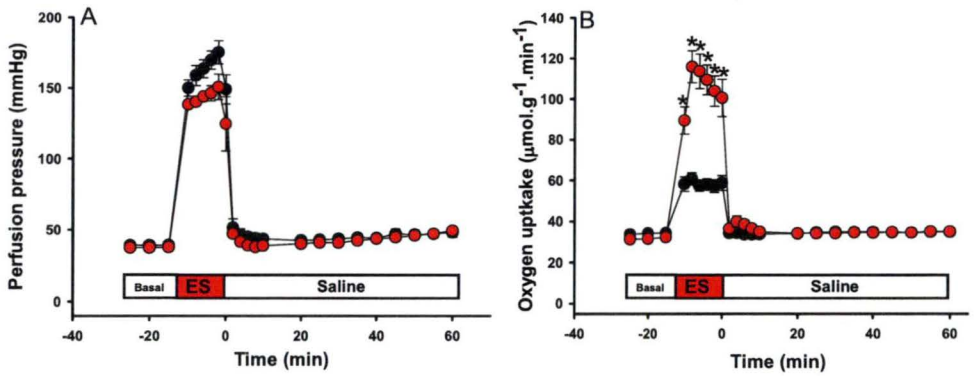

FIGURE 4.11: Effect of saline (●) or contraction (●) on perfusion pressure (panel A) and oxygen consumption (panel B) in the perfused hindlimb system during contraction of the perfused hind leg and up to 60 min post contraction. The flow rate was 4 ml.min^{-1} at basal and during the post-contraction period, and 15 ml.min^{-1} during contraction. Values are means ± SEM (n=5). *, significantly different to saline (p<0.05).

4.3.4.2 Glucose uptake and lactate release

In perfusion, there was a trend for hindlimb glucose uptake to increase with contraction, however due to great variability in this measurement statistical significance (p<0.05) was not reached (Fig. 4.12A). During the contraction period there was a spike in lactate release during the saline control experiments due to the increase in flow rate, however this was quickly reversed and lactate release (which generally accompanies increased glucose uptake) was significantly increased (p<0.05) during contraction compared to saline experiments (Fig. 4.12B). Both glucose uptake and lactate release returned to basal levels immediately post-contraction and remained stable for the remainder of the experiment. There was no significant difference in these parameters in the recovery period between the saline and contraction experiments.

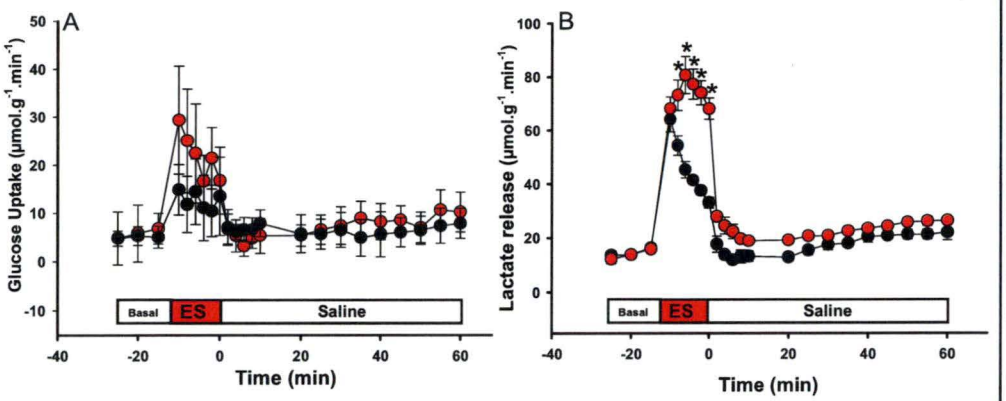

FIGURE 4.12: Effect of saline (●) or contraction (●) on glucose uptake (panel A) and lactate release (panel B) in the perfused hindlimb system during contraction of the perfused hind leg and up to 60 min post contraction. The flow rate was 4 ml.min^{-1} at basal and during the post-contraction period, and 15 ml.min^{-1} during contraction. Values are means ± SEM (n=5). *, significantly different to saline (p<0.05).

4.4 DISCUSSION

The main finding of this study was that microvascular perfusion increased 3.5-fold relevant to basal during 10 min of twitch contraction, and although having decreased by almost half, it remained at 2-fold over basal at 60 min post-contraction (Fig. 4.8). In contrast, femoral blood flow and vascular resistance (Fig. 4.7) returned to resting levels within 5 min post-contraction.

Microvascular volume, a key indicator of microvascular perfusion, measured by CEU with continuous 15 s pulsing intervals was still significantly ($p<0.05$) increased above basal levels at 60 min (Fig. 4.8). This shows that total blood flow and microvascular perfusion are unrelated and thus, possibly controlled by separate stimuli. This also suggests that while the increase in glucose uptake during recovery from contraction is not related to total blood flow, it may be tightly linked to the enhanced microvascular perfusion seen during this period.

In the isolated pump-perfused hindlimb where a microvascular response is not present, there was an increase in oxygen consumption, glucose uptake or lactate

release (Fig. 4.11 and 4.12). However, these parameters had returned to basal levels within 5 min post-contraction, suggesting changes in microvascular perfusion may play a part in the enhanced glucose uptake response seen during recovery from contraction.

Zhang et al. [29], using the 1-MX disappearance method, showed that microvascular perfusion had reversed between 15-30 min after a hyperinsulinaemic euglycaemic clamp (once plasma insulin concentrations had returned to basal). The continuous imaging data shows that capillary volume remains increased up to 60 min post-contraction, which may be functionally relevant as the capillaries may remain perfused to aid in nutrient delivery and waste removal. This may be the result of a redistribution of basal blood flow, from a primarily non-nutritive route, consisting of short capillaries, to more nutritive long tortuous capillaries in close contact with the muscle [299]. With greater capillary surface area available during the post-contraction period, insulin-mediated glucose uptake may be more sensitive to endogenous insulin. Thus, relatively low doses of insulin are able to restore muscle glycogen and maintain blood glucose concentrations during this recovery period. This enhanced perfusion during recovery may be mediated by nitric oxide, as studies have shown that while inhibition of nitric oxide synthase has no effect on exercise hyperaemia and blood flow during exercise, it results in a decrease in blood flow at basal and during recovery from contraction [77, 148, 300]. Furthermore, as nitric oxide contributes to the increase in glucose uptake during exercise, it may also be involved in the insulin sensitisation seen during recovery from exercise [139, 149].

Glucose uptake was significantly increased ($p<0.05$) up to 60 min (Fig. 4.9A and 4.10) after a short 10 min bout of twitch contraction, which is in line with the findings of previous studies [125, 301, 302]. There was no difference in plasma insulin levels between control experiments with saline and those with contraction (Table 4.1), suggesting that the increase in glucose uptake may be due to an increased sensitisation of the muscle to endogenous insulin. The muscles which showed the greatest increase (over 400%) in glucose uptake at 60 min post-contraction, were the white gastrocnemius, extensor digitorum longus and tibialis anterior, muscle which are predominantly fast twitch fibre type. The more insulin sensitive plantaris and red gastrocnemius muscles showed a more modest ~100% increase in glucose uptake,

while contraction had no effect in the predominantly red fibre type insulin sensitive soleus muscle (Fig 4.10). Blood flow during contraction has been shown to be specific to fibre type [303], which may explain the different pattern of glucose uptake between the different calf muscles examined in this study. Laughlin et al. [66] found that bulk blood flow in rats that were exercised by running, increased in a direct relationship to the fast twitch, high oxidative fibre composition of the muscles, and as in the present study, found no increase in blood flow to the soleus muscle. Therefore it may be that these working muscle have been primed to be more sensitive to insulin's haemodynamic actions. Interestingly, in the perfused hindlimb there was no increase in glucose uptake post-contraction (Fig. 4.12), suggesting that changes in microvascular perfusion due to contraction seen *in vivo* may be involved. This contributes to the retained post-contraction glucose uptake and this does not occur when the hindlimb is surgically isolated and perfused by pump. Even though there may be a contribution by the microvasculature to increased post-contraction glucose uptake there are definite changes that take place in the myocyte. Thus the increase in glucose uptake may also result from a greater recruitment of white fibre type muscles during contraction, leading to an increase in the translocation of GLUT4 to the plasma membrane in these muscles. In this regard, GLUT4 total protein and mRNA levels have been shown increase in the post exercise period, and remain elevated up to 16 h post exercise [115, 119, 304]. This increase in GLUT4 protein has also been shown to be regulated by the glycogen state of the muscle [117, 119]. However, given that in this study only rats were only subjected to a short 10 min bout of twitch contraction, which is unlikely to fully deplete muscle glycogen, it would suggest that glycogen replenishment may not be the primary factor involved in this increased sensitisation.

As only one third of muscle capillaries are perfused at rest [15], and data in this thesis and other studies [28, 288] have shown that microvascular perfusion can increase in response to insulin and exercise, it would not be expected that the capillaries would remain perfused for long periods of time without a stimulus. This would result in the microvascular remaining fully recruited at all times, negating its function, and contradicting the available data concerning a capillary reserve for muscle at rest [15]. The microvasculature is very sensitive to the metabolic needs of the muscle [16, 305], and it is these needs which form the stimuli which cause the initial increase in reactive hyperaemia and increased perfusion at the start of contraction. This magnitude of this

initial response is dependent on the intensity, duration and type of exercise [66], and as shown by Bangsbo et al. [306] the metabolic and muscle blood flow response during recovery from exercise is also dependent on the type and duration of exercise.

Basal oxygen uptake may also be increased in the post-contraction period, particularly if the exercise is intense. Thus, a single bout of aerobic exercise also results in elevated oxygen consumption during recovery from exercise known as excess post exercise oxygen consumption (EPOC). The magnitude of EPOC is also dependent on the duration, intensity and mode of exercise, but the reason behind this elevation has still not been elucidated, with studies showing that changes in creatine phosphate, ATP, lactate removal, increased body temperature and glycogen resynthesis are unable to account for the increased oxygen consumption [307]. Williams et al. [303] and Bangsbo et al. [306] have shown that EPOC remains elevated after mean arterial pressure, leg blood flow and leg vascular conductance had returned to pre exercise levels, however in these study only total blood flow was assessed. The present study found that using the isolated perfused hindlimb, where a contribution due to changes in microvascular perfusion is unlikely, perfusion pressure and oxygen consumption were not elevated during recovery (Fig. 4.11), and there was no increase in glucose uptake or lactate release (Fig. 4.12). *In vivo* however, although oxygen consumption was not measured, both microvascular perfusion and glucose uptake were increased, suggesting a link between microvascular perfusion and EPOC during recovery can not be overlooked. Furthermore, while hindlimb glucose uptake remained elevated 60 min post-contraction, there was no increase in hindlimb lactate release compared to the saline control (Fig. 4.9), suggesting that glucose uptake had occurred primarily through the aerobic pathway which may theoretically should have caused cause an increase in oxygen consumption.

The advantage of the current study is that the effects of contraction during the post-contraction period were examined *in vivo* with the benefit of using the contra-lateral resting leg as an internal control for comparisons. Many studies have also examined the post-contraction period by undertaking contraction *in vivo* and then removing the muscle in order to examine post-exercise glucose uptake during incubation or in the perfused hindlimb [105, 112]. Such an approach negates any haemodynamic, endocrine, paracrine or neural effects which may have occurred during recovery period, or

indeed, may have been released during contraction. Furthermore, higher concentrations of insulin are required in incubated muscle preparations than *in vivo*, and therefore the relevance of these results may be questioned. Also, studies which remove or manipulate the muscle and the nerves surrounding it in any way, may induce haemodynamic changes, a sympathetic response or cause damage to the muscle, changing its characteristics and it response to stimulation. In this study, by examining the post exercise response *in vivo*, the effects of contraction on multiple muscles and a range of muscle fibre types may be examined, making the results more physiologically relevant.

In conclusion, this study shows that the femoral blood flow response to contraction is rapidly reversed, within the first 5 min of recovery. However, microvascular perfusion remains enhanced up to 60 min post-contraction. This may be explained by a shift from the perfusion of short non-nutritive capillaries at basal, to long tortuous nutritive capillaries during recovery as the body tries to maintain a homeostatic balance by increasing glucose uptake to replenish glycogen and nutrient stores, and regulate blood glucose levels. The vasculature, as well as the skeletal muscle, may also be more sensitive to insulin stimulation resulting in an increase in microvascular perfusion at a lower concentration than would usually be required to elicit such a response. This in turn may account for the increase in skeletal muscle glucose uptake in the post-contraction period.

CHAPTER 5:

NITRIC OXIDE SYNTHASE INHIBITION AND MICROVASCULAR FLOW DURING CONTRACTION

5.1 INTRODUCTION

The skeletal muscle plays an important role in glucose homeostasis accounting for over 85% of glucose uptake during insulin stimulation [11]. Both insulin stimulation and exercise result in an increased level of GLUT4 protein translocation to the plasma membrane resulting in increased glucose uptake into the cell, however the mechanism through which these stimuli act appear to be different. This can be seen in patients with type 2 diabetes where there is a decreased rate of GLUT4 translocation to the membrane in response to insulin stimulation (despite normal levels of GLUT 4 protein), however glucose uptake and GLUT4 translocation during exercise appear normal [101, 308]. The insulin signalling pathway for GLUT4 translocation is PI3-kinase dependent. The exercise mediated signalling pathway has not been fully elucidated, but may involve protein kinase C, CaMK, AMP-activated protein kinase (AMPK) and/or nitric oxide [308].

Type 2 diabetes is associated with impaired nitric oxide synthase activity (NOS) in skeletal muscle [166, 167]. Infusion of a NOS inhibitor N^G-nitro-L-arginine methyl ester (L -NAME) during a hyperinsulinaemic clamp decreased total blood flow, microvascular perfusion and reduced muscle glucose uptake by 50% [164]. Roy et al. [165] found similar results *in vivo* and showed from *in vitro* experiments that L -NAME failed to affect basal or insulin-stimulated glucose transport in isolated muscles. Such studies suggest a role for nitric oxide in insulin mediated glucose uptake which is possibly mediated by changes in microvascular perfusion. There are however, great discrepancies in the available data concerning the role of nitric oxide during exercise, either in relation to blood flow or glucose uptake.

In humans, NOS inhibition with N^G-monomethyl-L-arginine (L-NMMA) during cycling significantly attenuated the normal increase in leg glucose uptake compared with saline infusion, without affecting leg blood flow or arterial glucose and insulin concentrations [149]. Co-infusion of L-arginine restored glucose uptake during L-NMMA infusion to levels similar to control subjects [149, 150]. Similar experiments were also performed in people with type 2 diabetes with results showing these patients to be more sensitive to NOS blockade during exercise, as the reduction in glucose uptake was significantly greater than the levels seen in normal control

subjects [151]. There are however, controversies surrounding the role of nitric oxide during exercise in humans, in particularly regarding blood flow with either a decrease [300, 309, 310] or no change [77, 148] in bulk flow reported.

Animal studies have also yielded conflicting results with many of these studies assessing glucose uptake post-exercise and/or *in vitro* which negate the important haemodynamic effects of nitric oxide [143, 153, 154]. For those studies conducted *in vivo*, blood flow and more particularly microvascular perfusion was not assessed and the effect of nitric oxide on glucose uptake differed [152, 155].

There are many studies focusing on the involvement of nitric oxide in exercise (with some controversy), with the inconsistencies possibly resulting from a number of methodological issues. Firstly, in regards to blood flow, it is important the blood flow is measured during exercise and not immediately following exercise (as is the case during measurements of flow with venous occlusion plethysmography), as this gives a measure of flow during recovery from exercise. Furthermore, measures of glucose uptake should also be made during contraction of the muscle and not post-contraction, as the results may be further influenced by the type of exercise and recovery of the muscle, as well as variations in the time frame in which measures are taken. Some discrepancies may result from the systemic infusion of the NOS inhibitor which may cause heart rate and mean arterial pressure changes which may affect the local environment, both in terms of blood flow and metabolism. The time frame between contraction and the inhibition of NOS may also play a role.

In this study, we examined whether a locally infused NOS inhibitor (L -NAME) attenuated the increase in glucose uptake seen *during* contraction. We also determined bulk flow and microvascular flow changes *in vivo*, in response to NOS inhibition throughout the muscle contraction period using contrast enhanced ultrasound.

5.2 METHODS

5.2.1 Animals

Male hooded Wistar rats weighing 247 ± 2 g were used during theses experiments. They were raised as described in section 2.2.1.

5.2.2 Surgery

Experiments were conducted using the anaesthetised rat model, with surgery as described in section 2.2.2 and 2.2.2.1.

5.2.3 Experimental procedure

After a 45 min equilibration period, the rat hindlimb was contracted via electrical stimulation of one calf muscle (as described in section 2.3.5) for 30 min. After 10 min of stimulation, L-NAME (final concentration of 5 μM) was infused locally into the contracting hindlimb via the epigastric artery for 20 min (Figure 1). The infusion volume was matched by the equivalent volume of isotonic saline in control experiments. At the conclusion of all experiments the calf muscles (soleus, SOL; plantaris PLA; red gastrocnemius, RG and white gastrocnemius, WG) of both the control and treatment legs were freeze-clamped as a group under liquid nitrogen. This process took no longer than 2 min. The muscle samples were then stored at -80°C until required for determination of muscle glucose uptake and other signalling processes.

The infusion rate of L-NAME was adjusted according to femoral blood flow in order to maintain a final concentration of 5 μM in the hindlimb. However, the infusion of microbubbles used to measure microvascular perfusion with contrast enhanced ultrasound (CEU; described in section 2.3.2.2) interferes with the Doppler signal of the flow probes used to measure femoral blood flow. Therefore two groups of experiments were required in order to measure change in both macrovascular and microvascular blood flow.

The first group of experiments was designed to determine changes in femoral blood flow (via a Transonic™ flow probe around each femoral artery) caused by contraction and L-NAME infusion. These data was then used to adjust the L-NAME infusion rate

during the CEU group of experiments. Also, muscle glucose uptake of both the treatment and control legs was measured using a method adapted from Kregan et al. [311]. Briefly, a bolus of 2-deoxy-D-[1-^{14}C] glucose (2-DG; specific activity 56.0 mCi.mmol^{-1}; Amersham Life Science, NSW, Australia) in isotonic saline was administered via the jugular vein at 20 min. Immediately after the administration of the 2-DG an arterial blood sample (0.5 ml) was withdrawn by a syringe pump at 50 µl.min^{-1} over 10 min. From this blood sample a plasma sample (25 µl) was collected to determine the average plasma specific radioactivity of [^{14}C] 2-DG. At the conclusion of the experiment the lower leg muscles (SOL, PLA, RG and WG) from the test and contra-lateral legs were freeze-clamped *in situ* using liquid nitrogen-cooled tongs and stored at -80°C. The muscle glucose uptake was then determined from the separation of free and phosphorylated 2-DG in the muscle as described in Section 2.3.3.

The second group of experiments (Fig. 5.1) involved the use of CEU (refer to section 2.3.2.2) to measure microvascular perfusion during twitch contraction and local L-NAME infusion. The transducer was placed over the calf muscle region allowing imaging of the soleus, plantaris, red and white gastrocnemius muscles during electrical stimulation. CEU measurements were made using a 7-4 MHz transducer interfaced with an ultrasound system (HDI-5000; Philips Medical Systems, Andover, MA), in harmonic imaging mode. The mechanical index was set to 0.8, and gain settings were standardised for all experiments.

A 50-fold dilution of octofluoro-propane gassed phospholipid microbubble solution (see Section 2.1.1; 'microbubbble contrast agent' for composition) was infused at a rate of 40 µl.min^{-1} into the rat, via the jugular vein. The infusion pump and syringe containing the microbubble solution was continuously mixed to ensure the microbubbles maintained an even suspension and the delivery line to the rat was also vibrated. Microbubbles were infused 5 min prior to commencing a pulsing interval curve to allow the microbubble concentration to reach steady state. Microvascular volume and flow rate was determined by a pulsing interval curve with intervals of 0.5, 1, 2, 3, 5, 8, 12 and 15 s. Each pulsing interval curve took approximately 5 min, and measurements were taken at basal, after 10 min of contraction and at 30 min during contraction with L-NAME (or saline) infusion (Fig. 5.1).

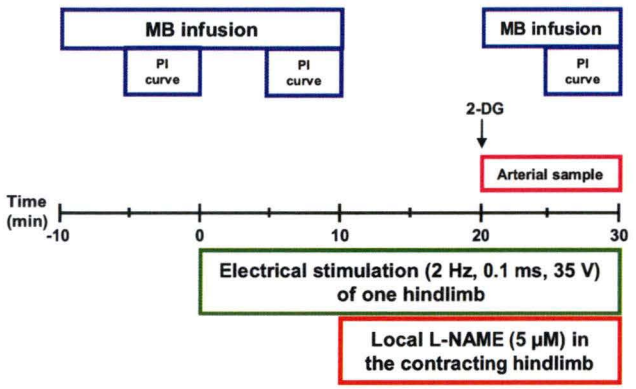

FIGURE 5.1: CONTRACTION AND L-NAME EXPERIMENTAL PROTOCOLS. The rat's hindlimb was contracted by electrical stimulation (2Hz, 0.1msec pulse, 35 V) for 30 min. Following 10 min of stimulation, saline or L-NAME (final concentration of 5µM) was locally infused, via the epigastric artery, for the remaining 20 min. During the first group of experiments, femoral blood flow was measured by flow probes around the femoral artery in the control and test legs. To determine muscle glucose uptake 2-Deoxy-D-[1-^{14}C] glucose (2-DG) was administered as a bolus at 20 min. Arterial blood was then continuously withdrawn (50 µl.min^{-1}) for 10 min to determine the concentration of 2-DG in the blood during this time. During the second group of experiments, microvascular perfusion of the contracting calf muscle was assessed by contrast enhanced ultrasound. Pulsing interval (PI) curves were conducted at 0 (basal), 10 min (contraction) and 30 min (contraction with L-NAME or saline). Phospholipid microbubbles (MB) were infused via the jugular vein 5 min prior to each PI curve to ensure arterial concentrations were at steady state. The calf muscles of the control and treatment legs were freeze-clamped under liquid nitrogen at the conclusion of all experiments for further analysis.

Horizontal bars represent stimulation, microbubble infusion, CEU measurements(PI curve), local infusions and arterial sampling as marked, *arrow* represents bolus injection of 2-DG.

5.2.4 Preparation of whole muscle lysates

For NOS activity, phosphorylation and AMPK signalling, frozen muscle was ground under liquid nitrogen into a powder and homogenized (10 µl of buffer per mg of muscle) in freshly prepared ice-cold buffer [50 mM Tris at pH 7.5 containing 1 mM EDTA, 10% v/v glycerol, 1% v/v Triton X-100, 50 mM NaF, 5 mM $Na_4P_2O_7$, 1 mM DTT, 1 mM PMSF, 1 µl.ml^{-1} trypsin inhibitor and 5 µl.ml^{-1} Protease Inhibitor Cocktail (P8340, Sigma, St. Louis, MO]). Tissue lysates were incubated on ice for 20 min and then spun at 16,000 × g for 20 min at 4°C. Protein concentration was determined using a bicinchoninic (BCA) protein assay (Pierce, Rockford, Il) with BSA as the standard. An aliquot of the whole muscle lysates was solublised in

Laemmli sample buffer and frozen at -20°C for later measurement of AMPK signalling.

NOS was affinity purified from whole muscle lysates using 2'5'-ADP Sepharose 4B beads (Amersham Biosciences, Piscataway, NJ), which had been pre-equilibrated in lysis buffer. Following purification, an aliquot of the ADP-sepharose beads were solublised in Laemmli sample buffer and frozen at -20°C for later measurement of NOS phosphorylation. The remaining ADP-Sepharose beads were used to measure NOS activity.

5.2.5 NOS activity assay

ADP-Sepharose beads were added to 100 µl of pre-heated (37°C) assay buffer, which contained (in final concentrations) 50 mM Tris-HCl (pH 7.5), 1.15 mM NADPH, 4 µM BH_4, 100 nM CaM, 0.7 mM $CaCl_2$, 10 µM L-arginine, 0.63 µM FAD, and 3 µM L-[U-^{14}C]-arginine (Amersham Biosciences, Piscataway, NJ). Samples were incubated in the presence of either H_2O or 1mM L-NAME for 10 min at 37°C, which was within the pre-determined linear range for rat skeletal muscle. The concentration of L-NAME used was sufficient to fully block NOS activity (data not shown), and inter- and intra-assay coefficient of variations were both 9%. NOS activity represents the difference between samples incubated in the absence and presence of L-NAME, and is expressed as pmol of L-[^{14}C]-arginine converted to L-[^{14}C]-citrulline per minute per mg of protein (pmol.min^{-1}.mg protein^{-1}).

5.2.6 AMPK signalling and NOS phosphorylation

For NOS phosphorylation, equal amounts of purified proteins and for determination of AMPKα threonine^{172} (AMPKα Thr^{172}) and ACCβ serine^{222} (ACCβ Ser^{222}) phosphorylation, 90 µg of total protein were all subjected to SDS-PAGE. Binding of purified proteins was detected by immunoblotting with either polyclonal rabbit antibodies raised against the phospho-peptide of rat nNOS pSer^{1412} antibody (RLRSESpIAFIE) that recognizes the predominant nNOSµ pSer^{1446} variant in skeletal muscle and the eNOS pThr^{1177} antibody based on the amino acid sequence of human eNOS (RIRTQSpFSLQER)[312]. For eNOS pThr^{1177}, AICAR-stimulated rat heart (0.5 mg.g^{-1} body weight I.P.) was used as a positive control. Membranes were then

reprobed with either anti-nNOS or anti-eNOS mouse monoclonal antibodies (BD Transduction Laboratories, NSW, Australia), respectively. Binding of whole cell lysates was also detected by immunoblotting with either anti-phospho-ACCβ Ser^{222} polyclonal antibody [313] or AMPKα Cell Signaling Technology (New England BioLabs, Hartsfordshire, England). Binding was detected with IRDye™ 800-conjugated anti-rabbit IgG (Rockland, Gilbertsville, PA) or IRDye™ 680-conjugated anti-mouse IgG (Molecular Probes, Eugene, OR) secondary antibodies. Direct fluorescence was detected and quantified using the Odyssey infrared imaging system (LI-COR Biosciences, Lincoln, NB, USA). For AMPK signalling, membranes were then stripped (2% SDS (w/v) in 1 M glycine, pH 2.0) and reprobed with IRDye™ 800-labeled streptavidin (LI-COR Biosciences) and affinity purified anti-phospho-AMPK Thr^{172} antibody, raised against AMPK alpha peptide (KDGEFLRTpSCGSPNY) [314]. Phosphorylation was expressed relative to protein abundance.

5.2.7 Skeletal muscle Nitrate and Nitrite (NOx) levels

Approximately 30 mg of frozen powdered muscle was homogenized (20 μl of buffer per mg of muscle) in freshly prepared ice-cold buffer (50 mM Tris at pH 7.5 containing 1 mM EDTA, 10% v/v glycerol, 1% v/v Triton X-100, 50 mM NaF, 5 mM $Na_4P_2O_7$, 1 mM PMSF, 1 $\mu l.ml^{-1}$ trypsin inhibitor and 5 $\mu l.ml^{-1}$ Protease Inhibitor Cocktail (P8340, Sigma)). Tissue lysates were incubated on ice for 20 min and then spun at 16,000 × g for 20 min at 4^0C. Samples were purified by spinning 450 μl of supernatant through pre-wetted 10 kDa molecular weight cut-off filters (Millipore, NSW, Australia) at 16,000 × g for 80 min at 4°C. Total nitrate and nitrite levels in the purified samples were determined using Nitrate/Nitrite Colorimetric Assay Kit (Cayman Chemical Co., Ann Arbor, MI). Values are expressed relative to the total protein concentration of the purified samples via the BCA protein assay (Pierce Rockford, Il).

5.2.8 Data analysis

All data are expressed as means ± SE. Heart rate, mean arterial pressure, femoral blood flow and vascular resistance data were calculated as described in section 2.4. CEU data were analysed using Qlab advanced quantification software (Phillips

Medical Systems, Nederland, B.V). The signal intensity from the larger vessels at 0.5 s was subtracted from the signal of the smaller vessels (pulsing intervals (1 to 15 s) to gain a true measure of microvascular perfusion. Pulsing interval curves were constructed, and microvascular volume (A) and microvascular flow rate ($A \times \beta$) values were determined as described in section 2.3.2.2.

5.2.9 Statistical Analysis

To ascertain differences between treatment groups at 30 min, a one-way repeated measures ANOVA was used. Comparisons were made between treatment groups over the course of the experiment using a two-way repeated measures ANOVA and Student-Newman-Keuls post hoc test. Significance was accepted at a level of $p< 0.05$. All tests were performed using SigmaStat software (Systat Software Inc., USA).

5.3 RESULTS

5.3.1 Experimental groups

There were two experimental groups, contraction with a local saline infusion and contraction with a local L-NAME infusion. Local infusion was via the epigastric artery in the contracted leg from 10 min. The contra-lateral leg in each experiment was used as an internal control.

5.3.2 Heart rate and blood pressure

Heart rate significantly increased ($p<0.05$) in response to contraction of the hindlimb from 332 beats.min^{-1} at basal to ~360 beats.min^{-1} after 15 min of contraction. Heart rate remained steady for the remainder of the experiment and was not affected by the local infusion of L-NAME into the contracting leg (Fig 5.2A). Contraction also had a small, but significant ($p<0.05$) effect on mean arterial pressure causing an increase from 110 mmHg at basal to ~116 mmHg after 10 min of contraction and ~120 mmHg after 30 min of contraction (Fig 5.2B). Local L-NAME infusion into the contracting leg had no effect on mean arterial pressure suggesting that any spill-over of the NOS inhibitor was insufficient to cause systemic effects.

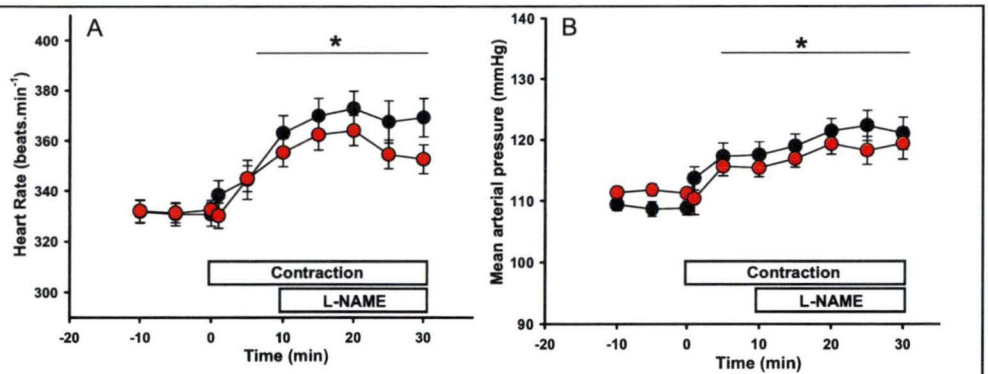

FIGURE 5.2: Effect of saline (●) or local L-NAME (●) on heart rate and mean arterial pressure during contraction of one hind leg. Heart rate (A) and mean arterial pressure (B) were measured by a catheter placed in the carotid artery. Values are means ± SEM (n=24 and 26 for contraction and contraction plus L-NAME, respectively). *, significantly different to -10 min (p<0.05).

5.3.3 Femoral blood flow and vascular resistance

Femoral blood flow was measured in both the test and contra-lateral control legs in each rat, by a flow probe around each femoral artery (n = 11). As expected, contraction significantly (p<0.05) increased femoral blood flow by ~3.8 ml.min^{-1}. Although there was no significant effect of L-NAME on femoral blood flow (absolute values) during contraction (Fig. 5.3A), the change in femoral blood flow from 10 mins (the beginning of local L-NAME infusion) revealed that L-NAME caused a significant (p<0.05) decrease in bulk flow (Fig. 5.3B). Femoral blood flow remained stable in the contra-lateral control leg of both groups and was unaffected by contraction or L-NAME infusion in the test leg.

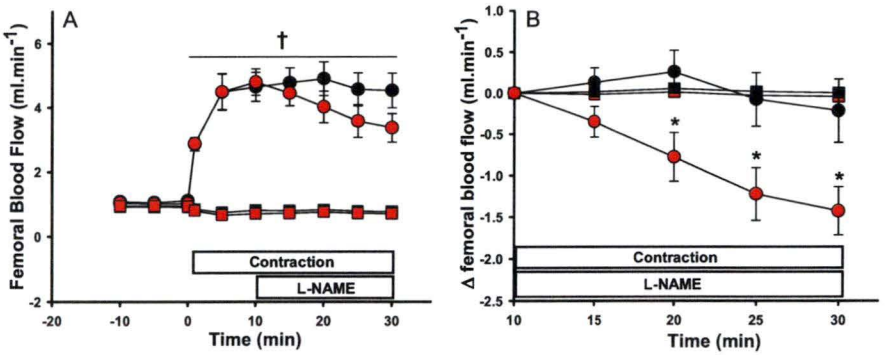

FIGURE 5.3: Effect of saline (**black** symbols) or local L-NAME (**red** symbols) on absolute femoral blood flow (A) and change in femoral blood flow from 10 min (the start of the L-NAME infusion) (B) in the contracted test leg (circles) and contra-lateral control leg (squares). Flow probes were positioned around the femoral arteries of each leg. Values are means ± SEM (n=11). †, significantly different to -10 min (p<0.05); *, significantly different to contraction alone and values for the contra-lateral leg (p<0.05).

Contraction caused vascular resistance to significantly decrease in the contracting leg and to significantly increase in the control leg (p<0.05; Fig 5.4). However neither was affected by L-NAME infusion in the test leg (Fig 5.4).

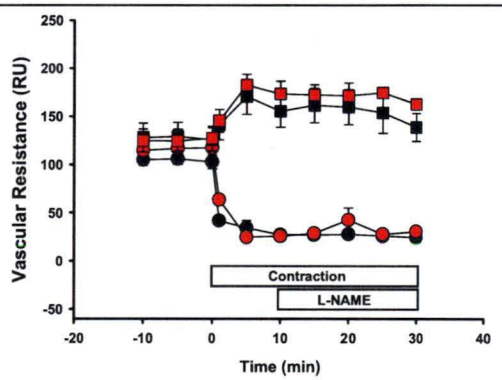

FIGURE 5.4: Effect of saline (**black** symbols) or local L-NAME (**red** symbols) on vascular resistance in the contracted test leg (circles) and contra-lateral control leg (squares). Vascular resistance was calculated by dividing blood pressure by femoral blood flow. Values are means ± SEM (n=11).

5.3.4 Microvascular perfusion

The ultrasound transducer was positioned over the calf muscles (SOL, PLA, RG and WG) of the contracting leg and thus only values for the contracting leg are shown (n=8). The signal intensity at the 0.5 s pulsing intervals (representative of the larger vessels) was subtracted from the intensity value at longer pulsing intervals to gain a true measure of microvascular perfusion. The pulsing interval curves from a typical experiment are shown in Fig. 5.5, with a curve at basal, during contraction at 10 min and during contraction with L-NAME at 30 min.

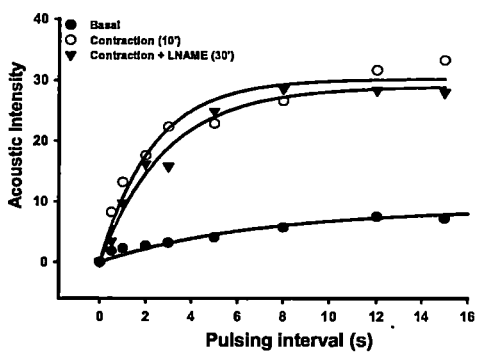

FIGURE 5.5: PULSING INTERVAL CURVES FROM A TYPICAL EXPERIMENT. Measurements were made at basal, after 10 min of contraction, and during contraction with L-NAME at 30 min. The signal intensity at the 0.5 s pulsing interval has been subtracted from the intensity value at longer pulsing intervals to give a measure of microvascular perfusion.

Contraction significantly ($p<0.05$) increased the microvascular volume (A value), microvascular flow rate constant (β values) and microvascular flow rate (β values). The local infusion of L-NAME had no effect on these parameters (Fig. 5.6).

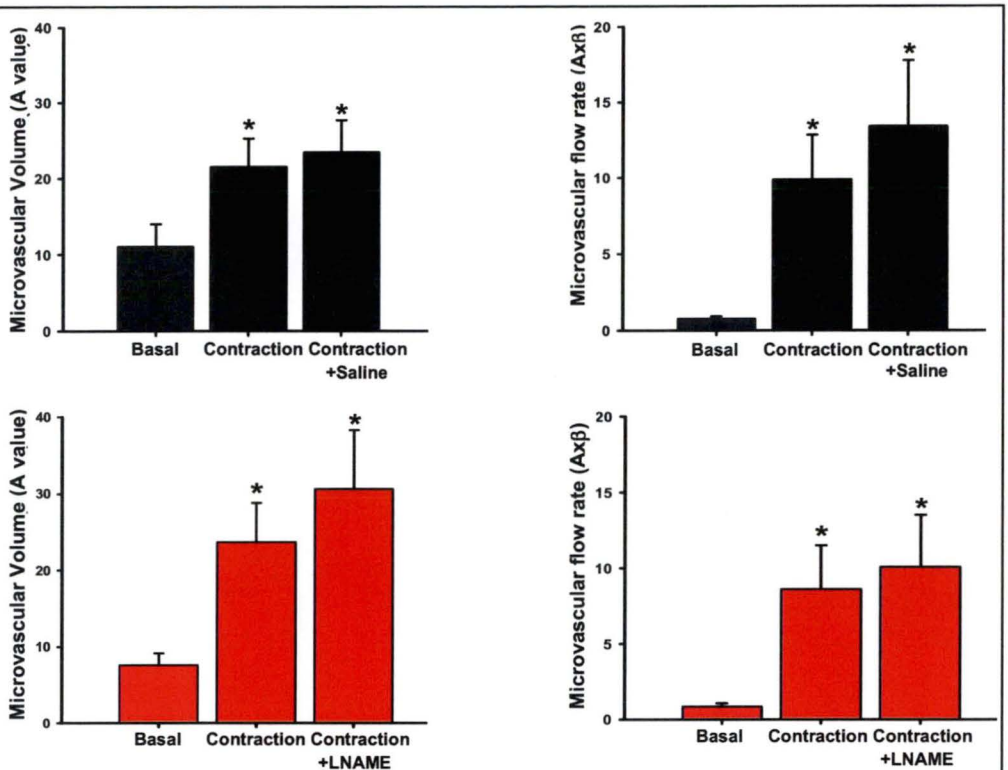

FIGURE 5.6: Effect of saline (■) or L-NAME (■) on microvascular volume (*A* value) and microvascular flow rate (*A* x *β*) in the contracted test leg. Microvascular volume and flow rate were measured by contrast enhanced ultrasound using phospholipid microbubbles before commencement of contraction (Basal); after 10 min of contraction and before L-NAME infusion (Contraction); and at the end of the protocol during L-NAME infusion (Contraction+ L-NAME). Values are means ± SEM (n=8). *, significantly different from basal (p<0.05)

5.3.5 Force development

Force development due to muscle contraction was measured by an isometric transducer attached to the Achilles tendon of the contracting leg (see section 2.3.5). Electrical stimulation resulted in a maximum tension of ~ 320 g that decrease to ~250 g after 10 min of contraction. This level of force development was sustained for the subsequent 20 min of the experimental period and was unaffected by local L-NAME infusion (Fig. 5.7).

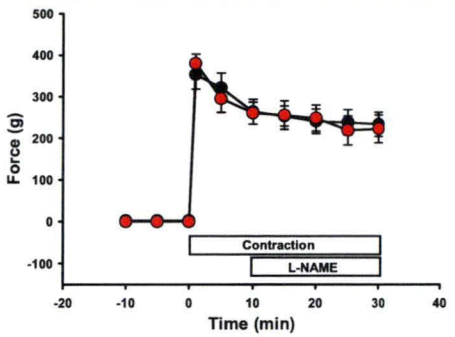

FIGURE 5.7: Effect of saline (●) or L-NAME (●) on electrical stimulation-mediated force development in lower leg muscles of test leg. Force was determined by an isometric force transducer attached to the Achilles tendon. L-NAME was only infused (locally) in the test leg. Values are means ± SEM (n=5).

5.3.6 Muscle glucose uptake

Muscle glucose uptake (R'g, measured by the 2-DG uptake) was measured in both the contracted test leg and contra-lateral control leg of each rat. Contraction resulted in a 16-fold increase in glucose uptake relative to the contra-lateral control leg (Fig. 5.8). Local L-NAME infusion into the contracting hindlimb significantly decreased ($p<0.05$) muscle glucose uptake in this leg by ~35%, with no effect on the contra-lateral control leg. There was no difference in plasma insulin concentrations (measured by an ELISA kit; Mercodia AB, Sweden) between the local saline (245 ± 44 pmol.l^{-1}) and local L-NAME (220 ± 46 pmol.l^{-1}) infused groups.

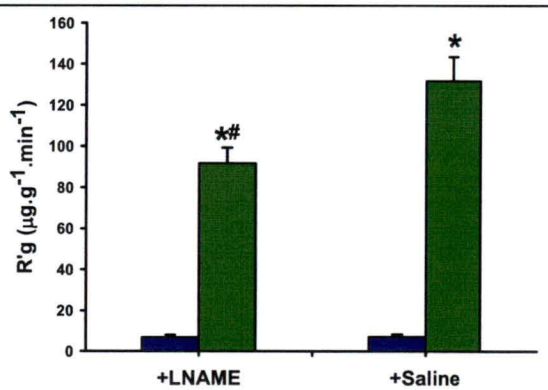

FIGURE 5.8: Effect of saline or L-NAME on 2-deoxyglucose uptake (R'g) in the contracted test leg (green bar) and contra-lateral control leg (blue bar). L-NAME was only infused (locally) in the test leg *, significantly different from control leg ($p<0.05$); #, significantly different from saline ($p<0.05$). R'g was measured over the final 10 min and the results are expressed as means ± SEM (n=6).

5.3.7 AMPKα phosphorylation and ACCβ phosphorylation

Contraction caused a 2-3 fold increase in AMPKα phosphorylation and ACCβ phosphorylation. Local L-NAME infusion into the contracting leg had no effect on the extent of this phosphorylation (Fig. 5.9). In addition L NAME infusion into the contracting hindlimb had no effect on AMPK α phosphorylation or ACCβ phosphorylation in the contra-lateral control (rest) leg (Fig. 5.9).

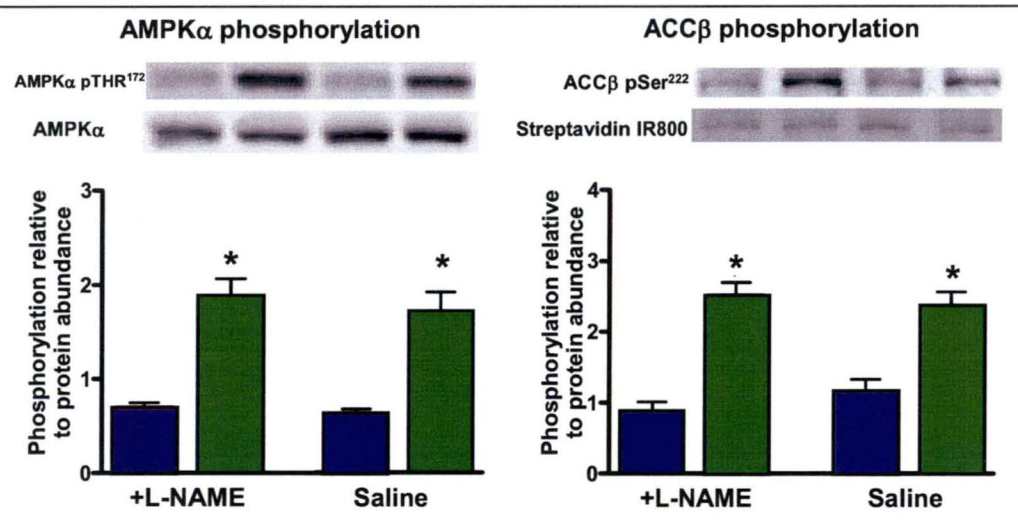

FIGURE 5.9: Effect of L-NAME on Thr^{172} phosphorylation of AMPKα (A) and Ser^{222} of ACCβ (B) in the contracted test leg (green bar) and contra-lateral control leg (blue bar). Values are means ± SEM. (n=6) *, significantly different to contra-lateral control leg (p<0.05).

5.3.8 NOS activity, nitrates and nitrites (NOx), nNOS phosphorylation and eNOS phosphorylation.

Contraction significantly increased skeletal muscle NOS activity and this increase was prevented by local L-NAME infusion during contractions (Fig. 5.10). A similar response was observed with skeletal muscle NOx content, although the increase with exercise was not significant (Fig. 5.10).

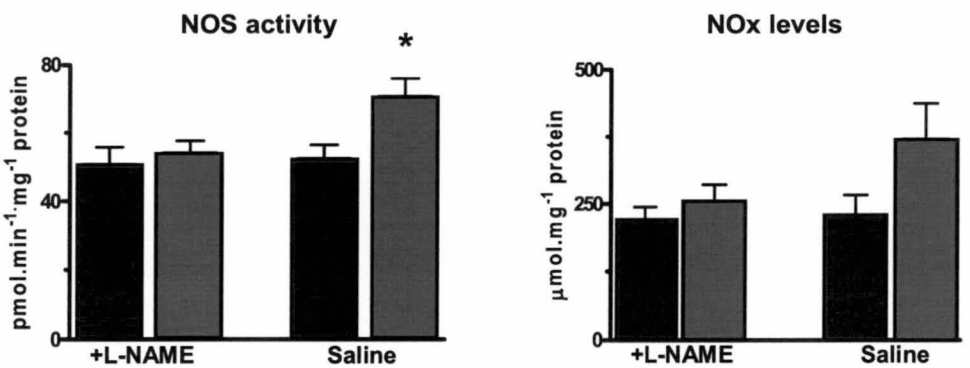

FIGURE 5.10: Effect of L-NAME on muscle NOS activity and NOx in the contracted test leg (green bar) and contra-lateral control leg (blue bar). Values are means ± SEM. (n=6) *, significantly different from the contra-lateral control leg (p<0.05).

Contraction caused a 2-3 fold increase in nNOS phosphorylation and, as was the case for AMPKα phosphorylation, L-NAME infusion during contraction had no effect on the extent of nNOS phosphorylation (Fig. 5.11).

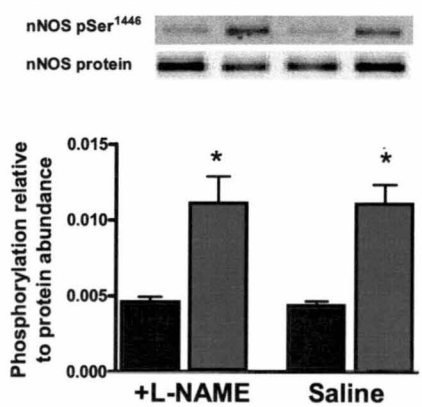

FIGURE 5.11: Effect of L-NAME on Ser^{1446} phosphorylation of nNOS in the muscle of the contracted test leg (green bar) and contra-lateral control leg (blue bar). Values are means ± SEM. (n=6) *, significantly different from the contra-lateral control leg (p<0.05).

L-NAME infusion into the contracting test leg had no effect on NOS activity, NOx content or nNOS phosphorylation in the contra-lateral control (rest) leg (Fig. 10 and 11).

A substantial eNOS phosphorylation in rat heart was observed following IP AICAR administration (as a control), but there was no detectable skeletal muscle eNOS phosphorylation at rest or following contractions (Fig 12).

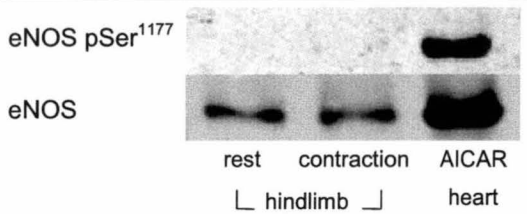

FIGURE 5.12: The effect of contraction on eNOS phosphorylation. IP AICAR administration was used as a control.

5.4 DISCUSSION

The major finding of this study was that local NOS inhibition attenuated the increase in skeletal muscle glucose uptake during *in situ* contractions without influencing muscle microvascular perfusion. In addition, AMPK activation was not altered by NOS inhibition suggesting the reduction in glucose uptake was specific to a reduction in nitric oxide and not to secondary effects on AMPK.

The results of this study are consistent with previous human studies which found a decreased glucose uptake with NOS inhibition [149], and the increase in NOS due to contraction, although modest, is similar to results seen in treadmill run rats [145]. This increase is almost certainly due to production of nitric oxide in the muscle, however there is a possibility that the vascular endothelial cells may contribute to this production. Their contribution would be minimal however, as vascular endothelial cells comprise only 3.4% of skeletal muscle [315].

Local L-NAME infusion blocked the activation of NOS and NOx in the contracted hindlimb, however muscle glucose uptake was only reduced by 35% (Fig 5.8). This suggests nitric oxide may play a role in contraction-mediated glucose uptake, however other factors are also involved. AMPK has been suggested to play a role in contraction-mediated glucose uptake, and has been shown to interact with nitric oxide. In human aortic endothelial cells, activation of AMPK by AICAR increases

NOS phosphorylation and nitric oxide production [316], while sodium nitroprusside increases the activation of AMPKα1 in rat skeletal muscle [153]. Furthermore peroxynitrite, (which is found when nitric oxide combines with superoxide) activates AMPK in endothelial cells [317].

In this study, AMPKα and ACCβ phosphorylation increased with contraction however the level of activation was not affected by NOS inhibition, suggesting that nitric oxide is not acting upstream of AMPK. It is possible, as NOS inhibition only decreased glucose uptake by one third, that AMPK may be responsible for the remaining 65% of contraction-mediated glucose uptake. Li et al.[318] found that NOS or guanylate cyclase inhibition decreased AICAR stimulated glucose uptake by ~20% and ~25% respectively, suggesting the majority of AMPK mediated glucose uptake is independent of NOS activation. Alternatively, Fryer et al.[319] showed AICAR increased NOS activity and glucose transport in mouse H-2K muscle cells, an effect which was blocked by NOS inhibition, a finding supported by Shearer et al. *in vivo*. As AICAR has been shown to activate NOS it would be possible that NOS is acting downstream of AMPK, and therefore we would not expect L-NAME to affect AMPK phosphorylation.

There may be inconsistencies regarding data using AICAR as a stimulus for AMPK in comparison to contraction. Stephens et al.[320] showed that AICAR stimulation increased glucose transport in rat epitrochlearis muscle 209% from basal. NOS inhibition caused this percentage to drop to 184%. In comparison, contraction mediated glucose uptake (by electrical stimulation *in vitro*) increased glucose transport 107% from basal while NOS inhibition caused glucose transport to drop to 31% above basal (similar to the values found in the present study, Fig 5.8). That study [320] suggests that the activation of AMPK by AICAR may be an over representation of the naturally occurring process of contraction mediated activation of AMPK. Furthermore, Jorgensen et al. [321] found that the AMPKα2 knockout mouse has abolished AICAR-, but not contraction-induced glucose uptake in skeletal muscle. Those studies show that and AICAR may stimulate AMPK through different mechanism to contraction and therefore may not be a useful means for comparison when assessing nitric oxide and AMPK activation or vice versa. There is also evidence to suggest that the level of AMPK activation and involvement in contraction

mediated glucose uptake is highly dependent on the glycogen stores in the muscle [322] and that contraction may increase glucose uptake without the activation of AMPK [323]. Therefore, while AMPK may play a role in contraction mediated glucose uptake it is not necessarily a key regulatory protein, and there are many possible pathways leading to increased glucose uptake during contraction [10, 137].

There is *in vitro* evidence to suggest that nitric oxide directly regulates glucose transport. Incubation with the nitric oxide donor sodium nitroprusside [143, 154, 324] has been shown to increase glucose transport, and GLUT4 translocation (independent from PI3-kinase mechanisms) possibly by nitric oxide activation of cGMP [168]. The data from the present study suggests that nitric oxide and AMPK are acting through independent pathways to increase glucose uptake during contraction, however further research is required to clarify these mechanisms and signalling pathways involved.

AMPK phosphorylates nNOSμ in skeletal muscle during exercise in humans [169, 325]. In the current study the increase in skeletal muscle nNOSμ phosphorylation during contractions was not affected by L-NAME (Fig 5.10). This is not surprising since AMPK activation during contractions was also unaffected by L-NAME (Fig 5.9). AMPK phosphorylation of nNOSμ at Ser^{1446} has little effect on nNOSμ activity (Lee-Young, Wadley, Chen, Kemp and McConell et al. University of Melbourne, unpublished observations). However, the question then is how is it that L-NAME prevented the increase in NOS activity with contractions if it did not effect nNOSμ phosphorylation at Ser^{1446}. Since L-NAME is a competitive inhibitor it would have been diluted and lost during the extraction and purification steps employed for the NOS activity assay. Therefore there must have been alterations in phosphorylation of sites other than Ser^{1446} and/or other covalent events resulting from L-NAME infusion during contraction. Since rodent muscle expresses both nNOSμ and eNOS [326], and AMPK phosphorylates and activates eNOS [327], eNOS phosphorylation was also examined. However, no eNOS phosphorylation either at rest or following contraction was detected. This suggests that nNOSμ plays a more important role in exercise metabolism than eNOS, since downstream NOS signalling (i.e. increased cGMP levels) occurs during contractions in normal muscle and $eNOS^{-/-}$ muscle, but not in $nNOS\mu^{-/-}$ muscle [326]. It is also possible that L-NAME affected other covalent events

on nNOSμ. Irrespective of the mechanism, this study has shown that NOS inhibition reduces NOS activity during contractions and attenuates increases in skeletal muscle glucose uptake which is an important finding.

This study also shows that contraction increases femoral blood flow four-fold and microvascular perfusion, adding weight to the hypothesis that only a third of the capillary bed is perfused at rest, creating a capillary reserve for times of stress and increased nutrient requirements such as during contraction [15, 328]. NOS inhibition decreased femoral blood flow, but had no effect on microvascular perfusion (Fig. 5.3 and Fig. 6.6). This is in contrast to the effects of NOS inhibition on insulin action. Similar to contraction, insulin has been shown to increase femoral blood flow (at higher doses) and microvascular perfusion [25, 29, 31]. NOS inhibition during insulin infusion attenuates the increase in both femoral blood flow and microvascular perfusion and results in a decreased glucose uptake [162-164]. Importantly, the degree of glucose uptake is correlated with the degree of microvascular perfusion and not total blood flow [21, 40] and it is the increase in microvascular perfusion that accounts for ~50% of insulin-mediated glucose uptake [29, 56, 95]. Thus, the decrease in flow during contraction with L-NAME is unlikely to be the cause of the decreased glucose uptake, especially as the extraction of glucose across the leg was only 15%, indicating the delivery of glucose was not limited by the total flow. Such data supports the notion that insulin and contraction act through different signalling pathways [87].

These data also demonstrate the redundancy that exists in the control of contraction-mediated glucose uptake and perfusion. Although femoral blood flow is decreased during NOS inhibition, microvascular perfusion, unlike that during insulin infusion, is unaffected. This difference may be due to the nature of the stimulus, as contraction changes the state of the muscle rapidly, increasing the energy requirements and the level of energy production required in the cell. From an evolutionary perspective contraction is an important mechanism and therefore may be mediated by a number of different pathways building a level of redundancy into the system. If one aspect of the contraction mediated pathway is inhibited there is a compensatory response to ensure the muscle is able to function efficiently. This was demonstrated by Schrage et al. [81] who showed that combined inhibition of prostaglandins and nitric oxide inhibited forearm blood flow during handgrip exercises, however prostaglandin

inhibition alone had a transient influence on blood flow, suggesting other vasodilitary mechanisms can compensate for its loss of function. A chronic inhibition is found in type 2 diabetes where a state of endothelial dysfunction is often present. These patients have a greater reliance on nitric oxide to mediate a vasodilitary response during exercise than healthy humans [151], demonstrating how the body can adapt to allow the muscle to function effectively during exercise.

The present study is novel as L -NAME is infused locally into the muscle during contraction, so that the effects of NOS inhibition are localised to the stimulated hindlimb. Other studies have used systemic infusion of NOS inhibitors which can increase mean arterial pressure triggering compensatory responses such as the withdrawal of sympathetic efferent activity, decreasing heart rate, and vasoconstrictor tone in the muscle and possibly inducing insulin resistance [148, 329]. Furthermore, systemic infusion of NOS inhibition increases entry of the inhibitor into the brain, which has been shown during ICV administration to induce a state of insulin resistance by increasing basal glucose concentrations and decreasing insulin mediated glucose disposal [176]. The present study also has the advantage of the unstimulated contra-lateral leg acting as an internal control, as any spill over of NOS inhibitor could be detected, firstly by changes in mean arterial pressure and heart rate (Fig 5.2), but also by changes in vascular resistance (Fig 5.4) and femoral blood flow (Fig 5.3) in the contra-lateral control leg. These parameters did not change in the contra-lateral leg showing the inhibition was limited to the contracting hindlimb.

In conclusion, this study demonstrated that local L -NAME infusion prevents contraction-induced increases in skeletal muscle NOS activity and NOx content and attenuates the increase in skeletal muscle glucose uptake during contractions without influencing skeletal muscle microvascular perfusion. These effects were independent of skeletal muscle AMPK activation during contraction and suggest that nitric oxide is critical for part of the normal increase in skeletal muscle glucose uptake during contraction.

CHAPTER 6:

ENDOTHELIN-1 AND INSULIN ACTION *IN VIVO*

6.1 INTRODUCTION

Endothelin-1 (ET-1) is a vasoactive peptide released from the vascular endothelial cells. It has a role in maintaining vasomotor tone and regulates blood flow by binding to its receptors located on the endothelial or smooth muscle cells. This leads to an increase in intracellular calcium stores resulting in vasoconstriction or the release of prostaglandins and nitric oxide resulting in vasodilation [181, 185, 186].

ET-1 has strong vasoconstrictor actions, and elevated plasma levels of this peptide have been implicated in disease states such as type 2 diabetes, hypertension, coronary artery disease and peripheral vascular disease [7, 182, 198, 330]. Over secretion of ET-1 may also contribute to endothelial dysfunction by disrupting the homeostatic regulation of the vasculature. There are many studies demonstrating ET-1's strong vasoconstrictor actions (and associated decrease in glucose uptake) in the gut, splanchnic and kidney regions [178, 187-189, 193]. Data concerning ET-1's affects on blood flow and glucose uptake in the skeletal muscle have also been examined, with some studies showing that ET-1 may cause a decrease in insulin mediated glucose uptake without showing a decrease in total flow to the muscle [178, 189, 193]. The microvascular effect of ET-1 in the skeletal muscle *in vivo* however, has not been explored.

Experiments utilising the perfused hindlimb technique in this laboratory, have shown that ET-1 modulates microvascular flow distribution, causing a stimulation of metabolism at low concentrations and inhibition at high concentrations. Insulin was found to block these inhibitory effects [190]. Therefore, the aim of this study was to test the hypothesis that elevated plasma levels of ET-1, through its vasoconstrictor effects, may prevent full perfusion of muscle, limiting the delivery of insulin and glucose. This study also assessed if high levels of insulin would reverse this inhibitory effect. We examined the effects of ET-1 *in vivo*, alone and in combination with insulin, on femoral blood flow, microvascular perfusion and glucose metabolism.

6.2 METHODS

6.2.1 Animals

Male hooded Wistar rats weighing 247 ± 2 g were used during theses experiments. They were raised as described in section 2.2.1.

6.2.2 Surgery

Experiments were conducted using the anaesthetised rat model, with surgery as described in section 2.2.2.

6.2.3 Experimental procedure

After a 45 min equilibration period, a hyperinsulinaemic-euglycaemic clamp was performed in which insulin (Humulin R, Eli Lilly ®; USA) was infused into the rat intravenously at a dose of 10 or 15 $mU.min^{-1}.kg^{-1}$ for 2 h (Fig 6.1; protocol 2). To test the effect of ET-1 on insulin action, ET-1 (50 $pmol.min^{-1}.kg^{-1}$) was infused into the rat 30 min prior to insulin infusion (10 $mU.min^{-1}.kg^{-1}$) and continued during the 2 h insulin clamp (Fig. 6.1; protocol 3). The infusion rate of ET-1 (50 $pmol.min^{-1}.kg^{-1}$) was chosen as preliminary experiments showed this rate was capable of increasing mean arterial pressure without affecting heart rate or femoral blood flow.

During experiments involving insulin infusion, a glucose solution (30% w/v) was also infused at variable rates to maintain blood glucose levels at 4.8 $mmol.l^{-1}$, and this infusion rate was plotted as GIR expressed in $mg.min^{-1}.kg^{-1}$. When ET-1 (50 $pmol.min^{-1}.kg^{-1}$; Calbiochem ®, USA) was infused alone (Fig 6.1; protocol 1), glucose was not infused and blood glucose levels were allowed to self-regulate. Infusion volumes of insulin, glucose and ET-1 were matched by the equivalent volume of vehicle (isotonic saline) in control experiments (Fig. 6.1).

Blood samples were taken at the times indicated in Figure 6.1 and analysed for blood glucose and lactate (refer to section 2.3.4).

The 1-MX method (refer to section 2.3.2.1) was used to determine microvascular perfusion and muscle glucose uptake was determined by using 2-deoxy-D-[1-^{14}C]

glucose (2-DG; specific activity = 56.0 mCi.mmol^{-1}, Amersham Pharmacia Biotech) as described in section 2.3.3.

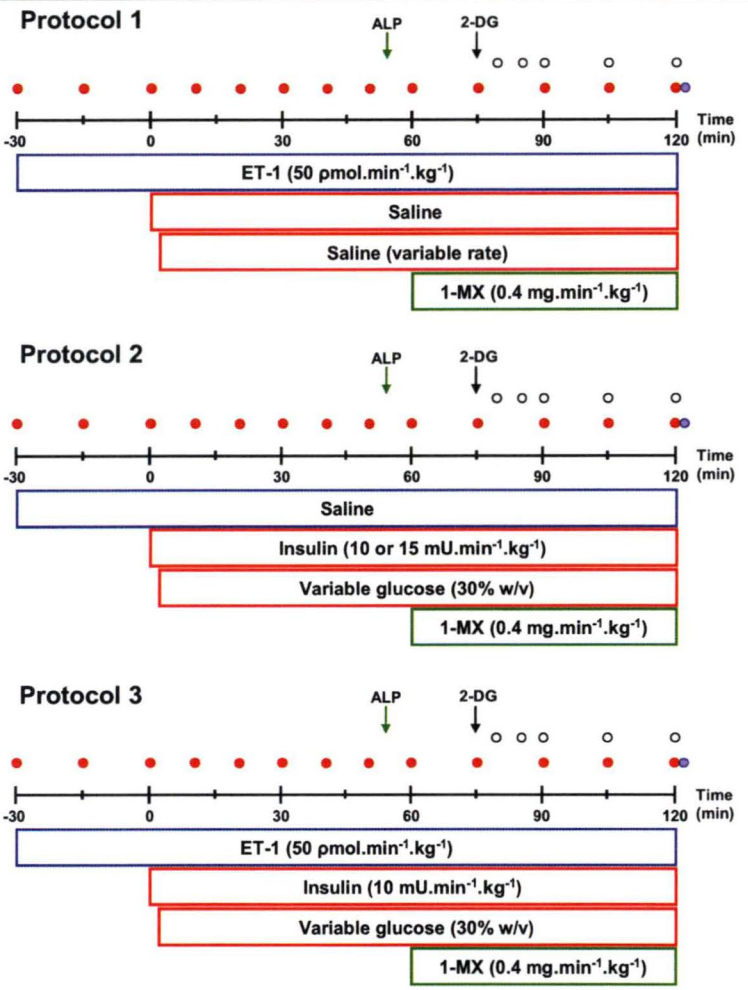

FIGURE 6.1. ET-1 EXPERIMENTAL PROTOCOLS. Experiments included an ET-1 control experiment where ET-1 (50 pmol.min^{-1}.kg^{-1}) was infused alone for 150 min (Protocol 1), a 2 h hyperinsulinaemic-euglycaemic clamp (10 or 15 mU.min^{-1}.kg^{-1}) (Protocol 2), and experiments designed to show the effect of ET-1 infusion on insulin action where ET-1 (50 pmol.min^{-1}.kg^{-1}) was infused 30 min prior to a 10mU.min^{-1}.kg^{-1} hyperinsulinaemic euglycaemic clamp (Protocol 3). During all protocols, a bolus injection of 2-deoxy-D-[1-^{14}C] glucose (2-DG) was administered at 75 min to determine muscle glucose uptake and 1-MX was continuously infused for the last hour of the experiment to determine microvascular perfusion.

Horizontal bars represent venous infusions, • represent arterial blood samples for determination of blood glucose and lactate, • represents venous blood sample to determine arterio-venous differences, ○ represent arterial blood samples taken to determine the clearance rate of 2-DG, *arrows* indicate bolus injections of allopurinol (ALP) or radioactive 2-DG.

6.2.4 Insulin clearance

A separate set of experiments was conducted in order to determine the insulin clearance rate (Fig. 6.2). A bolus of fluorescein isothiocyanate (FITC)-labelled insulin (200 µl, 1 $mg.ml^{-1}$, Sigma Aldrich ®; USA) was administered 45 min prior to the completion of a 2.5 h saline or ET-1 (50 $pmol.min^{-1}.kg^{-1}$) infusion. Blood samples were taken at 2, 5, 10, 15, 30 and 45 min after the bolus, centrifuged and the plasma removed. Fluorescence of the plasma samples (50 µl) were measured at an excitation wavelength of 480 nm and an emission wavelength of 530 nm, and plotted against time. From this graph, the clearance rate was determined by multiplying the *k* value obtained from the graph and the distribution volume (calculated by multiplying the concentration of insulin used by the number of µg per ml injected into the rat).

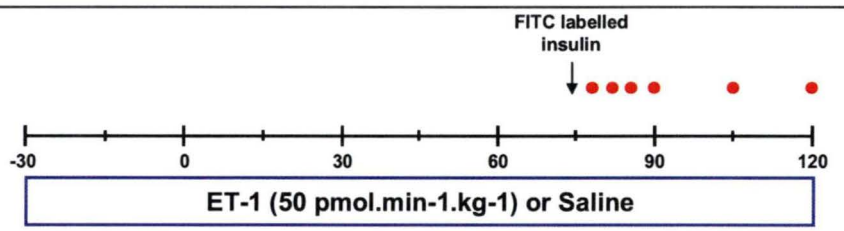

Figure 6.2: **INSULIN CLEARANCE PROTOCOL.** The insulin clearance experiments involved a 150min ET-1 or saline infusion. A bolus of FITC-labelled insulin was administered at 75 min, and blood samples were taken at 77, 80, 85, 95, 105 and 120 min to determine the insulin clearance rate.

Horizontal bar, represent venous infusions, *Arrow,* represents bolus injection via jugular vein, • represent arterial blood samples for determination insulin clearance.

6.2.5 Determination of insulin, C-peptide and endothelin

Arterial blood samples were taken prior to the start of the experiment and at 120 min, centrifuged and the plasma was removed and stored at -20°C until required. The plasma was used to determine arterial insulin (Mercodia AB; Sweden), endothelin (Biomedica; Austria) and C-peptide (rat C-peptide; Japan) levels using ELISA kits as indicated in parentheses. Plasma from femoral vein samples taken at 120 min was also used for the determination of venous plasma insulin (Mercodia AB; Sweden) levels by ELISA.

6.2.6 Data analysis

All data are expressed as means ± SEM. Data were calculated as described in section 2.4.

6.2.7 Statistical Analysis

To ascertain differences between treatment groups at the 120 min time point, a one-way ANOVA was used. Differences between initial (-30 min) and final (120 min) values were assessed using a paired *t*-test. Comparisons were made between treatment groups over the course of the experiment using a two-way repeated measures ANOVA and Student-Newman-Keuls post hoc test. Significance was accepted at a level of $p< 0.05$. All tests were performed using SigmaStat software (Systat Software Inc., USA).

6.3 RESULTS

6.3.1 Experimental Groups

There were four experimental groups: ET-1 (ET1; n=5), 10 $mU.min^{-1}.kg^{-1}$ insulin (INS10; n=8), ET-1 infusion 30 min prior to 10 $mU.min^{-1}.kg^{-1}$ insulin (ETINS10; n=7) and 15 $mU.min^{-1}.kg^{-1}$ insulin (INS15; n=6).

6.3.2 Plasma endothelin, insulin and C-peptide concentrations

Table 6.1 shows the initial (-30 min) and final (120 min) arterial plasma endothelin, insulin and C-peptide concentrations. There was no significant difference between the initial (-30 min) arterial plasma endothelin levels between the four groups (~6 $pmol.l^{-1}$). ET-1 infusion (with or without insulin) significantly (p<0.05) increased plasma endothelin levels to approximately 130 $pmol.l^{-1}$ by 120 min. Intermittent concentrations following the commencement of endothelin-1 infusion at -30 min were 48 ± 16 (0 min), 104 ± 28 (30 min), 92 ± 27 (60 min), and 89 ± 28 $pmol.l^{-1}$ (90 min). The increase was gradual and was reflected in the time course of other measurements such as mean arterial pressure and femoral blood flow. Insulin (INS10 and INS15) infusion (without ET-1 infusion) also caused a small but significant (p<0.05) increase in plasma endothelin concentrations reaching approximately 20 $pmol.l^{-1}$ by 120 min.

As with endothelin, there was no significant difference in the initial (-30 min) plasma insulin concentrations between the four experimental groups (~250 pmol.l^{-1}). Insulin (INS10) infusion significantly (p<0.05) increased plasma insulin concentrations to 2 120 ± 188 pmol.l^{-1}. When this same dose of insulin was infused with ET-1 (ETINS10), plasma concentrations reached 4 740 ± 908 pmol.l^{-1}, significantly (p<0.05) greater than INS10 alone. This increased plasma insulin concentration with ET-1 infusion (ETINS10) is comparable to insulin at the higher dose of 15 mU.min^{-1}.kg^{-1} (INS15), which resulted in final plasma insulin concentrations of 4 920 ± 193 pmol.l^{-1}. While there were differences between the arterial plasma insulin concentrations, venous plasma insulin levels (taken from the femoral vein) when multiplied by femoral blood flow to reflect the local concentrations, showed no significant differences between INS10 (1 190 ± 287 fmol.min^{-1}) and ETINS10 (1410 ± 777 fmol.min^{-1}). The higher dose of insulin (INS15) had a significantly higher local concentration (3140 ± 979 fmol.min^{-1}) than the other three groups, and ET-1 alone had significantly lower concentrations of 45 ± 10 fmol.min^{-1}.

C-peptide levels showed a trend to decrease throughout the course of the experiments but there was no statistical differences between initial (-30 min) and final (120 min) concentrations.

6.3.3 Insulin clearance

Whole body rate of insulin clearance was investigated to determine if the plasma insulin concentrations increased during ET-1 infusion due to a decrease in insulin clearance. There was no significant difference in the calculated distribution volume of a FITC insulin bolus when administered during saline (3.3 ± 0.2 ml) or ET-1 (3.3 ± 0.1 ml) infusions. However, the whole body insulin clearance rate was significantly decreased (p=0.002) during ET-1 infusion (0.19 ± 0.02 ml.min^{-1}) when compared with saline infusion (0.35 ± 0.6 ml.min^{-1}).

TABLE 6.1: PLASMA ENDOTHELIN, INSULIN AND C-PEPTIDE VALUES BEFORE (-30 MIN) AND AFTER TREATMENT (120 MIN)

	ET-1	10mU.min^{-1}.kg^{-1} insulin	ET-1+ 10mU.min^{-1}.kg^{-1} insulin	15mU.min^{-1}.kg^{-1} insulin
Plasma ET (pmol.l^{-1})				
Initial (-30 min)	10 ± 8	2 ± 0.4	3 ± 0.6	9 ± 3
Final (120 min)	130 ± 7$^{*\#}$	20 ± 3*	140 ± 6$^{*\#}$	20 ± 2*
Plasma insulin (pmol.l^{-1})				
Initial arterial (-30 min)	195 ± 13	260 ± 91	230 ± 22	3560 ± 75
Final arterial(120 min)	210 ± 34†	2 120 ± 188*	4 740 ± 908*†	4 920 ± 193*†
Final venous (120 min) (fmol.min^{-1})	45 ± 11	1 190 ± 287	1 410 ± 777	3 140 ± 979
Plasma C-peptide (pmol.l^{-1})				
Initial (-30 min)	1 320 ± 469	790 ± 0.1	1 170 ± 271	1 880 ± 254
Final (120 min)	1 035 ± 348	530 ± 48	960 ± 278	950 ± 198

Values are means ± SEM. *, significantly different from initial values ($p<0.05$); #, significantly different to 10 and 15 mU.min^{-1}.kg^{-1} insulin ($p<0.05$); †, significantly different to 10 mU.min^{-1}.kg^{-1} insulin ($p<0.05$).

6.3.4 Mean arterial pressure and heart rate

ET-1 infusion (ET1 and ETINS10 groups), significantly ($p<0.05$) increased mean arterial pressure in a time dependent manner reaching approximately 130 mmHg at 120 min (Fig. 6.3). This increase in mean arterial pressure corresponded with increases in plasma endothelin concentrations, and was unaffected by co-infusion with insulin. Insulin alone (INS10 and INS15) had no effect on mean arterial pressure, which was significantly ($p<0.05$) lower than the ET-1 groups (ET1 and ETINS10) from the 60 min time point (Fig.5.3A).

The infusion of ET-1 with insulin (ETINS10) caused a progressive decrease in heart rate resulting in a 10% decrease by the end of the experiment (Fig. 5.3B). This decrease became significantly ($p<0.05$) different to the INS10, INS15 and ET-1 groups from 75 min. Heart rate remained stable throughout the experiment for all other groups (Fig. 5.3B). Data for Figure 5.3B have been normalised relative to HR at 0 min; absolute values at 0 min were: 359 ± 14 (ET-1 alone), 377 ± 7 (10 mU.min^{-}

^{1}.kg^{-1} insulin), 392 ± 14 (15 mU.min^{-1}.kg^{-1} insulin), and 385 ± 11 (ET-1 + 10 mU.min^{-1}.kg^{-1} insulin) beats.min^{-1}.

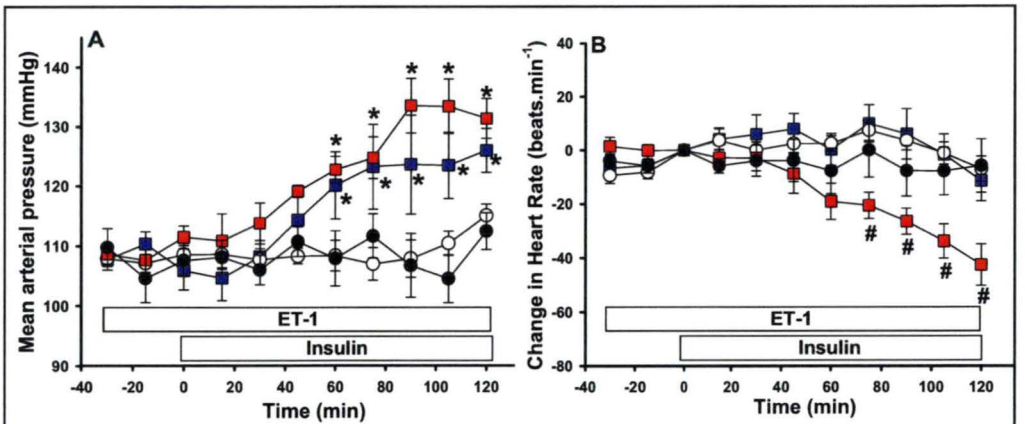

FIGURE 6.3: Time course for mean arterial pressure (A) and the change in hear rate (normalised at t=0 min; B) as a result of ET-1 and/or insulin infusion. Values are means ± SEM. *, significantly different from 10 and 15mU.min^{-1}.kg^{-1} (p<0.05). #, significantly different from all other groups (p<0.05). ○ 15mU.min^{-1}.kg^{-1} insulin; ● 10mU.min^{-1}.kg^{-1} insulin; ■ ET-1; ■ ET-1 prior to 10mU.min^{-1}.kg^{-1} insulin.

6.3.5 Femoral blood flow and vascular resistance

There was no change in femoral blood flow when ET-1 was infused alone (Fig. 6.4A). Insulin infusion resulted in a significant increase in femoral blood flow (p<0.05), however the infusion of ET-1 with insulin opposed this stimulatory effect ((p<0.05; Fig. 5.4A). Data for Figure 6.4A has been normalised relative to the femoral blood flow at 0 min; absolute values were 1.6 ± 0.2 (ET-1), 1.1 ± 0.1 (INS10), 1.2 ± 0.1 (INS15) and 1.2 ± 0.1 (ETINS10) ml.min^{-1}. A similar pattern was observed for vascular resistance involving infusion of ET-1 before and during insulin infusion (Fig. 6.4B). In this case ET-1 attenuated the decrease in vascular resistance caused by insulin infusion. Figure 6.4B also shows that ET-1 infusion alone caused a small but significant increase in vascular resistance (p<0.05) between 20 to 60 min, however this increase was no longer significant by 120 min. Again, data for Figure 6.4B has been normalised relative to the vascular resistance at 0 min; absolute values were 76 ± 13 (ET-1), 108 ± 8 (INS10), 91 ± 6 (INS15), and 101 ± 11 (ETINS10) RU.

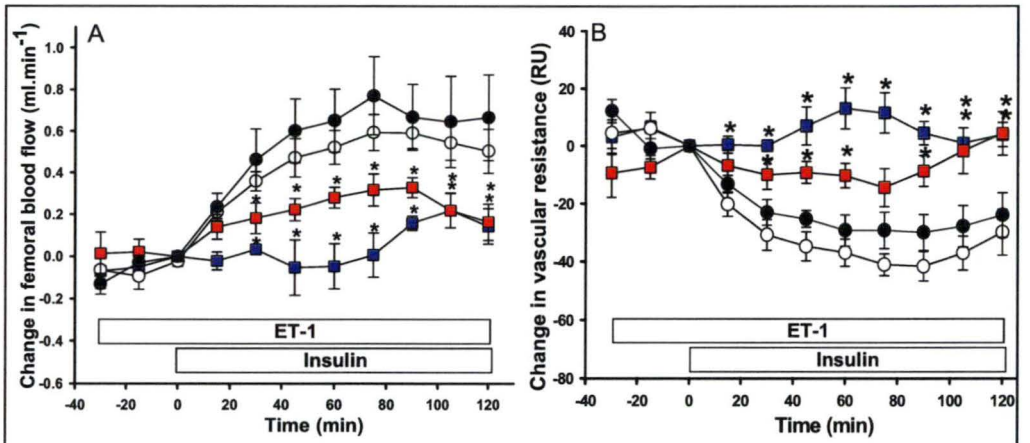

FIGURE 6.4: Time course for the change in femoral blood flow (A) and vascular resistance (B) as a result of ET-1 and/or insulin infusion. Values are normalised at t=0 min, and values are means ± SEM. *, significantly different from 10 and 15mU.min^{-1}.kg^{-1} (p<0.05). ○ 15mU.min^{-1}.kg^{-1} insulin; ● 10mU.min^{-1}.kg^{-1} insulin; ■ ET-1; ■ ET-1 prior to 10mU.min^{-1}.kg^{-1} insulin.

6.3.6 Microvascular Perfusion

No significant difference in arterial plasma concentrations of 1-MX or oxypurinol (the metabolite of allopurinol and inhibitor of xanthine oxidase) were found between the four experimental groups (Table 6.2). The infusion of insulin significantly ($p < 0.05$) increased the rate of 1-MX metabolism from 4.9 ± 0.6 nmol.min^{-1} with ET-1 alone to 8.4 ± 0.8 nmol.min^{-1} with 10 mU·min^{-1}·kg^{-1} insulin and to 8.3 ± 0.6 nmol.min^{-1} with 15 mU·min^{-1}·kg^{-1} insulin. However the infusion of ET-1 prior to insulin attenuated this stimulatory effect (ETINS10: 5.7 ± 0.8 nmol.min^{-1}) ($p < 0.05$).

TABLE 6.2: 1-METHYLXANTHINE METABOLISM AFTER ET AND/OR INSULIN INFUSION

	ET-1	10mU.min^{-1}.kg^{-1} insulin	ET-1 + 10mU.min^{-1}.kg^{-1} insulin	15mU.min^{-1}.kg^{-1} insulin
Oxypurinol (μM)	6.7 ± 1.1	6.3 ± 0.8	7.6 ± 0.4	7.4 ± 0.4
Arterial 1-MX (μM)	24.5 ± 5.2	21.4 ± 1.7	30.2 ± 3.8	17.9 ± 1.3
1-MX disappearance (nmol.min^{-1})	4.9 ± 0.6	8.4 ± 0.8*	5.7 ± 0.8	8.3 ± 0.6*

Values are means ± SEM. *, significantly different from ET-1 and ET-1+10 mU.min^{-1}.kg^{-1} insulin (p<0.05)

6.3.7 Glucose metabolism

Blood glucose was clamped at 4.8 mmol.l^{-1} throughout insulin infusions. The time course for the glucose infusion rate (GIR) to maintain euglycaemia during INS15 experiments reached a plateau at 31.3 ± 1.6 mg.min^{-1}.kg^{-1} and was significantly higher (p<0.05) than either INS10 (23.0 ± 0.7 mg.min^{-1}.kg^{-1}) or ETINS (22.5 ± 1.2 mg.min^{-1}.kg^{-1}). There was no difference between INS10 and ETINS10 (Fig 6.5).

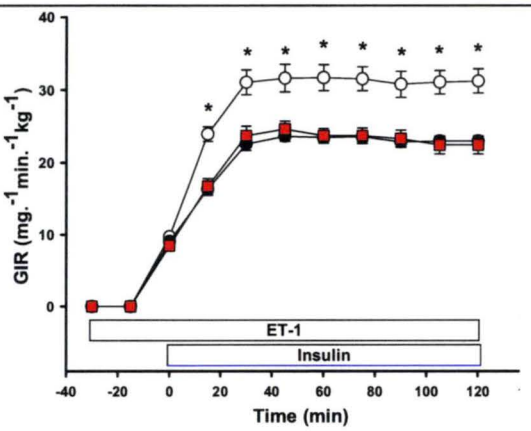

FIGURE 6.5: Time course for the change in glucose infusion rate (GIR) as a result of insulin alone, or insulin and ET-1 infusion. Values are means ± SEM. *, significantly different from ET-1 + 10 mU.min^{-1}.kg^{-1} and 10mU.min^{-1}.kg^{-1} (p<0.05). ○ 15mU.min^{-1}.kg^{-1} insulin; ● 10mU.min^{-1}.kg^{-1} insulin; ■ ET-1 prior to 10mU.min^{-1}.kg^{-1} insulin.

During infusion of ET-1 alone there was a small decrease in blood glucose which became significantly different from other groups at 75 min (p < 0.05) and remained significantly different for the remainder of the experiment (Fig. 6.6A). Blood lactate levels significantly increased from their initial values in all four groups (p < 0.05), however the blood lactate concentrations of the ETINS10 group increased significantly over all other groups at 90, 105 and 120 min (p < 0.05; Fig. 6.6B).

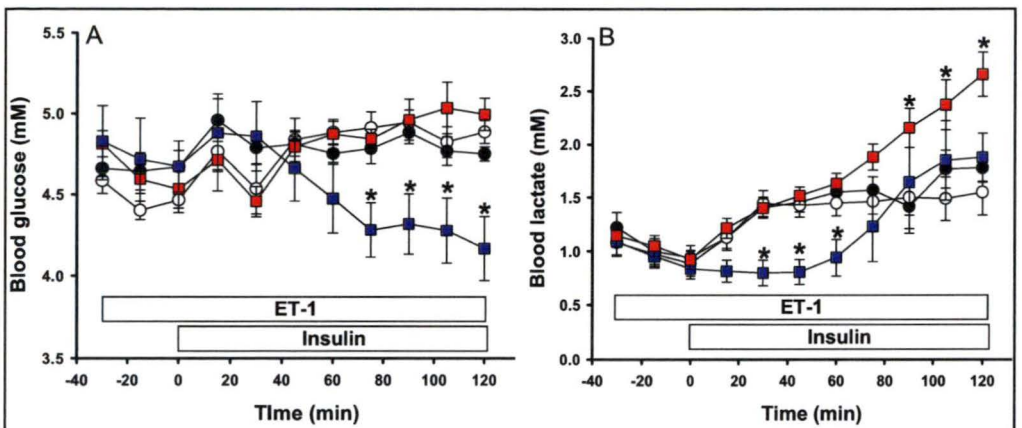

FIGURE 6.6: Time course for the change in blood glucose (A) and blood lactate (B) concentrations as a result of ET-1 and/or insulin infusion. Values are means ± SEM. *, significantly different from 10 and 15mU.min^{-1}.kg^{-1} (p<0.05). ○ 15mU.min^{-1}.kg^{-1} insulin; ● 10mU.min^{-1}.kg^{-1} insulin; ■ ET-1; ■ ET-1 prior to 10mU.min^{-1}.kg^{-1} insulin.

Figure 6.7A shows 2-DG uptake (R'g) for individual muscles of the lower leg (SOL, PLA, RG, WG, EDL, TIB) excised at the completion of the experiment. As expected the infusion of insulin significantly increased muscle glucose uptake in all muscles compared to the infusion of ET-1 alone (p<0.05). The infusion of INS15 had a significantly higher R'g than INS10 and ETINS15 in all individual muscles (except the soleus) and the combined value which is aggregated on proportion of weight (p<0.05; Figure 5.7B). There was no difference between the R'g for INS10 and ETINS10 in the individual muscle or when combined.

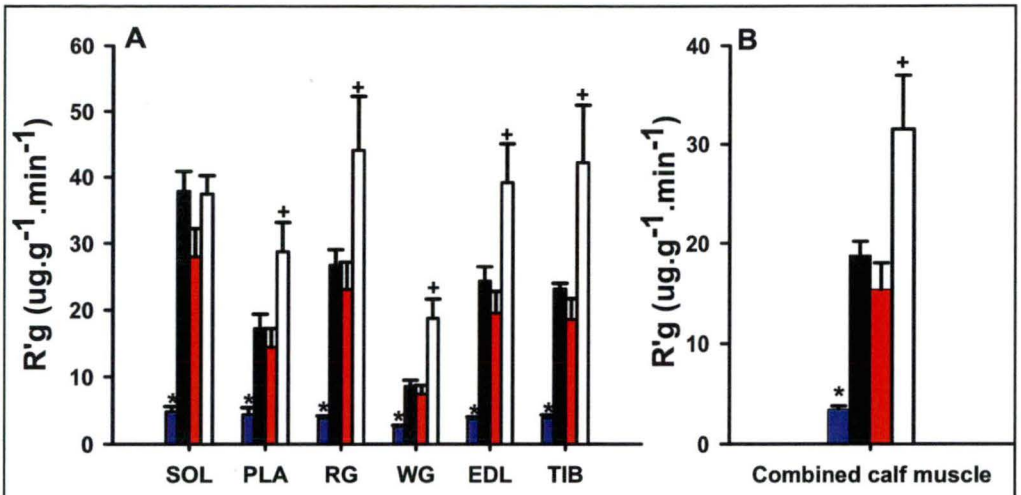

FIGURE 6.7: Muscle radioactive 2-DG uptake (R'g) for individual muscles of the lower leg (A) and the combined calf muscle (aggregated on proportional weight) (B) due to ET-1 and/or insulin infusion. 2-DG was administered at as a bolus at 75 min (Figure 6.1) and individual muscles (SOL, soleus; PLA, plantaris; RG, red gastrocnemius; WG, white gastrocnemius; EDL, extensor digitorum longus; TIB, tibialis anterior) were excised at the completion of the experiment. Values are means ± SEM. *, significantly different to all other groups ($p<0.05$), +, significantly different to ET-1+10mU.min^{-1}.kg^{-1} insulin ($p<0.05$). □ 15mU.min^{-1}.kg^{-1} insulin; ■10mU.min^{-1}.kg^{-1} insulin; ■ ET-1; ■ ET-1 prior to 10mU.min^{-1}.kg^{-1} insulin.

6.4 DISCUSSION

The main finding of this study was that ET-1 infusion *in vivo*, severely blunted insulin's stimulatory effects on microvascular perfusion and femoral blood flow. In conjunction with this inhibition, ET-1 also caused an increase in mean arterial pressure and a decrease in glucose infusion rate and muscle glucose uptake. However, these effects on glucose uptake are not obvious unless plasma insulin concentrations are assessed, as ET-1 (through its vasoconstrictor actions) caused a significant decrease insulin clearance rate leading to an increase in plasma insulin concentrations ($p<0.05$).

ET-1 infusion prior to a 10 mU.min^{-1}.kg^{-1} insulin clamp resulted in a ~2 fold increase in plasma insulin concentrations from 2 120 ± 190 pmol.l^{-1} to 4 740 ± 910 pmol.l^{-1}, levels equivalent to a higher insulin dose of 15 mU.min^{-1}.kg^{-1} where plasma insulin concentrations reached 4 920 ± 193 pmol.l^{-1}. De Carlo et al. [331] have shown that ET-

1 stimulates insulin secretion from rat pancreatic islets, however incubated cell preparations do not take into account ET-1's vascular actions, which have been shown to cause strong vasoconstriction to the pancreas [191, 192] and a decreased secretory response *in vivo* [332]. In the present study C-peptide levels in all groups remained unchanged during the experiment and ET-1 infusion alone did not affect basal plasma insulin levels (Table 6.1). These data suggest that ET-1 had increased plasma insulin concentrations by decreasing insulin clearance and not by increasing insulin secretion. This was confirmed by experiments using FTIC labelled insulin, which revealed that ET-1 caused a 50% decrease in the rate of insulin clearance ($p<0.002$), a new finding for studies *in vivo*.

The finding that insulin clearance is decreased with ET-1 infusion allows us to uncover the negative effect of ET-1 infusion on glucose uptake. If the data are assessed on the basis of plasma insulin concentrations, where ET-1 infusion prior to a 10 $mU.min^{-1}.kg^{-1}$ insulin clamp is compared to a 15 $mU.min^{-1}.kg^{-1}$ insulin clamp, ET-1 caused a 49% decrease in muscle glucose uptake (Fig. 6.7) and a 29% decrease in GIR (representative of whole body glucose uptake) (Fig. 6.6). However, there was no difference in glucose uptake measures between ET-1 infusion prior to 10 $mU.min^{-1}.kg^{-1}$ insulin clamp and 10 $mU.min^{-1}.kg^{-1}$ insulin clamp alone. This suggests that the vasculature is more sensitive to ET-1 than the muscle tissue and demonstrates that in the short term, increased plasma insulin concentrations may compensate for under-perfused tissues (particularly in muscle), and allow insulin to maintain its actions on glucose uptake. Over time however, hyperinsulinaemia has been shown to cause an increase in ET_A receptor expression [200, 201], leading to an increased vasoconstriction. Chronic hyperinsulinaemia is not a desirable trait and in conjunction with increased mean arterial pressure caused by ET-1, can lead to hypertension, insulin resistance, endothelial dysfunction and cardiovascular disease.

Another important finding in this study was that the infusion of ET-1 in conjunction with insulin, augmented insulin's haemodynamic actions. Insulin alone increased femoral blood flow and decreased vascular resistance in the hindlimb. More importantly, insulin increased microvascular perfusion, increasing its own access and that of glucose to the muscle. ET-1 suppressed insulin's haemodynamic effects by suppressing increases in femoral blood flow and microvascular perfusion, and

prevented the decrease in vascular resistance seen by insulin alone. These alterations in perfusion are the most likely cause of the decrease in insulin stimulated glucose uptake seen with ET-1 infusion.

It may be speculated that ET-1 caused muscle insulin resistance by suppressing the increase in femoral blood flow seen with insulin alone. However, Ottosson-Seeberger et al. [193] showed ET-1 infusion decreased muscle glucose uptake with no changes in total blood flow to the muscle, supporting the notion that total blood flow changes have little influence on glucose uptake. For example, a 3 $mU.min^{-1}.kg^{-1}$ hyperinsulinaemic-euglycaemic clamp increases muscle glucose uptake and microvascular perfusion without an increase in femoral blood flow [29] and previous studies using models of insulin resistance (such as the obese Zucker rat) have shown that an impairment in muscle glucose uptake may be attributed to inhibition of insulin mediated microvascular perfusion [41, 97, 196, 333]. Therefore, the extent of microvascular perfusion, which accounts for approximately 50% of muscle glucose uptake [29, 56] is an important determinant of glucose uptake in the muscle. Thus, by decreasing the surface area available for insulin and glucose to interact with the muscle, ET-1 infusion has resulted in a 49% decrease in insulin stimulated muscle glucose uptake (Fig. 6.7).

It appears that the decreased insulin clearance rate may also be attributed to ET-1's haemodynamic effects. It is well documented that ET-1 causes decreased blood flow to the kidneys and liver, two organs which account for approximately 65% of insulin clearance [334]. This study also shows that blood flow (and microvascular perfusion) to the hindlimb muscle, which has been shown to play a significant role in insulin clearance in spontaneously hypertensive rats, was also decreased. Therefore by decreasing blood flow to these organs, ET-1 has decreased the opportunity for insulin clearance resulting in elevated plasma concentrations. However, it is important to note that this phenomenon was only evident when exogenous insulin was infused, as there was no increase in plasma insulin concentration when ET-1 was infused alone. This may be due to the low circulating levels of insulin, where its clearance is concentration dependent unless other factors interfere. Alternatively, the change in concentration of ~100 $pmol.l^{-1}$ may be too small to be detected by ELISA with a small sample group of five rats.

A high dose of ET-1 was employed in this study and plasma levels at 120 min exceed plasma levels reported under pathological conditions. This dose of ET-1 was used as it was found to induce physiological hypertension without affecting heart rate during preliminary experiments. Also, plasma concentrations slowly increased throughout the experiment and it took over 60 min of ET-1 infusion for blood pressure to rise above resting levels. The results may have been even more dramatic if ET-1 had been infused at a higher rate, or was given as a bolus prior to insulin infusion. Therefore, as the secretion of ET-1 in the body is abluminal, and not directly in to the blood stream, this model may be considered representative of a disease state, such as diabetes or hypertension, where there is an over-secretion of ET-1.

Many studies have identified ET-1 concentrations to be elevated in diseases such as hypertension, type 2 diabetes and endothelial dysfunction, all of which are implicated in cardiovascular disease [7, 182-184]. The cause of ET-1 over secretion and increased plasma concentrations is yet to be determined and requires further investigation due to the severity of its actions. It is possible that hyperinsulinaemia seen in the diabetic state may up-regulate ET-1 secretion and receptor expression [200, 201] causing further vasoconstriction and potentate the hyperinsulinaemic state. Alternatively, increased ET-1 secretion (stimulated by other means) may lead to hyperinsulinaemia, as demonstrated in this study, which will in turn lead to a further over secretion of ET-1. ET-1's detrimental effects appear to be mediated through its vasoconstrictor actions induced by its binding to the ET_A receptor [85, 178, 187]. Blockade of this receptor may prove to be a beneficial therapy for patients suffering from cardiovascular disease and type 2 diabetes, however further research is required [335].

In summary, this study shows ET-1 infusion blocks insulin's haemodynamic actions, resulting in a decreased insulin clearance rate, muscle glucose uptake and whole body GIR. Based on previous work, this decreased glucose uptake may be attributed to a decrease in microvascular perfusion resulting in insulin resistance. This study implies that elevated plasma levels of ET-1 may contribute to insulin resistance and hypertension through its vascular effects.

CHAPTER 7:

INTERLEUKIN-6 AND INSULIN ACTION *IN VIVO*

7.1 INTRODUCTION

Interleukin-6 (IL-6) is an inflammatory cytokine which is also thought to be involved in glucose homeostasis. At rest, IL-6 is secreted from a number of tissues including adipose tissue, which is believed to be the tissue responsible for the increased concentrations of plasma IL-6 in type 2 diabetic and obese patients [90, 219, 336]. While the skeletal muscle contributes little to plasma IL-6 at rest, during exercise the muscle is responsible for a rise in plasma levels of IL-6 which increase from 1 $pg.ml^{-1}$ at rest up to 100 $pg.ml^{-1}$ after strenuous exercise [224, 225]. It is thought that IL-6 acts to regulate energy stores and maintain glucose homeostasis during exercise as its release is related to the level of stored glycogen in muscle, and is associated with an increase in AMPK activation [244, 247].

Studies *in vivo*, show that acute IL-6 administration causes an increase in lipolysis and fatty acid oxidation in adipose tissue [250, 253], without having an effect on basal glucose disposal, glucose uptake or hepatic glucose production. The available data concerning IL-6 infusion during insulin administration however, is ambiguous with studies finding an increase in glucose uptake [248], no change [266] or a decrease in insulin action [268]. In skeletal muscle a recent study has suggested that only supraphysiological doses of IL-6 (>10$ng.ml^{-1}$), up to ten times higher than those which occur during exercise, will cause glucose uptake [258]. Alternatively, a study by Carey et al.[248] found glucose uptake increased in a dose dependent manner from 1 to 10 $ng.ml^{-1}$ in L6 myotubes, with no further increases at doses of 100 or 1000 $ng.ml^{-1}$ IL-6. They also found that only higher concentrations of 10 to 1000 $ng.ml^{-1}$ IL-6 increased insulin stimulated glucose uptake, with no effect at the lower doses. However, both these studies were conducted with incubated muscle and cell culture, which do not take into account the possible haemodynamic effects of IL-6. Furthermore, when compared to the *in vivo* system, incubated muscles or cells generally require greater amounts of hormone/cytokine to cause an increase in glucose uptake [337]. While the involvement of IL-6 in glucose metabolism and insulin resistance in the adipose tissue and skeletal muscle is controversial, it has been consistently found that IL-6 causes a state of insulin resistance in the liver, through the activation of suppressor of cytokine signalling (SOCS) -3 proteins, interference of insulin receptor signalling, and decreased glycogen synthesis [276, 278, 279].

Previous work from this laboratory at the University of Tasmania has shown that infusion of TNF-α (at a dose of 0.5 $\mu g.kg^{-1}.h^{-1}$), another inflammatory cytokine, inhibits insulin mediated increases in femoral blood flow and microvascular perfusion in the rat. Furthermore, this inhibition also caused a 50% reduction in muscle glucose uptake causing a state of acute insulin resistance in the muscle.

The present study investigates if IL-6 inhibits insulin action in the same manner as TNF-α *in vivo*. Two doses of IL-6 are employed, one equivalent to the inhibitory dose of TNF-α used in previous studies, and a dose 10 times higher, corresponding to the increased concentrations seen during exercise. The effect of these two doses of IL-6 infusion on basal and insulin mediated haemodynamic and metabolic actions are assessed.

7.2 METHODS

7.2.1 Animals

Male hooded Wistar rats weighing 240 ± 2 g were used during theses experiments. They were raised as described in section 2.2.1.

7.2.2 Surgery

Experiments were conducted using the anaesthetised rat model, with surgery as described in section 2.2.2.

7.2.3 Experimental procedure

After a 45 min equilibration period rats were infused intravenously with IL-6 (recombinant rat IL-6; R & D Systems, USA) at 0.5 $\mu g.kg^{-1}.h^{-1}$ (low dose) or 5 $\mu g.kg^{-1}.h^{-1}$ (high dose) for 3 hours (Fig. 7.1). To test the effect of IL-6 on insulin action, a hyperinsulinaemic-euglycaemic clamp, in which insulin (Humulin R, Eli Lilly ®; USA) was infused into the rat at 3 $mU.min^{-1}.kg^{-1}$ for 2 h, was started after 1 h of IL-6 infusion (Fig. 7.1). The muscles of the lower leg (soleus, SOL; plantaris, PLA; red gastrocnemius, RG; white gastrocnemius, WG; extensor digitorum longus, EDL and

tibialis anterior, TIB) and the epididymal fat pads were excised, freeze-clamped in liquid nitrogen and stored at -80°C until required for analysis.

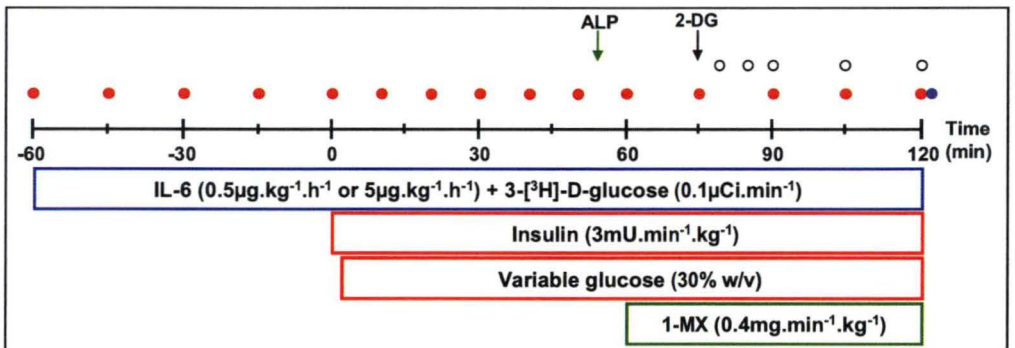

FIG. 7.1: IL-6 AND INSULIN EXPERIMENTAL PROTOCOL. Experiments consisted of a 3 h intravenous infusion of IL-6 at either 0.5 or 5 $\mu g.kg^{-1}.h^{-1}$ alone or during a hyperinsulinaemic euglycaemic clamp (3 $mU.min^{-1}.kg^{-1}$). Infusion volumes of insulin and glucose were matched by the equivalent volume of isotonic saline. IL-6 was replaced with a vehicle solution during control experiments. 3-[^{3}H]-D-glucose was infused throughout the experiment to determine glucose turnover. A bolus injection of 2-deoxy-D-[1-^{14}C] glucose (2-DG) was administered at 75 min for determination of muscle glucose uptake and 1-MX was continuously infused for the last hour of the experiment to determine microvascular perfusion. The muscles of the calf were excised and freeze-clamped with liquid nitrogen at the conclusion of the experiment.

Horizontal bars represent venous infusions, *red circles* represent arterial blood samples for determination of blood glucose and lactate, *blue circle* represents venous blood sample to determine arterio-venous differences, *white circles* represent arterial blood samples taken to determine the clearance rate of 2-DG, and *arrows* indicate bolus injections of allopurinol (ALP) or radioactive 2-DG as indicated.

During all experiments a glucose solution (30% w/v) was infused at variable rates to maintain blood glucose levels at 4.8 $mmol.l^{-1}$. This infusion rate was plotted as GIR expressed in $mg.min^{-1}.kg^{-1}$. Infusion volumes of insulin and glucose were matched by the equivalent volume of isotonic saline, and a solution (45% CH_3CN, 0.1% triflouroacetic acid in phosphate-buffered saline) was used as a vehicle substitute for IL-6 during control experiments (Fig 7.1).

Blood samples were taken at the times indicated in Fig. 7.1 and 7.2 and analysed for blood glucose and lactate (refer to section 2.3.4).

The 1-MX method (refer to section 2.3.2.1) was used to determine microvascular perfusion and muscle glucose uptake was determined by using 2-deoxy-D-[1-^{14}C] glucose (specific activity = 56.0 mCi.mmol^{-1}, Amersham Pharmacia Biotech) as described in section 2.3.3.

During IL-6 and insulin experiments, a primed (2 μCi), continuous infusion of 3-[^{3}H]-D-glucose (0.1 μCi.min^{-1}, specific activity of 16.6 Ci.mmol^{-1}, Amersham Pharmacia Biotech) was administered throughout the experiment in order to determine the glucose turnover (the rate of appearance and disappearance of glucose). Arterial samples were taken 15 min prior to, and on completion of the experiment, centrifuged and the plasma removed. The plasma was then deproteinised using 2 M perchloric acid, evaporated to dryness to remove $^{3}H_2O$ and re-suspended in distilled water. Biodegradable Counting Scintillant (Amersham, Arlington Heights, IL) was added to each sample and [^{3}H] glucose radioactivity was determined using a scintillation counter. The rates of appearance (Ra) and disappearance (Rd) of glucose were calculated using the isotope dilution equation:

$$Ra = Rd = F / SA$$

Where:

F = the rate of tracer infusion

SA = the specific activity of glucose (calculated by dividing the plasma radioactivity by the glucose concentration)

The hepatic glucose production (Ra) was then calculated by subtracting the glucose infusion rate (GIR) from the Rd as described by Burnol and colleagues [338].

7.2.4 Determination of insulin and IL-6

Arterial blood samples were taken prior to the start of the experiment and at 120 min, centrifuged and the plasma was removed and stored at -20°C until required. The plasma was used to determine arterial insulin (Mercodia AB; Sweden) and IL-6 (Pierce; Rockford, USA) concentrations using ELISA kits as indicated in parentheses.

7.2.5 Western blot analyses of Akt

For Western blot analyses muscles from the animals were homogenized in ice-cold lysis buffer consisting of 50 mM HEPES, 150 mM NaCl, 10 mM NaF, 1 mM Na_3VO_4, 5 mM EDTA, 0.5% Triton X-100, 10% glycerol (v/v), 2 $\mu g.ml^{-1}$ leupeptin, 100 $\mu g.ml^{-1}$ phenylmethylsulfonyl fluoride, and 2 $\mu g.ml^{-1}$ aprotinin. Homogenates were spun at 16,000 g for 60 min at 4°C, and the supernatant was removed and rapidly frozen in liquid nitrogen. Protein concentration of the muscle lysates was subsequently determined (Pierce). Lysates were solubilised in Laemmli sample buffer and boiled for 5 min, resolved by SDS-PAGE on 6% polyacrylamide gels, transferred to a nitrocellulose membrane, blocked with 5% milk, and immunoblotted overnight with phospho (Ser^{473}) and total Akt antibodies (1:1000, Cell Signaling, Beverley, MA). After incubation with horseradish peroxidase-conjugated secondary antibody (1:2000, Amersham Biosciences), the immunoreactive proteins were detected with enhanced chemiluminescence (PerkinElmer Life Sciences) and quantified by densitometry.

7.2.6 Data analysis

All data are expressed as means ± SEM. Data were calculated as described in section 2.4.

7.2.7 Statistical Analysis

To ascertain differences between treatment groups at the 120 min time point, a one-way ANOVA was used. Differences between initial (-60 min) and final (120 min) values were assessed using a paired *t*-test. Comparisons were made between treatment groups over the course of the experiment using a two-way repeated measures ANOVA and Student-Newman-Keuls post hoc test. Significance was accepted at a level of $p < 0.05$. All tests were performed using SigmaStat software (Systat Software Inc., USA).

7.3 RESULTS

7.3.1 Experimental groups

The experimental groups and the number of experiments in each (*n* value) are shown in the table below:

TABLE 7.1: IL-6 AND INSULIN EXPERIMENTAL GROUPS

Treatment group	*n* value
Vehicle	7
3 $mU.min^{-1}.kg^{-1}$ insulin	7
Low dose IL-6 (0.5 $\mu g.h^{-1}.kg^{-1}$)	5
Low dose IL-6 (0.5 $\mu g.h^{-1}.kg^{-1}$) + 3 $mU.min^{-1}.kg^{-1}$ insulin	5
High dose IL-6 (5 $\mu g.h^{-1}.kg^{-1}$)	8
High dose IL-6 (5 $\mu g.h^{-1}.kg^{-1}$) + 3 $mU.min^{-1}.kg^{-1}$ insulin	8

7.3.2 Plasma IL-6 and insulin concentrations

Table 7.2 shows the initial (-60 min) and final (120 min) arterial plasma IL-6 and insulin concentrations. There was no significant difference between the initial (-60 min) arterial plasma IL-6 levels between the experimental groups (~ 200 $pg.ml^{-1}$). Low dose IL-6 infusion (with or without insulin) had no effect on the levels of IL-6 in the plasma. High dose IL-6 infusion at 5 $\mu g.kg^{-1}.h^{-1}$, with or without insulin infusion, caused a significant increase in circulating levels to between 2500 and 3000 $pg.ml^{-1}$.

There was no significant difference between the initial (-60 min) arterial plasma insulin concentration between the experimental groups. Insulin infusion significantly increased circulating concentrations, with levels tending to be higher during IL-6 infusion, however this was not statistically significant.

TABLE 7.2: PLASMA CONCENTRATIONS OF IL-6 AND INSULIN BEFORE (-60 MIN) AND AFTER (120 MIN) IL-6 AND/OR INSULIN INFUSION

			0.5 μg.kg^{-1}.h^{-1} IL-6		5 μg.kg^{-1}.h^{-1} IL-6	
	Vehicle	3 mU·min^{-1}·kg^{-1} insulin	IL-6	IL-6 + insulin	IL-6	IL-6 + insulin
Plasma IL-6 concentrations (pg.ml^{-1})						
Initial (-60 min)	225 ± 10	164 ± 33	126 ± 32	165 ± 36	195 ± 7	225 ± 15
Final (120 min)	281 ± 31	281 ± 48	265 ± 31	608 ± 164	2519 ± 678*	3040 ± 726*
Plasma insulin concentrations (pmol.l^{-1})						
Initial (-60 min)	316 ± 44	346 ± 86	213 ± 62	445 ± 73	198 ± 14	342 ± 93
Final (120 min)	380 ± 89	774 ± 135*	460 ± 72	1231 ± 286*	284 ± 22	920 ± 192*

Values are means ± SEM. *, significantly different all other groups (p<0.05)

7.3.3 Heart rate and mean arterial pressure

Heart rate remained constant throughout the experiment for all groups, with neither IL-6 nor insulin alone, or in combination, having an effect on this parameter. Heart rate ranged from ~360 to 410 beats.min^{-1} for the duration of the experiment (Fig. 7.3).

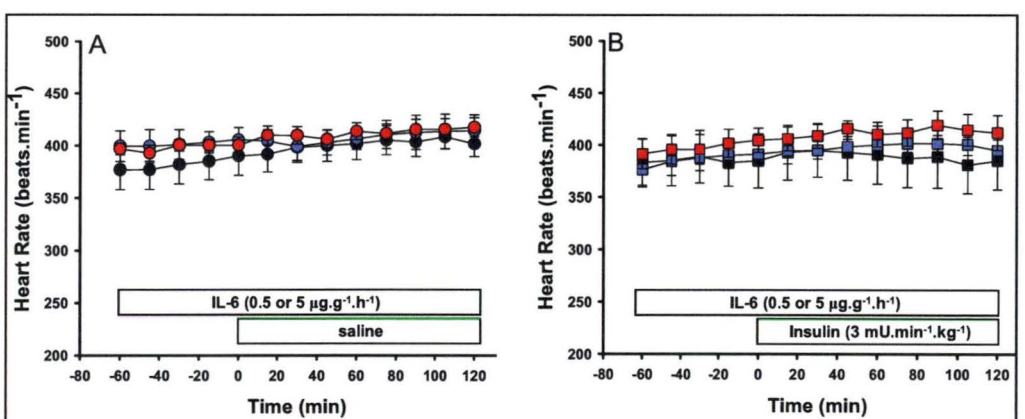

Figure 7.3: Time course for heart rate as a result of IL-6 infusion (panel A) or IL-6 infusion with 3mU.min^{-1}.kg^{-1} insulin infusion (panel B). Heart rate is measured by a catheter placed in the carotid artery. Values are means ± SEM. ● vehicle; ● 0.5 μg.kg^{-1}.h^{-1} IL-6; ● 5 μg.kg^{-1}.h^{-1} IL-6; ■ 3 mU.min^{-1}.kg^{-1} insulin; ■ 0.5 μg.kg^{-1}.h^{-1} IL-6 + insulin; ■ 5 μg.kg^{-1}.h^{-1} IL-6 + insulin.

Like heart rate, mean arterial pressure remained constant throughout the experiment for all groups, with neither IL-6 nor insulin alone, or in combination, having an effect

on this parameter. Mean arterial pressure ranged from ~100 to 120 mmHg for the duration of the experiment (Fig. 7.4).

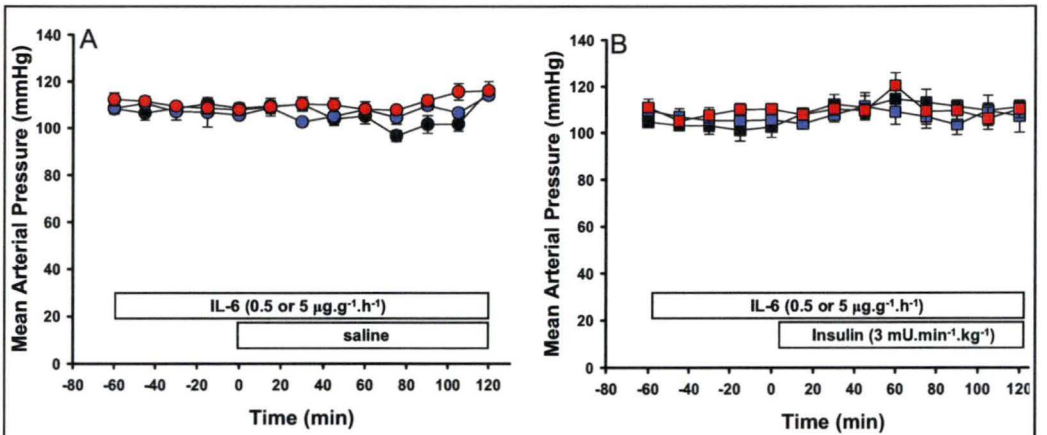

Figure 7.4: Time course for mean arterial pressure as a result of IL-6 infusion (panel A) or IL-6 infusion with 3mU.min^{-1}.kg^{-1} insulin infusion (panel B). Mean arterial pressure was measured by a catheter placed in the carotid artery. Values are means ± SEM. ● vehicle; ● 0.5 μg.kg^{-1}.h^{-1} IL-6; ● 5 μg.kg^{-1}.h^{-1} IL-6; ■ 3 mU.min^{-1}.kg^{-1} insulin; ■ 0.5 μg.kg^{-1}.h^{-1} IL-6 + insulin; ■ 5 μg.kg^{-1}.h^{-1} IL-6 + insulin.

7.3.4 Femoral blood flow and vascular resistance

Femoral blood flow remained steady for the duration of the experiment and was unaffected by the vehicle infusion, or insulin infusion alone or in combination with either dose of IL-6. The low dose of IL-6 had no effect on femoral blood flow however the high dose of 5 μg.kg^{-1}.h^{-1} IL-6 caused a small decrease in femoral blood flow throughout the experiment. Femoral blood flow was ~1.2 ml.min^{-1} before IL-6 infusion commenced, and was significantly decreased (p<0.05) by 15 min (compared to it initial starting value at -60 min and the vehicle infused group) reaching ~0.9 ml.min^{-1} by the end of the experiment (Fig. 7.5).

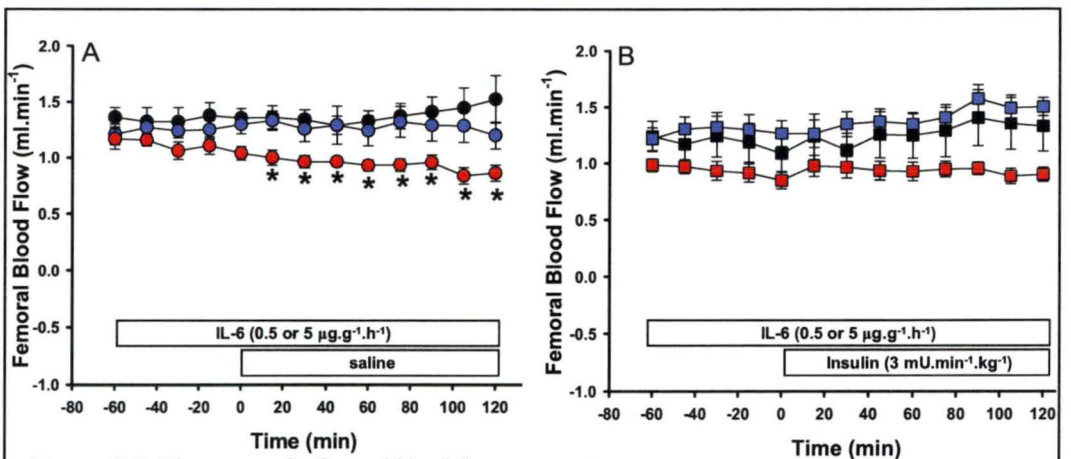

FIGURE 7.5: Time course for femoral blood flow as a result of IL-6 infusion (panel A) or IL-6 infusion with 3mU.min^{-1}.kg^{-1} insulin infusion (panel B). Flow probes were positioned around the femoral arteries of each leg. Values are means ± SEM. *, significantly different from vehicle infusion. ● vehicle; ● 0.5 µg.kg^{-1}.h^{-1} IL-6; ● 5 µg.kg^{-1}.h^{-1} IL-6; ■ 3 mU.min^{-1}.kg^{-1} insulin; ■ 0.5 µg.kg^{-1}.h^{-1} IL-6 + insulin; ■ 5 µg.kg^{-1}.h^{-1} IL-6 + insulin.

The time course for vascular resistance follows a similar pattern to femoral blood flow. While vehicle infusion and insulin infusion alone or in conjunction with IL-6 had no effect on vascular resistance, the high dose IL-6 (5 µg.kg^{-1}.h^{-1}) caused vascular resistance to increase (p<0.05) from ~95 at basal to ~125 at 120 min (Fig. 7.6).

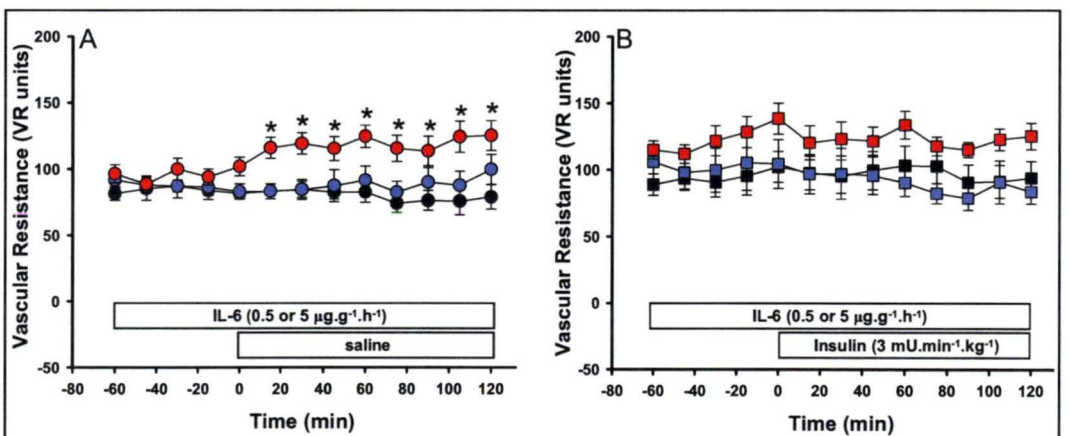

FIGURE 7.6: Time course for vascular resistance as a result of IL-6 infusion (panel A) or IL-6 infusion with 3mU.min^{-1}.kg^{-1} insulin infusion (panel B). Vascular resistance was calculated by dividing mean arterial pressure by femoral blood flow at a given time point. Values are means ± SEM. *, significantly difference to vehicle infusion (p<0.05)● vehicle; ● 0.5 µg.kg^{-1}.h^{-1} IL-6; ● 5 µg.kg^{-1}.h^{-1} IL-6; ■ 3 mU.min^{-1}.kg^{-1} insulin; ■ 0.5 µg.kg^{-1}.h^{-1} IL-6 + insulin; ■ 5 µg.kg^{-1}.h^{-1} IL-6 + insulin.

7.3.5 Microvascular perfusion

No significant difference in arterial plasma concentrations of 1-MX or oxypurinol (the metabolite of allopurinol and inhibitor of xanthine oxidase) were found between the experimental groups (Table 7.3). The infusion of insulin significantly ($p < 0.05$) increased the rate of 1-MX metabolism from 5.16 ± 0.95 nmol.min^{-1} with the vehicle solution to 8.12 ± 0.85 nmol.min^{-1} with 3 mU·min^{-1}·kg^{-1} insulin. IL-6 alone had no effect on 1-MX metabolism when compared to vehicle infusion however, infusion of both the low dose of IL-6 (6.10 ± 1.03 nmol.min^{-1}) and the high dose of IL-6 (6.77 ± 0.32 nmol.min^{-1}) significantly ($p < 0.05$) attenuated insulin's stimulatory on 1-MX metabolism and microvascular perfusion (Table 7.3).

TABLE 7.3: 1-METHYLXANTHINE METABOLISM AFTER IL-6 AND/OR INSULIN INFUSION

			0.5 μg.kg^{-1}.h^{-1} IL-6		5 μg.kg^{-1}.h^{-1} IL-6	
	Vehicle	3 mU.min^{-1}.kg^{-1} insulin	IL-6	IL-6 + insulin	IL-6	IL-6 + insulin
Oxypurinol (μM)	5.38 ± 0.52	6.16 ± 0.71	5.81 ± 0.28	6.17 ± 0.34	7.30 ± 0.45	6.77 ± 0.32
Arterial 1-MX (μM)	16.94 ± 1.14	23.42 ± 3.07	17.33 ± 1.94	16.72 ± 0.91	23.36 ± 3.72	21.08 ± 1.7
1-MX disappearance (nmol.min^{-1})	5.16 ± 0.95	8.12 ± 0.85*	5.56 ± 0.46	6.10 ± 1.03	5.63 ± 0.91	6.77 ± 0.32

Values are means ± SEM. *, significantly different all other groups ($p<0.05$)

7.3.6 Glucose metabolism

Blood glucose was clamped at 4.8 mmol.l^{-1} throughout the experiment. There was no difference in blood glucose between the experimental groups containing insulin, however it appears that the blood glucose concentration is higher in the high dose IL-6 treatment group. During treatment with high dose IL-6, glucose infusion was required to maintain euglycaemia during the middle portion of the experiment (0-60 min; see Fig 7.8), after which time, blood glucose concentrations were rising without the need for glucose infusion. There was no statistical difference between the blood glucose concentrations at basal compared to 120 min between any of the treatment groups (Fig. 7.7).

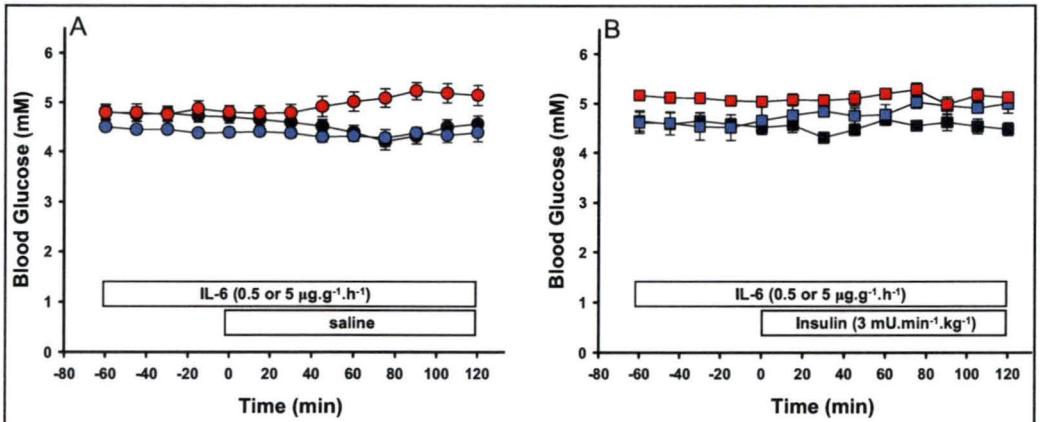

FIGURE 7.7: Time course for blood glucose concentrations as a result of IL-6 infusion (panel A) or IL-6 infusion with 3mU.min^{-1}.kg^{-1} insulin infusion (panel B). Values are means ± SEM. • vehicle; • 0.5 μg.kg^{-1}.hr^{-1} IL-6; • 5 μg.kg^{-1}.hr^{-1} IL-6; ■ 3 mU.min^{-1}.kg^{-1} insulin; ■ 0.5 μg.kg^{-1}.hr^{-1} IL-6 + insulin; ■ 5 μg.kg^{-1}.hr^{-1} IL-6 + insulin.

The glucose infusion rate (GIR) required to maintain euglycaemia during insulin infusion reached a plateau of 15.19 ± 0.91 mg.min^{-1}.kg^{-1}. Neither the low dose (GIR; 14.18 ± 1.53 mg.min^{-1}.kg^{-1}) nor high dose (GIR; 15.36 ± 1.45 mg.min^{-1}.kg^{-1}) of IL-6 had an affect on insulin stimulated glucose infusion rate, above that of insulin alone (Fig. 7.7). Preliminary experiments showed that if glucose was not infused during high dose IL-6 (5 μg.kg^{-1}.h^{-1}) infusion, blood glucose concentrations fell by ~1 mM throughout the 180 min experiment. Therefore a small amount of glucose (~1-2 mg.min^{-1}.kg^{-1}) was required during high dose of IL-6 infusion, generally between 0 and 60 min. Glucose was not infused during vehicle or low dose IL-6 (0.5 μg.kg^{-1}.h^{-1}) infusion (Fig. 7.7).

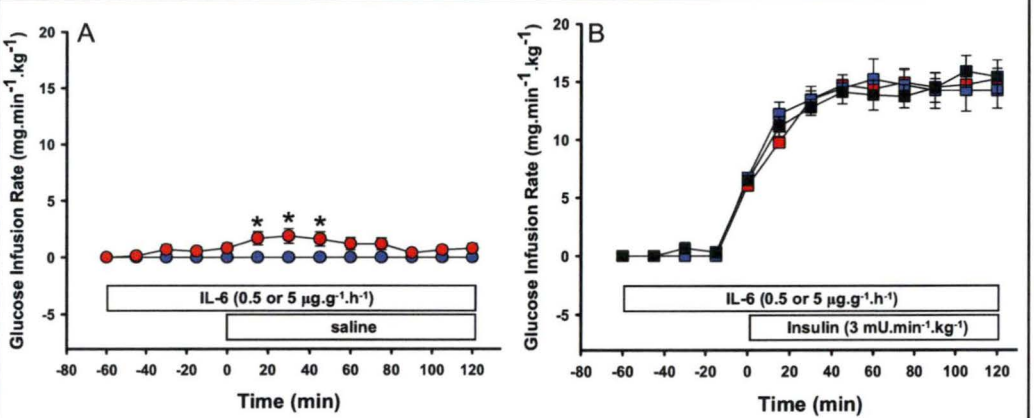

FIGURE 7.8: Time course for glucose infusion rate as a result of IL-6 infusion (panel A) or IL-6 infusion with 3mU.min^{-1}.kg^{-1} insulin infusion (panel B). Blood glucose levels were maintained at 4.8 mM. Values are means ± SEM. *, significantly different from vehicle infusion (p<0.05). ● vehicle; ● 0.5 µg.kg^{-1}.h^{-1} IL-6; ● 5 µg.kg^{-1}.h^{-1} IL-6; ■ 3 mU.min^{-1}.kg^{-1} insulin; ■ 0.5 µg.kg^{-1}.h^{-1} IL-6 + insulin; ■ 5 µg.kg^{-1}.h^{-1} IL-6 + insulin.

Figure 7.9 shows 2-DG uptake (R'g) for individual muscles of the lower leg (SOL, PLA, RG, WG, EDL, TIB) and the epididymal fat pads (FAT) excised and freeze-clamped at the completion of the experiment. As expected the infusion of insulin significantly (p<0.05) increased glucose uptake in all muscles compared to the infusion of vehicle and IL-6 alone. Low dose IL-6 (0.5 µg.kg^{-1}.h^{-1}) alone did not increase glucose uptake above basal and had no affect on insulin stimulated glucose uptake in the muscle. High dose IL-6 (5 µg.kg^{-1}.h^{-1}) alone however, increased glucose uptake compared to vehicle infusion in the red gastrocnemius muscle (p=0.035) and epididymal fat pad (p=0.021). Similarly, high dose IL-6 infused with insulin tended to further increase glucose uptake in the red gastrocnemius muscle and fat pads above insulin infusion alone, however this was not statistically significant (Fig 7.9).

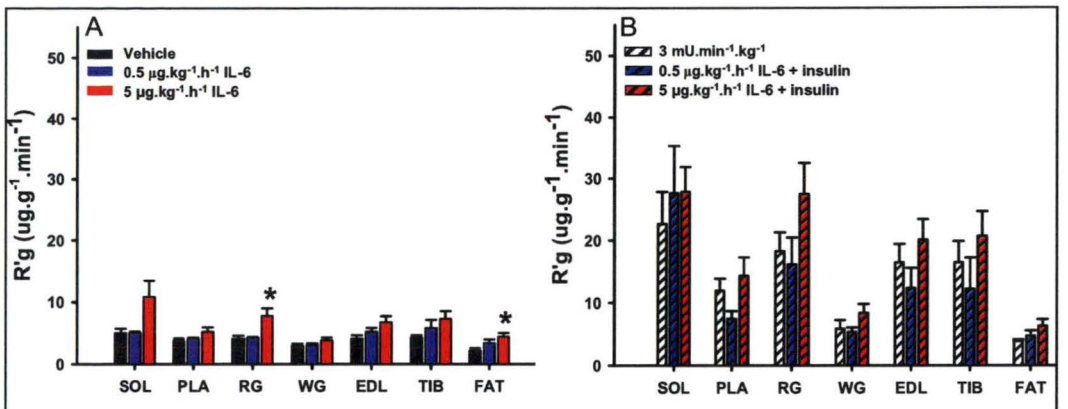

FIGURE 7.9: Muscle and adipose tissue radioactive 2-DG uptake (R'g) for individual muscles of the lower leg as a result of IL-6 infusion (panel A) or IL-6 infusion with 3mU.min^{-1}.kg^{-1} insulin infusion (panel B). 2-DG was administered at as a bolus at 75 min (Figure 6.1) and individual muscles (SOL, soleus; PLA, plantaris; RG, red gastrocnemius; WG, white gastrocnemius; EDL, extensor digitorum longus; TIB, tibialis anterior) and the epididymal fat pads (FAT)were excised at the completion of the experiment. Values are means ± SEM. *, significantly different to vehicle (p<0.05).

The combined calf muscle glucose uptake (aggregated on proportional weight) showed that insulin infusion increased muscle glucose uptake above values obtained with a vehicle infusion. Low dose IL-6 infusion (0.5 µg.kg^{-1}.h^{-1}) had no significant (p<0.05) effect on basal or insulin stimulated glucose infusion. High dose IL-6 infusion (5 µg.kg^{-1}.h^{-1}) alone tended to increase glucose uptake, however this was not statistically significant (p = 0.057). High dose IL-6 had no effect on insulin stimulated glucose uptake (Fig. 7.10).

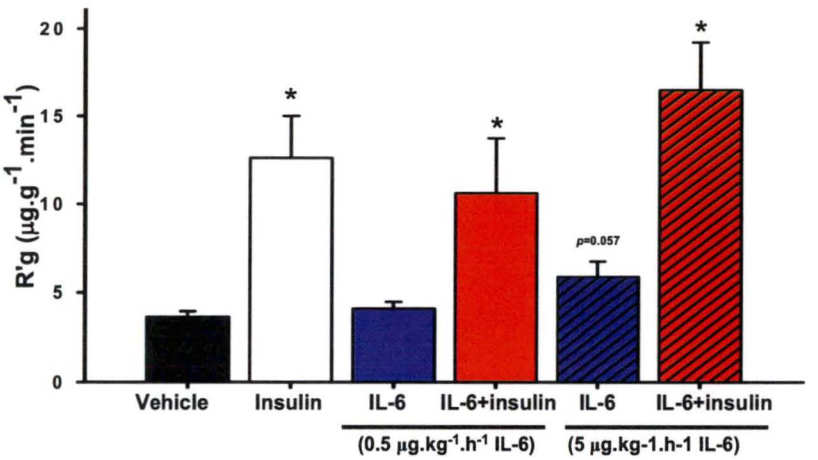

FIGURE 7.10: Muscle radioactive 2-DG uptake (R'g) for the combined calf muscle (aggregated on proportional weight) due to low dose IL-6 or high dose IL-6 and/or insulin infusion. 2-DG was administered at as a bolus at 75 min (Figure 6.1) and individual muscles (SOL, soleus; PLA, plantaris; RG, red gastrocnemius; WG, white gastrocnemius; EDL, extensor digitorum longus; TIB, tibialis anterior) were excised at the completion of the experiment. Values are means ± SEM. *, significantly different to vehicle ($p<0.05$).

7.3.7 Blood lactate concentrations

Blood lactate concentrations remained unchanged in response to vehicle and IL-6 infusion. Insulin infusion tended to increase blood lactate concentrations above basal (1.16 ± 0.10 mM versus 0.84 ± 0.19 mM at 120 min) although this was not significant. Co-infusion of insulin with high dose IL-6 caused a further increase in blood lactate concentration and the difference became significant ($p<0.05$) to insulin alone at 60 min with concentrations reaching 1.43 ± 0.10 mM at 120 min (Fig. 7.11).

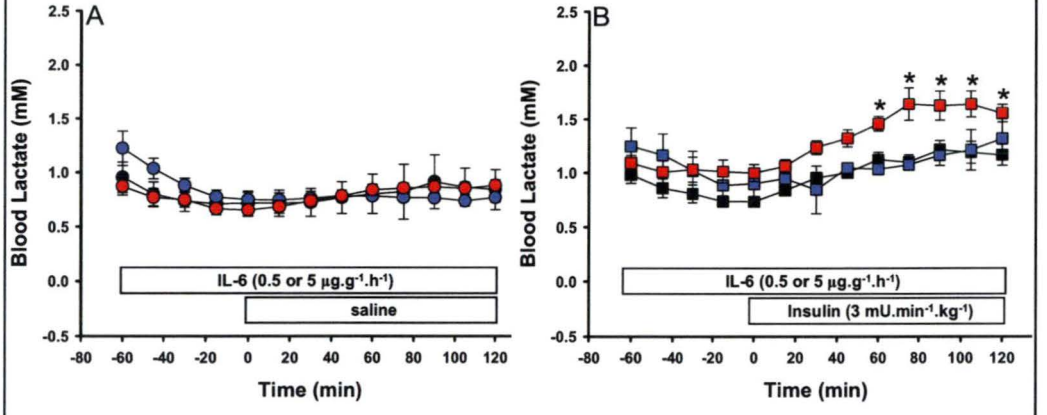

FIGURE 7.11: Time course for blood lactate concentrations as a result of IL-6 infusion (panel A) or IL-6 infusion with 3mU.min^{-1}.kg^{-1} insulin infusion (panel B). Values are means ± SEM. *, significantly different to 3 mU.min^{-1}.kg^{-1} (p<0.05). ● vehicle; ● 0.5 µg.kg^{-1}.h^{-1} IL-6; ● 5 µg.kg^{-1}.h^{-1} IL-6; ■ 3 mU.min^{-1}.kg^{-1} insulin; ■ 0.5 µg.kg^{-1}.h^{-1} IL-6 + insulin; ■ 5 µg.kg^{-1}.h^{-1} IL-6 + insulin.

7.3.8 Glucose turnover

Hepatic glucose production (measured via the metabolism of 3-[^{3}H]-D-glucose) was suppressed by insulin infusion. This suppression persisted during infusion with low dose IL-6, however high dose IL-6 (5 µg.kg^{-1}.h^{-1}) resulted in a significant increase in hepatic glucose production compared to insulin alone. Interestingly, the co-infusion of high dose IL-6 and insulin resulted in a significant increase (p<0.05) in glucose disappearance compared insulin alone (Fig 7.12).

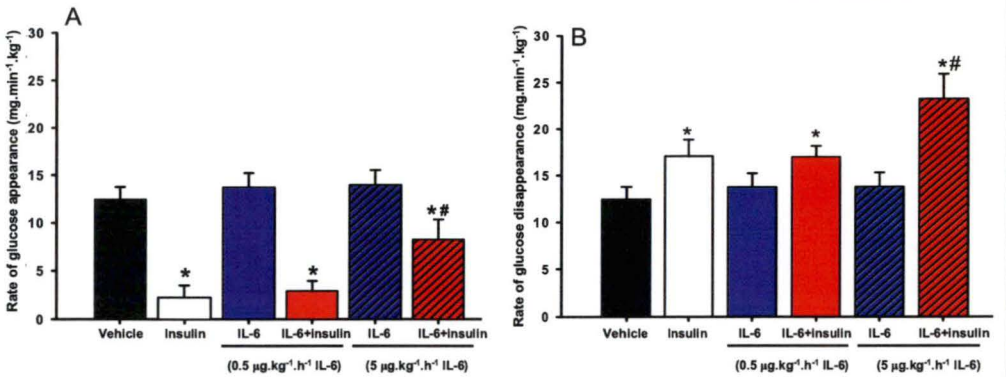

FIGURE 7.12: The rate of glucose appearance (hepatic glucose production; panel A) and glucose disappearance (glucose uptake; panel B) as a result of low dose or high dose IL-6 and/or insulin infusion. Values are means ± SEM. *, significantly different to vehicle ($p<0.05$); #, significantly different to insulin ($p<0.05$).

7.3.9 Akt phosphorylation

Total Akt and Akt phosphorylation (Ser^{473}) was measured in the combined calf muscle (SOL, PLA, RG, WG) which were excised and freeze clamped as one sample on completion of the experiment. Vehicle infusion had little effect on Akt phosphorylation (Ser^{473}). Both IL-6 and insulin infusion alone and in combination significantly ($p<0.05$) increased Akt phosphorylation (Ser^{473}) above that seen in the vehicle infused treatment group (Fig. 7.13).

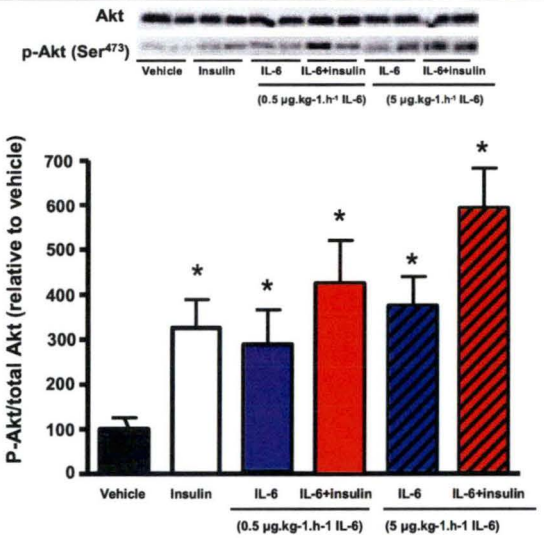

FIGURE 7.13: The ratio of Akt phosphorylation (Ser ^{473}) to total Akt protein as a result of low dose or high dose IL-6 and/or insulin infusion. A representative western blot of total and phosphorylated Akt for each treatment group is shown. Values are means ± SEM (n=6). *, significantly different to vehicle (p<0.05).

7.4 DISCUSSION

The main finding of this study is that IL-6 has a number of haemodynamic effects being able to decrease femoral blood flow, increase vascular resistance and attenuate insulin's ability to increase microvascular perfusion. While IL-6 opposes insulin's stimulatory effect on microvascular perfusion, it is able to compensate for any loss in glucose metabolism in the short term by its ability to increase glucose uptake.

Plasma concentrations of IL-6 reached ~300 pg.l^{-1} during 0.5 µg.kg^{-1}.h^{-1} IL-6 infusion and ~2700 pg.l^{-1} during 5 µg.kg^{-1}.h^{-1} IL-6 infusion (Table 7.2). Circulating plasma concentrations in humans have been reported to be between ~1-2 pg.l^{-1} [221, 224] in healthy subjects, and ~2-3 pg.l^{-1} in type 2 diabetic [220, 339] and obese patients [218, 219]. Studies using microdialysis have also shown that interstitial concentrations are ~100 greater than those in the plasma [340, 341]. In the present study, circulating IL-6 concentrations at basal were ~ 250 pg.l^{-1} suggesting that plasma concentrations are not directly comparable between humans and animal models and that the

concentrations required to elicit a response in humans may be different to those used in animal models. The infusion of high dose IL-6 in this study lead to a 100 fold increase in circulating levels (as is seen during exercise in humans), therefore assuming the clearance rate of the cytokine is similar between species, this concentration may be likened to that seen during exercise in humans.

IL-6 infusion at the high dose (5 $\mu g.kg^{-1}.h^{-1}$), but not the low dose (0.5 $\mu g.kg^{-1}.h^{-1}$), caused femoral blood flow to decrease resulting in an increase in vascular resistance. These were only small changes over the course of the experiment (femoral blood flow decreased by ~ 0.3 $ml.min^{-1}$ over three hours) however this did reach statistical significance ($p<0.05$). This effect on total blood flow was not apparent during co-infusion with insulin, as insulin's well known vasodilatory actions may have been strong enough to compensate from such a small decrease in blood flow. In these experiments however, co-infusion with either dose of IL-6 significantly ($p<0.05$) attenuated insulin mediated increase in microvascular perfusion, suggesting that the microvasculature is more sensitive to inhibition by IL-6 than the larger vessels. While the haemodynamic effects of IL-6 have not been studied in depth, a similar inflammatory cytokine in TNF-α, which stimulates IL-6 release from adipose tissue, has been shown to inhibit insulin mediated haemodynamic actions (both total flow and microvascular perfusion) [95, 97, 342]. Studies have also shown that TNF-α stimulated the release of the vasoconstrictor endothlein-1 [343, 344], which may result in an insulin resistant state through a decrease in insulin stimulated microvascular perfusion (Chapter 7). Furthermore, as shown in Chapter 7 of this thesis, ET-1 release may decrease insulin clearance, and given that the plasma insulin concentrations of both doses of IL-6 are slightly higher (but not statistically significant) than insulin alone, a small increase in ET-1 may be possible. An Endothelin ELISA (Biomedica; Austria) performed on the plasma samples from these experiments was unable to detect any increase in endothelin above basal, however as ET-1 is released abluminally, and it is possible that small increase in secretion will not be detected in the circulating plasma.

Insulin induced vasodilation results from the an increase in nitric oxide synthase activity and nitric oxide production in the endothelium [162]. It is therefore possible that IL-6 may decrease insulin stimulated microvascular perfusion by inhibiting nitric

oxide production. A recent study by Andreozzi et al. [345] showed that IL-6 interferes with insulin's ability to phosphorylate eNOS by regulating its phosphorylation at Ser^{117} and Th^{495}. This study [345] also showed through chemical inhibition and siRNA that IL-6 activation of the JNK and ERK1/2 pathways was responsible for the inhibitory effect of IL-6 on insulin stimulation of NOS activity and production. More research is required to investigate if IL-6, like TNF-α, modifies blood flow through the stimulation of ET-1 secretion, or if this occurs through a separate mechanism involving inhibition of nitric oxide production.

In contrast to it's inhibitory effects on blood flow, IL-6 at a dose of 5 $\mu g.kg^{-1}.h^{-1}$ (but not the low dose of 0.5 $\mu g.kg^{-1}.h^{-1}$) resulted in a trend to stimulate muscle glucose uptake (measured by 2-DG uptake) in the individual muscles of the calf, with a significant increase (p=0.035) in the red gastrocnemius muscle. There was also a significant increase (p=0.021) in 2-DG uptake in the epididymal fat pads compared with a vehicle infusion (Fig.7.9). The effect of IL-6 to increase glucose metabolism is further supported as a glucose infusion was required during these experiments to maintain euglycaemia. Preliminary studies showed that failure to infused glucose during IL-6 treatment resulted in blood glucose decreasing by ~ 1mM over the course of the experiment. Similarly, during a 3 $mU.min^{-1}.kg^{-1}$ insulin clamp, there is a trend for co-infusion of IL-6 to further increase glucose uptake of the combined calf muscle (p=0.057; Fig 7.10) and in the individual muscles of the calf and the epididymal fat pads (Fig. 7.9) above that achieved by insulin infusion alone,. The rate of glucose disappearance measured by 3-[^{3}H] glucose, an indicator of the whole body glucose disappearance, was also significantly increased (p<0.02) with co-infusion of IL-6 and insulin above that of insulin alone (Fig. 12). In addition the blood lactate concentrations (p>0.05; Fig. 11) were increased over the course of the experiment, which together suggested an increase in glucose metabolism. Incubated muscle and cell culture experiments support the view that IL-6 is able to exert a positive effect on glucose uptake in the muscle and adipose tissue, and that it further enhances insulin mediated glucose uptake [248, 259, 264].

Interestingly, there was no difference between the glucose infusion rate of insulin alone and during co-infusion of high dose IL-6 (Fig. 7.8). This may be attributed to the inhibition of insulin's action to suppress hepatic glucose production (Fig. 12),

causing a higher blood glucose concentration, and consequently requiring less infused glucose to maintain euglycaemia. A number of studies *in vitro* [276, 277] and *in vivo* [268, 278] have shown that IL-6 increases glycogenolysis during insulin stimulation and causes hepatic insulin resistance, through the induction of SOCS3 protein and inhibition of insulin receptor signal transduction [279]. However, as shown by Klover et al. [278] while IL-6 caused hepatic insulin receptor autophosphorylation and tyrosine phosphorylation of IRS-1 to decrease by 60%, insulin signal transduction in the skeletal muscle remained unaffected.

The present study shows that IL-6 is able to phosphorylate Akt at Ser^{473}, to a similar extent as insulin, and may help to elucidate the signalling pathway IL-6 activates to increase glucose uptake (Fig. 7.13). The same phosphorylation in response to IL-6 was also found by Weigert et al. [257] in incubated human myotubes, and it was discussed that while it is the phosphorylation of the Thr^{308} residue of Akt which activates the protein, the phosphorylation of Ser^{473} only increases the susceptibility of Thr^{308} to phosphorylation by PI3-kinase, leading to an increase in insulin sensitivity. In that study, this effect was inhibited by incubation with wortmanin. Similarly, Al-kahalili et al. [256] found that IL-6 increased glucose metabolism and glycogen synthesis by PI3-kinase dependent mechanisms in human skeletal muscle cell culture. That study [256] also showed that the increased lipid oxidation in response to IL-6 incubation was regulated by an AMPK dependent mechanisms, separate to glucose metabolism. In contrast, Glund et al. [259] found that incubation of skeletal muscle strips from the vastus lateralis muscle in humans with IL-6 lead to an increase in resting glucose uptake through activation of the AMPK and MAPK signalling pathways without affecting PI3-kinase, Akt or AS160 phosphorylation. Similarly, Carey et al. [248] found that L6 myotubes infected with a dominant-negative AMPK alpha-subunit decreased glucose uptake, GLUT4 translocation and fatty acid oxidation.

The activation of signalling proteins by IL-6 appears to be a transient effect and may explain why in this study, there was no detectable increase in IRS-1 or AMPK phosphorylation in the skeletal muscle (data not shown), as samples were collected after 3 hour of IL-6 infusion. Other studies have shown that treatment of cultured skeletal muscle cells and human umbilical vein endothelial cells with IL-6 results in a

modification of IRS-1 through a rapid phosphorylation of Ser^{318} which begins to decrease 30 min after stimulation [260, 345].

In humans, IL-6 is only released during strenuous or long duration exercise [242, 346] which require prolonged periods of increased fuel utilisation. Furthermore, IL-6 release is particularly sensitive to a decrease in muscle glycogen [243] suggesting that IL-6 may act as an additional mechanism to regulate glucose uptake during times of increased fuel metabolism. IL-6 and contraction have been shown to activate AMPK [248, 258], a kinase involved in fuel regulation known to increase lipid metabolism and to conserve glycogen and glucose stores. IL-6 may be released as a mechanism to assist in energy mobilisation during exercise, by increasing the release of glucose by the liver (Fig. 12), and by increasing glucose uptake in the muscle through an alternative pathway (Fig. 10). The mechanism through which IL-6 signalling occurs however still requires on going research to elucidate the tissue specific pathways involved in glucose and lipid metabolism at rest, during insulin stimulation and contraction.

The increase in plasma concentrations of IL-6 during exercise is transient and appears to be mediated by a need for fuel redistribution to the working muscles during exercise allowing an increase in muscle glucose uptake. However the effect of chronically elevated IL-6 at basal may be problematic. The data in the present study suggests that a chronic increase in circulating IL-6 concentrations may result in insulin resistance through inhibition of insulin mediated microvascular perfusion, a process which appears to be more sensitive to IL-6 than the signalling mechanism which leads to an increase in glucose uptake (demonstrated by the differences in low and high dose IL-6 infusion). In the short term, the ability of IL-6 to increase glucose uptake is able to compensate for an increased vascular resistance at basal and for a loss in insulin mediated microvascular perfusion. In the long term however, the inhibition of insulin's suppression of hepatic glucose uptake may result in chronic hyperglycaemia. The ability of the body to dispose of this increase in glucose concentrations will result in an increase in insulin secretion, however due to IL-6 suppression of insulin's haemodynamic actions, may cause a form of acute insulin resistance as insulin is not able to efficiently dispose of the excess glucose. If this cycle persists, hyperinsulinaemia and insulin resistance may develop. This is also

confounded by the fact that IL-6 is an inflammatory cytokine involved in the acute phase response which may also lead to complications involving the vasculature through increased blood viscosity and atherosclerosis, as well as an increase in central obesity and hypertension (through association with the hypothalamic-pituitary-adrenal axis), risk factors for both cardiovascular disease and insulin resistance [347].

In conclusion, IL-6 causes an increase in vascular resistance under basal conditions and an inhibition of increased microvascular perfusion during insulin stimulation. Glucose uptake however is not inhibited, as IL-6 is able to compensate for any loss in vascular function by directly increasing glucose uptake in the skeletal muscle and adipose tissue through signalling mechanism which may involve phosphorylation of Akt. This may also be an alternative pathway used by contraction to assist in glucose regulation and increasing the availability of glucose for the working muscle during prolonged exercise. In the long term however, an increase in circulating IL-6 may lead to insulin resistance due to its ability to not only inhibit insulin mediated increase in microvascular perfusion, but also by attenuating insulin's action to suppress glucose production.

CHAPTER 8:

DISCUSSION

8.1 DISCUSSION

This thesis has examined the role of insulin and contraction mediated increases in microvascular perfusion on glucose uptake and insulin resistance. Focus has been on skeletal muscle as it contributes to 85% of glucose disposal during hyperinsulinaemic euglycaemia, and is the main site of insulin resistance [11]. The techniques of CEU and 1-MX metabolism have been used to measure changes in microvascular perfusion during contraction and insulin stimulation, as they are able to measure flow changes in the microvasculature without being influenced by changes in bulk flow which may occur with either or both of these stimuli.

Circulating concentrations of IL-6 and ET-1 are both elevated in obese and insulin resistant subjects [182, 219, 336] and studies in this thesis have revealed that both IL-6 and ET-1 inhibit insulin-meditated increases in skeletal muscle microvascular perfusion. Both these substances may act by inhibiting insulin-stimulated nitric oxide production to cause a decrease in perfusion, and they may also cause hyperinsulinaemia through vasoconstriction and hepatic effects. Nitric oxide may also be involved in the increases in microvascular perfusion (compared to basal) and muscle glucose uptake seen during recovery from contraction. However, it seems that while nitric oxide may play a role in vascular tone at basal, and be involved in both the increase in glucose uptake and microvascular perfusion in response to insulin, only glucose uptake is affected by nitric oxide synthase inhibition during contraction. This suggests that contraction has separate and distinct pathways for increasing microvascular perfusion and glucose uptake and may stimulate the vasculature and myocyte through different signalling mechanisms. Elucidating these mechanisms may be important for the development of new therapeutic target for the treatment of insulin resistance and type 2 diabetes.

8.2 SUMMARY OF KEY FINDINGS

8.2.1 Contrast enhanced ultrasound technique for measuring microvascular perfusion

The use of capillary models was used to show that contrast enhanced ultrasound (CEU) imaging technique may distinguish between changes in microvascular perfusion independently of changes in bulk flow. Furthermore, while the technique can also detect changes in microvascular volume and the filling rate of the capillaries, this technique can not be used to determine changes in flow pattern. Thus, flow redistribution from short to long tortuous capillaries, or flow pattern changes involving sharing of flow from one to a number of capillaries can not be distinguished using CEU. Most importantly, this study shows that CEU may be used to measure changes in microvascular perfusion in response to contraction or insulin stimulation and not be affected by the concomitant changes in total blood flow.

8.2.2 Microvascular perfusion post-contraction

This study found that a short 10 min bout of contraction (by electrical stimulation of one hindlimb) *in vivo* increased microvascular perfusion during contraction, but led to a sustained increase for some time after. Thus while femoral blood flow returned to basal levels immediately after the bout of contraction, perfusion of the microvasculature remained enhanced (compared to basal levels) for up to 60 min post-contraction. Muscle glucose uptake also remained significantly increased in the contracted leg at this time, without the stimulus of exogenously added insulin, or an increase in circulating plasma insulin concentrations. Similar experiments, in the perfused hindlimb model, however had no effect on glucose uptake (or lactate release) after 60 min of recovery from contraction, and all parameters returned to basal levels within 5 minutes of the end of exercise. Taken together these data would suggest that enhanced glucose uptake is not the result of an increase in bulk blood flow, or plasma insulin concentrations, but is most likely the result, at least in part, of increased microvascular perfusion. Although changes in the myocyte may occur, the data suggest that the enhance microvascular perfusion during this post-contraction period may play a key role in the increase in glucose uptake and insulin sensitivity seen during recovery from contraction.

8.2.3 The effect of nitric oxide synthase inhibition during contraction

Insulin mediated increases in microvascular perfusion and glucose uptake have recently been shown to be mediated by nitric oxide. This study found that local infusion of a nitric oxide synthase inhibitor (via the epigastric artery of one leg) during contraction had no effect on the contraction mediated increase in microvascular perfusion. NOS inhibition did however decrease muscle glucose uptake by ~30%. The inhibition of nitric oxide release during contraction may have been compensated for by the release of other vasodilitary factors which are secreted during contraction [58]. Glucose uptake however was partially dependent on nitric oxide release, and the decrease in muscle glucose uptake was independent of AMPK or nNOSμ phosphorylation. Therefore nitric oxide is critical for the muscle glucose uptake, but not the increase in microvascular perfusion response to contraction. This study reiterates that the signalling pathways controlling microvascular perfusion at rest, during insulin stimulation and during exercise are controlled by separate mechanisms. Furthermore, the mechanisms which act to increase microvascular perfusion and those which affect glucose uptake also appear to be mediated by separate stimuli.

8.2.4 Enodothelin-1 and insulin action

The intravenous infusion of the vasoconstrictor ET-1 with insulin *in vivo*, resulted in elevated mean arterial pressure and an attenuation of insulin mediated femoral blood flow and microvascular perfusion. ET-1 infusion also caused a 50% decrease in the rate of insulin clearance to compensate for a decrease in microvascular perfusion and to maintain an increase muscle glucose uptake due to insulin stimulation. When circulating plasma insulin concentrations were compared between experiments (as opposed to comparing the infusion rate of insulin), it was found that ET-1 also caused a decrease in whole body (as measured by glucose infusion rate) and muscle glucose uptake (measured by 2-DG uptake). The hyperinsulinaemia resulting from a decrease in insulin clearance rate, could be attributed to the vasoconstrictor actions of ET-1 to decrease blood flow to the kidney and liver [187, 188], the major sites of insulin clearance [334]. This vasoconstrictor action also resulted in a decreased delivery of insulin to the skeletal muscle by inhibiting insulin mediated increases in microvascular perfusion. This denied the access of insulin to the muscle cells,

resulting in a decrease in muscle glucose uptake, and again showing an association between these two actions.

8.2.5 Interleukin 6: Effects on insulin action and contraction

Co-infusion of the inflammatory cytokine IL-6 (5 $\mu g.kg^{-1}.h^{-1}$) with insulin caused a decrease in insulin mediated microvascular perfusion, but resulted in a small increase in insulin mediated glucose uptake. IL-6 infusion also resulted in the attenuation of insulin's suppression of hepatic glucose production. This latter affect accounts for the similar glucose infusions rates between insulin infusion alone and in conjunction with IL-6, even though the glucose disappearance rate was increased during IL-6 infusion. The increase in muscle and adipose tissue glucose uptake in response to IL-6 infusion could be attributed to the phosphorylation of Akt at Ser^{473}, leading to an increase in insulin sensitivity by enhancing the susceptibility of the Thr^{308} residue to be phosphorylated by PI3-Kinase [257]. Co-infusion of a low dose (0.5 $\mu g.kg^{-1}.h^{-1}$) of IL-6 suppressed insulin mediated microvascular perfusion, but had no significant affect on glucose metabolism. The difference in results between these two doses of IL-6 suggests that microvascular perfusion is more sensitive than glucose uptake to the effects of this inflammatory cytokine, and while IL-6 is able to sustain an increase glucose metabolism in the short term, its haemodynamic effects and attenuation of insulin's suppression of hepatic glucose output may result in insulin resistance if circulating concentrations remain chronically elevated.

8.3 MEASUREMENT OF MICROVASCULAR PERFUSION: ADVANTAGES AND DISADVANTAGES

Due to the size of the capillaries, and the dynamic nature of blood flow measurements of microvascular perfusion can be difficult. A number of techniques are available, such as microdialysis [35],laser Doppler flowmetry [30] and intravital microscopy [348] and while these are valuable methods, they only enable assessment of blood flow in one small region of the muscle. Measurements may be inconsistent between experiments due to the subjective nature of the placement of the probes. These methods also require blood flow to be at a steady state, and may be influenced by changes in bulk flow. Furthermore, microdialysis also requires the insertion of a large needle when placing the probe in the muscle which may cause damage to the

surrounding tissue and possibly invoke an inflammatory response. Measurement by positron emission tomography (PET) is also possible, but resolution is not sufficiently fine enough to determine microvascular perfusion as a separate component of nutrient delivery (eg. see Bertoldo et al. [349]). Other methods including lymph sampling [350] are only suitable for larger animals such as the dog.

This study has used two methods to measure microvascular perfusion, 1-MX metabolism and CEU, as these techniques enables data to be collected for a large percentage of muscle tissue, minimising any variability which may be seen when only assessing one muscle or a specific fibre type, and allow relatively sensitive measures of change in microvascular perfusion. The 1-MX metabolism technique only requires an intravenous infusion of 1-MX throughout the experiment, and therefore does not disrupt the muscle tissue. This method is not influenced by changes in bulk flow, however it may only be used as an end point measure due to the volume of plasma required for sampling (which may otherwise disrupt blood flow if taken during the experiment). The advantage of the CEU technique is that the microbubble contrast agents are infused intravenously, and an entire region of muscle (eg. the muscles of the calf) may be examined simultaneously, without disrupting the muscle tissue. Furthermore, as shown in chapter 3, the method may distinguish between changes in bulk flow and changes in microvascular perfusion, as well as obtaining information about the filling rate of the capillaries. In addition, multiple measurements can be made throughout an experiment using CEU allowing a time course study of changes in capillary volume may be assessed with this technique, making it a very effective technique for measuring changes in microvascular perfusion.

8.4 MECHANISMS OF VASCULAR AND METABOLIC CONTROL

8.4.1 Mechanisms of insulin mediated microvascular perfusion and glucose uptake

This thesis has further helped to confirm the relationship between insulin mediated microvascular perfusion and insulin mediated glucose metabolism. The insulin signalling pathway acts to control microvascular perfusion by stimulating the production of the vasodilator nitric oxide, and the vasoconstrictor ET-1 from the vascular endothelium [351, 352]. Insulin stimulates the release of these two substances

through separate pathways (described below). The secretion of nitric oxide acts to inhibit ET-1 production and increase vasodilation [199] with the interactions between these two substances helping to regulate vascular tone. An imbalance in their secretion contributes to endothelial dysfunction, often associated with insulin resistance, and may result in hypertension and atherosclerosis due to a decrease in nitric oxide dependent vascular activity [197, 347].

Inhibition of PI3-kinase reduces insulin stimulated nitric oxide production by up to 50% [159] suggesting that stimulation of nitric oxide production by insulin is predominantly via the PI3-kinase pathway. This signalling pathway is initiate by insulin receptor tyrosine phosphorylation, the phosphorylation of IRS-1, PDK-1 [161] and Akt. eNOS Ser^{1179} is phosphorylated by Akt and is independent of Ca^{2+} [140]. Interestingly, this is the same signalling pathway which leads to an increase in GLUT4 translocation to the plasma membrane in response to insulin suggesting a possible link between insulin mediated control of nitric oxide production and glucose uptake in the muscle cell. Insulin does not regulate glucose uptake in the endothelial cells, so the signalling pathway in these cells is directed towards nitric oxide production, vasodilation and microvascular perfusion. Increased microvascular perfusion can clearly lead to an increased glucose uptake by the myocytes. Inhibition of PI3-Kinase and NOS in endothelial cells also results in an increase in insulin mediated ET-1 release and vasoconstriction [196, 351] via MAPK activation [197]. Both basal and insulin stimulated muscle NOS activity is impaired in type 2 diabetic patients [166], which may result in an increase in insulin stimulated ET-1 release, as nitric oxide is not present in large enough quantities to inhibit ET-1 production and counteract the vasoconstrictor actions. Chronically, an imbalance in these insulin stimulated vasoactive substance will result in endothelial dysfunction [197, 198], and as shown in this thesis, an increase in circulating ET-1 will also block insulin mediated microvascular perfusion, and decrease insulin clearance. The resulting hyperinsulinaemia and decrease in muscle glucose uptake perpetuates the cycle of an imbalance in the insulin haemodynamic response and insulin resistance.

Endothelial dysfunction and insulin resistance is also associated with an increase in inflammatory markers such as TNF-α and IL-6 [347, 353]. Previous studies have shown that TNF-α leads to a decrease in muscle glucose uptake by inhibiting insulin

signalling [93, 354], and insulin mediated haemodynamic effects [95, 97]. This thesis shows that although IL-6 does not inhibit muscle glucose uptake and is able to compensate for any loss in insulin action, it attenuates insulin mediated increases in microvascular perfusion. The vascular effects of both these cytokines can be attributed to their inhibition of insulin mediated eNOS phosphorylation and decreased nitric oxide production. In human umbilical vein endothelial cells, Andreozzi et al. [345] found that incubation with IL-6 decreases the phosphorylation of IRS-1 at Tyr^{612}, which is essential for PI3-kinase activation, through its activation of the JNK and ERK1/2 pathway. This resulted in a decrease in Akt associated phosphorylation of eNOS Ser^{1177}, and consequent inhibition of nitric oxide production. Inhibition of the JNK and ERK1/2 pathway (by JNK inhibitor I or PD98059) restored insulin signalling and nitric oxide production [345]. Similarly, TNF-α inhibits IRS-1 associated PI3-kinase activity and eNOS phosphorylation [355], with this pathway restored by inhibition of p38 MAPK [356].

In addition to the direct interference of IL-6 and TNF-α on the insulin signalling pathway, these cytokines also inhibit lipoprotein lipase activity, and TNF-α also stimulated hormone sensitive lipase in the adipose tissue leading to an increase in lipolysis [251, 271, 272]. An increase in circulating fatty acid levels *in vivo* is also associated with a decrease in endothelial function and vasodilation [357, 358] and at high levels inhibits insulin meditated microvascular perfusion and glucose uptake [280]. This inhibition is thought to be caused by an inhibition of insulin signalling and Akt mediated eNOS activation [359]. Interestingly, TNF-α has been shown to stimulate ET-1 release [343, 344], and like TNF-α, ET-1 also stimulates IL-6 synthesis [360]. *In vivo*, the interaction between IL-6 and ET-1 may result in hyperinsulinaemia and insulin resistance, due IL-6 attenuating insulin's ability to suppress hepatic glucose production. This leads to an increase in circulating glucose concentrations and insulin secretion, which is problematic, as ET-1 decreases the clearance rate of circulating insulin through its vasoconstrictor actions, causing hyperinsulinaemia. Figure 8.1 shows the insulin signalling pathway and the involvement of ET-1 and cytokines (TNF-α and IL-6) in insulin resistance.

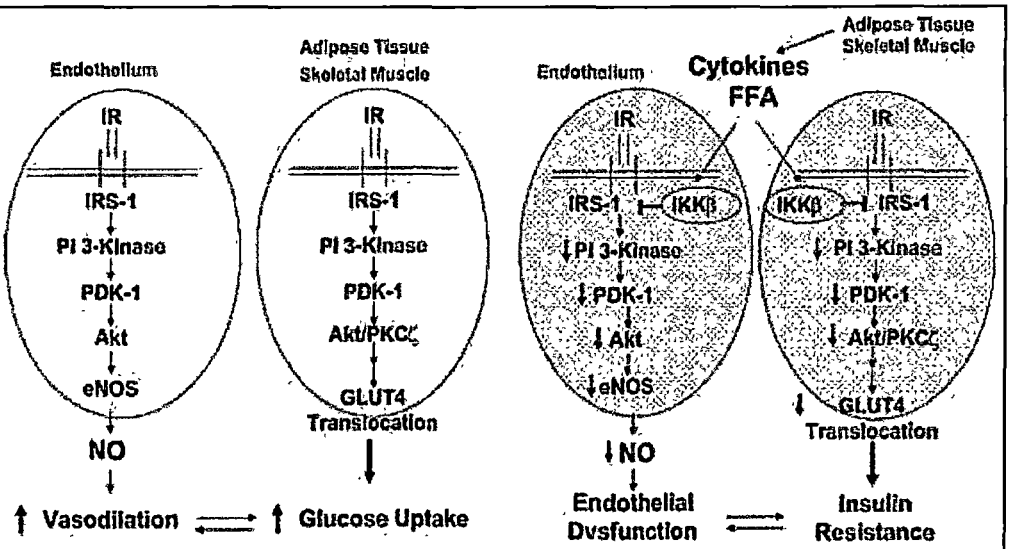

Figure 8.1: The insulin signalling pathway in vascular and metabolic tissues under normal healthy conditions (left) and during metabolic and cardiovascular diseases (right) involving increased circulating free fatty acids (FFA) and inflammation due to elevated cytokine concentrations. (Diagram from Kim et al. [8]).

8.4.2 Mechanisms of contraction mediated microvascular perfusion

While nitric oxide appears to play an important role in insulin mediated vasodilation and insulin resistance, its function during exercise hyperaemia and contraction mediated microvascular perfusion is less significant. The nature of exercise and its historical relevance as a survival mechanism has lead to a robust signalling process which mediates the haemodynamic response to contraction. As discussed in Chapter 1, a number of vasodilitary mechanisms are involved in inducing hyperaemia in response to contraction, including the propagation of signal by gap junctions, the muscle pump, neural mechanisms, acetylcholine, adenosine, potassium ions, nitric oxide and prostaglandins to name a few. The maintenance of perfusion during contraction appears to be mediated by separate mechanisms to the initial hyperaemia, and has a degree of redundancy built in to the signalling process. This is demonstrated by the multiple cellular sources which may release vaodilators in response to contraction and the ability of the body to compensate for an inhibition of one vasodilator by the increased secretion of another [58, 309].

8.4.3 Mechanisms of contraction mediated glucose uptake

As is the case for contraction mediated vasodilation, contraction mediated glucose uptake also appears to have a number of signalling pathways, which aim to increase GLUT4 translocation to the plasma membrane and fuel availability for the muscle. These pathways are independent of PI3-kinase, which may explain why contraction is able to stimulate glucose uptake in insulin resistant subjects [87, 101]. Contraction causes the release of Ca^{2+} from the sacroplasmic reticulum due to the depolarisation of the plasma membrane and transverse-tubules, therefore it would seem likely that calcium would be involved as a contraction mediated signalling mechanism. The signalling pathway down stream from Ca^{2+} is still not clear, but may involve activation of calmodulin, a Ca^{2+} receptor protein that binds to a number of downstream targets such as calmodulin regulated protein kinase II [361]. Ca^{2+} dependent protein kinase C (PKC) isoforms may also be activated, which have a range of effects involving metabolism, cell differentiation and growth. Inhibition of PKC by calphostin C has been shown to specifically inhibit contraction mediated glucose uptake, suggesting a role for PKC in the contraction mediated response [362]. AMPK activation however was unaffected demonstrating the range of different pathways activated by contraction to increase glucose uptake. AMPK is an energy sensing kinase which is also activated during contraction in response to an increased ratio of AMP to ATP and creatine to phosphocreatine ratio signifying the low energy state of the muscle. AMPK acts to inhibit energy consuming processes and stimulate alternate pathways for ATP generation such as increased fatty acid oxidation through the phosphorylation of acetyl-CoA carboxylase and increasing glucose uptake into the cell by increasing GLUT 4 translocation [363]. Contraction also activates MAPK pathways increasing the transcriptional activity during exercise and recovery, however it is not known if this pathway is able to increase GLUT4 translocation [363]. The precise signalling pathways involved in contraction mediated glucose uptake are still unclear (Fig. 8.2) and more research is required to unravel the individual pathways which are involved in both contraction mediated glucose uptake and microvascular perfusion.

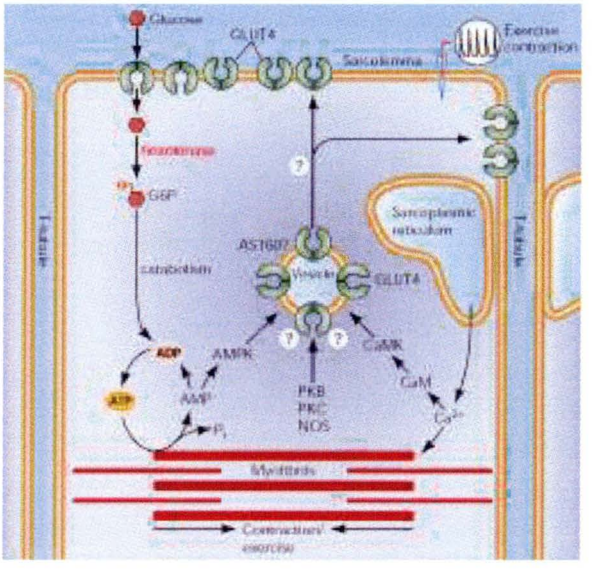

Figure 8.2: A schematic representation of the contraction mediated signalling pathways involved in increasing glucose metabolism via GLUT4 translocation to the sarcolemma and transverse tubules (T-tubules). The precise mechanism and signalling intermediates are still to be elucidated but are thought to involve signalling through increased Ca2+ release and AMPK. Question marks refer to unidentified signalling and structural molecules involved in GLUT4 translocation. G6P, glucose-6-phosphate; AS160, Akt substrate 160; AMPK, 5'AMP activated protein kinase; CaM, calmodulin; CaMK, calmodulin dependent protein kinase; PKB, protein kinase B (Akt); PKC, protein kinase C; NOS, nitric oxide synthase. (Diagram from Rose et al. [361])

Studies represented in this thesis show that inhibition of nitric oxide had no effect on microvascular perfusion *during* contraction, however glucose uptake was decreased by 30%. This suggests that unlike the insulin signalling pathway, the mechanism though which contraction increases and maintains blood flow may be separate to the signalling pathway activating glucose uptake. Insulin acts through PI3-kinase to stimulate nitric oxide release. Contraction mediated nitric oxide production however is mediated by Ca^{2+}/calmodulin dependent mechanisms. This is demonstrated by the contraction induced increases in Ca^{2+} causing a dose dependent increase in nitric oxide production, an affect which is blocked by inhibition of the Ca^{2+}/calmodulin pathway [364, 365]. In addition, nitric oxide release also appears to be stimulated by an AMPK (via Akt) dependent pathway. AMPK activates Akt (via small GTPase Rac1) in order to stimulate eNOS phosphorylation [365]. This is shown by the siRNA knockdown of AMPK α1 which led to an impairment in Akt phosphorylation. siRNA knockdown of Akt, however had no effect on AMPK activation [365]. Furthermore,

transfection of endothelial cells with a dominant negative AMPKα subunit abolished nitric oxide production [366]. This suggests that Akt (which activates eNOS) lies upstream of AMPK in the signalling pathway and may explain why in chapter 5 of this thesis, glucose uptake was decreased during contraction without affecting AMPK or ACC phosphorylation. There are two aspects to this argument. Firstly, contraction mediated microvascular perfusion may not involve nitric oxide (Chapter 5 of this thesis) or may compensate for any inhibition through the release of other vasodilatory substances. Secondly, contraction increases nitric oxide through a number of different mechanisms, which unlike insulin, is not dependent on the PI3-kinase signalling pathway, and is therefore less susceptible, or able to compensate for any inhibition due to IL-6.

Interestingly, even though overregulation/secretion of ET-1 and IL-6 may result in insulin resistance, both are released in high quantities during contraction which has a positive effect on glucose metabolism. ET-1 aids in the redistribution of blood flow by causing increase in blood flow to the working muscles and constriction to the non working muscles and the gut [207, 211], while IL-6 is released in response to a depletion of energy, and aids in mobilizing glycogen from the liver by stimulating hepatic glucose production and increasing glucose uptake in the muscle tissue [231]. Circulating ET-1 concentrations have returned to basal by 30 min post-contraction, however circulating IL-6 concentrations may remain elevated for 24 h after an exercise bout [224, 234]. Insulin sensitivity however is increased during this period post exercise, suggesting that this increase in glucose uptake during recovery from exercise may occur through a mixture of the contraction mediated and insulin mediated pathways.

8.4.4 Mechanisms of post-contraction microvascular perfusion and glucose uptake

While the increase in glucose uptake is important during contraction, and the mechanism appears to be intact in insulin resistant subjects, it is the post exercise period which may also be of importance in the benefits of exercise to type 2 diabetic patients. The post exercise glucose uptake and microvascular perfusion appear to be mediated by yet another set of signalling mechanisms. Very little is known about the signalling events which occur during the post-contraction period, as the response to an

exercise bout may range from a period of acute insulin resistance [111] to an increase in insulin sensitivity 48 h after a bout of exercise [109] and is heavily influenced by the intensity, duration and mode of exercise. Interestingly, post-contraction glucose uptake is enhanced regardless of a decrease in IRS-1 phosphorylation and IRS-1 associated PI3-kinase activity in rodents [124] and is still present in the muscle specific insulin receptor knockout mouse, which only responds to insulin during recovery from contraction [125].

This thesis has shown that in addition to the increase in insulin sensitivity post contraction, microvascular perfusion also remains increased, compared to basal, for up to 60 min post contraction. This may explain the enhanced glucose uptake post contraction as the nutritive capillaries of the skeletal muscle remained recruited during recovery potentially allowing increased delivery of both glucose and insulin through the muscle. This may involve nitric oxide production (activated by a PI3-kinase independent mechanism), and may also result in insulin further stimulating microvascular perfusion (through PI3-kinase dependent mechanisms), to partly explain the additive effects of insulin and contraction together). Thorell et al. [367] found that a 2 hour hyperinsulinaemic euglycaemic clamp resulted in a 32% increase in GLUT4 translocation and 640% increase in Akt phosphorylation above basal (note, these assays were conducted in white muscle and although containing vascular elements, the data would largely reflect changes occurring in the myocytes). Similarly, a 60 min exercise bout performed before the insulin clamp resulted in an increase in insulin sensitivity up to 90 min post exercise and a 44% increase in GLUT4 translocation accompanied by a 1000% increase in Akt phosphorylation [367]. A increase in Akt phosphorylation and glucose uptake was also seen post-contraction by Wojtaszewski et al. [125] in the muscle-specific insulin receptor knock out mouse suggesting that Akt activation (assumed to be predominantly myocyte Akt) may be involved in the post-contraction signalling pathways. Furthermore, while the data surrounding nitric oxide involvement (both myocyte and endothelial) during contraction is varied, it is generally found that NOS inhibition during the post-exercise period results in a decrease in blood flow [77, 300]. Therefore it is possible that both the increase in glucose uptake and microvascular perfusion during recovery may be due to Akt phosphorylation in both myocytes and endothelial cells and nitric oxide

release by endothelium. In addition, myocyte Akt may also stimulate AS160 phosphorylation resulting in an increase in GLUT4 translocation [105, 131].

Insulin sensitivity during recovery is affected by the glycogen content of the muscle, with a decrease in muscle glycogen resulting in a prolonged elevation of GLUT4 protein content at the plasma membrane and longer period of insulin sensitivity [117, 368]. A small period of contraction such as that used in this thesis (10 min twitch contraction) would not be expected to deplete muscle glycogen stores, however glucose uptake was still significantly elevated after 60 min of recovery. This may suggest that glycogen content may influence the time frame of the increased sensitivity but may not be the only mechanism involved in this enhanced response. Future experiments are required to examine the time course between microvascular perfusion and glucose uptake over a longer period of recovery and to assess the effect of glycogen depletion on microvascular perfusion in the post contraction period.

8.5 IMPLICATIONS FOR DISEASE

The circulating plasma concentrations of ET-1, IL-6 and TNF-α are increased in insulin resistant and obese patients [88, 183, 219, 269, 369]. The interaction of these three substances may lead to insulin resistance through a number of different pathways with the result of decreasing insulin mediated nitric oxide release and thus vasodilation. Studies which have inhibited nitric oxide synthase during insulin stimulation have found a decrease in total blood flow [162], microvascular perfusion [164], as well as a decrease in glucose uptake in both the skeletal muscle and adipose tissue [165]. Furthermore, eNOS knockout mice developed hyperinsulinaemia, hypertension, hyperlipidaemia, had a 40% decrease in insulin mediated glucose uptake and were unable to suppress hepatic glucose output during insulin stimulation compared to control mice [138, 171]. Those studies help to demonstrate the importance of nitric oxide in mediating insulin's vasodilitary response, and show that over secretion of ET-1, TNF-a or IL-6 alone or in combination, through their signalling cascades may greatly inhibit the amount of nitric oxide produced, resulting in insulin resistance

This thesis has shown that although ET-1 and IL-6 may decrease insulin mediated microvascular perfusion, they do not have inhibitory affects on perfusion and glucose

uptake in the basal state, a phenomenon which has also been seen in other studies [95, 204]. At basal, only ~30% of the microvasculature is perfused at any one time [15] and nitric oxide synthase inhibition has been shown to decrease blood flow at rest [77, 300]. Generally, the level of microvascular perfusion is matched to the metabolic requirements of the cells. Therefore in the basal state, the energy needs of the muscle are not high, and blood flow is thought to be predominantly through the short shunt like capillaries which principally feed the connective and adipose tissues (possibly as a greater proportion of the bodies energy needs at rest are met by the metabolism of fats [370]). Once insulin or contraction stimulate metabolism, blood flows through the more 'nutritive', long tortuous capillaries of the muscle where energy needs are high [299]. The results from this study would suggest that the stimulus of ET-1 and IL-6 at basal may not have been great enough to cause a change in the metabolic needs of the cells, and therefore a change in the state of perfusion may not have been required. Another explanation may be that the signalling pathway regulating vascular tone at basal is different to that during insulin stimulation, thus as ET-1 and IL-6 inhibit the insulin signalling pathway, they would not have an effect on the basal mechanism of nitric oxide production. Furthermore, the changes in nitric oxide production and ET-1 release are relatively low, and therefore an inhibition may not have had a great effect over a short time period. Chronically however, the basal state of perfusion may change in response to these factors. For example, Mather et al. [198] found that obese and type 2 diabetic patients have an increase in the basal endothelin mediated constrictor tone compared to lean subjects. Treatment of these patients with an ET_A antagonist resulted in a significant vasodilation, however lean subjects were unaffected. Therefore, as lean rodents were used in this thesis, they may not have been affected, or were able to compensate for a small change in vascular tone.

Previous studies and the data presented in this thesis suggest that ET-1 could be a mediator of insulin resistance and hypertension, and could be a target for therapeutic intervention. Endothelin-1 appears to mediate its potentially harmful vasoconstrictor effects through the ET_A receptor located on the vascular smooth muscle cells [181]. Acute inhibition of this receptor through the use of an ET_A receptor antagonist (but not an ET_B receptor agonist) normalised glucose metabolism and blocked the ET-1 induced reduction in insulin sensitivity and vasoconstriction in the liver, kidney and gut [178, 187], and has also been shown to regulate the increase in vascular tone seen in

type 2 diabetic and obese patients at basal [198]. Long term treatment (six weeks) of the Zucker fatty rat with the ET_A receptor selective antagonist atrasentan, improved whole body glucose metabolism during a hyperinsulinaemic clamp, by improving insulin signalling in the liver [202]. Furthermore, the stimulation of IL-6 by ET-1 is inhibited by an ET_A receptor agonist [360, 371]. These studies help to demonstrate that an elevation in ET-1 may cause significant modifications to the vasculature through its potent vasoconstrictor actions, and would suggest that inhibition of the ET_A receptor mediated events may help to decrease the harmful effects mediated by ET-1 and could possibly be a beneficial therapy for the treatment of insulin resistance.

Over 70% of type 2 diabetic patients are obese [372], and recent studies have suggested that obesity and type 2 diabetes may be associated with a state of low-grade inflammation [369]. The adipose tissue is a major site of cytokine secretion at rest [272], with IL-6 and TNF-α acting to decrease lipid accumulation within the adipose tissue and regulate cell size by stimulating lipolysis. TNF-α is also involved in apoptosis and IL-6 also acts on the hypothalamus in conjunction leptin to regulate satiety. Therefore, in healthy subject IL-6 and TNF- have a regulatory role, and act to regulate energy metabolism and fuel storage. A similar effect occurs in the IL-6 knockout mouse which develops mature onset obesity [275]. An increase in adipose tissue will lead to an increase in the secretion of inflammatory cytokines, and as shown in this thesis and eluded to above, a chronic increase in circulating cytokines will result in an increase in hepatic glucose production, and interference in insulin signalling.

IL-6 secretion is associated with an increase in adipose tissue mass and the body mass index [90, 219] and while obese patients have an increase in subcutaneous adipose tissue, they also have an increase in visceral fat and fat deposits surrounding the blood vessels, and more importantly the arterioles. Yudkin et al. [373] proposed that in a calorie rich environment these fat deposits may protect the muscle from an oversupply of substrates, by secreting factors such as TNF-α and IL-6 which interfere with insulin's ability to increase perfusion and nutrient delivery, preventing the accumulation of fat stores in the muscle which causes insulin resistance. Ironically however, it is the increase in circulating TNF-α and IL-6 which will contribute to insulin resistance and possible result in atherosclerosis and heart disease [222, 347]. The signalling pathways and regulatory function of TNF-α and IL-6 still requires further

investigation, however due to their important immune functions and actions during exercise, as well as their protective effect on muscle insulin resistance, it is unlikely that the antagonism or suppression of these cytokines will result in a sustainable pharmacological intervention for the treatment of type 2 diabetes.

Exercise is still the most important means of both prevention and treatment of a number of diseases such as type 2 diabetes, obesity and heart disease, with the benefits seen not only during the exercise bout but also during recovery. Insulin resistant subjects have a relatively normal response during contraction, and also maintain the same insulin sensitivity in the post-contraction period as do lean subjects. Whether this increase in sensitivity is due to a vascular response involving increased microvascular perfusion, in conjunction with a myocyte response involving glycogen synthesis, signalling through Akt or other pathways is not known. However it is important that further studies on the mechanisms of this positive effect are made so that a treatment option for these patients may be developed. This treatment may be in the form of a new pharmaceutical therapy or through a better understanding of the most effective exercise programmes to benefit these patients and maximise their insulin sensitivity during recovery.

The use of hormones, cytokines and vasoactive peptides in *in vivo* studies as reported herein, allows us to assess the relationships between vascular function and glucose metabolism. This does not however enable us to determine the cause of the increase in circulating agents, nor whether their increased stimulation is due to the up-regulation of other factors, the release of these substances as a protective mechanism, or if they are the cause of insulin resistance. Further research is thus required to fully understand the signalling processes which contribute to the beneficial effects of insulin and contraction, and the regulatory process which govern them.

8.6 CONCLUSION

In conclusion, studies in this thesis confirm that changes in bulk flow and microvascular perfusion are two separate and largely unrelated events. Furthermore, it is the change in the microvascular perfusion of the muscle, and not bulk flow, which is associated with change in glucose uptake. These two points are clearly

demonstrated in the study examining the role of microvascular perfusion during recovery from contraction. Thus, using contrast enhanced ultrasound, which is able to discriminate between changes in bulk flow and microvascular volume, it was shown that while femoral blood flow returned to basal levels rapidly after contraction, microvascular perfusion and glucose uptake remained elevated for 60 min post-contraction. Such data suggests that the increase in glucose uptake and the sensitisation of the muscle to insulin seen during recovery may involve a vascular component.

This thesis has also shown that the microvascular perfusion and muscle glucose uptake may be controlled by separate stimuli, as nitric oxide synthase inhibition during contraction, had no effect on the contraction mediated increase in microvascular perfusion, but caused a 30% decrease in glucose uptake. This result was unexpected, and suggests a non-vascular myocyte source of nitric oxide that is involved contraction-mediated glucose uptake.

In additional studies, both IL-6 and ET-1 inhibited insulin mediated microvascular perfusion, but, in the short term, changed insulin clearance (ET-1) or hepatic glucose output (IL-6) in order to maintain euglycaemia and insulin mediated glucose uptake. Chronically however, there is evidence to suggest that both ET-1 and IL-6 may lead to hyperinsulinaemia and insulin resistance by causing an imbalance in the vasoactive substances controlling vascular tone and microvascular perfusion.

Collectively these studies show that the vasculature is an important component of both contraction- and insulin-mediated actions, and that while microvascular perfusion and glucose uptake appear to be associated, the pathways activated in order to mediate these effects appear to be different. Therefore, the mechanisms through which contraction and insulin increase microvascular perfusion and glucose uptake need to be closely examined and further research is required to separate the effects of these stimuli on the myocyte and the endothelial cells of the vasculature.

REFERENCES

9.0 REFERENCES

1. Australian Bureau of Statistics. 2006. 2004-2005 Australian Bureau of Statistics National Health Survey: Summary of results.1-92. Viewed March 2007. www.abs.gov.org.
2. American Diabetes Association. 2007. The American Diabetes Association. Viewed March 2007. www.diabetes.org
3. World Health Oragnisation. 2007. World Health Organisation diabetes facts and figures. Viewed March 2007. www.who.org
4. Steinberger, J., and Daniels, S.R. 2003. Obesity, insulin resistance, diabetes, and cardiovascular risk in children: an American Heart Association scientific statement from the Atherosclerosis, Hypertension, and Obesity in the Young Committee (Council on Cardiovascular Disease in the Young) and the Diabetes Committee (Council on Nutrition, Physical Activity, and Metabolism). *Circulation* 107:1448-1453.
5. Nigro, J., Osman, N., Dart, A.M., and Little, P.J. 2006. Insulin resistance and atherosclerosis. *Endocr Rev* 27:242-259.
6. Abdul-Ghani, M.A., Tripathy, D., and DeFronzo, R.A. 2006. Contributions of beta-cell dysfunction and insulin resistance to the pathogenesis of impaired glucose tolerance and impaired fasting glucose. *Diabetes Care* 29:1130-1139.
7. Shichiri, M., Hirata, Y., Ando, K., Emori, T., Ohta, K., Kimoto, S., Ogura, M., Inoue, A., and Marumo, F. 1990. Plasma endothelin levels in hypertension and chronic renal failure. *Hypertension* 15:493-496.
8. Kim, J.A., Montagnani, M., Koh, K.K., and Quon, M.J. 2006. Reciprocal relationships between insulin resistance and endothelial dysfunction: molecular and pathophysiological mechanisms. *Circulation* 113:1888-1904.
9. Wellen, K.E., and Hotamisligil, G.S. 2005. Inflammation, stress, and diabetes. *J Clin Invest* 115:1111-1119.
10. Goodyear, L.J., and Kahn, B.B. 1998. Exercise, glucose transport, and insulin sensitivity. *Annu Rev Med* 49:235-261.
11. DeFronzo, R.A., Gunnarsson, R., Bjorkman, O., Olsson, M., and Wahren, J. 1985. Effects of insulin on peripheral and splanchnic glucose metabolism in noninsulin-dependent (type II) diabetes mellitus. *J Clin Invest* 76:149-155.
12. Ryder, J.W., Chibalin, A.V., and Zierath, J.R. 2001. Intracellular mechanisms underlying increases in glucose uptake in response to insulin or exercise in skeletal muscle. *Acta Physiol Scand* 171:249-257.
13. Vaag, A., Henriksen, J.E., and Beck-Nielsen, H. 1992. Decreased insulin activation of glycogen synthase in skeletal muscles in young nonobese Caucasian first-degree relatives of patients with non-insulin-dependent diabetes mellitus. *J Clin Invest* 89:782-788.
14. Wasserman, D.H., and Ayala, J.E. 2005. Interaction of physiological mechanisms in control of muscle glucose uptake. *Clin Exp Pharmacol Physiol* 32:319-323.
15. Krogh, A. 1967. A contribuion to the physiology of the capillaries. In *Nobel lecture; Physiology or Medicine 1901-1921,*. Amsterdam: Elsevier Publishing Company.
16. Murrant, C.L., and Sarelius, I.H. 2000. Coupling of muscle metabolism and muscle blood flow in capillary units during contraction. *Acta Physiol Scand* 168:531-541.

17. Sarelius, I.H., Cohen, K.D., and Murrant, C.L. 2000. Role for capillaries in coupling blood flow with metabolism. *Clin Exp Pharmacol Physiol* 27:826-829.
18. Williams, D.A., and Segal, S.S. 1993. Feed artery role in blood flow control to rat hindlimb skeletal muscles. *J Physiol* 463:631-646.
19. Sweeney, T.E., and Sarelius, I.H. 1989. Arteriolar control of capillary cell flow in striated muscle. *Circ Res* 64:112-120.
20. Berg, B.R., and Sarelius, I.H. 1995. Functional capillary organization in striated muscle. *Am J Physiol* 268:H1215-1222.
21. Rattigan, S., Clark, M.G., and Barrett, E.J. 1997. Hemodynamic actions of insulin in rat skeletal muscle: evidence for capillary recruitment. *Diabetes* 46:1381-1388.
22. Bruder, G., Heid, H., Jarasch, E.D., Keenan, T.W., and Mather, I.H. 1982. Characteristics of membrane-bound and soluble forms of xanthine oxidase from milk and endothelial cells of capillaries. *Biochim Biophys Acta* 701:357-369.
23. Jarasch, E.D., Grund, C., Bruder, G., Heid, H.W., Keenan, T.W., and Franke, W.W. 1981. Localization of xanthine oxidase in mammary-gland epithelium and capillary endothelium. *Cell* 25:67-82.
24. Parks, D.A., and Granger, D.N. 1986. Xanthine oxidase: biochemistry, distribution and physiology. *Acta Physiol Scand Suppl* 548:87-99.
25. Coggins, M., Lindner, J., Rattigan, S., Jahn, L., Fasy, E., Kaul, S., and Barrett, E. 2001. Physiologic hyperinsulinemia enhances human skeletal muscle perfusion by capillary recruitment. *Diabetes* 50:2682-2690.
26. Wei, K., Jayaweera, A.R., Firoozan, S., Linka, A., Skyba, D.M., and Kaul, S. 1998. Quantification of myocardial blood flow with ultrasound-induced destruction of microbubbles administered as a constant venous infusion. *Circulation* 97:473-483.
27. Kaul, S. 1997. Myocardial contrast echocardiography: 15 years of research and development. *Circulation* 96:3745-3760.
28. Dawson, D., Vincent, M.A., Barrett, E.J., Kaul, S., Clark, A., Leong-Poi, H., and Lindner, J.R. 2002. Vascular recruitment in skeletal muscle during exercise and hyperinsulinemia assessed by contrast ultrasound. *Am J Physiol Endocrinol Metab* 282:E714-720.
29. Zhang, L., Vincent, M.A., Richards, S.M., Clerk, L.H., Rattigan, S., Clark, M.G., and Barrett, E.J. 2004. Insulin sensitivity of muscle capillary recruitment in vivo. *Diabetes* 53:447-453.
30. de Jongh, R.T., Clark, A.D., RG, I.J., Serne, E.H., de Vries, G., and Stehouwer, C.D. 2004. Physiological hyperinsulinaemia increases intramuscular microvascular reactive hyperaemia and vasomotion in healthy volunteers. *Diabetologia* 47:978-986.
31. Serne, E.H., RG, I.J., Gans, R.O., Nijveldt, R., De Vries, G., Evertz, R., Donker, A.J., and Stehouwer, C.D. 2002. Direct evidence for insulin-induced capillary recruitment in skin of healthy subjects during physiological hyperinsulinemia. *Diabetes* 51:1515-1522.
32. Clark, A.D., Barrett, E.J., Rattigan, S., Wallis, M.G., and Clark, M.G. 2001. Insulin stimulates laser Doppler signal by rat muscle in vivo, consistent with nutritive flow recruitment. *Clin Sci (Lond)* 100:283-290.

33. Clark, M.G., Clark, A.D., and Rattigan, S. 2000. Failure of laser Doppler signal to correlate with total flow in muscle: is this a question of vessel architecture? *Microvasc Res* 60:294-301.
34. Newman, J.M., Rattigan, S., and Clark, M.G. 2002. Nutritive blood flow improves interstitial glucose and lactate exchange in perfused rat hindlimb. *Am J Physiol Heart Circ Physiol* 283:H186-192.
35. Gudbjornsdottir, S., Sjostrand, M., Strindberg, L., and Lonnroth, P. 2005. Decreased muscle capillary permeability surface area in type 2 diabetic subjects. *J Clin Endocrinol Metab* 90:1078-1082.
36. Abramson, D.I., Schkloven, N., Margolis, M.N., and Mirsky, I.A. 1939. Influence of massive doses of insulin on peripheral blood flow in man. *American Journal of Physiology* 128:124-132.
37. Liang, C., Doherty, J.U., Faillace, R., Maekawa, K., Arnold, S., Gavras, H., and Hood, W.B., Jr. 1982. Insulin infusion in conscious dogs. Effects on systemic and coronary hemodynamics, regional blood flows, and plasma catecholamines. *J Clin Invest* 69:1321-1336.
38. Vincent, M.A., Dawson, D., Clark, A.D., Lindner, J.R., Rattigan, S., Clark, M.G., and Barrett, E.J. 2002. Skeletal muscle microvascular recruitment by physiological hyperinsulinemia precedes increases in total blood flow. *Diabetes* 51:42-48.
39. James, D.E., Jenkins, A.B., and Kraegen, E.W. 1985. Heterogeneity of insulin action in individual muscles in vivo: euglycemic clamp studies in rats. *Am J Physiol* 248:E567-574.
40. Rattigan, S., Clark, M.G., and Barrett, E.J. 1999. Acute vasoconstriction-induced insulin resistance in rat muscle in vivo. *Diabetes* 48:564-569.
41. Wallis, M.G., Wheatley, C.M., Rattigan, S., Barrett, E.J., Clark, A.D., and Clark, M.G. 2002. Insulin-mediated hemodynamic changes are impaired in muscle of Zucker obese rats. *Diabetes* 51:3492-3498.
42. Anderson, E.A., Hoffman, R.P., Balon, T.W., Sinkey, C.A., and Mark, A.L. 1991. Hyperinsulinemia produces both sympathetic neural activation and vasodilation in normal humans. *J Clin Invest* 87:2246-2252.
43. Baron, A.D., and Brechtel, G. 1993. Insulin differentially regulates systemic and skeletal muscle vascular resistance. *Am J Physiol* 265:E61-67.
44. Laakso, M., Edelman, S.V., Brechtel, G., and Baron, A.D. 1990. Decreased effect of insulin to stimulate skeletal muscle blood flow in obese man. A novel mechanism for insulin resistance. *J Clin Invest* 85:1844-1852.
45. Utriainen, T., Malmstrom, R., Makimattila, S., and Yki-Jarvinen, H. 1995. Methodological aspects, dose-response characteristics and causes of interindividual variation in insulin stimulation of limb blood flow in normal subjects. *Diabetologia* 38:555-564.
46. Ebeling, P., Bourey, R., Koranyi, L., Tuominen, J.A., Groop, L.C., Henriksson, J., Mueckler, M., Sovijarvi, A., and Koivisto, V.A. 1993. Mechanism of enhanced insulin sensitivity in athletes. Increased blood flow, muscle glucose transport protein (GLUT-4) concentration, and glycogen synthase activity. *J Clin Invest* 92:1623-1631.
47. Allwood, M.J., Hensel, H., and Papenberg, J. 1959. Muscle and skin blood flow in the human forearm during insulin hypoglycaemia. *J Physiol* 147:269-273.

48. Yki-Jarvinen, H., Young, A.A., Lamkin, C., and Foley, J.E. 1987. Kinetics of glucose disposal in whole body and across the forearm in man. *J Clin Invest* 79:1713-1719.
49. Andres, R., Baltzan, M.A., Cader, G., and Zierler, K.L. 1962. Effect of insulin on carbohydrate metabolism and on potassium in the forearm of man. *J Clin Invest* 41:108-115.
50. Tack, C.J., Schefman, A.E., Willems, J.L., Thien, T., Lutterman, J.A., and Smits, P. 1996. Direct vasodilator effects of physiological hyperinsulin-aemia in human skeletal muscle. *Eur J Clin Invest* 26:772-778.
51. Høst, U., Kelbaek, H., Rasmusen, H., Court-Payen, M., Christensen, N.J., Pedersen-Bjergaard, U., and Lorenzen, T. 1996. Haemodynamic effects of eating: the role of meal composition. *Clin Sci (Lond)* 90:269-276.
52. Fugmann, A., Millgard, J., Sarabi, M., Berne, C., and Lind, L. 2003. Central and peripheral haemodynamic effects of hyperglycaemia, hyperinsulinaemia, hyperlipidaemia or a mixed meal. *Clin Sci (Lond)* 105:715-721.
53. Clark, M.G., Wallis, M.G., Barrett, E.J., Vincent, M.A., Richards, S.M., Clerk, L.H., and Rattigan, S. 2003. Blood flow and muscle metabolism: a focus on insulin action. *Am J Physiol Endocrinol Metab* 284:E241-258.
54. Baron, A.D. 1994. Hemodynamic actions of insulin. *Am J Physiol* 267:E187-202.
55. Newman, J.M., Dora, K.A., Rattigan, S., Edwards, S.J., Colquhoun, E.Q., and Clark, M.G. 1996. Norepinephrine and serotonin vasoconstriction in rat hindlimb control different vascular flow routes. *Am J Physiol* 270:E689-699.
56. Vincent, M.A., Clerk, L.H., Lindner, J.R., Klibanov, A.L., Clark, M.G., Rattigan, S., and Barrett, E.J. 2004. Microvascular recruitment is an early insulin effect that regulates skeletal muscle glucose uptake in vivo. *Diabetes* 53:1418-1423.
57. Wunsch, S.A., Muller-Delp, J., and Delp, M.D. 2000. Time course of vasodilatory responses in skeletal muscle arterioles: role in hyperemia at onset of exercise. *Am J Physiol Heart Circ Physiol* 279:H1715-1723.
58. Clifford, P.S., and Hellsten, Y. 2004. Vasodilatory mechanisms in contracting skeletal muscle. *J Appl Physiol* 97:393-403.
59. Segal, S.S. 2000. Integration of blood flow control to skeletal muscle: key role of feed arteries. *Acta Physiol Scand* 168:511-518.
60. Gorczynski, R.J., Klitzman, B., and Duling, B.R. 1978. Interrelations between contracting striated muscle and precapillary microvessels. *Am J Physiol* 235:H494-504.
61. Hilton, S.M. 1959. A peripheral arterial conducting mechanism underlying dilatation of the femoral artery and concerned in functional vasodilatation in skeletal muscle. *J Physiol* 149:93-111.
62. Radegran, G., and Saltin, B. 1998. Muscle blood flow at onset of dynamic exercise in humans. *Am J Physiol* 274:H314-322.
63. Rattigan, S., Wheatley, C., Richards, S.M., Barrett, E.J., and Clark, M.G. 2005. Exercise and insulin-mediated capillary recruitment in muscle. *Exerc Sport Sci Rev* 33:43-48.
64. Welsh, D.G., and Segal, S.S. 1997. Coactivation of resistance vessels and muscle fibers with acetylcholine release from motor nerves. *Am J Physiol* 273:H156-163.
65. Nuutila, P., Peltoniemi, P., Oikonen, V., Larmola, K., Kemppainen, J., Takala, T., Sipila, H., Oksanen, A., Ruotsalainen, U., Bolli, G.B., et al. 2000.

Enhanced stimulation of glucose uptake by insulin increases exercise-stimulated glucose uptake in skeletal muscle in humans: studies using [15O]O2, [15O]H2O, [18F]fluoro-deoxy-glucose, and positron emission tomography. *Diabetes* 49:1084-1091.

66. Laughlin, M.H., and Armstrong, R.B. 1982. Muscular blood flow distribution patterns as a function of running speed in rats. *Am J Physiol* 243:H296-306.
67. Lott, M.E., Hogeman, C.S., Vickery, L., Kunselman, A.R., Sinoway, L.I., and MacLean, D.A. 2001. Effects of dynamic exercise on mean blood velocity and muscle interstitial metabolite responses in humans. *Am J Physiol Heart Circ Physiol* 281:H1734-1741.
68. Tschakovsky, M.E., Shoemaker, J.K., and Hughson, R.L. 1996. Vasodilation and muscle pump contribution to immediate exercise hyperemia. *Am J Physiol* 271:H1697-1701.
69. Glavind-Kristensen, M., Matchkov, V., Hansen, V.B., Forman, A., Nilsson, H., and Aalkjaer, C. 2004. KATP-channel-induced vasodilation is modulated by the Na,K-pump activity in rabbit coronary small arteries. *Br J Pharmacol* 143:872-880.
70. De Clerck, I., Pannier, J.L., and Van de Voorde, J. 2006. K+ potentiates hyperosmolarity-induced vasorelaxations in rat skeletal muscle arterioles. *Eur J Appl Physiol* 96:679-685.
71. MacLean, D.A., Imadojemu, V.A., and Sinoway, L.I. 2000. Interstitial pH, K(+), lactate, and phosphate determined with MSNA during exercise in humans. *Am J Physiol Regul Integr Comp Physiol* 278:R563-571.
72. Juel, C., Pilegaard, H., Nielsen, J.J., and Bangsbo, J. 2000. Interstitial K(+) in human skeletal muscle during and after dynamic graded exercise determined by microdialysis. *Am J Physiol Regul Integr Comp Physiol* 278:R400-406.
73. Kiens, B., Saltin, B., Walloe, L., and Wesche, J. 1989. Temporal relationship between blood flow changes and release of ions and metabolites from muscles upon single weak contractions. *Acta Physiol Scand* 136:551-559.
74. Martin, E.A., Nicholson, W.T., Eisenach, J.H., Charkoudian, N., and Joyner, M.J. 2006. Influences of adenosine receptor antagonism on vasodilator responses to adenosine and exercise in adenosine responders and nonresponders. *J Appl Physiol* 101:1678-1684.
75. Radegran, G., and Calbet, J.A. 2001. Role of adenosine in exercise-induced human skeletal muscle vasodilatation. *Acta Physiol Scand* 171:177-185.
76. Ballard, H.J., Cotterrell, D., and Karim, F. 1987. Appearance of adenosine in venous blood from the contracting gracilis muscle and its role in vasodilatation in the dog. *J Physiol* 387:401-413.
77. Radegran, G., and Saltin, B. 1999. Nitric oxide in the regulation of vasomotor tone in human skeletal muscle. *Am J Physiol* 276:H1951-1960.
78. Segal, S.S., and Jacobs, T.L. 2001. Role for endothelial cell conduction in ascending vasodilatation and exercise hyperaemia in hamster skeletal muscle. *J Physiol* 536:937-946.
79. Wilson, J.R., and Kapoor, S.C. 1993. Contribution of prostaglandins to exercise-induced vasodilation in humans. *Am J Physiol* 265:H171-175.
80. Shoemaker, J.K., Naylor, H.L., Pozeg, Z.I., and Hughson, R.L. 1996. Failure of prostaglandins to modulate the time course of blood flow during dynamic forearm exercise in humans. *J Appl Physiol* 81:1516-1521.

81. Schrage, W.G., Joyner, M.J., and Dinenno, F.A. 2004. Local inhibition of nitric oxide and prostaglandins independently reduces forearm exercise hyperaemia in humans. *J Physiol* 557:599-611.
82. Baron, A.D., Brechtel-Hook, G., Johnson, A., and Hardin, D. 1993. Skeletal muscle blood flow. A possible link between insulin resistance and blood pressure. *Hypertension* 21:129-135.
83. Ivy, J.L., Brozinick, J.T., Jr., Torgan, C.E., and Kastello, G.M. 1989. Skeletal muscle glucose transport in obese Zucker rats after exercise training. *J Appl Physiol* 66:2635-2641.
84. Xiang, L., Naik, J., and Hester, R.L. 2005. Exercise-induced increase in skeletal muscle vasodilatory responses in obese Zucker rats. *Am J Physiol Regul Integr Comp Physiol* 288:R987-991.
85. Berthiaume, N., Wessale, J.L., Opgenorth, T.J., and Zinker, B.A. 2005. Metabolic responses with endothelin antagonism in a model of insulin resistance. *Metabolism* 54:735-740.
86. Kurtz, T.W., Morris, R.C., and Pershadsingh, H.A. 1989. The Zucker fatty rat as a genetic model of obesity and hypertension. *Hypertension* 13:896-901.
87. Wheatley, C.M., Rattigan, S., Richards, S.M., Barrett, E.J., and Clark, M.G. 2004. Skeletal Muscle Contraction Stimulates Capillary Recruitment and Glucose Uptake in Insulin Resistant Obese Zucker Rats. *Am J Physiol Endocrinol Metab.*
88. Saghizadeh, M., Ong, J.M., Garvey, W.T., Henry, R.R., and Kern, P.A. 1996. The expression of TNF alpha by human muscle. Relationship to insulin resistance. *J Clin Invest* 97:1111-1116.
89. Hotamisligil, G.S., Budavari, A., Murray, D., and Spiegelman, B.M. 1994. Reduced tyrosine kinase activity of the insulin receptor in obesity-diabetes. Central role of tumor necrosis factor-alpha. *J Clin Invest* 94:1543-1549.
90. Kern, P.A., Ranganathan, S., Li, C., Wood, L., and Ranganathan, G. 2001. Adipose tissue tumor necrosis factor and interleukin-6 expression in human obesity and insulin resistance. *Am J Physiol Endocrinol Metab* 280:E745-751.
91. Nolte, L.A., Hansen, P.A., Chen, M.M., Schluter, J.M., Gulve, E.A., and Holloszy, J.O. 1998. Short-term exposure to tumor necrosis factor-alpha does not affect insulin-stimulated glucose uptake in skeletal muscle. *Diabetes* 47:721-726.
92. Kanety, H., Feinstein, R., Papa, M.Z., Hemi, R., and Karasik, A. 1995. Tumor necrosis factor alpha-induced phosphorylation of insulin receptor substrate-1 (IRS-1). Possible mechanism for suppression of insulin-stimulated tyrosine phosphorylation of IRS-1. *J Biol Chem* 270:23780-23784.
93. Hotamisligil, G.S., Peraldi, P., Budavari, A., Ellis, R., White, M.F., and Spiegelman, B.M. 1996. IRS-1-mediated inhibition of insulin receptor tyrosine kinase activity in TNF-alpha- and obesity-induced insulin resistance. *Science* 271:665-668.
94. Kroder, G., Bossenmaier, B., Kellerer, M., Capp, E., Stoyanov, B., Muhlhofer, A., Berti, L., Horikoshi, H., Ullrich, A., and Haring, H. 1996. Tumor necrosis factor-alpha- and hyperglycemia-induced insulin resistance. Evidence for different mechanisms and different effects on insulin signaling. *J Clin Invest* 97:1471-1477.
95. Youd, J.M., Rattigan, S., and Clark, M.G. 2000. Acute impairment of insulin-mediated capillary recruitment and glucose uptake in rat skeletal muscle in vivo by TNF-alpha. *Diabetes* 49:1904-1909.

96. Lang, C.H., Dobrescu, C., and Bagby, G.J. 1992. Tumor necrosis factor impairs insulin action on peripheral glucose disposal and hepatic glucose output. *Endocrinology* 130:43-52.
97. Zhang, L., Wheatley, C.M., Richards, S.M., Barrett, E.J., Clark, M.G., and Rattigan, S. 2003. TNF-alpha acutely inhibits vascular effects of physiological but not high insulin or contraction. *Am J Physiol Endocrinol Metab* 285:E654-660.
98. Kingwell, B.A., Formosa, M., Muhlmann, M., Bradley, S.J., and McConell, G.K. 2003. Type 2 diabetic individuals have impaired leg blood flow responses to exercise: role of endothelium-dependent vasodilation. *Diabetes Care* 26:899-904.
99. Clerk, L.H., Vincent, M.A., Jahn, L.A., Liu, Z., Lindner, J.R., and Barrett, E.J. 2006. Obesity blunts insulin-mediated microvascular recruitment in human forearm muscle. *Diabetes* 55:1436-1442.
100. Zierath, J.R., He, L., Guma, A., Odegoard Wahlstrom, E., Klip, A., and Wallberg-Henriksson, H. 1996. Insulin action on glucose transport and plasma membrane GLUT4 content in skeletal muscle from patients with NIDDM. *Diabetologia* 39:1180-1189.
101. Kennedy, J.W., Hirshman, M.F., Gervino, E.V., Ocel, J.V., Forse, R.A., Hoenig, S.J., Aronson, D., Goodyear, L.J., and Horton, E.S. 1999. Acute exercise induces GLUT4 translocation in skeletal muscle of normal human subjects and subjects with type 2 diabetes. *Diabetes* 48:1192-1197.
102. Teran-Garcia, M., Rankinen, T., Koza, R.A., Rao, D.C., and Bouchard, C. 2005. Endurance training-induced changes in insulin sensitivity and gene expression. *Am J Physiol Endocrinol Metab* 288:E1168-1178.
103. Koyama, Y., Galassetti, P., Coker, R.H., Pencek, R.R., Lacy, D.B., Davis, S.N., and Wasserman, D.H. 2002. Prior exercise and the response to insulin-induced hypoglycemia in the dog. *Am J Physiol Endocrinol Metab* 282:E1128-1138.
104. Howlett, K.F., Sakamoto, K., Hirshman, M.F., Aschenbach, W.G., Dow, M., White, M.F., and Goodyear, L.J. 2002. Insulin signaling after exercise in insulin receptor substrate-2-deficient mice. *Diabetes* 51:479-483.
105. Arias, E.B., Kim, J., Funai, K., and Cartee, G.D. 2007. Prior exercise increases phosphorylation of Akt substrate of 160 kDa (AS160) in rat skeletal muscle. *Am J Physiol Endocrinol Metab* 292:E1191-1200.
106. Bogardus, C., Thuillez, P., Ravussin, E., Vasquez, B., Narimiga, M., and Azhar, S. 1983. Effect of muscle glycogen depletion on in vivo insulin action in man. *J Clin Invest* 72:1605-1610.
107. Devlin, J.T., Hirshman, M., Horton, E.D., and Horton, E.S. 1987. Enhanced peripheral and splanchnic insulin sensitivity in NIDDM men after single bout of exercise. *Diabetes* 36:434-439.
108. Perseghin, G., Price, T.B., Petersen, K.F., Roden, M., Cline, G.W., Gerow, K., Rothman, D.L., and Shulman, G.I. 1996. Increased glucose transport-phosphorylation and muscle glycogen synthesis after exercise training in insulin-resistant subjects. *N Engl J Med* 335:1357-1362.
109. Mikines, K.J., Sonne, B., Farrell, P.A., Tronier, B., and Galbo, H. 1988. Effect of physical exercise on sensitivity and responsiveness to insulin in humans. *Am J Physiol* 254:E248-259.

110. Wojtaszewski, J.F., Jorgensen, S.B., Frosig, C., MacDonald, C., Birk, J.B., and Richter, E.A. 2003. Insulin signalling: effects of prior exercise. *Acta Physiol Scand* 178:321-328.
111. Del Aguila, L.F., Krishnan, R.K., Ulbrecht, J.S., Farrell, P.A., Correll, P.H., Lang, C.H., Zierath, J.R., and Kirwan, J.P. 2000. Muscle damage impairs insulin stimulation of IRS-1, PI 3-kinase, and Akt-kinase in human skeletal muscle. *Am J Physiol Endocrinol Metab* 279:E206-212.
112. Richter, E.A., Garetto, L.P., Goodman, M.N., and Ruderman, N.B. 1982. Muscle glucose metabolism following exercise in the rat: increased sensitivity to insulin. *J Clin Invest* 69:785-793.
113. Garetto, L.P., Richter, E.A., Goodman, M.N., and Ruderman, N.B. 1984. Enhanced muscle glucose metabolism after exercise in the rat: the two phases. *Am J Physiol* 246:E471-475.
114. Kawanaka, K., Han, D.H., Nolte, L.A., Hansen, P.A., Nakatani, A., and Holloszy, J.O. 1999. Decreased insulin-stimulated GLUT-4 translocation in glycogen-supercompensated muscles of exercised rats. *Am J Physiol* 276:E907-912.
115. Ren, J.M., Semenkovich, C.F., Gulve, E.A., Gao, J., and Holloszy, J.O. 1994. Exercise induces rapid increases in GLUT4 expression, glucose transport capacity, and insulin-stimulated glycogen storage in muscle. *J Biol Chem* 269:14396-14401.
116. Kawanaka, K., Nolte, L.A., Han, D.H., Hansen, P.A., and Holloszy, J.O. 2000. Mechanisms underlying impaired GLUT-4 translocation in glycogen-supercompensated muscles of exercised rats. *Am J Physiol Endocrinol Metab* 279:E1311-1318.
117. Garcia-Roves, P.M., Han, D.H., Song, Z., Jones, T.E., Hucker, K.A., and Holloszy, J.O. 2003. Prevention of glycogen supercompensation prolongs the increase in muscle GLUT4 after exercise. *Am J Physiol Endocrinol Metab* 285:E729-736.
118. Cartee, G.D., Young, D.A., Sleeper, M.D., Zierath, J., Wallberg-Henriksson, H., and Holloszy, J.O. 1989. Prolonged increase in insulin-stimulated glucose transport in muscle after exercise. *Am J Physiol* 256:E494-499.
119. Chou, C.H., Tsai, Y.L., Hou, C.W., Lee, H.H., Chang, W.H., Lin, T.W., Hsu, T.H., Huang, Y.J., and Kuo, C.H. 2005. Glycogen overload by postexercise insulin administration abolished the exercise-induced increase in GLUT4 protein. *J Biomed Sci* 12:991-998.
120. Richter, E.A., Hansen, S.A., and Hansen, B.F. 1988. Mechanisms limiting glycogen storage in muscle during prolonged insulin stimulation. *Am J Physiol* 255:E621-628.
121. Henriksen, E.J., and Halseth, A.E. 1994. Early alterations in soleus GLUT-4, glucose transport, and glycogen in voluntary running rats. *J Appl Physiol* 76:1862-1867.
122. Fell, R.D., Terblanche, S.E., Ivy, J.L., Young, J.C., and Holloszy, J.O. 1982. Effect of muscle glycogen content on glucose uptake following exercise. *J Appl Physiol* 52:434-437.
123. Wojtaszewski, J.F., Hansen, B.F., Gade, Kiens, B., Markuns, J.F., Goodyear, L.J., and Richter, E.A. 2000. Insulin signaling and insulin sensitivity after exercise in human skeletal muscle. *Diabetes* 49:325-331.

124. Goodyear, L.J., Giorgino, F., Balon, T.W., Condorelli, G., and Smith, R.J. 1995. Effects of contractile activity on tyrosine phosphoproteins and PI 3-kinase activity in rat skeletal muscle. *Am J Physiol* 268:E987-995.
125. Wojtaszewski, J.F., Higaki, Y., Hirshman, M.F., Michael, M.D., Dufresne, S.D., Kahn, C.R., and Goodyear, L.J. 1999. Exercise modulates postreceptor insulin signaling and glucose transport in muscle-specific insulin receptor knockout mice. *J Clin Invest* 104:1257-1264.
126. Howlett, K.F., Sakamoto, K., Yu, H., Goodyear, L.J., and Hargreaves, M. 2006. Insulin-stimulated insulin receptor substrate-2-associated phosphatidylinositol 3-kinase activity is enhanced in human skeletal muscle after exercise. *Metabolism* 55:1046-1052.
127. Cartee, G.D., and Wojtaszewski, J.F. 2007. Role of Akt substrate of 160 kDa in insulin-stimulated and contraction-stimulated glucose transport. *Appl Physiol Nutr Metab* 32:557-566.
128. Kramer, H.F., Witczak, C.A., Fujii, N., Jessen, N., Taylor, E.B., Arnolds, D.E., Sakamoto, K., Hirshman, M.F., and Goodyear, L.J. 2006. Distinct signals regulate AS160 phosphorylation in response to insulin, AICAR, and contraction in mouse skeletal muscle. *Diabetes* 55:2067-2076.
129. Wojtaszewski, J.F., and Richter, E.A. 2006. Effects of acute exercise and training on insulin action and sensitivity: focus on molecular mechanisms in muscle. *Essays Biochem* 42:31-46.
130. Ramm, G., Larance, M., Guilhaus, M., and James, D.E. 2006. A role for 14-3-3 in insulin-stimulated GLUT4 translocation through its interaction with the RabGAP AS160. *J Biol Chem* 281:29174-29180.
131. Bruss, M.D., Arias, E.B., Lienhard, G.E., and Cartee, G.D. 2005. Increased phosphorylation of Akt substrate of 160 kDa (AS160) in rat skeletal muscle in response to insulin or contractile activity. *Diabetes* 54:41-50.
132. Karlsson, H.K., Zierath, J.R., Kane, S., Krook, A., Lienhard, G.E., and Wallberg-Henriksson, H. 2005. Insulin-stimulated phosphorylation of the Akt substrate AS160 is impaired in skeletal muscle of type 2 diabetic subjects. *Diabetes* 54:1692-1697.
133. Thyfault, J.P., Cree, M.G., Zheng, D., Zwetsloot, J.J., Tapscott, E.B., Koves, T.R., Ilkayeva, O., Wolfe, R.R., Muoio, D.M., and Dohm, G.L. 2007. Contraction of insulin-resistant muscle normalizes insulin action in association with increased mitochondrial activity and fatty acid catabolism. *Am J Physiol Cell Physiol* 292:C729-739.
134. Treebak, J.T., Birk, J.B., Rose, A.J., Kiens, B., Richter, E.A., and Wojtaszewski, J.F. 2007. AS160 phosphorylation is associated with activation of alpha2beta2gamma1- but not alpha2beta2gamma3-AMPK trimeric complex in skeletal muscle during exercise in humans. *Am J Physiol Endocrinol Metab* 292:E715-722.
135. Sriwijitkamol, A., Coletta, D.K., Wajcberg, E., Balbontin, G.B., Reyna, S.M., Barrientes, J., Eagan, P.A., Jenkinson, C.P., Cersosimo, E., DeFronzo, R.A., et al. 2007. Effect of acute exercise on AMPK signaling in skeletal muscle of subjects with type 2 diabetes: a time-course and dose-response study. *Diabetes* 56:836-848.
136. Treebak, J.T., Glund, S., Deshmukh, A., Klein, D.K., Long, Y.C., Jensen, T.E., Jorgensen, S.B., Viollet, B., Andersson, L., Neumann, D., et al. 2006. AMPK-Mediated AS160 Phosphorylation in Skeletal Muscle Is Dependent on AMPK Catalytic and Regulatory Subunits. *Diabetes* 55:2051-2058.

137. Reid, M.B. 1998. Role of nitric oxide in skeletal muscle: synthesis, distribution and functional importance. *Acta Physiol Scand* 162:401-409.
138. Shankar, R.R., Wu, Y., Shen, H.Q., Zhu, J.S., and Baron, A.D. 2000. Mice with gene disruption of both endothelial and neuronal nitric oxide synthase exhibit insulin resistance. *Diabetes* 49:684-687.
139. McConell, G.K., and Kingwell, B.A. 2006. Does nitric oxide regulate skeletal muscle glucose uptake during exercise? *Exerc Sport Sci Rev* 34:36-41.
140. Montagnani, M., Chen, H., Barr, V.A., and Quon, M.J. 2001. Insulin-stimulated activation of eNOS is independent of Ca2+ but requires phosphorylation by Akt at Ser(1179). *J Biol Chem* 276:30392-30398.
141. Crawford, J.H., Isbell, T.S., Huang, Z., Shiva, S., Chacko, B.K., Schechter, A.N., Darley-Usmar, V.M., Kerby, J.D., Lang, J.D., Jr., Kraus, D., et al. 2006. Hypoxia, red blood cells, and nitrite regulate NO-dependent hypoxic vasodilation. *Blood* 107:566-574.
142. Cosby, K., Partovi, K.S., Crawford, J.H., Patel, R.P., Reiter, C.D., Martyr, S., Yang, B.K., Waclawiw, M.A., Zalos, G., Xu, X., et al. 2003. Nitrite reduction to nitric oxide by deoxyhemoglobin vasodilates the human circulation. *Nat Med* 9:1498-1505.
143. Balon, T.W., and Nadler, J.L. 1997. Evidence that nitric oxide increases glucose transport in skeletal muscle. *J Appl Physiol* 82:359-363.
144. Delp, M.D., and Laughlin, M.H. 1998. Regulation of skeletal muscle perfusion during exercise. *Acta Physiol Scand* 162:411-419.
145. Roberts, C.K., Barnard, R.J., Jasman, A., and Balon, T.W. 1999. Acute exercise increases nitric oxide synthase activity in skeletal muscle. *Am J Physiol* 277:E390-394.
146. McConell, G.K., Bradley, S.J., Stephens, T.J., Canny, B.J., Kingwell, B.A., and Lee-Young, R.S. 2007. Skeletal muscle nNOS{micro} protein content is incresaed by exercise training in humans. *Am J Physiol Regul Integr Comp Physiol.*
147. Vassilakopoulos, T., Deckman, G., Kebbewar, M., Rallis, G., Harfouche, R., and Hussain, S.N. 2003. Regulation of nitric oxide production in limb and ventilatory muscles during chronic exercise training. *Am J Physiol Lung Cell Mol Physiol* 284:L452-457.
148. Frandsen, U., Bangsbo, J., Sander, M., Hoffner, L., Betak, A., Saltin, B., and Hellsten, Y. 2001. Exercise-induced hyperaemia and leg oxygen uptake are not altered during effective inhibition of nitric oxide synthase with N(G)-nitro-L-arginine methyl ester in humans. *J Physiol* 531:257-264.
149. Bradley, S.J., Kingwell, B.A., and McConell, G.K. 1999. Nitric oxide synthase inhibition reduces leg glucose uptake but not blood flow during dynamic exercise in humans. *Diabetes* 48:1815-1821.
150. McConell, G.K., Huynh, N.N., Lee-Young, R.S., Canny, B.J., and Wadley, G.D. 2006. L-Arginine infusion increases glucose clearance during prolonged exercise in humans. *Am J Physiol Endocrinol Metab* 290:E60-E66.
151. Kingwell, B.A., Formosa, M., Muhlmann, M., Bradley, S.J., and McConell, G.K. 2002. Nitric oxide synthase inhibition reduces glucose uptake during exercise in individuals with type 2 diabetes more than in control subjects. *Diabetes* 51:2572-2580.
152. Roberts, C.K., Barnard, R.J., Scheck, S.H., and Balon, T.W. 1997. Exercise-stimulated glucose transport in skeletal muscle is nitric oxide dependent. *Am J Physiol* 273:E220-225.

153. Higaki, Y., Hirshman, M.F., Fujii, N., and Goodyear, L.J. 2001. Nitric oxide increases glucose uptake through a mechanism that is distinct from the insulin and contraction pathways in rat skeletal muscle. *Diabetes* 50:241-247.
154. Etgen, G.J., Jr., Fryburg, D.A., and Gibbs, E.M. 1997. Nitric oxide stimulates skeletal muscle glucose transport through a calcium/contraction- and phosphatidylinositol-3-kinase-independent pathway. *Diabetes* 46:1915-1919.
155. Rottman, J.N., Bracy, D., Malabanan, C., Yue, Z., Clanton, J., and Wasserman, D.H. 2002. Contrasting effects of exercise and NOS inhibition on tissue-specific fatty acid and glucose uptake in mice. *Am J Physiol Endocrinol Metab* 283:E116-123.
156. Hirai, T., Visneski, M.D., Kearns, K.J., Zelis, R., and Musch, T.I. 1994. Effects of NO synthase inhibition on the muscular blood flow response to treadmill exercise in rats. *J Appl Physiol* 77:1288-1293.
157. Musch, T.I., McAllister, R.M., Symons, J.D., Stebbins, C.L., Hirai, T., Hageman, K.S., and Poole, D.C. 2001. Effects of nitric oxide synthase inhibition on vascular conductance during high speed treadmill exercise in rats. *Exp Physiol* 86:749-757.
158. Kahn, N.N., Acharya, K., Bhattacharya, S., Acharya, R., Mazumder, S., Bauman, W.A., and Sinha, A.K. 2000. Nitric oxide: the "second messenger" of insulin. *IUBMB Life* 49:441-450.
159. Zeng, G., and Quon, M.J. 1996. Insulin-stimulated production of nitric oxide is inhibited by wortmannin. Direct measurement in vascular endothelial cells. *J Clin Invest* 98:894-898.
160. Kuboki, K., Jiang, Z.Y., Takahara, N., Ha, S.W., Igarashi, M., Yamauchi, T., Feener, E.P., Herbert, T.P., Rhodes, C.J., and King, G.L. 2000. Regulation of endothelial constitutive nitric oxide synthase gene expression in endothelial cells and in vivo : a specific vascular action of insulin. *Circulation* 101:676-681.
161. Montagnani, M., Ravichandran, L.V., Chen, H., Esposito, D.L., and Quon, M.J. 2002. Insulin receptor substrate-1 and phosphoinositide-dependent kinase-1 are required for insulin-stimulated production of nitric oxide in endothelial cells. *Mol Endocrinol* 16:1931-1942.
162. Steinberg, H.O., Brechtel, G., Johnson, A., Fineberg, N., and Baron, A.D. 1994. Insulin-mediated skeletal muscle vasodilation is nitric oxide dependent. A novel action of insulin to increase nitric oxide release. *J Clin Invest* 94:1172-1179.
163. Scherrer, U., Randin, D., Vollenweider, P., Vollenweider, L., and Nicod, P. 1994. Nitric oxide release accounts for insulin's vascular effects in humans. *J Clin Invest* 94:2511-2515.
164. Vincent, M.A., Barrett, E.J., Lindner, J.R., Clark, M.G., and Rattigan, S. 2003. Inhibiting NOS blocks microvascular recruitment and blunts muscle glucose uptake in response to insulin. *Am J Physiol Endocrinol Metab* 285:E123-129.
165. Roy, D., Perreault, M., and Marette, A. 1998. Insulin stimulation of glucose uptake in skeletal muscles and adipose tissues in vivo is NO dependent. *Am J Physiol* 274:E692-699.
166. Kashyap, S.R., Roman, L.J., Lamont, J., Masters, B.S., Bajaj, M., Suraamornkul, S., Belfort, R., Berria, R., Kellogg, D.L., Jr., Liu, Y., et al. 2005. Insulin resistance is associated with impaired nitric oxide synthase activity in skeletal muscle of type 2 diabetic subjects. *J Clin Endocrinol Metab* 90:1100-1105.

167. Doronzo, G., Russo, I., Mattiello, L., Anfossi, G., Bosia, A., and Trovati, M. 2004. Insulin activates vascular endothelial growth factor in vascular smooth muscle cells: influence of nitric oxide and of insulin resistance. *Eur J Clin Invest* 34:664-673.
168. Hickner, R.C., Kemeny, G., Stallings, H.W., Manning, S.M., and McIver, K.L. 2006. Relationship between body composition and skeletal muscle eNOS. *Int J Obes (Lond)* 30:308-312.
169. Young, M.E., and Leighton, B. 1998. Evidence for altered sensitivity of the nitric oxide/cGMP signalling cascade in insulin-resistant skeletal muscle. *Biochem J* 329 (Pt 1):73-79.
170. Ishii, H., Jirousek, M.R., Koya, D., Takagi, C., Xia, P., Clermont, A., Bursell, S.E., Kern, T.S., Ballas, L.M., Heath, W.F., et al. 1996. Amelioration of vascular dysfunctions in diabetic rats by an oral PKC beta inhibitor. *Science* 272:728-731.
171. Duplain, H., Burcelin, R., Sartori, C., Cook, S., Egli, M., Lepori, M., Vollenweider, P., Pedrazzini, T., Nicod, P., Thorens, B., et al. 2001. Insulin resistance, hyperlipidemia, and hypertension in mice lacking endothelial nitric oxide synthase. *Circulation* 104:342-345.
172. Shesely, E.G., Maeda, N., Kim, H.S., Desai, K.M., Krege, J.H., Laubach, V.E., Sherman, P.A., Sessa, W.C., and Smithies, O. 1996. Elevated blood pressures in mice lacking endothelial nitric oxide synthase. *Proc Natl Acad Sci U S A* 93:13176-13181.
173. Stauss, H.M., Godecke, A., Mrowka, R., Schrader, J., and Persson, P.B. 1999. Enhanced blood pressure variability in eNOS knockout mice. *Hypertension* 33:1359-1363.
174. Koller, A., and Huang, A. 1995. Shear stress-induced dilation is attenuated in skeletal muscle arterioles of hypertensive rats. *Hypertension* 25:758-763.
175. Koller, A., and Huang, A. 1994. Impaired nitric oxide-mediated flow-induced dilation in arterioles of spontaneously hypertensive rats. *Circ Res* 74:416-421.
176. Shankar, R., Zhu, J.S., Ladd, B., Henry, D., Shen, H.Q., and Baron, A.D. 1998. Central nervous system nitric oxide synthase activity regulates insulin secretion and insulin action. *J Clin Invest* 102:1403-1412.
177. Scherrer, U., and Sartori, C. 2000. Defective nitric oxide synthesis: a link between metabolic insulin resistance, sympathetic overactivity and cardiovascular morbidity. *Eur J Endocrinol* 142:315-323.
178. Ahlborg, G., and Lindstrom, J. 2002. Insulin sensitivity and big ET-1 conversion to ET-1 after ETA- or ETB-receptor blockade in humans. *J Appl Physiol* 93:2112-2121.
179. Levin, E.R. 1995. Endothelins. *N Engl J Med* 333:356-363.
180. Vierhapper, H., Wagner, O., Nowotny, P., and Waldhausl, W. 1990. Effect of endothelin-1 in man. *Circulation* 81:1415-1418.
181. Pollock, D.M., Keith, T.L., and Highsmith, R.F. 1995. Endothelin receptors and calcium signaling. *Faseb J* 9:1196-1204.
182. Ferri, C., Bellini, C., Desideri, G., Di Francesco, L., Baldoncini, R., Santucci, A., and De Mattia, G. 1995. Plasma endothelin-1 levels in obese hypertensive and normotensive men. *Diabetes* 44:431-436.
183. Takahashi, K., Ghatei, M.A., Lam, H.C., O'Halloran, D.J., and Bloom, S.R. 1990. Elevated plasma endothelin in patients with diabetes mellitus. *Diabetologia* 33:306-310.

184. Donatelli, M., Hoffmann, E., Colletti, I., Andolina, G., Russo, V., Bucalo, M.L., Valenti, T.M., Compagno, V., Cataldo, M.G., and Morici, M.L. 1996. Circulating endothelin-1 levels in type 2 diabetic patients with ischaemic heart disease. *Acta Diabetol* 33:246-248.
185. de Nucci, G., Thomas, R., D'Orleans-Juste, P., Antunes, E., Walder, C., Warner, T.D., and Vane, J.R. 1988. Pressor effects of circulating endothelin are limited by its removal in the pulmonary circulation and by the release of prostacyclin and endothelium-derived relaxing factor. *Proc Natl Acad Sci U S A* 85:9797-9800.
186. Filep, J.G., Foldes-Filep, E., Rousseau, A., Sirois, P., and Fournier, A. 1993. Vascular responses to endothelin-1 following inhibition of nitric oxide synthesis in the conscious rat. *Br J Pharmacol* 110:1213-1221.
187. King-VanVlack, C.E., Mewburn, J.D., and Chapler, C.K. 1999. Receptor-mediated vascular and metabolic actions of endothelin-1 in canine small intestine. *Am J Physiol* 276:G1131-1136.
188. Ahlborg, G., Weitzberg, E., and Lundberg, J.M. 1995. Circulating endothelin-1 reduces splanchnic and renal blood flow and splanchnic glucose production in humans. *J Appl Physiol* 79:141-145.
189. Gardiner, S.M., Compton, A.M., and Bennett, T. 1989. Regional hemodynamic effects of endothelin-1 in conscious, unrestrained, Wistar rats. *J Cardiovasc Pharmacol* 13 Suppl 5:S202-204.
190. Kolka, C.M., Rattigan, S., Richards, S., and Clark, M.G. 2005. Metabolic and vascular actions of endothelin-1 are inhibited by insulin-mediated vasodilation in perfused rat hindlimb muscle. *Br J Pharmacol* 145:992-1000.
191. Takaori, K., Inoue, K., Kogire, M., Higashide, S., Tun, T., Aung, T., Doi, R., Fujii, N., and Tobe, T. 1992. Effects of endothelin on microcirculation of the pancreas. *Life Sci* 51:615-622.
192. Lai, E.Y., Persson, A.E., Bodin, B., Kallskog, O., Andersson, A., Pettersson, U., Hansell, P., and Jansson, L. 2007. Endothelin-1 and Pancreatic Islet Vasculature: Studies in Vivo and on Isolated, Vascularly Perfused Pancreatic Islets. *Am J Physiol Endocrinol Metab.*
193. Ottosson-Seeberger, A., Lundberg, J.M., Alvestrand, A., and Ahlborg, G. 1997. Exogenous endothelin-1 causes peripheral insulin resistance in healthy humans. *Acta Physiol Scand* 161:211-220.
194. Mitchell, D., Bihari, A., Sandig, M., and Tyml, K. 2002. Endothelin-a receptor in rat skeletal muscle microvasculature. *Microvasc Res* 64:179-185.
195. Maeda, S., Miyauchi, T., Sakane, M., Saito, M., Maki, S., Goto, K., and Matsuda, M. 1997. Does endothelin-1 participate in the exercise-induced changes of blood flow distribution of muscles in humans? *J Appl Physiol* 82:1107-1111.
196. Potenza, M.A., Marasciulo, F.L., Chieppa, D.M., Brigiani, G.S., Formoso, G., Quon, M.J., and Montagnani, M. 2005. Insulin resistance in spontaneously hypertensive rats is associated with endothelial dysfunction characterized by imbalance between NO and ET-1 production. *Am J Physiol Heart Circ Physiol* 289:H813-822.
197. Muniyappa, R., and Quon, M.J. 2007. Insulin action and insulin resistance in vascular endothelium. *Curr Opin Clin Nutr Metab Care* 10:523-530.
198. Mather, K.J., Mirzamohammadi, B., Lteif, A., Steinberg, H.O., and Baron, A.D. 2002. Endothelin contributes to basal vascular tone and endothelial dysfunction in human obesity and type 2 diabetes. *Diabetes* 51:3517-3523.

199. Ahlborg, G., and Lundberg, J.M. 1997. Nitric oxide-endothelin-1 interaction in humans. *J Appl Physiol* 82:1593-1600.
200. Wu, S.Q., Hopfner, R.L., McNeill, J.R., Wilson, T.W., and Gopalakrishnan, V. 2000. Altered paracrine effect of endothelin in blood vessels of the hyperinsulinemic, insulin resistant obese Zucker rat. *Cardiovasc Res* 45:994-1000.
201. Hopfner, R.L., Hasnadka, R.V., Wilson, T.W., McNeill, J.R., and Gopalakrishnan, V. 1998. Insulin increases endothelin-1-evoked intracellular free calcium responses by increased ET(A) receptor expression in rat aortic smooth muscle cells. *Diabetes* 47:937-944.
202. Berthiaume, N., Carlson, C.J., Rondinone, C.M., and Zinker, B.A. 2005. Endothelin antagonism improves hepatic insulin sensitivity associated with insulin signaling in Zucker fatty rats. *Metabolism* 54:1515-1523.
203. Wilkes, J.J., Hevener, A., and Olefsky, J. 2003. Chronic endothelin-1 treatment leads to insulin resistance in vivo. *Diabetes* 52:1904-1909.
204. Idris, I., Patiag, D., Gray, S., and Donnelly, R. 2001. Tissue- and time-dependent effects of endothelin-1 on insulin-stimulated glucose uptake. *Biochem Pharmacol* 62:1705-1708.
205. Ishibashi, K.I., Imamura, T., Sharma, P.M., Huang, J., Ugi, S., and Olefsky, J.M. 2001. Chronic endothelin-1 treatment leads to heterologous desensitization of insulin signaling in 3T3-L1 adipocytes. *J Clin Invest* 107:1193-1202.
206. Shaw, S.G., and Boden, P.J. 2005. Insulin resistance, obesity and the metabolic syndrome. Is there a therapeutic role for endothelin-1 antagonists? *Curr Vasc Pharmacol* 3:359-363.
207. Tanabe, K., Yamamoto, A., Suzuki, N., Yokoyama, Y., Osada, N., Nakayama, M., Akashi, Y., Seki, A., Samejima, H., Oya, M., et al. 2000. Physiological role of endothelin-1 in nonworking muscles during exercise in healthy subjects. *Jpn Circ J* 64:27-31.
208. Yousufuddin, M., Shamim, W., Chambers, J.S., Henein, M., Amin, F.R., Anker, S.D., Kemp, M., Hooper, J., and Coats, A.J. 2000. Superiority of endothelin-1 over norepinephrine in exercise-induced alterations of the conduit artery tone of the non-exercised arm in patients with chronic heart failure. *Int J Cardiol* 73:15-25.
209. McEniery, C.M., Wilkinson, I.B., Jenkins, D.G., and Webb, D.J. 2002. Endogenous endothelin-1 limits exercise-induced vasodilation in hypertensive humans. *Hypertension* 40:202-206.
210. Ahlborg, G., Weitzberg, E., and Lundberg, J. 1995. Metabolic and vascular effects of circulating endothelin-1 during moderately heavy prolonged exercise. *J Appl Physiol* 78:2294-2300.
211. Maeda, S., Miyauchi, T., Iemitsu, M., Tanabe, T., Irukayama-Tomobe, Y., Goto, K., Yamaguchi, I., and Matsuda, M. 2002. Involvement of endogenous endothelin-1 in exercise-induced redistribution of tissue blood flow: an endothelin receptor antagonist reduces the redistribution. *Circulation* 106:2188-2193.
212. Kolka, C.M., Rattigan, S., Richards, S.M., and Clark, M.G. 2007. Potential for endothelin-1-mediated impairment of contractile activity in hypertension. *Clin Exp Pharmacol Physiol* 34:217-222.

213. Fernandez-Real, J.M., Broch, M., Vendrell, J., Gutierrez, C., Casamitjana, R., Pugeat, M., Richart, C., and Ricart, W. 2000. Interleukin-6 gene polymorphism and insulin sensitivity. *Diabetes* 49:517-520.
214. Keller, E.T., Wanagat, J., and Ershler, W.B. 1996. Molecular and cellular biology of interleukin-6 and its receptor. *Front Biosci* 1:d340-357.
215. Heinrich, P.C., Behrmann, I., Muller-Newen, G., Schaper, F., and Graeve, L. 1998. Interleukin-6-type cytokine signalling through the gp130/Jak/STAT pathway. *Biochem J* 334 (Pt 2):297-314.
216. Febbraio, M.A., Steensberg, A., Starkie, R.L., McConell, G.K., and Kingwell, B.A. 2003. Skeletal muscle interleukin-6 and tumor necrosis factor-alpha release in healthy subjects and patients with type 2 diabetes at rest and during exercise. *Metabolism* 52:939-944.
217. Pickup, J.C., Chusney, G.D., Thomas, S.M., and Burt, D. 2000. Plasma interleukin-6, tumour necrosis factor alpha and blood cytokine production in type 2 diabetes. *Life Sci* 67:291-300.
218. Bastard, J.P., Maachi, M., Van Nhieu, J.T., Jardel, C., Bruckert, E., Grimaldi, A., Robert, J.J., Capeau, J., and Hainque, B. 2002. Adipose tissue IL-6 content correlates with resistance to insulin activation of glucose uptake both in vivo and in vitro. *J Clin Endocrinol Metab* 87:2084-2089.
219. Vozarova, B., Weyer, C., Hanson, K., Tataranni, P.A., Bogardus, C., and Pratley, R.E. 2001. Circulating interleukin-6 in relation to adiposity, insulin action, and insulin secretion. *Obes Res* 9:414-417.
220. Pradhan, A.D., Manson, J.E., Rifai, N., Buring, J.E., and Ridker, P.M. 2001. C-reactive protein, interleukin 6, and risk of developing type 2 diabetes mellitus. *Jama* 286:327-334.
221. Ridker, P.M., Rifai, N., Stampfer, M.J., and Hennekens, C.H. 2000. Plasma concentration of interleukin-6 and the risk of future myocardial infarction among apparently healthy men. *Circulation* 101:1767-1772.
222. Jenny, N.S., Tracy, R.P., Ogg, M.S., Luong le, A., Kuller, L.H., Arnold, A.M., Sharrett, A.R., and Humphries, S.E. 2002. In the elderly, interleukin-6 plasma levels and the -174G>C polymorphism are associated with the development of cardiovascular disease. *Arterioscler Thromb Vasc Biol* 22:2066-2071.
223. Mohamed-Ali, V., Goodrick, S., Rawesh, A., Katz, D.R., Miles, J.M., Yudkin, J.S., Klein, S., and Coppack, S.W. 1997. Subcutaneous adipose tissue releases interleukin-6, but not tumor necrosis factor-alpha, in vivo. *J Clin Endocrinol Metab* 82:4196-4200.
224. Ostrowski, K., Rohde, T., Zacho, M., Asp, S., and Pedersen, B.K. 1998. Evidence that interleukin-6 is produced in human skeletal muscle during prolonged running. *J Physiol* 508 (Pt 3):949-953.
225. Ullum, H., Haahr, P.M., Diamant, M., Palmo, J., Halkjaer-Kristensen, J., and Pedersen, B.K. 1994. Bicycle exercise enhances plasma IL-6 but does not change IL-1 alpha, IL-1 beta, IL-6, or TNF-alpha pre-mRNA in BMNC. *J Appl Physiol* 77:93-97.
226. Hirano, T. 1998. Interleukin 6 and its receptor: ten years later. *Int Rev Immunol* 16:249-284.
227. Gerhartz, C., Dittrich, E., Stoyan, T., Rose-John, S., Yasukawa, K., Heinrich, P.C., and Graeve, L. 1994. Biosynthesis and half-life of the interleukin-6 receptor and its signal transducer gp130. *Eur J Biochem* 223:265-274.

228. Heinrich, P.C., Behrmann, I., Haan, S., Hermanns, H.M., Muller-Newen, G., and Schaper, F. 2003. Principles of interleukin (IL)-6-type cytokine signalling and its regulation. *Biochem J* 374:1-20.
229. Pedersen, B.K., Ostrowski, K., Rohde, T., and Bruunsgaard, H. 1998. The cytokine response to strenuous exercise. *Can J Physiol Pharmacol* 76:505-511.
230. Starkie, R.L., Rolland, J., Angus, D.J., Anderson, M.J., and Febbraio, M.A. 2001. Circulating monocytes are not the source of elevations in plasma IL-6 and TNF-alpha levels after prolonged running. *Am J Physiol Cell Physiol* 280:C769-774.
231. Keller, C., Steensberg, A., Pilegaard, H., Osada, T., Saltin, B., Pedersen, B.K., and Neufer, P.D. 2001. Transcriptional activation of the IL-6 gene in human contracting skeletal muscle: influence of muscle glycogen content. *Faseb J* 15:2748-2750.
232. Steensberg, A., van Hall, G., Osada, T., Sacchetti, M., Saltin, B., and Klarlund Pedersen, B. 2000. Production of interleukin-6 in contracting human skeletal muscles can account for the exercise-induced increase in plasma interleukin-6. *J Physiol* 529 Pt 1:237-242.
233. Jonsdottir, I.H., Schjerling, P., Ostrowski, K., Asp, S., Richter, E.A., and Pedersen, B.K. 2000. Muscle contractions induce interleukin-6 mRNA production in rat skeletal muscles. *J Physiol* 528 Pt 1:157-163.
234. Moldoveanu, A.I., Shephard, R.J., and Shek, P.N. 2000. Exercise elevates plasma levels but not gene expression of IL-1beta, IL-6, and TNF-alpha in blood mononuclear cells. *J Appl Physiol* 89:1499-1504.
235. Banzet, S., Koulmann, N., Sanchez, H., Serrurier, B., Peinnequin, A., Alonso, A., and Bigard, X. 2007. Contraction-induced interleukin-6 transcription in rat slow-type muscle is partly dependent on calcineurin activation. *J Cell Physiol* 210:596-601.
236. Nieman, D.C., Davis, J.M., Henson, D.A., Walberg-Rankin, J., Shute, M., Dumke, C.L., Utter, A.C., Vinci, D.M., Carson, J.A., Brown, A., et al. 2003. Carbohydrate ingestion influences skeletal muscle cytokine mRNA and plasma cytokine levels after a 3-h run. *J Appl Physiol* 94:1917-1925.
237. Starkie, R.L., Arkinstall, M.J., Koukoulas, I., Hawley, J.A., and Febbraio, M.A. 2001. Carbohydrate ingestion attenuates the increase in plasma interleukin-6, but not skeletal muscle interleukin-6 mRNA, during exercise in humans. *J Physiol* 533:585-591.
238. Vassilakopoulos, T., Karatza, M.H., Katsaounou, P., Kollintza, A., Zakynthinos, S., and Roussos, C. 2003. Antioxidants attenuate the plasma cytokine response to exercise in humans. *J Appl Physiol* 94:1025-1032.
239. Thompson, D., Williams, C., McGregor, S.J., Nicholas, C.W., McArdle, F., Jackson, M.J., and Powell, J.R. 2001. Prolonged vitamin C supplementation and recovery from demanding exercise. *Int J Sport Nutr Exerc Metab* 11:466-481.
240. Fischer, C.P. 2006. Interleukin-6 in acute exercise and training: what is the biological relevance? *Exerc Immunol Rev* 12:6-33.
241. Ronsen, O., Lea, T., Bahr, R., and Pedersen, B.K. 2002. Enhanced plasma IL-6 and IL-1ra responses to repeated vs. single bouts of prolonged cycling in elite athletes. *J Appl Physiol* 92:2547-2553.

242. Helge, J.W., Stallknecht, B., Pedersen, B.K., Galbo, H., Kiens, B., and Richter, E.A. 2003. The effect of graded exercise on IL-6 release and glucose uptake in human skeletal muscle. *J Physiol* 546:299-305.
243. Steensberg, A., Febbraio, M.A., Osada, T., Schjerling, P., van Hall, G., Saltin, B., and Pedersen, B.K. 2001. Interleukin-6 production in contracting human skeletal muscle is influenced by pre-exercise muscle glycogen content. *J Physiol* 537:633-639.
244. MacDonald, C., Wojtaszewski, J.F., Pedersen, B.K., Kiens, B., and Richter, E.A. 2003. Interleukin-6 release from human skeletal muscle during exercise: relation to AMPK activity. *J Appl Physiol.*
245. Nehlsen-Cannarella, S.L., Fagoaga, O.R., Nieman, D.C., Henson, D.A., Butterworth, D.E., Schmitt, R.L., Bailey, E.M., Warren, B.J., Utter, A., and Davis, J.M. 1997. Carbohydrate and the cytokine response to 2.5 h of running. *J Appl Physiol* 82:1662-1667.
246. Wojtaszewski, J.F., MacDonald, C., Nielsen, J.N., Hellsten, Y., Hardie, D.G., Kemp, B.E., Kiens, B., and Richter, E.A. 2003. Regulation of 5'AMP-activated protein kinase activity and substrate utilization in exercising human skeletal muscle. *Am J Physiol Endocrinol Metab* 284:E813-822.
247. Kelly, M., Keller, C., Avilucea, P.R., Keller, P., Luo, Z., Xiang, X., Giralt, M., Hidalgo, J., Saha, A.K., Pedersen, B.K., et al. 2004. AMPK activity is diminished in tissues of IL-6 knockout mice: the effect of exercise. *Biochem Biophys Res Commun* 320:449-454.
248. Carey, A.L., Steinberg, G.R., Macaulay, S.L., Thomas, W.G., Holmes, A.G., Ramm, G., Prelovsek, O., Hohnen-Behrens, C., Watt, M.J., James, D.E., et al. 2006. Interleukin-6 increases insulin-stimulated glucose disposal in humans and glucose uptake and fatty acid oxidation in vitro via AMP-activated protein kinase. *Diabetes* 55:2688-2697.
249. Al-Khalili, L., Bouzakri, K., Glund, S., Lonnqvist, F., Koistinen, H.A., and Krook, A. 2006. Signaling specificity of interleukin-6 action on glucose and lipid metabolism in skeletal muscle. *Mol Endocrinol.*
250. Lyngso, D., Simonsen, L., and Bulow, J. 2002. Metabolic effects of interleukin-6 in human splanchnic and adipose tissue. *J Physiol* 543:379-386.
251. van Hall, G., Steensberg, A., Sacchetti, M., Fischer, C., Keller, C., Schjerling, P., Hiscock, N., Moller, K., Saltin, B., Febbraio, M.A., et al. 2003. Interleukin-6 stimulates lipolysis and fat oxidation in humans. *J Clin Endocrinol Metab* 88:3005-3010.
252. Richter, E.A., Turcotte, L., Hespel, P., and Kiens, B. 1992. Metabolic responses to exercise. Effects of endurance training and implications for diabetes. *Diabetes Care* 15:1767-1776.
253. Petersen, E.W., Carey, A.L., Sacchetti, M., Steinberg, G.R., Macaulay, S.L., Febbraio, M.A., and Pedersen, B.K. 2005. Acute IL-6 treatment increases fatty acid turnover in elderly humans in vivo and in tissue culture in vitro. *Am J Physiol Endocrinol Metab* 288:E155-162.
254. Bruce, C.R., and Dyck, D.J. 2004. Cytokine regulation of skeletal muscle fatty acid metabolism: effect of interleukin-6 and tumor necrosis factor-alpha. *Am J Physiol Endocrinol Metab* 287:E616-621.
255. Path, G., Bornstein, S.R., Gurniak, M., Chrousos, G.P., Scherbaum, W.A., and Hauner, H. 2001. Human breast adipocytes express interleukin-6 (IL-6) and its receptor system: increased IL-6 production by beta-adrenergic activation and effects of IL-6 on adipocyte function. *J Clin Endocrinol Metab* 86:2281-2288.

256. Al-Khalili, L., Bouzakri, K., Glund, S., Lonnqvist, F., Koistinen, H.A., and Krook, A. 2006. Signaling specificity of interleukin-6 action on glucose and lipid metabolism in skeletal muscle. *Mol Endocrinol* 20:3364-3375.
257. Weigert, C., Hennige, A.M., Brodbeck, K., Haring, H.U., and Schleicher, E.D. 2005. Interleukin-6 acts as insulin sensitizer on glycogen synthesis in human skeletal muscle cells by phosphorylation of Ser473 of Akt. *Am J Physiol Endocrinol Metab* 289:E251-257.
258. Geiger, P.C., Hancock, C., Wright, D.C., Han, D.H., and Holloszy, J.O. 2007. IL-6 increases muscle insulin sensitivity only at superphysiological levels. *Am J Physiol Endocrinol Metab* 292:E1842-1846.
259. Glund, S., Deshmukh, A., Long, Y.C., Moller, T., Koistinen, H.A., Caidahl, K., Zierath, J.R., and Krook, A. 2007. Interleukin-6 directly increases glucose metabolism in resting human skeletal muscle. *Diabetes* 56:1630-1637.
260. Weigert, C., Hennige, A.M., Lehmann, R., Brodbeck, K., Baumgartner, F., Schauble, M., Haring, H.U., and Schleicher, E.D. 2006. Direct cross-talk of interleukin-6 and insulin signal transduction via insulin receptor substrate-1 in skeletal muscle cells. *J Biol Chem* 281:7060-7067.
261. Rotter, V., Nagaev, I., and Smith, U. 2003. Interleukin-6 (IL-6) induces insulin resistance in 3T3-L1 adipocytes and is, like IL-8 and tumor necrosis factor-alpha, overexpressed in human fat cells from insulin-resistant subjects. *J Biol Chem* 278:45777-45784.
262. Fasshauer, M., Kralisch, S., Klier, M., Lossner, U., Bluher, M., Klein, J., and Paschke, R. 2004. Insulin resistance-inducing cytokines differentially regulate SOCS mRNA expression via growth factor- and Jak/Stat-signaling pathways in 3T3-L1 adipocytes. *J Endocrinol* 181:129-138.
263. Lagathu, C., Bastard, J.P., Auclair, M., Maachi, M., Capeau, J., and Caron, M. 2003. Chronic interleukin-6 (IL-6) treatment increased IL-6 secretion and induced insulin resistance in adipocyte: prevention by rosiglitazone. *Biochem Biophys Res Commun* 311:372-379.
264. Stouthard, J.M., Oude Elferink, R.P., and Sauerwein, H.P. 1996. Interleukin-6 enhances glucose transport in 3T3-L1 adipocytes. *Biochem Biophys Res Commun* 220:241-245.
265. Steensberg, A., Fischer, C.P., Sacchetti, M., Keller, C., Osada, T., Schjerling, P., van Hall, G., Febbraio, M.A., and Pedersen, B.K. 2003. Acute interleukin-6 administration does not impair muscle glucose uptake or whole-body glucose disposal in healthy humans. *J Physiol* 548:631-638.
266. Rotter Sopasakis, V., Larsson, B.M., Johansson, A., Holmang, A., and Smith, U. 2004. Short-term infusion of interleukin-6 does not induce insulin resistance in vivo or impair insulin signalling in rats. *Diabetologia* 47:1879-1887.
267. Stith, R.D., and Luo, J. 1994. Endocrine and carbohydrate responses to interleukin-6 in vivo. *Circ Shock* 44:210-215.
268. Kim, H.J., Higashimori, T., Park, S.Y., Choi, H., Dong, J., Kim, Y.J., Noh, H.L., Cho, Y.R., Cline, G., Kim, Y.B., et al. 2004. Differential effects of interleukin-6 and -10 on skeletal muscle and liver insulin action in vivo. *Diabetes* 53:1060-1067.
269. Miyazaki, Y., Pipek, R., Mandarino, L.J., and DeFronzo, R.A. 2003. Tumor necrosis factor alpha and insulin resistance in obese type 2 diabetic patients. *Int J Obes Relat Metab Disord* 27:88-94.

270. Huvers, F.C., Popa, C., Netea, M.G., van den Hoogen, F.H., and Tack, C.J. 2007. Improved insulin sensitivity by anti-TNFalpha antibody treatment in patients with rheumatic diseases. *Ann Rheum Dis* 66:558-559.
271. Greenberg, A.S., Nordan, R.P., McIntosh, J., Calvo, J.C., Scow, R.O., and Jablons, D. 1992. Interleukin 6 reduces lipoprotein lipase activity in adipose tissue of mice in vivo and in 3T3-L1 adipocytes: a possible role for interleukin 6 in cancer cachexia. *Cancer Res* 52:4113-4116.
272. Coppack, S.W. 2001. Pro-inflammatory cytokines and adipose tissue. *Proc Nutr Soc* 60:349-356.
273. Nishimoto, N., Yoshizaki, K., Miyasaka, N., Yamamoto, K., Kawai, S., Takeuchi, T., Hashimoto, J., Azuma, J., and Kishimoto, T. 2004. Treatment of rheumatoid arthritis with humanized anti-interleukin-6 receptor antibody: a multicenter, double-blind, placebo-controlled trial. *Arthritis Rheum* 50:1761-1769.
274. Choy, E.H., Isenberg, D.A., Garrood, T., Farrow, S., Ioannou, Y., Bird, H., Cheung, N., Williams, B., Hazleman, B., Price, R., et al. 2002. Therapeutic benefit of blocking interleukin-6 activity with an anti-interleukin-6 receptor monoclonal antibody in rheumatoid arthritis: a randomized, double-blind, placebo-controlled, dose-escalation trial. *Arthritis Rheum* 46:3143-3150.
275. Wallenius, V., Wallenius, K., Ahren, B., Rudling, M., Carlsten, H., Dickson, S.L., Ohlsson, C., and Jansson, J.O. 2002. Interleukin-6-deficient mice develop mature-onset obesity. *Nat Med* 8:75-79.
276. Kanemaki, T., Kitade, H., Kaibori, M., Sakitani, K., Hiramatsu, Y., Kamiyama, Y., Ito, S., and Okumura, T. 1998. Interleukin 1beta and interleukin 6, but not tumor necrosis factor alpha, inhibit insulin-stimulated glycogen synthesis in rat hepatocytes. *Hepatology* 27:1296-1303.
277. Senn, J.J., Klover, P.J., Nowak, I.A., and Mooney, R.A. 2002. Interleukin-6 induces cellular insulin resistance in hepatocytes. *Diabetes* 51:3391-3399.
278. Klover, P.J., Zimmers, T.A., Koniaris, L.G., and Mooney, R.A. 2003. Chronic exposure to interleukin-6 causes hepatic insulin resistance in mice. *Diabetes* 52:2784-2789.
279. Senn, J.J., Klover, P.J., Nowak, I.A., Zimmers, T.A., Koniaris, L.G., Furlanetto, R.W., and Mooney, R.A. 2003. Suppressor of cytokine signaling-3 (SOCS-3), a potential mediator of interleukin-6-dependent insulin resistance in hepatocytes. *J Biol Chem* 278:13740-13746.
280. Clerk, L.H., Rattigan, S., Clark, M.G., Coggins, M., Lindner, J., Jahn, L., Fasy, E., Kaul, S., and Barrett, E. 2002. Lipid infusion impairs physiologic insulin-mediated capillary recruitment and muscle glucose uptake in vivo. *Diabetes* 51:1138-1145.
281. Mahajan, H., Richards, S.M., Rattigan, S., and Clark, M.G. 2004. Local methacholine but not bradykinin potentiates insulin-mediated glucose uptake in muscle in vivo by augmenting capillary recruitment. *Diabetologia* 47:2226-2234.
282. Jarasch, E.D., Bruder, G., and Heid, H.W. 1986. Significance of xanthine oxidase in capillary endothelial cells. *Acta Physiol Scand Suppl* 548:39-46.
283. Asp, S., Watkinson, A., Oakes, N.D., and Kraegen, E.W. 1997. Prior eccentric contractions impair maximal insulin action on muscle glucose uptake in the conscious rat. *J Appl Physiol* 82:1327-1332.

284. Emmerson, B.T., Gordon, R.B., Cross, M., and Thomson, D.B. 1987. Plasma oxipurinol concentrations during allopurinol therapy. *Br J Rheumatol* 26:445-449.
285. Kraegen, E.W., James, D.E., Jenkins, A.B., and Chisholm, D.J. 1985. Dose-response curves for in vivo insulin sensitivity in individual tissues in rats. 248:E353-E362.
286. James, D.E., Jenkins, A.B., and Kraegen, E.W. 1985. Heterogeneity of insulin action in individual muscles in vivo: euglycemic clamp studies in rats. 248:E567-E574.
287. Lindner, J.R., Skyba, D.M., Goodman, N.C., Jayaweera, A.R., and Kaul, S. 1997. Changes in myocardial blood volume with graded coronary stenosis. *Am J Physiol* 272:H567-575.
288. Vincent, M.A., Clerk, L.H., Lindner, J.R., Price, W.J., Jahn, L.A., Leong-Poi, H., and Barrett, E.J. 2006. Mixed meal and light exercise each recruit muscle capillaries in healthy humans. *Am J Physiol Endocrinol Metab* 290:E1191-1197.
289. Eringa, E.C., Stehouwer, C.D., van Nieuw Amerongen, G.P., Ouwehand, L., Westerhof, N., and Sipkema, P. 2004. Vasoconstrictor effects of insulin in skeletal muscle arterioles are mediated by ERK1/2 activation in endothelium. *Am J Physiol Heart Circ Physiol* 287:H2043-2048.
290. Kaufmann, B.A., Wei, K., and Lindner, J.R. 2007. Contrast echocardiography. *Curr Probl Cardiol* 32:51-96.
291. Ploug, T., Galbo, H., and Richter, E.A. 1984. Increased muscle glucose uptake during contractions: no need for insulin. *Am J Physiol* 247:E726-731.
292. Wallberg-Henriksson, H., and Holloszy, J.O. 1984. Contractile activity increases glucose uptake by muscle in severely diabetic rats. *J Appl Physiol* 57:1045-1049.
293. DeFronzo, R.A., Ferrannini, E., Sato, Y., Felig, P., and Wahren, J. 1981. Synergistic interaction between exercise and insulin on peripheral glucose uptake. *J Clin Invest* 68:1468-1474.
294. Honig, C.R., Odoroff, C.L., and Frierson, J.L. 1982. Active and passive capillary control in red muscle at rest and in exercise. *Am J Physiol* 243:H196-206.
295. Klitzman, B., Damon, D.N., Gorczynski, R.J., and Duling, B.R. 1982. Augmented tissue oxygen supply during striated muscle contraction in the hamster. Relative contributions of capillary recruitment, functional dilation, and reduced tissue PO2. *Circ Res* 51:711-721.
296. Ruderman, N.B., Houghton, C.R., and Hems, R. 1971. Evaluation of the isolated perfused rat hindquarter for the study of muscle metabolism. *Biochem J* 124:639-651.
297. Ross, B.D. 1972. *Perfusion techniques in biochemistry:a laboratory manual.* Oxford: Clarendon Press.
298. Greene, E.C. 1968. *Anatomy of the rat.* USA: Hafner Publishing Co.
299. Clark, M.G., Rattigan, S., Clerk, L.H., Vincent, M.A., Clark, A.D., Youd, J.M., and Newman, J.M. 2000. Nutritive and non-nutritive blood flow: rest and exercise. *Acta Physiol Scand* 168:519-530.
300. Gordon, M.B., Jain, R., Beckman, J.A., and Creager, M.A. 2002. The contribution of nitric oxide to exercise hyperemia in the human forearm. *Vasc Med* 7:163-168.

301. Richter, E.A., Mikines, K.J., Galbo, H., and Kiens, B. 1989. Effect of exercise on insulin action in human skeletal muscle. *J Appl Physiol* 66:876-885.
302. Richter, E.A., Garetto, L.P., Goodman, M.N., and Ruderman, N.B. 1984. Enhanced muscle glucose metabolism after exercise: modulation by local factors. *Am J Physiol* 246:E476-482.
303. Williams, J.T., Pricher, M.P., and Halliwill, J.R. 2005. Is postexercise hypotension related to excess postexercise oxygen consumption through changes in leg blood flow? *J Appl Physiol* 98:1463-1468.
304. Ivy, J.L., and Kuo, C.H. 1998. Regulation of GLUT4 protein and glycogen synthase during muscle glycogen synthesis after exercise. *Acta Physiol Scand* 162:295-304.
305. Mohrman, D.E., and Regal, R.R. 1988. Relation of blood flow to VO2, PO2, and PCO2 in dog gastrocnemius muscle. *Am J Physiol* 255:H1004-1010.
306. Bangsbo, J., and Hellsten, Y. 1998. Muscle blood flow and oxygen uptake in recovery from exercise. *Acta Physiol Scand* 162:305-312.
307. Borsheim, E., and Bahr, R. 2003. Effect of exercise intensity, duration and mode on post-exercise oxygen consumption. *Sports Med* 33:1037-1060.
308. Richter, E.A., Derave, W., and Wojtaszewski, J.F. 2001. Glucose, exercise and insulin: emerging concepts. *J Physiol* 535:313-322.
309. Schrage, W.G., Dietz, N.M., and Joyner, M.J. 2006. Effects of combined inhibition of ATP-sensitive potassium channels, nitric oxide, and prostaglandins on hyperemia during moderate exercise. *J Appl Physiol* 100:1506-1512.
310. Gilligan, D.M., Panza, J.A., Kilcoyne, C.M., Waclawiw, M.A., Casino, P.R., and Quyyumi, A.A. 1994. Contribution of endothelium-derived nitric oxide to exercise-induced vasodilation. *Circulation* 90:2853-2858.
311. Kraegen, E.W., James, D.E., Jenkins, A.B., and Chisholm, D.J. 1985. Dose-response curves for in vivo insulin sensitivity in individual tissues in rats. *Am J Physiol* 248:E353-362.
312. Chen, Z.P., Mitchelhill, K.I., Michell, B.J., Stapleton, D., Rodriguez-Crespo, I., Witters, L.A., Power, D.A., Ortiz de Montellano, P.R., and Kemp, B.E. 1999. AMP-activated protein kinase phosphorylation of endothelial NO synthase. *FEBS Lett* 443:285-289.
313. Chen, Z.P., McConell, G.K., Michell, B.J., Snow, R.J., Canny, B.J., and Kemp, B.E. 2000. AMPK signaling in contracting human skeletal muscle: acetyl-CoA carboxylase and NO synthase phosphorylation. *Am J Physiol Endocrinol Metab* 279:E1202-1206.
314. Wadley, G.D., Lee-Young, R.S., Canny, B.J., Wasuntarawat, C., Chen, Z.P., Hargreaves, M., Kemp, B.E., and McConell, G.K. 2006. Effect of exercise intensity and hypoxia on skeletal muscle AMPK signaling and substrate metabolism in humans. *Am J Physiol Endocrinol Metab* 290:E694-702.
315. Paul, R. 1980. Chemical energetics of vascular smooth muscle. . In *Handbook of Physiology. The Cardiovascular System II.* D. Bohr, A. Somlyo, and H. Sparks, editors. Baltimore: Waverly Press. 201-235.
316. Morrow, V.A., Foufelle, F., Connell, J.M., Petrie, J.R., Gould, G.W., and Salt, I.P. 2003. Direct activation of AMP-activated protein kinase stimulates nitric-oxide synthesis in human aortic endothelial cells. *J Biol Chem* 278:31629-31639.
317. Zou, M.H., Hou, X.Y., Shi, C.M., Kirkpatick, S., Liu, F., Goldman, M.H., and Cohen, R.A. 2003. Activation of 5'-AMP-activated kinase is mediated through

c-Src and phosphoinositide 3-kinase activity during hypoxia-reoxygenation of bovine aortic endothelial cells. Role of peroxynitrite. *J Biol Chem* 278:34003-34010.

318. Li, J., Hu, X., Selvakumar, P., Russell, R.R., 3rd, Cushman, S.W., Holman, G.D., and Young, L.H. 2004. Role of the nitric oxide pathway in AMPK-mediated glucose uptake and GLUT4 translocation in heart muscle. *Am J Physiol Endocrinol Metab* 287:E834-841.
319. Fryer, L.G., Hajduch, E., Rencurel, F., Salt, I.P., Hundal, H.S., Hardie, D.G., and Carling, D. 2000. Activation of glucose transport by AMP-activated protein kinase via stimulation of nitric oxide synthase. *Diabetes* 49:1978-1985.
320. Stephens, T.J., Canny, B.J., Snow, R.J., and McConell, G.K. 2004. 5'-aminoimidazole-4-carboxyamide-ribonucleoside-activated glucose transport is not prevented by nitric oxide synthase inhibition in rat isolated skeletal muscle. *Clin Exp Pharmacol Physiol* 31:419-423.
321. Jorgensen, S.B., Viollet, B., Andreelli, F., Frosig, C., Birk, J.B., Schjerling, P., Vaulont, S., Richter, E.A., and Wojtaszewski, J.F. 2004. Knockout of the alpha2 but not alpha1 5'-AMP-activated protein kinase isoform abolishes 5-aminoimidazole-4-carboxamide-1-beta-4-ribofuranosidebut not contraction-induced glucose uptake in skeletal muscle. *J Biol Chem* 279:1070-1079.
322. Wojtaszewski, J.F., Jorgensen, S.B., Hellsten, Y., Hardie, D.G., and Richter, E.A. 2002. Glycogen-dependent effects of 5-aminoimidazole-4-carboxamide (AICA)-riboside on AMP-activated protein kinase and glycogen synthase activities in rat skeletal muscle. *Diabetes* 51:284-292.
323. Wojtaszewski, J.F., Mourtzakis, M., Hillig, T., Saltin, B., and Pilegaard, H. 2002. Dissociation of AMPK activity and ACCbeta phosphorylation in human muscle during prolonged exercise. *Biochem Biophys Res Commun* 298:309-316.
324. Young, M.E., Radda, G.K., and Leighton, B. 1997. Nitric oxide stimulates glucose transport and metabolism in rat skeletal muscle in vitro. *Biochem J* 322 (Pt 1):223-228.
325. Richter, E.A., Nielsen, J.N., Jorgensen, S.B., Frosig, C., Birk, J.B., and Wojtaszewski, J.F. 2004. Exercise signalling to glucose transport in skeletal muscle. *Proc Nutr Soc* 63:211-216.
326. Lau, K.S., Grange, R.W., Isotani, E., Sarelius, I.H., Kamm, K.E., Huang, P.L., and Stull, J.T. 2000. nNOS and eNOS modulate cGMP formation and vascular response in contracting fast-twitch skeletal muscle. *Physiol Genomics* 2:21-27.
327. Chen, Z.P., Stephens, T.J., Murthy, S., Canny, B.J., Hargreaves, M., Witters, L.A., Kemp, B.E., and McConell, G.K. 2003. Effect of exercise intensity on skeletal muscle AMPK signaling in humans. *Diabetes* 52:2205-2212.
328. Lindbom, L., Tuma, R.F., and Arfors, K.E. 1980. Influence of oxygen on perfused capillary density and capillary red cell velocity in rabbit skeletal muscle. *Microvasc Res* 19:197-208.
329. Baron, A.D., Zhu, J.S., Marshall, S., Irsula, O., Brechtel, G., and Keech, C. 1995. Insulin resistance after hypertension induced by the nitric oxide synthesis inhibitor L-NMMA in rats. *Am J Physiol* 269:E709-715.
330. Tsui, J.C., and Dashwood, M.R. 2005. A role for endothelin-1 in peripheral vascular disease. *Curr Vasc Pharmacol* 3:325-332.

331. De Carlo, E., Milanesi, A., Martini, C., Maffei, P., Sicolo, N., and Scandellari, C. 2000. Endothelin-1 and endothelin-3 stimulate insulin release by isolated rat pancreatic islets. *J Endocrinol Invest* 23:240-245.
332. Teuscher, A.U., Lerch, M., Shaw, S., Pacini, G., Ferrari, P., and Weidmann, P. 1998. Endothelin-1 infusion inhibits plasma insulin responsiveness in normal men. *J Hypertens* 16:1279-1284.
333. McAuley, D.F., Nugent, A.G., McGurk, C., Maguire, S., Hayes, J.R., and Johnston, G.D. 2000. Vasoconstriction to endogenous endothelin-1 is impaired in patients with type II diabetes mellitus. *Clin Sci (Lond)* 99:175-179.
334. Duckworth, W.C., Bennett, R.G., and Hamel, F.G. 1998. Insulin degradation: progress and potential. *Endocr Rev* 19:608-624.
335. Lteif, A., Vaishnava, P., Baron, A.D., and Mather, K.J. 2007. Endothelin limits insulin action in obese/insulin-resistant humans. *Diabetes* 56:728-734.
336. van Tits, L.J., Arioglu-Oral, E., Sweep, C.G., Smits, P., Stalenhoef, A.F., and Tack, C.J. 2005. Anti-inflammatory effects of troglitazone in nondiabetic obese subjects independent of changes in insulin sensitivity. *Neth J Med* 63:250-255.
337. Baron, A.D., and Clark, M.G. 1997. Role of blood flow in the regulation of muscle glucose uptake. *Annu Rev Nutr* 17:487-499.
338. Burnol, A.F., Leturque, A., Ferre, P., and Girard, J. 1983. A method for quantifying insulin sensitivity in vivo in the anesthetized rat: the euglycemic insulin clamp technique coupled with isotopic measurement of glucose turnover. *Reprod Nutr Dev* 23:429-435.
339. Hu, F.B., Meigs, J.B., Li, T.Y., Rifai, N., and Manson, J.E. 2004. Inflammatory markers and risk of developing type 2 diabetes in women. *Diabetes* 53:693-700.
340. Rosendal, L., Sogaard, K., Kjaer, M., Sjogaard, G., Langberg, H., and Kristiansen, J. 2005. Increase in interstitial interleukin-6 of human skeletal muscle with repetitive low-force exercise. *J Appl Physiol* 98:477-481.
341. Sopasakis, V.R., Sandqvist, M., Gustafson, B., Hammarstedt, A., Schmelz, M., Yang, X., Jansson, P.A., and Smith, U. 2004. High local concentrations and effects on differentiation implicate interleukin-6 as a paracrine regulator. *Obes Res* 12:454-460.
342. Ijzerman, R.G., Voordouw, J.J., Van Weissenbruch, M.M., Yudkin, J.S., Serne, E.H., Delemarre-van de Waal, H.A., and Stehouwer, C.D. 2006. TNF-alpha levels are associated with skin capillary recruitment in humans: a potential cxplanation for the relationship between TNF-alpha and insulin resistance. *Clin Sci (Lond)* 110:361-368.
343. Patel, J.N., Jager, A., Schalkwijk, C., Corder, R., Douthwaite, J.A., Yudkin, J.S., Coppack, S.W., and Stehouwer, C.D. 2002. Effects of tumour necrosis factor-alpha in the human forearm: blood flow and endothelin-1 release. *Clin Sci (Lond)* 103:409-415.
344. Klemm, P., Warner, T.D., Hohlfeld, T., Corder, R., and Vane, J.R. 1995. Endothelin 1 mediates ex vivo coronary vasoconstriction caused by exogenous and endogenous cytokines. *Proc Natl Acad Sci U S A* 92:2691-2695.
345. Andreozzi, F., Laratta, E., Procopio, C., Hribal, M.L., Sciacqua, A., Perticone, M., Miele, C., Perticone, F., and Sesti, G. 2007. Interleukin-6 impairs the insulin signaling pathway, promoting production of nitric oxide in human umbilical vein endothelial cells. *Mol Cell Biol* 27:2372-2383.

346. Ostrowski, K., Schjerling, P., and Pedersen, B.K. 2000. Physical activity and plasma interleukin-6 in humans--effect of intensity of exercise. *Eur J Appl Physiol* 83:512-515.
347. Yudkin, J.S., Kumari, M., Humphries, S.E., and Mohamed-Ali, V. 2000. Inflammation, obesity, stress and coronary heart disease: is interleukin-6 the link? *Atherosclerosis* 148:209-214.
348. Renaudin, C., Michoud, E., Rapin, J.R., Lagarde, M., and Wiernsperger, N. 1998. Hyperglycaemia modifies the reaction of microvessels to insulin in rat skeletal muscle. *Diabetologia* 41:26-33.
349. Bertoldo, A., Pencek, R.R., Azuma, K., Price, J.C., Kelley, C., Cobelli, C., and Kelley, D.E. 2006. Interactions between delivery, transport, and phosphorylation of glucose in governing uptake into human skeletal muscle. *Diabetes* 55:3028-3037.
350. Ellmerer, M., Hamilton-Wessler, M., Kim, S.P., Huecking, K., Kirkman, E., Chiu, J., Richey, J., and Bergman, R.N. 2006. Reduced access to insulin-sensitive tissues in dogs with obesity secondary to increased fat intake. *Diabetes* 55:1769-1775.
351. Eringa, E.C., Stehouwer, C.D., Merlijn, T., Westerhof, N., and Sipkema, P. 2002. Physiological concentrations of insulin induce endothelin-mediated vasoconstriction during inhibition of NOS or PI3-kinase in skeletal muscle arterioles. *Cardiovasc Res* 56:464-471.
352. Cardillo, C., Nambi, S.S., Kilcoyne, C.M., Choucair, W.K., Katz, A., Quon, M.J., and Panza, J.A. 1999. Insulin stimulates both endothelin and nitric oxide activity in the human forearm. *Circulation* 100:820-825.
353. Rask-Madsen, C., and King, G.L. 2007. Mechanisms of Disease: endothelial dysfunction in insulin resistance and diabetes. *Nat Clin Pract Endocrinol Metab* 3:46-56.
354. del Aguila, L.F., Claffey, K.P., and Kirwan, J.P. 1999. TNF-alpha impairs insulin signaling and insulin stimulation of glucose uptake in C2C12 muscle cells. *Am J Physiol* 276:E849-855.
355. Kim, F., Gallis, B., and Corson, M.A. 2001. TNF-alpha inhibits flow and insulin signaling leading to NO production in aortic endothelial cells. *Am J Physiol Cell Physiol* 280:C1057-1065.
356. Li, G., Barrett, E.J., Barrett, M.O., Cao, W., and Liu, Z. 2007. Tumor necrosis factor-alpha induces insulin resistance in endothelial cells via a p38 mitogen-activated protein kinase-dependent pathway. *Endocrinology* 148:3356-3363.
357. Steinberg, H.O., Tarshoby, M., Monestel, R., Hook, G., Cronin, J., Johnson, A., Bayazeed, B., and Baron, A.D. 1997. Elevated circulating free fatty acid levels impair endothelium-dependent vasodilation. *J Clin Invest* 100:1230-1239.
358. Rongen, G.A., and Tack, C.J. 2001. Triglycerides and endothelial function in type 2 diabetes. *Eur J Clin Invest* 31:560-562.
359. Wang, X.L., Zhang, L., Youker, K., Zhang, M.X., Wang, J., LeMaire, S.A., Coselli, J.S., and Shen, Y.H. 2006. Free fatty acids inhibit insulin signaling-stimulated endothelial nitric oxide synthase activation through upregulating PTEN or inhibiting Akt kinase. *Diabetes* 55:2301-2310.
360. Browatzki, M., Schmidt, J., Kubler, W., and Kranzhofer, R. 2000. Endothelin-1 induces interleukin-6 release via activation of the transcription factor NF-kappaB in human vascular smooth muscle cells. *Basic Res Cardiol* 95:98-105.

361. Rose, A.J., and Richter, E.A. 2005. Skeletal Muscle Glucose Uptake During Exercise: How is it Regulated? *Physiology (Bethesda)* 20:260-270.
362. Ihlemann, J., Galbo, H., and Ploug, T. 1999. Calphostin C is an inhibitor of contraction, but not insulin-stimulated glucose transport, in skeletal muscle. *Acta Physiol Scand* 167:69-75.
363. Sakamoto, K., and Goodyear, L.J. 2002. Invited review: intracellular signaling in contracting skeletal muscle. *J Appl Physiol* 93:369-383.
364. Dedkova, E.N., Wang, Y.G., Ji, X., Blatter, L.A., Samarel, A.M., and Lipsius, S.L. 2007. Signalling mechanisms in contraction-mediated stimulation of intracellular NO production in cat ventricular myocytes. *J Physiol* 580:327-345.
365. Levine, Y.C., Li, G.K., and Michel, T. 2007. Agonist-modulated regulation of AMP-activated protein kinase (AMPK) in endothelial cells. Evidence for an AMPK -> Rac1 -> Akt -> endothelial nitric-oxide synthase pathway. *J Biol Chem* 282:20351-20364.
366. Reihill, J.A., Ewart, M.A., Hardie, D.G., and Salt, I.P. 2007. AMP-activated protein kinase mediates VEGF-stimulated endothelial NO production. *Biochem Biophys Res Commun* 354:1084-1088.
367. Thorell, A., Hirshman, M.F., Nygren, J., Jorfeldt, L., Wojtaszewski, J.F., Dufresne, S.D., Horton, E.S., Ljungqvist, O., and Goodyear, L.J. 1999. Exercise and insulin cause GLUT-4 translocation in human skeletal muscle. *Am J Physiol* 277:E733-741.
368. Holloszy, J.O. 2005. Exercise-induced increase in muscle insulin sensitivity. *J Appl Physiol* 99:338-343.
369. Yudkin, J.S., Juhan-Vague, I., Hawe, E., Humphries, S.E., di Minno, G., Margaglione, M., Tremoli, E., Kooistra, T., Morange, P.E., Lundman, P., et al. 2004. Low-grade inflammation may play a role in the etiology of the metabolic syndrome in patients with coronary heart disease: the HIFMECH study. *Metabolism* 53:852-857.
370. van Hall, G., Sacchetti, M., Radegran, G., and Saltin, B. 2002. Human skeletal muscle fatty acid and glycerol metabolism during rest, exercise and recovery. *J Physiol* 543:1047-1058.
371. Matsuno, M., Kozawa, O., Suzuki, A., Tokuda, H., Kaida, T., Matsuno, H., Niwa, M., and Uematsu, T. 1998. Involvement of protein kinase C activation in endothelin-1-induced secretion of interleukin-6 in osteoblast-like cells. *Cell Signal* 10:107-111.
372. Hotamisligil, G.S. 1999. The role of TNFalpha and TNF receptors in obesity and insulin resistance. *J Intern Med* 245:621-625.
373. Yudkin, J.S., Eringa, E., and Stehouwer, C.D. 2005. "Vasocrine" signalling from perivascular fat: a mechanism linking insulin resistance to vascular disease. *Lancet* 365:1817-1820.